

UNIVERSITY OF CINCINNATI

Date: 27 April, 2005

I, Sylian J. Rodríguez-Lattuada,
hereby submit this work as part of the requirements for the degree of:
Doctorate of Philosophy (Ph.D)

in:

Environmental Engineering

It is entitled:

Characterization Of Soil Biofilms For The Biodegradation
Of Polycyclic Aromatic Hydrocarbons

This work and its defense approved by:

Chair: Dr. Paul L. Bishop
Dr. George Sorial
Dr. Daniel Oerther
Dr. Brian Kinkle

Characterization Of Soil Biofilms For The Biodegradation Of Polycyclic Aromatic Hydrocarbons

A Dissertation submitted to the

Division of Research and Advanced Studies
of the University of Cincinnati

in partial fulfillment of the requirements for the degree of

DOCTORATE OF PHILOSOPHY

in the Department of Civil and Environmental Engineering
of the College of Engineering

2005

by

Sylian Joy Rodríguez-Lattuada

B.S., Civil Engineering, Escuela Colombiana de Ingeniería, 1997

Specialist, Environmental Sanitation, Escuela Colombiana de Ingeniería, 1998

M.S., Environmental Engineering, University of Cincinnati, 2001

Committee Chair: Paul L. Bishop, Ph.D, P.E., D.E.E.

Abstract

Polycyclic Aromatic Hydrocarbons (PAHs) are common contaminants in soils and groundwater aquifers, resulting from anthropogenic activities. Major concerns with these compounds are their recalcitrance, toxicity and other unique characteristics in the environment. *In situ* bioremediation has been successfully used for some PAH degradation in soils, but the optimum conditions for the continuous active growth of microbial communities are not well-understood, so biodegradation processes cannot be properly enhanced.

Lab-scale column reactors simulating sandy aquifer environments were used as attachment medium for the biofilm. The biological degradation of a low molecular weight PAH, naphthalene, was investigated, resulting in a 93.5% removal using acetate as a co-substrate. Biofilm mass and extracellular polymeric substances were greatly improved by the presence of acetate, which also promoted the degradation of naphthalene. Biofilm morphology and structure were characterized qualitatively and quantitatively by using confocal microscopy and image analysis, suggesting that porous media biofilms are complex matrixes that develop and change with specific environmental conditions.

Sole-substrates, as well as binary/tertiary mixtures of 2-, 3- and 4-ringed PAHs, were examined for competitive/inhibitive interactions on porous media biofilms. While phenanthrene and pyrene could not be degraded as sole carbon sources, binary systems of the 3- and 4-ring PAHs with acetate and naphthalene supplements stimulated their

degradation, with up to 87.9% and 70.1% removal efficiencies, respectively. However, inhibition of pyrene degradation by phenanthrene was observed in the tertiary systems. Heterogeneous surface films and a variety of biological aggregate structures and growth patterns were observed by confocal microscopy.

A nonionic surfactant was tested for water solubility enhancements of naphthalene, phenanthrene and pyrene. Solutions of Triton X-100 above the critical micelle concentration (CMC) showed great solubilization of the three PAHs. Batch experiments were also conducted to investigate the sorption effects of PAHs and/or Triton X-100 to the porous media, as well as the partitioning to live/killed biofilms. Low amounts of surfactant were found to be adsorbed onto sand and biofilm; Triton X-100 appeared to increase PAH sorption, but sorbed concentrations were still considered negligible.

The effects of the nonionic surfactant on the biodegradation of PAHs were also investigated. Column experiments showed that the degradation of the 2-ring PAH alone was not affected and only a small enhancement of 3- and 4-ring PAH (as sole-substrates) degradation occurred by Triton X-100 addition. Higher biodegradations were always achieved by having just PAH mixtures without the surfactant, indicating the importance of cross feeding / cometabolic mechanisms over improved solubilization of PAHs.

Acknowledgements

I am deeply thankful to my advisor Dr. Paul L. Bishop for his guidance, assistance and support throughout my time in the doctoral program at UC. He has been a superb example of both personal and professional qualities, who inspired me to search always for excellence in any aspect of my life. Dr. Bishop allowed the autonomy I needed while still keeping me pointed down the path of research. I am also grateful to the other members of my committee, Dr. George Sorial, Dr. Daniel Oerther and Dr. Brian Kinkle for their time, advice and interest.

My gratitude also goes to the National Institute of Environmental Health Sciences (NIEHS), under the Superfund Basic Research Program (SBRP), which provided the funding for this present work. I have to thank also Dr. Nancy Kleene at the Center for Biological Microscopy (University of Cincinnati Medical Center) for her amazing technical support with the confocal image analysis.

My friends and colleagues at the Department of Civil and Environmental Engineering deserve also special thanks, because they have contributed a lot with their friendship, help and advice in the lab, in the office and in the everyday life: Jian, Peng, Alberto, Jeff, Youngwoo, Am and Maria. I would like to thank also former group members Denise, Elena and Baikun, for helping me at the beginning of my Ph.D. Gloria, Andrea, Angie and Norma are long-distance friends who kept me encouraged all this time: thanks to them too. My very special thanks go to my boyfriend and best friend Robert, for his continuous love, patience and support.

I would like to dedicate this dissertation to my parents Daly and Jaime: without their love, encouragement and help, none of this would have been possible. I am also grateful to my brother Vladimir, who has been a constant source of support and advice.

Table of Contents

Abstract	ii
Acknowledgements	v
Table of Contents	vi
List of Tables	ix
List of Figures	x
Chapter 1 INTRODUCTION	1
1.1 Problem Statement	1
1.2 Research Significance	3
1.3 Overall Goals and Specific Objectives	4
1.4 Organization of the Dissertation	6
1.5 References	8
Chapter 2 BACKGROUND	10
2.1 Introduction	10
2.2 Interest on PAHs	11
2.3 PAH Biodegradation	14
2.3.1 <i>In Situ</i> PAH Biodegradation	18
2.3.2 Porous Media Biofilms	21
2.4 Effects of Surfactant Addition on PAH Biodegradation	27
2.5 References	29
Chapter 3 RESEARCH MATERIALS AND METHODS	36
3.1 Introduction	36
3.2 Experimental Design and Setup	37
3.3 Feed and Nutrient Solutions	41
3.4 Chemicals	41
3.5 Analytical Methods	42
3.5.1 Acetate	42
3.5.2 Bacterial Viability	43
3.5.3 Carbohydrates	43
3.5.4 Dissolved Oxygen	44
3.5.5 Lipid-Phosphates	44
3.5.6 Optical Density	45
3.5.7 Polycyclic Aromatic Hydrocarbons	45
3.5.8 pH	46
3.5.9 Proteins	46
3.5.10 Triton X-100	47
3.5.11 Volatile Solids	47

3.6 Other Research Tools	47
3.6.1 Flow cells	47
3.6.2 Confocal Laser Scanning Microscopy	48
3.7 Quality Assurance/Quality Control	49
3.8 References	50

**Chapter 4 BIOFILM FUNCTION-STRUCTURE STUDIES DURING
BIODEGRADATION OF A LOW-MOLECULAR WEIGHT
PAH 52**

4.1 Abstract	52
4.2 Introduction	53
4.3 Materials and Methods	54
4.4 Results and Discussion	56
4.4.1 Biodegradation Studies	57
4.4.2 Naphthalene Adsorption onto Sand Medium	61
4.4.3 Biofilm Composition	62
4.4.4 Biofilm Structure	71
4.4.5 Three-Dimensional Biofilm Quantification	73
4.5 Conclusions	83
4.6 References	84

**Chapter 5 BIOFILM FUNCTION-STRUCTURE STUDIES DURING
BIODEGRADATION OF MEDIUM-MOLECULAR WEIGHT
PAHS AND MIXTURES 87**

5.1 Abstract	87
5.2 Introduction	88
5.3 Materials and Methods	89
5.4 Results and Discussion	91
5.4.1 Phenanthrene Biodegradation Studies	92
5.4.2 Pyrene Biodegradation Studies	95
5.4.3 PAH Adsorption onto Sand Medium	98
5.4.4 Biofilm Composition	100
5.4.5 Biofilm Structure	114
5.5 Conclusions	121
5.6 References	123

**Chapter 6 SOLUBILIZATION AND SORPTION STUDIES OF PAHS
WITH A NONIONIC SURFACTANT 126**

6.1 Abstract	126
6.2 Introduction	127
6.3 Materials and Methods	130
6.4 Results and Discussion	134
6.4.1 Microbial Growth	135
6.4.2 Solubility of PAHs	138

6.4.3	Surfactant Sorption-to-Sand Tests	144
6.4.4	PAHs/Surfactant Sorption-to-Sand Tests	147
6.4.5	Surfactant Sorption-to-Biofilm Tests	152
6.4.6	PAHs/Surfactant Sorption-to-Biofilm Tests	154
6.5	Conclusions	157
6.6	References	160

Chapter 7 EFFECTS OF NONIONIC SURFACTANT ADDITION ON THE BIODEGRADATION OF PAHS 163

7.1	Abstract	163
7.2	Introduction	164
7.3	Materials and Methods	166
7.4	Results and Discussion	168
7.4.1	Biodegradation Studies at 100 mg/L of Triton X-100	169
7.4.2	Biodegradation Studies at 125 mg/L of Triton X-100	172
7.4.3	PAH/Surfactant Adsorption onto Sand Medium	179
7.4.4	Biofilm Composition	183
7.4.5	Biofilm Structure	190
7.5	Conclusions	194
7.6	References	196

Chapter 8 SUMMARY AND RECOMMENDATIONS 199

8.1	Conclusions	199
8.2	Recommendations for Future Study	201

Appendix A Sand Column Design and Operation 203

Appendix B Physical Properties of Sand Media 205

Appendix C Chemical and Physical Analysis Procedures 207

C.1	Naphthalene analysis by GC/FID	208
C.2	Phenanthrene analysis by GC/FID	209
C.3	Pyrene analysis by GC/FID	210
C.4	PAHs/Triton X-100 analysis by HPLC	211
C.5	Protein analysis	212
C.6	Carbohydrates analysis	213
C.7	Lipid-Phosphate analysis	214
C.8	Bacterial viability staining	216

Appendix D PAH feed Generation Columns 217

Tables

Table 2.1	Common contaminants at Superfund sites	12
Table 2.2	Structure and properties of most common PAHs	13
Table 3.1	Nutrient solution composition	42
Table 4.1	Summary of sequence of experiments	57
Table 4.2	Statistical parameters for cell volume measurements and diameter calculations	76
Table 4.3	Statistical parameters for biosurface area, biovolume and biothickness ..	78
Table 4.4	Statistical parameters for total, viable and non-viable areas and cell densities	80
Table 5.1	PAH feed generation column parameters	90
Table 5.2	Summary of sequence of experiments	92
Table 6.1	Selected properties of surfactant Triton X-100	130
Table 6.2	Solubilization parameters of PAHs by surfactant Triton X-100	142
Table 7.1	Summary of sequence of experiments	168
Table 7.2	Summary of effects of addition of Triton X-100 during PAH biodegradation	176

Figures

Figure 2.1	Distribution of typical hazardous waste from different industries11
Figure 2.2	Major metabolic pathways of PAHs17
Figure 2.3	Half-lives of most common PAHs18
Figure 2.4	Biofilm processes in porous media22
Figure 2.5	Biofilm structure and morphology24
Figure 3.1	Schematic diagram of sand column38
Figure 3.2	Flow cell detail38
Figure 3.3	Experimental setup of the system40
Figure 4.1	Removal efficiency of naphthalene (with and without co-substrate) over a period of 18 weeks58
Figure 4.2	Average naphthalene concentration profiles with and without co-substrate	60
Figure 4.3	Naphthalene adsorbed onto sand after 18 weeks61
Figure 4.4	Total biomass profile63
Figure 4.5	Viable biomass profile65
Figure 4.6	Firmly and loosely attached biomass profiles at (a) 1 week, (b) 11 weeks and (c) 18 weeks67,68
Figure 4.7	Carbohydrate profile69
Figure 4.8	Protein profile70
Figure 4.9	Optical sections of biofilms on sand grain surfaces at 7.5 cm (a) at 40x and (b) 20x magnifications, after 18 weeks72
Figure 4.10	Distribution of measured cell volumes74
Figure 4.11	Distribution of calculated cell diameters (n=32)75

Figure 4.12	Typical stack of 39 biofilm images77
Figure 4.13	Typical biosurface area distribution with biofilm depth82
Figure 4.14	Typical cell density per unit area distribution with total biosurface area	82
Figure 5.1	Removal efficiencies for sole-substrate and binary and tertiary mixtures of PAHs during phenanthrene studies93
Figure 5.2	Removal efficiencies for sole-substrate and binary and tertiary mixtures of PAHs during pyrene studies96
Figure 5.3	PAH adsorbed onto sand during phenanthrene studies after 22 weeks	..98
Figure 5.4	PAH adsorbed onto sand during pyrene studies after 22 weeks99
Figure 5.5	Total biomass profile during phenanthrene studies101
Figure 5.6	Total biomass during pyrene studies102
Figure 5.7	Viable biomass profile during phenanthrene studies103
Figure 5.8	Firmly and loosely attached biomass profiles at (a) 1 week, (b) 14 weeks and (c) 22 weeks, during phenanthrene studies105,106
Figure 5.9	Viable biomass profile during pyrene studies107
Figure 5.10	Firmly and loosely attached biomass profiles at (a) 1 week, (b) 14 weeks and (c) 22 weeks, during pyrene studies109,110
Figure 5.11	Carbohydrate profile during phenanthrene studies111
Figure 5.12	Carbohydrate profile during pyrene studies112
Figure 5.13	Protein profile during phenanthrene studies113
Figure 5.14	Protein profile during pyrene studies114
Figure 5.15	Optical sections of biofilms on sand grain surfaces at 7.5 cm (a) at 40x and (b) 20x magnifications, during phenanthrene studies after 14 weeks	116

Figure 5.16	Optical sections of biofilms on sand grain surfaces at 7.5 cm (a) at 40x and (b) 20x magnifications, during phenanthrene studies after 22 weeks	117
Figure 5.17	Optical sections of biofilms on sand grain surfaces at 7.5 cm (a) at 40x and (b) 20x magnifications, during pyrene studies after 14 weeks119
Figure 5.18	Optical sections of biofilms on sand grain surfaces at 7.5 cm (a) at 40x and (b) 20x magnifications, during pyrene studies after 22 weeks120
Figure 6.1	Microbial growth of naphthalene in the presence of Triton X-100136
Figure 6.2	Consumption of (a) naphthalene and (b) Triton X-100 by a mixed culture during microbial growth experiments137
Figure 6.3	Naphthalene solubility at different Triton X-100 concentrations139
Figure 6.4	Phenanthrene solubility at different Triton X-100 concentrations140
Figure 6.5	Pyrene solubility at different Triton X-100 concentrations140
Figure 6.6	Adsorption capacity of Triton X-100 (filled symbols, Y axis at left) and removal from solution (open symbols, Y axis at right) with sand dose (after 24 hours)144
Figure 6.7	Adsorption capacity onto sand of (a) Triton X-100 and (b) naphthalene (filled symbols, Y axis at left) and their removal from solution (open symbols, Y axis at right) with sand dose148
Figure 6.8	Adsorption capacity onto sand of (a) Triton X-100 and (b) phenanthrene (filled symbols, Y axis at left) and their removal from solution (open symbols, Y axis at right) with sand dose149
Figure 6.9	Adsorption capacity onto sand of (a) Triton X-100 and (b) pyrene (filled symbols, Y axis at left) and their removal from solution (open symbols, Y	

	axis at right) with sand dose	151
Figure 6.10	Adsorption capacity onto live biofilm (LB) and killed biofilm (KB) of Triton X-100 with time	153
Figure 6.11	Adsorption capacity onto live biofilm (LB) and killed biofilm (KB) of Triton X-100 with time, in the presence of PAHs	155
Figure 6.12	Adsorption capacity onto live biofilm (LB) of PAHs with time, in the presence of Triton X-100 (100 mg/L)	156
Figure 6.13	Adsorption capacity onto live biofilm (LB) of PAHs with time, in the presence of Triton X-100 (125 mg/L)	157
Figure 7.1	Removal efficiencies of PAHs in the presence of 100 mg/L Triton X-100	170
Figure 7.2	Removal efficiencies of PAHs in the presence of 125 mg/L Triton X-100	173
Figure 7.3	Sorption of (a) PAHs and (b) surfactant (100 mg/L) onto sand	180
Figure 7.4	Sorption of (a) PAHs and (b) surfactant (125 mg/L) onto sand	181
Figure 7.5	Total biomass profile in the presence of Triton X-100	184
Figure 7.6	Viable biomass in the presence of Triton X-100	185
Figure 7.7	Firmly and loosely attached biomass profiles in the presence of (a) 100 mg/L and (b) 125 mg/L of Triton X-100	186
Figure 7.8	Carbohydrate profile in the presence of Triton X-100	188
Figure 7.9	Protein profile in the presence of Triton X-100	189
Figure 7.10	Optical sections of biofilms on sand grain surfaces at 7.5 cm (a) at 40x and (b) 20x magnifications, in the presence of 100 mg/L of Triton, after 22 weeks	191
Figure 7.11	Optical sections of biofilms on sand grain surfaces at 7.5 cm (a) at 40x and (b) 20x magnifications, in the presence of 125 mg/L of Triton, after 22 weeks	192

Figure A.1	Experimental setup of single sand column and flowcells204
Figure A.2	Complete experimental setup204
Figure B.1	Particle size distribution for ASTM silica sand (C-190)206
Figure D.1	ESEM picture of typical PAH coating on glass beads at 200x and 500x magnifications219

Chapter 1

INTRODUCTION

1.1 PROBLEM STATEMENT

Polycyclic aromatic hydrocarbons (PAHs) are a class of several hundred individual compounds containing at least two condensed rings. They have received much attention since they were found in soils for the first time by Blumer (1961), mainly due to their toxicity to humans and their possible harmful effect on soil organisms and plants (Menzie, 1992). Their unique characteristics, such as high densities, low solubilities, high hydrophobicities, low vapor pressures and low biodegradabilities, make PAHs a continuous hot topic of interest for new research and investigation.

Many studies have reported on PAH biodegradation in soil. However, the biodegradation of these compounds is governed by several physical/chemical factors that appear to control microbial energetic and nutritional requirements, as well as the availability of the pollutants to microbial populations (Pignatello and Xing, 1996; Amella et al., 2001). Both *in situ* and *ex situ* bioremediation have been demonstrated to be successful for PAH contaminated soils, but *in situ* technologies have gained more attention due to lower costs of treatment. Even so, the addition of external electron acceptors and nutrients, as well as repeated inoculation to increase the bacterial population, are often needed (Beaudin et al., 1999; Schwartz et al., 2001).

A fundamental mechanism of interaction between biological processes and soils has been established through the formation of biofilms, or microbial communities that conglomerate and are held together by an organic polymeric matrix of extracellular material and debris (Bishop, 1997). Subsurface biofilms use porous media for attachment, colonization and proliferation, forming heterogeneous structures that vary in thickness, porosity, pore structure, etc., and which are even stratified at times (Zhang and Bishop, 1994). However, due to the complexity of this matrix, the role of biofilm has not been sufficiently investigated, especially because it is a dynamic matrix that may alter the mass transfer of nutrients and contaminants. Therefore, further research is needed to understand the useful properties of biofilms, so biodegradation of recalcitrant compounds like PAHs can be optimized.

Most of the studies regarding the biodegradability of PAHs have been carried out with single, low-molecular weight contaminants and/or pure cultures of microorganisms (Daugulis and McCracken, 2003; Mulder et al., 1998); biodegradation under these conditions has been successfully employed for remediation of contaminated soils. However, bioremediation strategies often have limited applicability when mixtures and medium- and high-molecular-weight PAHs are present, probably due to the tendency of these compounds to sorb strongly to natural soil organic matter, to the stabilities of their structures and their low water solubilities. Several authors (Yuan et al., 2001; Dean-Ross et al., 2002) have found both cometabolic and inhibitive effects of multisubstrate utilization of PAHs, but there are not conclusive results. In addition, the bioavailability of the pollutants has been examined by using surfactants, which improve mobilization and

solubility of the contaminants (Marquez-Rocha et al., 2000; Kim et al., 2001), but again, contradictory data has been found. A more realistic situation where several pollutants of homologous composition are present, as well as a mixed culture that has broader biodegradation capabilities, needs to be further investigated, and more studies on the enhancement of PAH bioavailability are required.

1.2 RESEARCH SIGNIFICANCE

In situ bioremediation has been proposed as a new alternative for PAH degradation in soils, and has shown excellent results. However, factors such as low water solubility, lack of appropriate microorganisms and/or nutrients, and the need for oxygen often limit the effectiveness of *in situ* bioremediation of PAHs.

Assuming black-box approaches, different studies have been conducted on soil pore water, often giving a poor description of the actual rates of disappearance of the PAHs. However, no research has been reported on the biofilm surrounding the soil particles, which is the primary site where biodegradation occurs.

Therefore, this research is aimed at improving bioremediation processes by maximizing the useful properties of soil biofilms. It is fundamental to elucidate the heterogeneity of biofilms grown and developed in porous media with recalcitrant compounds, such as PAHs, as their unique structure and composition in subsurface environments may influence the rate and kinetics of transport and degradation of the contaminants, and may

also vary according to specific environmental stresses. Microbial communities may thrive and remain viable during unfavorable periods of time, thanks to their adaptive capacity, but it is important also to investigate the optimum conditions for their continuous active growth, in order to enhance biodegradation processes.

The second major aim of this study is to provide more realistic conditions for PAH bioremediation, taking into account that the pollutants are often found as mixtures and sorbed to the soil particles, and different species or strains of microorganisms may be present in this environment. This will provide a better understanding of the degradation of PAH mixtures, the competitive metabolisms occurring within the biofilm and the impact of surfactant addition on degradation mechanisms.

The results of this research are intended to provide a fundamental guideline for the development of more effective bioremediation strategies in the future applications of biological barriers, as a means of subsurface environmental restoration.

1.3 OVERALL GOALS AND SPECIFIC OBJECTIVES

The overall goals of this research were:

- to gain an understanding of the transport and degradation mechanisms involved in soil bioremediation systems for low and medium molecular weight PAHs;
- to define the role of the biofilm matrix, in terms of growth and development, structure, composition and chemistry during *in situ* PAH biodegradation, and

- to understand the mass transport of nutrients and contaminants to biofilm microorganisms.

The following specific objectives were addressed for the characterization of soil biofilms growing in the presence of a variety of PAHs:

1. To investigate the biodegradation of low- and medium-molecular-weight PAHs, in sand column reactors, operating under aerobic conditions.
2. To compare degradation performances and competitive mechanisms of degradation of PAHs as sole-carbon sources, as well as binary and tertiary mixtures.
3. To determine the microbial biomass and especially the cell viability number per unit area and unit volume, in biofilms growing in the presence of PAHs.
4. To examine the extracellular polymeric substance production per sand mass/biomass and viable biomass per sand mass/total solids, and its influence on PAH biodegradation.
5. To describe the heterogeneity of the biofilm in terms of its physical structure, growth and development, degree of attachment and formation characteristics for a variety of PAHs and their mixtures.
6. To examine the effect of surfactant addition on the biodegradation of 2, 3 and 4-ring PAHs as single substrates and mixtures.
7. To investigate the impacts of the presence of a nonionic surfactant on the biofilm structure and composition.
8. To examine the sorption processes of the nonionic surfactant to the porous media and to the biofilms and its effects on biodegradation of PAHs.

1.4 ORGANIZATION OF THE DISSERTATION

The material in this dissertation is organized by chapters in the following manner. Chapter 1 is the section in which the problem statement, significance of the research and overall goals and specific objectives are described.

Chapter 2 focuses on the literature review, which emphasizes background information on PAH characteristics, health effects on humans and sources of their production. This chapter also illustrates the types of biological degradation of these recalcitrant compounds; common bacteria that metabolize them and pathways of biodegradation; *in situ* vs. *ex situ* methodologies of PAH biodegradation; the environmental factors affecting *in situ* bioremediation; biofilm formation, growth and structure in a porous media; typical biofilm responses to the presence of PAHs; the role of extracellular polymeric substances (EPS) with respect to PAH biodegradation; the use of surfactants as a method for improving PAH solubility; and the dual effects (inhibition-enhancement) on PAH biodegradation.

Chapter 3 provides a detailed description of the reactors' design and complete experimental setup, with the specific procedures of inoculation, preparation and operation of the system. It includes the composition of the feed and nutrient solutions, as well as chemicals used in the research. The analytical methods and other research tools utilized in the study are also discussed, including instrumentation, laboratory procedures and specific techniques. Finally, the quality assurance and quality control (QA/QC) plan

contains the description of measurements taken during sampling, instrument calibration and methods, in order to assure minimum experimental error.

In Chapter 4, the function-structure of biofilms growing on low-molecular-weight PAHs is presented. Biodegradation studies with naphthalene and its performance in the presence of acetate are discussed. Temporal and spatial distributions of naphthalene concentrations are also described in this chapter. The characterization of biofilms in terms of the physical structure and chemical composition are illustrated, as a means of formation, growth and development in soil systems. Image analysis is included, with the goal of describing morphologic characteristics of biofilms attached to sand grain surfaces.

Chapter 5 describes the function-structure of biofilms for medium molecular weight PAHs, such as phenanthrene and pyrene. Biodegradation studies on PAHs as sole-carbon sources, binary and tertiary mixtures are discussed in this chapter, as well as the different metabolism mechanisms influencing PAH biodegradation. The nature of biofilms are described by exopolymer and biomass composition, and the physical structures are examined using confocal microscopic analysis.

Chapter 6 examines the solubilization and sorption studies of PAHs with a nonionic surfactant. Microbial growth is evaluated at different concentrations of Triton X-100, in order to establish toxicity/inhibition effects on biomass growth. Solubility of low and medium molecular weight PAHs are investigated in the presence of two different concentrations of the nonionic surfactant Triton X-100. Also, sorption tests, including

surfactant-sand, surfactant-biofilm and surfactant-PAH-biofilm are discussed, so that the main mechanisms governing the system are elucidated.

Chapter 7 investigates the effects of surfactant addition on PAH biodegradation. The biodegradations of the 2-, 3- and 4-ring PAHs with Triton X-100 are evaluated as single substrates and mixtures in the sand columns. The structure and composition of biofilms growing under these conditions are described.

The last chapter, Chapter 8, presents a summary of the results found in this research and provides some recommendations for future work on the bioremediation of PAHs that can be initiated.

Appendices provide detailed information about sand column design and operation; sand media and its properties; laboratory procedures and analytical methods.

1.5 REFERENCES

Amella, N., Portal, J., Vogel, T., Berthelin, J., (2001), "Distribution and location of polycyclic aromatic hydrocarbons (PAHs) and PAH-degrading bacteria within polluted soil aggregates", *Biodegradation*, **12**, 49-57.

Beaudin, N., Caron, R.F., Legros, R., Ramsay, J., Ramsay, B., (1999), "Identification of the key factors affecting composting of a weathered hydrocarbon-contaminated soil", *Biodegradation*, **10**, 127-133.

Bishop, P.L., (1997), "Biofilm structure and kinetics", *Wat.Sci.Techn.*, **36**, 287-294.

Blumer, M., (1961), "Benzyprenes in soil", *Science*, **134**, 474-475.

Daugulis, A., McCracken, C., (2003), "Microbial degradation of high and low molecular weight polyaromatic hydrocarbons in a two-phase partitioning bioreactor by two strains of *Sphingomonas* sp.", *Biotechn.Lett.*, **25**, 1441-1444.

Dean-Ross D., Moody, J., Cerniglia, C., (2002), " Utilization of mixtures of polycyclic aromatic hydrocarbons by bacteria isolated from contaminated sediment", *Microb. Ecol.*, **41**, 1-7.

Kim, I., Park, J., Kim, K., (2001), "Enhanced biodegradation of polycyclic aromatic hydrocarbons using nonionic surfactants in soil slurry", *Appl.Geochem.*, **16**, 1419-1428.

Márquez-Rocha, F., Hernández-Rodríguez, V., Vázquez-Duhalt, R., (2000), "Biodegradation of soil-adsorbed polycyclic aromatic hydrocarbons by the white rot fungus *Pleurotus ostreatus*", *Biotechn.Lett.*, **22**, 469-472.

Menzie, C.A., Potocki, B., Santodonato, J., (1992), "Exposure to carcinogenic PAHs in the environment", *Env.Sci.&Techn.*, **26**, 1278-1283.

Mulder, H., Breure, A., Van Honschooten, D., Grotenhuis, J., Van Andel, J., Rulkens, W., (1998), "Effect of biofilm formation by *Pseudomonas* 8909N on the bioavailability of solid naphthalene", *Appl.Microb.Biotechn.*, **50**, 277-283.

Pignatello, J., Xing, B., (1996), "Mechanisms of slow sorption of organic chemicals to natural particles", *Env.Sci.&Techn.*, **30**, 1-11.

Schwartz, E., Scow, K., (2001), "Repeated inoculation as a strategy for the remediation of low concentrations of phenanthrene in soil", *Biodegradation*, **12**, 201-207.

Yuan, S.Y., Chang, J., Yen, J., Chang, B.V., (2001), "Biodegradation of phenanthrene in river sediment", *Chemosphere*, **43**, 273-278.

Zhang, T., Bishop, P., (1994), "Density, porosity and pore structure of biofilms", *Water Research*, **28**(11), 2267-2277.

Chapter 2

BACKGROUND

2.1 INTRODUCTION

Many hazardous materials, classified as any type of waste discarded from residential, commercial or industrial areas with specific properties (such as reactivity, ignitability, toxicity and corrosivity), have been listed in the Code of Federal Regulations (CFR) because of the risk they pose to the environment and human health.

Over 700 tons of hazardous wastes are produced each year in the U.S. at different industrial sites, such as chemical, electronics and electrical equipment, petroleum refining, metals, transportation and other related plants (Bishop, 2000). A graphical distribution of typical hazardous wastes produced is presented in **Figure 2.1**. Usually 96% of all hazardous wastes is still managed on site by storing, landfilling, waste immobilization by solidification/stabilization, incineration or other thermal treatment, while only 4% is handled by off-site treatment and disposal facilities (Corbitt, 1990); however, the types, quantities and degree of toxicity have a wide range of variation.

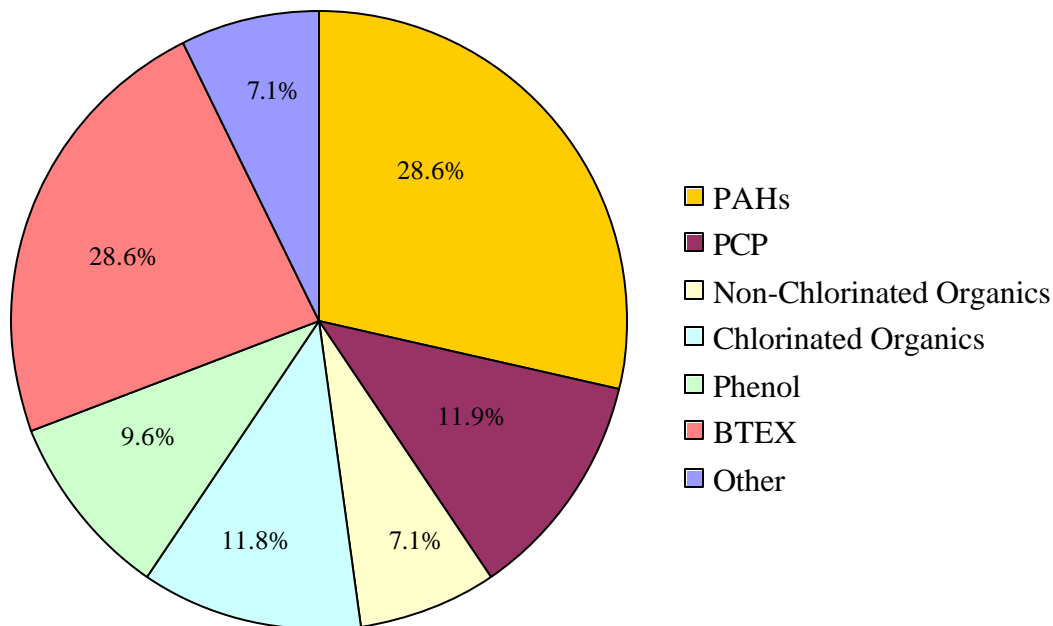


Figure 2.1 Distribution of typical hazardous waste from different industries (Bishop, 2000).

2.2 INTEREST IN PAHS

Significant amounts of toxic organics are contained in Superfund sites; the most common contaminants are depicted in **Table 2.1** (Bishop, 2000). Polycyclic aromatic hydrocarbons (PAHs) are frequently encountered there (ASTDR, 1995). The main concern with PAHs is based on their unique characteristics: 1) high levels of toxicity, 2) microbial recalcitrance, 3) high potential for bioaccumulation and 4) high occurrence in the environment (Ryan *et al.*, 1991).

PAHs are a group of aromatic compounds, usually produced by the incomplete combustion of coal, oil and gas, garbage and other organic substances; there is also

Table 2.1 Common contaminants at Superfund sites (Bishop, 2000).

Chemical	Occurrence (%)	Concentration (ppm)
Lead	51.4	309
Cadmium	44.7	2.19
Toluene	44.1	1120
Mercury	29.6	1.38
Benzene	28.5	58
Trichloroethylene	27.9	103
Ethylbenzene	26.9	540
Benzo[<i>a</i>]anthracene	12.3	148
Bromodichloromethane	7.0	0.02
Polychlorinated biphenyls (PCBs)	3.9	128
Toxaphene	0.6	12.36

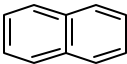
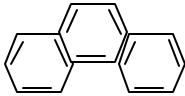
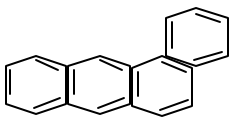
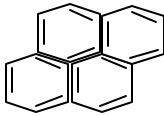
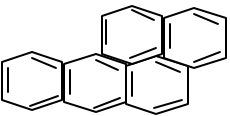
knowledge about the use of these chemicals in pharmaceutical and dyeing industries, for pesticides, plastics and wood preservation.

Contamination of soil and groundwater at Superfund sites by PAHs are very common. As of 2002, over 1300 sites in the U.S. are listed in the National Priorities List (NPL) by the Environmental Protection Agency (EPA) and are waiting for the Superfund cleanup process, according to the Comprehensive Environmental Response, Compensation, and Liability Act (CERCLA), established in 1980 (EPA, 2001; ASTDR, 1995). Not only are coal-tar production plants, coking plants, bitumen and asphalt production plants, coal-gasification sites and municipal refuse incinerators included in the Superfund list, but also partial coal combustion sites.

Polycyclic aromatic hydrocarbons (PAHs) are polynuclear chemicals containing at least two condensed rings. Their unique characteristics make them of interest for new research

and investigation: high densities, low solubilities, high hydrophobicities, low vapor pressures and therefore, low biodegradabilities. **Table 2.2** contains the most common PAHs, their structure and some properties (Merck & Co., 1996; Bishop, 2000). Usually PAHs are present in soil as NAPLs (non-aqueous phase liquids), meaning small globules of free liquid, which are very difficult to dissolve in water.

Table 2.2 Structure and properties of most common PAHs (Bishop, 2000).

Compound	Structure	Molecular weight (g/mol)	Solubility (mg/L)	Vapor pressure (mm Hg)	Specific Gravity
Toluene		92.15	515	22	0.87
Naphthalene		128.17	30	5.4×10^{-2}	1.15
Anthracene		178.24	4.5×10^{-2}	1.7×10^{-5}	1.28
Phenanthrene		178.24	1.9×10^{-3}	2.1×10^{-4}	0.98
Benzo[<i>a</i>]anthracene		228.3	5.7×10^{-3}	2.2×10^{-8}	1.27
Pyrene		202.26	0.13	2.5×10^{-6}	1.27
Benzo[<i>a</i>]pyrene		252.32	3.8×10^{-3}	5.6×10^{-9}	1.35

Serious human health effects and impacts on the environment have been found to be caused by PAHs. Animal studies have shown that PAHs can cause harmful consequences to the skin, body, fluids, ability to fight disease and mutagenicity after both short and long-term exposure; reports determined that individuals exposed by breathing or skin contact for long periods of time are susceptible to cancer (Menzie *et al.*, 1992). The most common PAH exposure pathways from soil contamination are: inhalation, dermal absorption, ingestion, consumption of plants or animals that have assimilated the PAH material, or consumption of contaminated drinking water (Calabrese, 1998).

The Occupational Safety and Health Administration (OSHA) has set a limit of 0.2 mg of PAHs per m³ of air, while in drinking water supplies the range varies between 4-24 ng/L. The OSHA Permissible Exposure Limit (PEL) for mineral oil mist that contains PAHs is 5 mg/m³ averaged over an 8-hour exposure period. The National Institute for Occupational Safety and Health (NIOSH) recommends that the average workplace air levels for coal tar products not exceed 0.1 mg/m³ for a 10-hour workday, within a 40-hour workweek (ASTDR, 1995).

2.3 PAH BIODEGRADATION

Biological degradation represents the major route through which PAHs are removed from contaminated sites (Vecchioli *et al.*, 1997; Guo, 1998). In most cases, lower molecular weight PAHs containing 2 or 3 rings are readily biodegraded, while higher molecular

weight PAHs are more resistant to biological action and tend to persist in the environment (Cerniglia, 1993).

In PAH biodegradation, natural microorganisms can be used in the controlled detoxification of contaminants. The metabolizing bacteria most frequently reported in the literature are: *Pseudomonas* (Schneider, 1996; Stelmack *et al.*, 1999), *Achromobacter* (Gannon *et al.*, 1991), *Arthrobacter* (Dorn *et al.*, 1978), *Mycobacterium* (Boldrin *et al.*, 1993; Tongpim *et al.*, 1996), *Flavobacterium* (Aprill *et al.*, 1990), *Rhodococcus* (Cerniglia *et al.*, 1992), *Acinetobacter* (Pendry, 1990) and *Comamonas* (McClennen *et al.*, 1990). There are also dominant fungal genera shown to degrade PAHs: *Phanerochaete* (Bradford *et al.*, 1991; Novotny *et al.*, 1999), *Cunninghamella* (Pothuluri *et al.*, 1998) and *Penicillium* (Huysmans *et al.*, 1991).

Under controlled conditions, pure cultures are capable of degrading individual PAHs, but they are often unable to degrade multiple pollutants found at contaminated sites. The use of mixed cultures is advantageous, since the products and by-products of one microorganism may provide the carbon and energy source for another microorganism through cometabolism (Bailey *et al.*, 1986). Mixed cultures have been shown to degrade several PAHs at significantly higher rates than individual bacterial strains because of their broader enzymatic capabilities (Yuan *et al.*, 2000).

Substrate interactions complicate the biodegradation kinetics in PAH-contaminated environments. When in mixtures, PAHs can influence positively or negatively the rate

and extent of biodegradation of other PAH components. Sometimes, cometabolic interactions enhance degradation of higher molecular weight PAHs, when soil consortia utilize inter-metabolites. In other cases, competitive inhibition was observed when PAHs were metabolized by a common enzyme system, with the degradation of 2- or 3-ring compounds preferred, and delay or decrease of the degradation of more persistent PAHs. Both cometabolic and inhibitory effects have frequently been observed and widely reported in the literature (McNally *et al.*, 1999; Bouchez *et al.*, 1999; Yuan *et al.*, 2001; Dean-Ross *et al.*, 2002).

Three types of PAH degradation have been shown to occur during laboratory studies with pure cultures (Mahro *et al.*, 1994):

- ***Complete Mineralization:*** oxidation is carried out by the incorporation of an oxygen molecule into the aromatic ring (Cerniglia, 1992; Pothuluri, 1998; Sutherland, 1995). The reaction is catalyzed by a dioxygenase and leads to *cis*-dihydrodiol intermediates. Through this process, bacteria are capable of growing on PAHs as a sole carbon and energy source. Complete mineralization is only valid for PAHs with less than four condensed rings.
- ***Cometabolic Degradation:*** this process differs from the first one in the sense that organisms do not use the PAHs for growth, and also that cometabolic degradation stops at a very early stage after initial oxidation.
- ***Unspecified Radical Oxidation:*** a specific kind of white fungi is able to degrade lignin, which can attack and oxidize aromatic constituents, since ligninases act as substrate-

unspecific peroxidases. The unspecified radical oxidation of PAHs leads to the formation of a wide variety of metabolic products.

The major pathways in the microbial metabolism of a typical polycyclic aromatic hydrocarbon are shown in **Figure 2.2** (Pothuluri, 1998). The incorporation of oxygen must always be included as the first step in the PAH biodegradation.

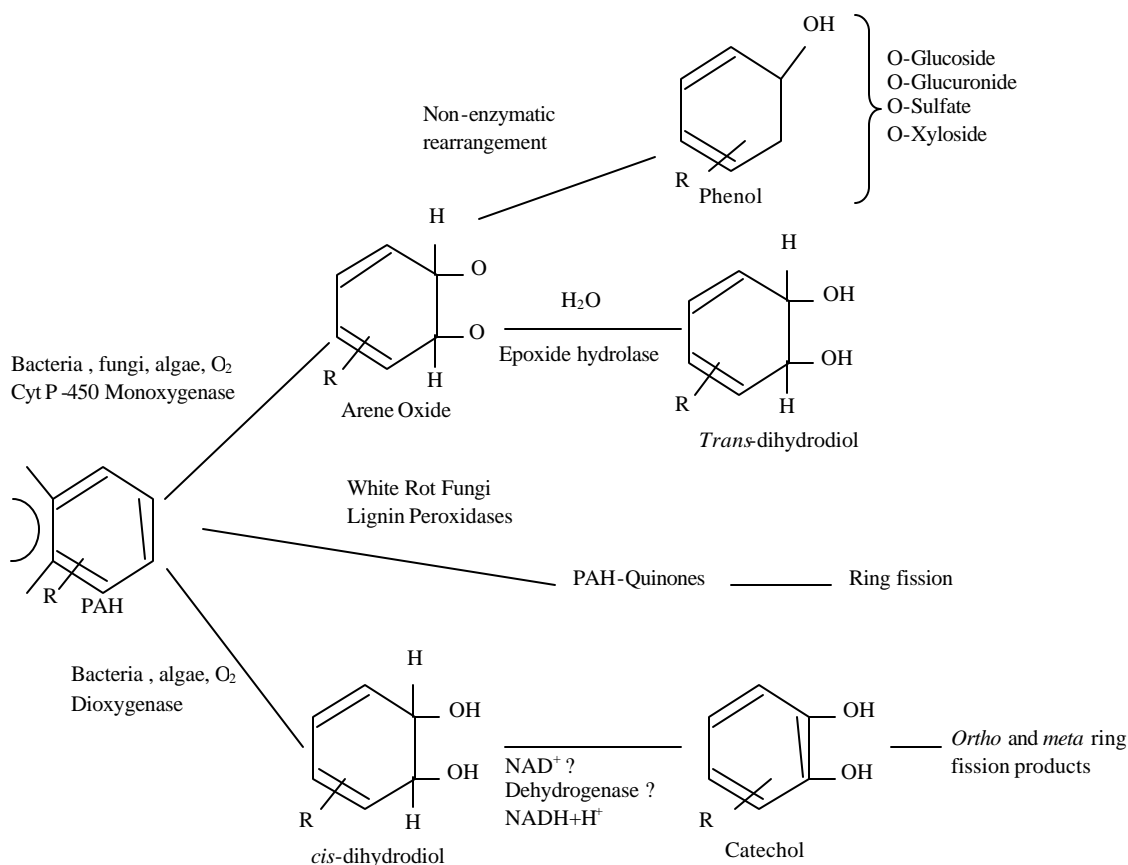


Figure 2.2 Major metabolic pathways of PAHs (Pothuluri, 1998).

Based on experimental results, the estimated half-lives of PAHs with three or fewer rings were found to be around 20 days, while biodegradation of high molecular weight PAHs were considerably longer, ranging from 20 to 400 days, as shown in **Figure 2.3**.

However, there are differences in the half-life values reported by several investigators, due to many environmental factors that may influence the rate of PAH degradation like pH, nutrients, oxygen concentration, temperature, moisture, PAH concentration, soil type, etc. (Park *et al.*, 1990).

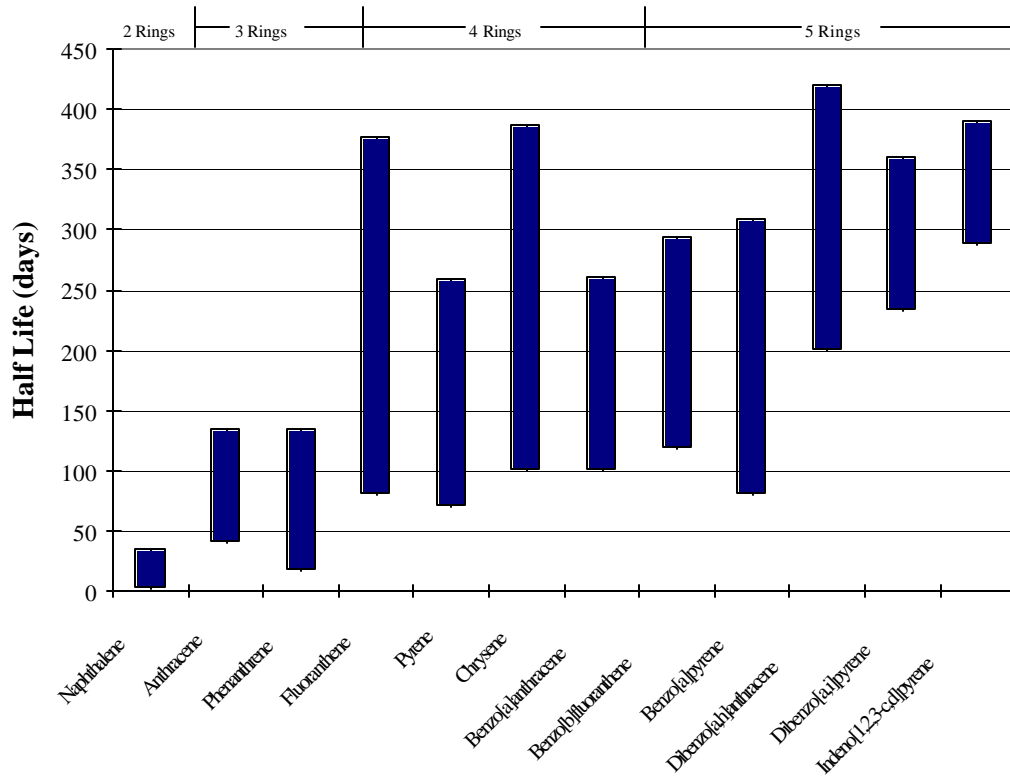


Figure 2.3 Half-lives of most common PAHs (Park *et al.*, 1990).

2.3.1 *In Situ* PAH Biodegradation

Bioremediation treatment technologies for PAH contaminated soils can be used by both *in situ* and *ex situ* stimulation, involving the enhancement of the biodegradation rate of

the organic contaminants within affected soil or in compost heaps or slurry bioreactors (Baker *et al.*, 1994; Blackburn *et al.*, 1993).

Usually *ex situ* methodologies provide better-controlled conditions (Zhang and Bouwer, 1997), but they also require excavation and transportation of the soil, which results in high costs of treatment. On the other hand, *in situ* bioremediation has acquired more importance in the last few years as an attractive alternative for biodegradation; in this case, it requires the stimulation of the degradative activities of endogenous microbial populations by the provision of nutrients (called biostimulation) and/or external electron acceptors (Beaudin *et al.*, 1999; Johnson *et al.*, 1999) or repeated inoculation (called bioaugmentation) to increase the bacterial population (Schwartz *et al.*, 2001).

The addition of nutrients to contaminated soils has been investigated with varying degrees of success (Beaudin *et al.*, 1999; Johnson *et al.*, 1999), often in combination with oxygen provided via percolation of oxygen-saturated water, air sparging, hydrogen peroxide or bioventing (Hinchee *et al.*, 1995).

Both the rate and the extent of microbial remediation of PAHs *in situ* are affected by a variety of environmental factors, some of which can be manipulated whereas others are difficult to modify within the contaminated site:

- **pH:** since the majority of bacteria exhibit optimum growth at or near neutral pH values, most PAH biodegradation studies have been carried out at this pH range. Adjustment of soil pH can significantly alter bioremediation rates (Verstraete *et al.*, 1976). It should

however, be kept in mind that alteration of the soil or sediment pH may affect the solubility, bioavailability and the chemical form of the organic pollutants and the soil macro- and micronutrients.

- **Nutrient availability:** nutrient supplementation is very important during *in situ* bioremediation; typically nitrogen and phosphorous addition results in improvement in degradation rates (Beaudin *et al.*, 1999; Atlas *et al.*, 1992; Leavitt *et al.*, 1994).
- **External electron availability:** in many *in situ* bioremediation techniques, oxygen is required to enhance respiratory breakdown of organic contaminants. O₂ is supplied either by percolation of oxygen-enriched water, air sparging, bioventing or oxygenation of returned groundwater in “pump and treat” systems (Baker *et al.*, 1994; Lu, 1994; Pardick *et al.*, 1992).
- **Bioavailability of pollutants:** this is an important factor governing the rate of *in situ* bioremediation. Low water solubility and a tendency to adsorb to particulate matter in soils and sediments are limiting elements that can severely decrease the biodegradation of PAHs (Singleton, 1994). Polycyclic aromatic hydrocarbons are highly nonpolar compounds that have a low solubility in water and tend to adsorb strongly to organic matter in soils and sediments (Ramaswami *et al.*, 1997; Yeom *et al.*, 1998; Bellin *et al.*, 1990).

The microenvironment of soil biofilm systems was described by Battaglia *et al.* (1992). PAH contaminated soils are usually made up of individual sand grains, aggregates of finer particles and pockets of non-aqueous phase PAHs (NAPLs). A film of bacteria usually surrounds them. The *in situ* biodegradation occurs when a PAH diffuses into the

biofilm where the bacteria are located, either from the NAPL or from the soluble PAHs; as PAHs are degraded, more PAH will solubilize and diffuse into the biofilm in order to maintain equilibrium. As pointed out before, the slow release of contaminants into the aqueous phase may limit the bioremediation (Ramaswami *et al.*, 1997; Yeom *et al.*, 1998).

2.3.2 Porous Media Biofilms

The formation of biofilms has long been recognized as an important mechanism of interaction between porous media and biological processes. Biofilm has been defined as an organic material consisting of microorganisms embedded in a polymer matrix of their own making, called extracellular polymeric substances (EPS) (Characklis *et al.*, 1990; Bishop, 1997).

In soil systems there is a large surface available for microorganisms that can either interact or attach to these surfaces, colonizing them and promoting their survival and growth. Viable cells find access to sorbed nutrients and increase their ability to grow and survive in changing environmental conditions.

Two interacting sets of factors influence the complex process of biofilm formation: 1) factors related to porous media characteristics and hydrodynamics and 2) microbiological factors. The individual processes that control the formation and persistence of biofilm, including adsorption, growth, attachment, desorption and detachment, are presented in

Figure 2.4 (Turner, 2000); these processes in turn are affected by hydrodynamic forces and transport processes in the porous media, including transport of unattached bacterial cells and growth-limiting nutrients (substrate), but also by the microbial community and liquid flow rate.

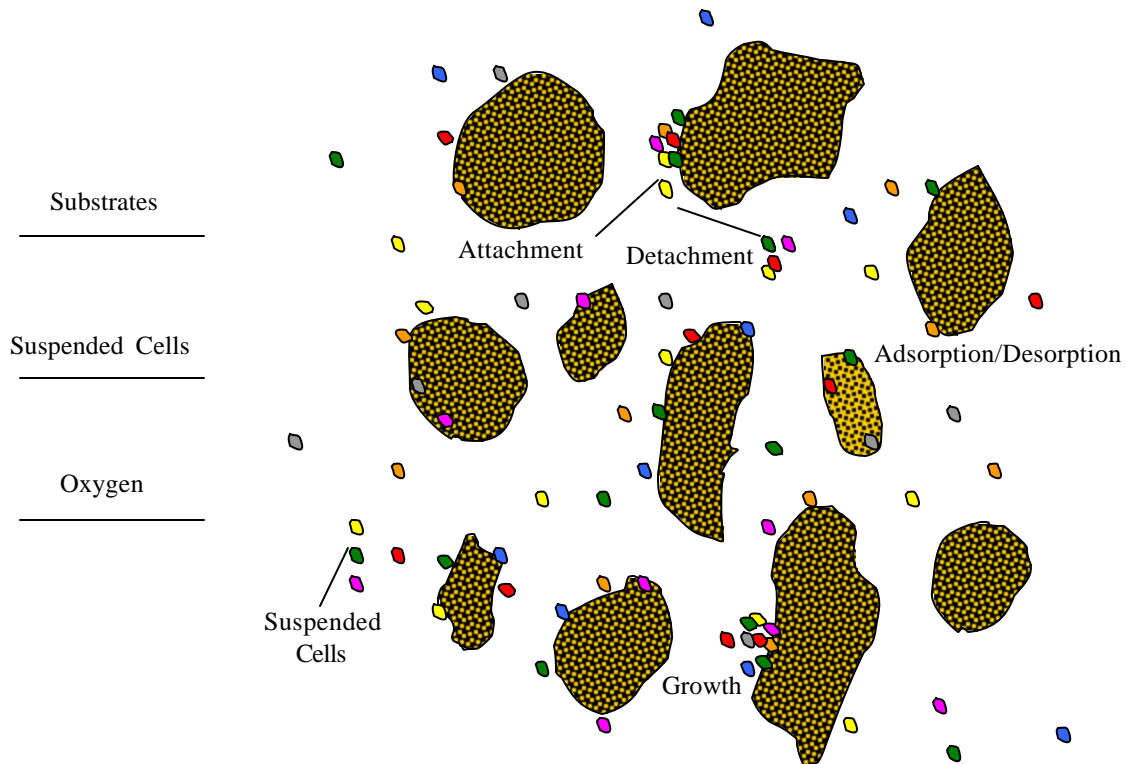


Figure 2.4 Biofilm processes in porous media (Turner, 2000).

Adsorption refers to the interphase accumulation or concentration of bacterial cells at the surface of soil particles. This process may be the result of physical forces (such as Van der Waals, hydrogen bonds, protonation, coordination bonds or water bridging) or chemical interactions (such as ionic or covalent bonding), or both. Growth describes the microbial processes that result in a bacterial reproduction and the production of

extracellular polymers. Attachment is the capture and/or entrapment of suspended bacterial cells from a biofilm into the surrounding fluid. Desorption is the reverse of adsorption and refers to the movement of cells from the interface back into the liquid phase; while attachment and detachment involve the movement of bacterial cells between biofilm and pore liquid, and adsorption and desorption refer the movement of cells between the soil particle surface and the fluid (Turner, 2000).

Biofilm structures vary with the utilized substrate (like glucose, acetate and methanol); however there are investigations that support the concept of continuous biofilm formation on the outer surfaces of the soil grain (Taylor *et al.*, 1990), which lead to the growth of layers of maximum thickness; this was later described as the “open pore” model for permeability reduction. Other studies (Vandevivere *et al.*, 1992a) suggest that bacterial aggregates develop in the pore spaces between coarse soil grains, giving sparse and heterogeneous coverage and limited exopolymer content. Mixed culture biofilm was developed in a simulated sandstone aquifer (Paulsen *et al.*, 1997) and showed a biofilm colonization at the beginning, followed by larger cell clusters, and finally development of a “bioweb” network of fibrillar strands, varying in size and shape depending on liquid flow velocity.

Preliminary studies in our lab (Ebihara *et al.*, 1997; Ebihara *et al.*, 1999) using soil columns for PAH biodegradation have determined the presence of continuous surface films on sand grains that are approximately 5 to 15 μm in thickness, but there are also a

variety of biological aggregate structures of 5 to 30 μm in diameter. A diagram of biofilm composition in terms of structure and morphology is shown in **Figure 2.5**.

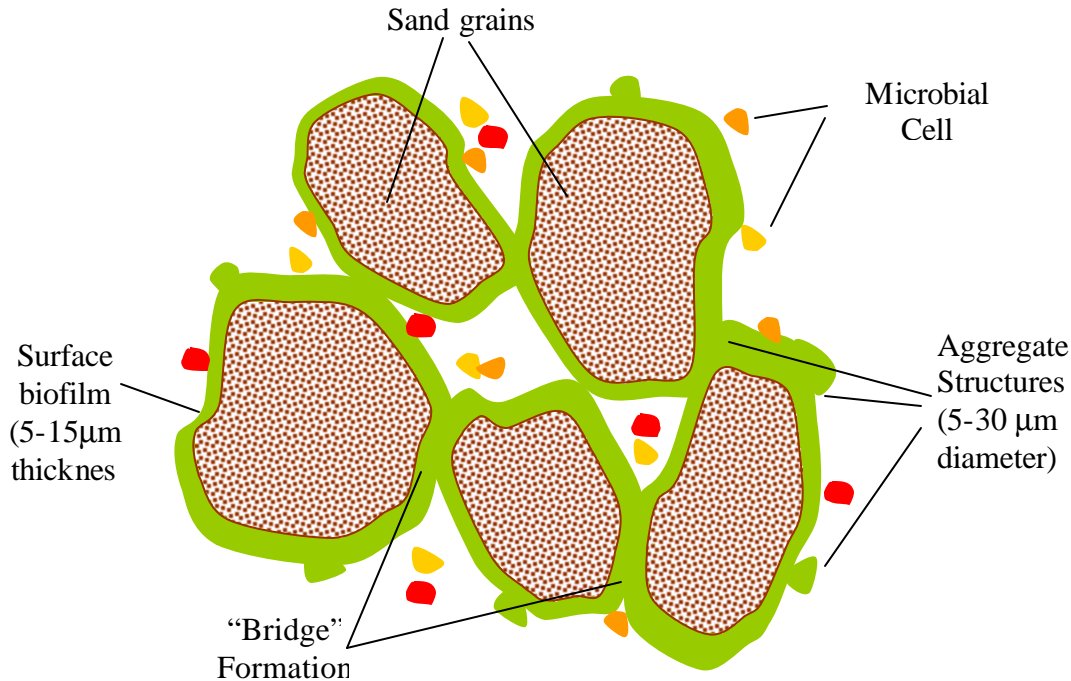


Figure 2.5 Biofilm structure and morphology.

There are different types of biofilm responses to the presence of PAHs, enhancing the degradative capabilities of the microbial communities; those are: 1) changes in community structure; 2) production of biosurfactants; 3) activation of solvent tolerance mechanisms and 4) changes in biofilm physical structure. All of them play important roles in the improvement of PAH bioremediation kinetics, including:

- **Changes in community structure:** this usually happens with the introduction of petroleum hydrocarbons, including PAHs, as the sole carbon source. A number of investigators (Cerniglia *et al.*, 1992) have reported the involvement of plasmids in the

biodegradation of different PAHs, showing the adaptation of a wide variety of microorganisms to utilize the PAH, due to higher plasmid transfer frequencies on solid surfaces.

- ***Production of biosurfactants:*** the availability of hydrophobic compounds as substrates for cell growth and energy is altered with their production by hydrocarbon degraders, such as bacteria, fungi or yeast (Lang *et al.*, 1987). These chemicals interact with the hydrocarbon-water interface to increase PAH availability for cell uptake and metabolism, by forming tiny droplets of hydrocarbons called micelles in aqueous suspensions. Several studies (Burd, 1996; Neu, 1996; Deziel, 1996) have shown the increased extent of PAH biodegradation and the prevention of flocculation, increasing the cell surface hydrophobicity and the affinity for the hydrocarbon phase.
- ***Activation of solvent tolerance mechanisms:*** when exposed to aromatic hydrocarbons, membrane damage or loss can occur, disrupting proton motive forces and barrier and protein functions. The production of phospholipids is a mechanism that prevents and compensates for this event, as shown by Pinkart *et al.* (1997), when using a solvent-tolerant strain of *Pseudomonas putida* which responded to the presence of xylene.
- ***Changes in biofilm physical structure:*** microbial communities have adaptive strategies in biofilm structure, cellular composition and spatial organization to facilitate utilization of recalcitrant organic compounds. No research is available with respect to PAHs; however it has been reported (Moller *et al.*, 1997) that different biofilm characteristics (such as cell density, biofilm thickness, cell morphology) can be observed when grown with several chlorinated compounds.

Extracellular polymeric substances (EPS) contained in the biofilm matrix play an important role in the biodegradation of PAHs, enhancing their bioremediation by 1) adsorbing PAHs from the aqueous environment, 2) reducing toxicity by sorbing heavy metals and 3) forming biological barriers that limit transport of PAHs:

- ***PAH sorption***: even though there are no reports concerning mechanisms of PAH sorption to biofilm EPS, several mechanisms are known to improve biodegradation or decrease contaminant transport: a) incorporation of PAH micelles, b) sorption of PAH containing particulates, and c) sorption of organic matter containing PAH.
- ***Metal binding***: microbial cells have interactions with a variety of trace metals for nutritional uptake, but they also have the capacity to bind a wide range of metallic ions, due to complexation to anionic organic ligands of EPS (Lion *et al.*, 1988). Metal binding occurs in bacterial cell walls with metals like copper, cobalt, iron, nickel, lead and zinc, and the functional groups responsible for metal binding include phosphoryl, carboxyl, sulfhydryl, and hydroxyl groups of membrane proteins, lipids, peptidoglycans and teichoic acids. A reduction in the toxicity has also been found to occur (Lion *et al.*, 1988), reflected by a free metal ion concentration decrease.
- ***Permeability reduction***: even though EPS formation could lead to clogging of treatment systems, other biological mechanisms, such as increases in cell number and chemical precipitates formed by byproducts of cellular activity, can improve bioremediation. While reducing hydraulic conductivity, a microbial barrier is formed, containing the movement of a contaminant plume.

2.4 INFLUENCE OF SURFACTANT ADDITION ON PAH BIODEGRADATION

Surfactants are compounds which possess both polar and nonpolar regions on the same molecule, forming spherical micelles (colloidal-size clusters) in solution (Cross, 1986; Haigh, 1996). It is the formation of micelles in solution that gives surfactants their excellent detergency and solubilization properties. For micellar solubilization of hydrophobic compounds such as PAHs, the surfactant concentration must be greater than the critical micellar concentration (CMC), value at which the surface-active molecules do not exist as monomers, but as aggregates with hydrophobic groups located at the center of the cluster and hydrophilic groups towards the solvent. However, solubilization is a function of the surfactant nature, solute, temperature, ionic strength, concentration, surfactant-soil interactions and time of contact between the contaminant and soil (Guha and Jaffe, 1996; Li and Chen, 2002).

Use of surfactants has been suggested as a means to increase the availability of sorbed contaminants, by lowering surface tension and increasing desorption and solubility (Mueller *et al.*, 1989; Backhus *et al.*, 1997). Most of the available studies have reported contradictory results concerning the influence of surfactants on PAH biodegradation. On one hand, some studies suggested enhanced effects, showing a significant increase in both the rate and the extent of mineralization of the hydrocarbons (Aronstein *et al.*, 1993; Churchill *et al.*, 1995; Allen *et al.*, 1999). Marquez-Rocha *et al.* (2000) showed improved biodegradation efficiencies of phenanthrene (from 64 to 76%), pyrene (from 40

to 74%) and anthracene (from 62 to 78%), by using Tween 40 surfactant. Biodegradations of three to seven-ring PAHs, in the presence of Brij 35 and Tergitol NP-10, were also tested by Boonchan et al.(1998); in all cases, it was evident that the overall biodegradation rate increased by 30% and the lag period normally seen for PAH degradation decreased. In the Kim *et al.* (2001) study, phenanthrene and naphthalene biodegradations were enhanced (occurred in less than 60 h) by utilizing Brij, which was reported to be easily biodegradable, and may have induced the coupled biodegradation of the PAHs.

On the other hand, some studies reported inhibitory effects, in which the presence of surfactant micelles slowed degradation. This has been explained by toxicity caused by the surfactants, interfering with cellular processes, surfactant degradation that may compete with PAH degradation, and the diversity of microbial populations that may lead to different outcomes. Doong and Lei (2003) reported the inhibition of *Pseudomonas putida* growth and the decrease of the mineralization rate of pyrene, by using Brij 35 and Tween 80 surfactants. Another study (Laha and Luthy, 1991) showed the inhibition of phenanthrene by nonionic surfactants, explained by micellization and the resultant decrease in available equilibrium free phenanthrene concentration to degrading microorganisms. Similar results have been shown by several authors (Thiem, 1994; Aronstein *et al.*, 1991; Putcha and Domack, 1993).

Overall, surfactants can be seen as potentially useful for aiding bioremediation of PAH-contaminated sites if these issues such as variable biodegradability can be resolved.

2.5 REFERENCES

Agency for Toxic Substances and Disease Registry (ASTDR), (1995), "Toxicological profile for polycyclic aromatic hydrocarbons", Atlanta, GA, U.S. Department of Health and Human Services, Public Health Service.

Allen, C., Boyd, D., Hempenstall, F., Larkin, M.J., Sharma, N., (1999), "Contrasting effects of a nonionic surfactant on the biotransformation of polycyclic aromatic hydrocarbons to cis-dihydrodiols by soil bacteria", *Appl. Environm. Microb.*, **65**, 1335-1339.

Aprill, W., Sims, R.C., Sims, J.L., Matthews, J.E., (1990), "Assessing detoxification and degradation of wood preservatives and petroleum wastes in contaminated soil", *Wast. Manag. & Research*, **8**, 46-65.

Aronstein, B.N., Calvillo, Y.M., Alexander, M., (1991), "Effect of surfactants at low concentrations on the desorption and biodegradation of sorbed aromatic compounds in soil", *Env. Science. Techn.*, **25**, 1728-1731.

Aronstein, B.N., Alexander, M., (1993), "Effect of a non-ionic surfactant added to the soil surface on the biodegradation of aromatic hydrocarbons within the soil", *Appl. Microbiol. Biotechn.*, **39**, 386-390.

Backhus, D., Picardal, F.W., Johnson, S., Knowles, T., Collins, R., Radue, A., Kim, S., (1997), "Soil- and surfactant- enhanced reductive dechlorination of carbon tetrachloride in the presence of *Shewanella putrefaciens* 200", *Journ. Contam. Hydrol.*, **28**, 337-361.

Bailey, A.M., Coffey, M.D., (1986), "Characterization of microorganisms involved in accelerated biodegradation of metaxyl and metolachlor in soils", *Can. J. Microbiol.*, **32**, 562-567.

Baker, K., Herson, D.S., (1994), "Microbiology and Biodegradation in Bioremediation", Baker, K. and Herson, D.S. Eds, Mc Graw-Hill, New York, pp 9-60.

Battaglia, A., Morgan, D.J., (1992), "Application of the GRI Accelerated treatability protocol to contaminated soils from manufactured gas plant sites", *Hydrocarbon Contaminated Soils*, Kostecki, P.T, Calabrese, E., Bonazountas, Eds., Lewis Publishers, II, Boca Raton, pp. 257-278.

Beaudin, N., Caron, R.F., Legros, R., Ramsay, J., Ramsay, B., (1999), "Identification of the key factors affecting composting of a weathered hydrocarbon-contaminated soil", *Biodegradation*, **10**, 127-133.

Bellin, C.A., O'Connor, G.A., Jin, Y., (1990), "Sorption and degradation of pentachlorophenol in sludge-amended soils", *J. Env. Qual.*, **19**, 603-608.

Bishop, P.L., Zhang, T., (1995), "Effect of biofilm structure, microbial distributions and mass transport on biodegradation processes", *Wat.Sci.Techn.*, **31**, 179-185.

Bishop, P.L., (1997), "Biofilm structure and kinetics", *Wat.Sci.Techn.*, **36**, 287-294.

Bishop, P.L., (2000), "Pollution Prevention: fundamentals and practice", McGraw-Hill Series Eds., pp. 114-117.

Blackburn, J.W., Hafker, W.R., (1993), "The impact of biochemistry, bioavailability and bioactivity on the selection of bioremediation techniques", *Trends Biotechn.*, **11**, 328-333.

Boldrin, B., Tiehm, A., Fritzsche, C., (1993), "Degradation of phenanthrene, fluorene, fluoranthrene, and pyrene by a *Mycobacterium* sp.", *Appl.Env.Microbiol.*, **59**, 1927-1930.

Boonchan, S., Britz, M.L., Stanley, G.A., (1998), "Surfactant-enhanced biodegradation of high-molecular weight polycyclic aromatic hydrocarbons by *Stenotrophomonas maltophilia*", *Biotechnol&Bioengin.*, **59**(4), 482-494.

Bouchez, M., D. Blanchet, V. Bardin, F. Haeseler, J.P. Vandecasteele 1999. "Efficiency of defined strains and of soil consortia in the biodegradation of polycyclic aromatic hydrocarbons (PAH) mixtures", *Biodegradation*, **10**, 429-435.

Bradford, M.L., Krishnamoorthy, R., (1991), "Consider bioremediation for waste site cleanup", *Chem.Eng.Prog.*, **87**(2).

Burd, G., Ward, O., (1996), "Involvement of surface-active high molecular weight factor in degradation of polycyclic aromatic hydrocarbons by *Pseudomonas marginalis*", *Canadian Journal of Microbiology*, **42**, 791-797.

Calabrese, E., Kostechi P.T., (1988), "Public Health implications of soils contaminated with petroleum products", *Soils Contaminated by Petroleum*, Calabrese, E., Kostechi, P.T., Fleischer, J., Eds., John Wiley & Sons, New York, pp. 191-229.

Cerniglia, C.E., (1992), "Biodegradation of polycyclic aromatic hydrocarbons", *Biodegradation*, **3**, 351-368.

Cerniglia, C.E., (1993), "Biodegradation of polycyclic aromatic hydrocarbons", *Current Opinion in Biotechnology*, **4**, 331-338.

Characklis, W.C., Marshall, K.C., (1990), "Biofilms: a basis for an interdisciplinary approach", in *Biofilms*, Characklis, W.C. and Marshall, K.C., Eds., New York, Wiley, pp. 3-15.

Churchill, P., Dudley, R., Churchill, S., (1995), "Surfactant-enhanced bioremediation", *Wast.Managem.*, **15**(5/6), 371-377.

Corbitt, R.A., (1990), "Standard handbook of Environmental Engineering", Corbitt Eds., Mc Graw-Hill, New York.

Cross, (1986), "Nonionic surfactants: chemical analysis (Surfactant Science Series)", Vol.19, Marcel Dekker, Inc. New York.

Dean-Ross D., J.Moody, C.E. Cerniglia 2002. " Utilization of mixtures of polycyclic aromatic hydrocarbons by bacteria isolated from contaminated sediment", *Microb. Ecolog.*, **41**, 1-7.

Deziel, E., (1996), "Biosurfactant production by a soil *Pseudomona* strain growing on polycyclic aromatic hydrocarbons", *Appl. & Env.Microbiol.*, **62** (6), 1908-1912.

Doong, R, Lei, W., (2003), "Solubilization and mineralization of polycyclic aromatic hydrocarbons by *Pseudomonas putida* in the presence of surfactant", *J.Hazard.Mater.*, **B96**, 15-27.

Dorn, E., Knackmuss, H.J., (1978), "Chemical structure and biodegradability of halogenated aromatic compounds", *Biochemical J.*, **174**, 73-83.

Ebihara, T., Bishop, P.L., (1997), "Examination of biofilms utilized in bioremediation of organic compounds using confocal scanning microscopy techniques", *Superfund Basic Research Program Conference: a decade of improving health through multi-disciplinary research*, Chapel Hill, NC.

Ebihara, T., Bishop, P.L., (1999), "Biofilm structural forms in porous media utilized in organic compounds degradation", *Wat.Sci.&Techn.*, **39**(7), 203-210.

EPA, (2001), "Superfund Annual Report to Congress", <http://www.epa.gov/superfund/accomp/sarc/index.htm>

Gannon, J.T., Mingelgrin, U., Alexander, M., Wagner, R.J., (1991), "Bacterial transport through homogeneous soil", *Soil Biol.Biochem.*, **23**(12), 1155-1160.

Guha, S., Jaffe, P., (1996), "Biodegradation kinetics of phenanthrene partitioned into the micellar phase of ionic surfactant", *Env.Sci.&Techn.*, **25**(30), 605-611.

Guo, J., (1998), "Biodegradation kinetics of polycyclic aromatic hydrocarbons in soil slurry and sand column reactors", *Chemical Engineering*, University of Cincinnati, Cincinnati, (OH), 82.

Haigh, S., (1996), "A review of the interaction of surfactants with organic contaminants in soil", *Sci.Tot.Environm.*, **185**, 161-170.

- Hinchee, R.E., Miller, R. N., Johnson, P.C., (1995), "In situ aeration: air sparging, bioventing and related remediation processes", Battelle Press, Columbus, OH.
- Huysmans, K.D., Frankenburger, W.T., (1991), "Evolution of trimethylarsine by *penicillium sp.* Isolated from agricultural evaporation pond water", *Sci.Total Env.*, **105**, 13-28.
- Johnson, C., Scow, K, (1999), "Effect of nitrogen and phosphorous addition on phenanthrene biodegradation in four soils", *Biodegradation*, **10**, 43-50.
- Kim, I., Park, J., Kim, K., (2001), "Enhanced biodegradation of polycyclic aromatic hydrocarbons using nonionic surfactants in soil slurry", *Appl.Geochem.*, **16**, 1419-1428.
- Laha, S., Luthy, R.G., (1991), "Inhibition of phenanthrene mineralization by nonionic surfactants in soil-water systems", *Env.Sci.Tecn.*, **25**, 1920-1930.
- Lang, S., Wagner, F., (1987), "Structure and properties of biosurfactants", *Biosurfactants and Biotechnology*, **25**, 21-45.
- Leavitt, M.E., Brown, K.L., (1994), "Biostimulation versus bioaugmentation-three case studies, in *Hydrocarbon Bioremediation*, Hinchee, R.E., Alleman, B.C., Hoeppe, R.E., Miller, R.N. Eds, CRC, Boca Raton, FL, pp. 323-328.
- Li, J.L., Chen, B.H., (2002), "Solubilization of model polycyclic aromatic hydrocarbons by nonionic surfactants", *Chem.Eng.Sci.*, **57**, 2825-2835.
- Lu, C.J., (1994), "Effects of hydrogen peroxide on the *in situ* biodegradation of organic chemicals in a simulated groundwater system", in *Hydrocarbon Bioremediation*, Hinchee, R.E., Alleman, B.C., Hoeppe, R.E., Miller, R.N. Eds, CRC, Boca Raton, FL, pp. 140-147.
- Mahro, B., Schaefer, G., (1994), "Pathways of microbial degradation of polycyclic aromatic hydrocarbons in soil", *Bioremediation of chlorinated and polycyclic aromatic hydrocarbons*, Hinchee R., Leeson, A., Semprini, L., Ong S., Lewis Publishers, Boca Raton, pp. 203-217.
- Márquez-Rocha, F., Hernández-Rodríguez, V., Vázquez-Duhalt, R., (2000), "Biodegradation of soil-adsorbed polycyclic aromatic hydrocarbons by the white rot fungus *Pleurotus ostreatus*", *Biotechn.Lett.*, **22**, 469-472.
- McClennen, W., Arnold, N., Roberts, K., Meuselaar, H., Lighty, J., Lindgren, E., (1990), "Fast, repetitive GC/MS analysis of thermally desorbed polycyclic aromatic hydrocarbons from contaminated soil", *Combust.Sci.&Techn.*, **74**, 297-309.

- McNally, D., J.R. Mihelcic, D. Luenking 1999. "Biodegradation of mixtures of polycyclic aromatic hydrocarbons under aerobic and nitrate-reducing conditions", *Chemosphere*, **38**(6), 1313-1321.
- Menzie, C.A., Potocki, B., Santodonato, J., (1992), "Exposure to carcinogenic PAHs in the environment", *Env.Sci.&Techn.*, **26**, 1278-1283.
- Merck &Co. (1996), *The Merck Index*, Whitehouse Station, NJ., Merck &Co., Inc.
- Mueller, J.G., Chapman, P.J., Pritchard, P.H., (1989), "Creosote-contaminated sites", *Env.Sci.&Techn.*, **23**, 1197-1201.
- Neu, T., (1996), "Significance of bacterial surface-active compounds in interaction of bacteria and interface", *Microbiol. Reviews*, **60** (1), 151-166.
- Novotny, C., Erbanova, P., Sasek, V., Kubatova, A., Cajthaml, T., Lang, E., Krahl, J., Zadrazil, F., (1999), "Extracellular oxidative enzyme production and PAH removal in soil by exploratory mycelium of white rot fungi", *Biodegradation*, **10**, 159-168.
- Pardick, D.L., Bouwer, E.J., Stone, A.T., (1992), "Hydrogen peroxide use to increase oxidant capacity for *in situ* bioremediation of contaminated soils and aquifers: a review", *J. Contaminant Hydrol.*, **9**, 221-227.
- Park, K.S., Sims, R.C., Dupont, R.R., (1990), "Transformation of PAHs in soil systems", *J. Environm.Engin.*, **116**(3), 632-640.
- Park, K.S., Sims, R.C., Dupont, R.R., (1990), "The fate of PAHs compounds in two soil types influence of volatilization abiotic loss and biological activity", *Environm.Toxic.Chem.*, **9**(2), 187-196.
- Paulsen, J., Oppen, E, Bakken. R., (1997), "Biofilm morphology in porous media: a study with microscopic and imaging techniques", *Wat.Sci.& Techn.*, **36**(1), 1-9.
- Pendrys, J.P., (1990), "The biodegradation of hydrocarbons by bacteria which excrete bioemulsifiers", *Gas, Oil&Coal Biotechn. II*, Atkins, C., and Smith, J. Eds, Institute of Gas Technology.
- Phothuluri, J., Cerniglia, C., (1998), "Current aspects of polycyclic aromatic hydrocarbons degradation processes", *Biodegradation Technology Developments*, Sikar, S., Irvine, R., Eds., Lancaster, Technomic publishing Co., Inc., II, pp.461-520.
- Pinkhart, H., White, D., (1997), "Phospholipid biosynthesis and solvent tolerance in *Pseudomonas putida* strains", *Journal of Bacteriology*, **179**(13), 4219-4226.
- Putch, R.V., Domack, M.M., (1993), "Fluorescence monitoring of polycyclic aromatic hydrocarbons biodegradation and effect of surfactants", *Environm.Progr.*, **12**, 81-85.

Ramaswami, A., Luthy, R.G., (1997), "Mass transfer and bioavailability of PAH compounds in coal tal NAPL-Slurry Systems. 1 Model Development", *Env.Sci.&Techn.*, **31**, 2260-2267.

Ramaswami, A., Luthy, R.G., (1997), "Mass transfer and bioavailability of PAH compounds in coal tal NAPL-Slurry Systems. 1 Experimental Evaluations", *Env.Sci.&Techn.*, **31**, 2268-2276.

Ryan, J.R., Loehr, R.C., Rucker, E., (1991), "Bioremediation of organic contaminated soils", *J.Hazard.Mat.*, **28**, 159-169.

Schneider, J., Grosser, R., (1996), "Degradation of pyrene, benzo[a]anthracene and benzo[a]pyrene by *Mycobacterium sp.* Strain RJGII. 135 isolated from a former coal gasification site", *Appl.Env.Microbiol.*, **62**, 13-19.

Schwartz, E., Scow, K., (2001), "Repeated inoculation as a strategy for the remediation of low concentrations of phenanthrene in soil", *Biodegradation*, **12**, 201-207.

Stelmack, P.L., Gray, M.R., Pickard, M.A., (1999), "Bacterial adhesion to soil contaminants in the presence of surfactants", *Appl.Env.Microbiol.*, **65**, 163-168.

Sutherland, J.B., Rafii, F., (1995), "Mechanisms of polycyclic aromatic hydrocarbon degradation", *Microbial Transformation and degradation of Toxic Organic Chemicals*, Young, L., Cerniglia, C., Wiley-Liss, New York, pp. 269-306.

Taylor, S., Jaffe, P., (1990), "Biofilm growth and the related changes in physical properties of a porous medium – 1. Experimental Investigation", *Wat.Res.Research.*, **26**(9), 2153-2159.

Thiem, A., (1994), "Degradation of polycyclic aromatic hydrocarbons in the presence of synthetic surfactants", *Appl.Envir.Microb.*, **60**, 258-263.

Tongpim, S., Pickard, M.A., (1996), "Growth of *Rhodococcus S1* on anthracene", *Can. J.Microbiol.*, **42**, 289-294.

Turner, P., (2000), "Biofilm in remediation of contaminated soils", in *Bioremediation of contaminated soils*, Wise, D., Trantolo, D., Cichon, E., Inrang, H. and Stottmeister, U. Eds, Marcel Dekker Inc., New York.

Vandevivere, P., Baveye, P., (1992), "Saturated hydraulic conductivity reduction caused by aerobic bacteria in sand columns", *Soil Science Society of America Journal*, **56**(1), 1-3.

Vecchioli, G., Constanza, O., Giorgieri, S., Remmler, M., (1997), "Extent of cleaning achievable by bioremediation of soil contaminated with petrochemical sludges", *J.Chem.Tech.Biotechn.*, **70**, 331-336.

Verstraete, W., Vanlooche, R., de Borjer, R., Verlinde, A., (1976), "Modelling of the breakdown and the mobilization of hydrocarbons in unsaturated soils layers", in Proceedings of the 3rd International Biodegradation Symposium, Applied Science, London, pp.99-112.

Yeom, I., Ghosh, M., (1998), "Mass transfer limitation in PAH-Contaminated Soil remediation", *Wat.Sci.& Techn.*, **37**(8), 111-118.

Yuan, S.Y., S.H. Wei, B.V. Chang 2000. "Biodegradation of polycyclic aromatic hydrocarbons in a mixed culture", *Chemosphere*, **41**, 1463-1468.

Yuan, S.Y., J.S. Chang, J.H. Yen, B.V. Chang 2001. "Biodegradation of phenanthrene in river sediment", *Chemosphere*, **43**, 273-278.

Zhang, W., Bouwer, E., (1997), "Biodegradation of benzene, toluene and naphthalene in soil-water slurry microcosms", *Biodegradation*, **8**, 167-175.

Chapter 3

RESEARCH MATERIALS AND METHODS

3.1 INTRODUCTION

This chapter presents the details of the experimental setup used in this study. The first part includes a full description of sand column reactors utilized in each series of experiments. In addition, it also provides information on the chemicals and specific reagents, as well on the composition of the mineral salt solution, co-substrates solution and PAH solution generation, which remained constant in all the phases of the operational work.

The second part provides a complete description of the analytical methods, procedures and instruments for the identification and quantification of all compounds of interest. Certain procedures that were specific for a particular set of experiments or unique conditions will be further included in the methodology section of the corresponding chapter.

3.2 EXPERIMENTAL DESIGN AND SETUP

Lab-scale reactors simulating a sandy contaminated aquifer were used to support the growth of biological film capable of degrading the PAHs. The experimental setup resembled an *in situ* bioremediation system, based on the idea of a bio-barrier.

Four identical, lab-scale reactors were constructed from 32-cm long by 3.8-cm diameter glass columns (Custom Glassblowing of Louisville Inc., Louisville, KY). **Figure 3.1** provides a schematic diagram of the sand column system, and a photograph is available in **Appendix A**. The reactors were equipped with ten (10) sample ports along the length of the column to allow for sampling. Six outlet ports on one side were used for liquid sampling of the influent and the pore water at five different depths along the column (5, 10, 15, 20 and 25 cm). The four on the other side were utilized for liquid and solid sampling (7.5, 12.5, 17.5 and 22.5 cm), which consisted of specially designed and attachable flow cell ports, that simulated the conditions within the column and were used for biofilm growth examination. Flow cells consisted of a small Nylon channel (volume: 1.68 cm³ and cross-sectional area: 0.48 cm²) with removable glass cover plates and were filled with the sand media. Biofilm in the flow cells represented the biofilm within the column at the same depth, with the advantage that it could be directly examined without disturbing the soil column. A schematic of a flow cell is shown in **Figure 3.2**.

The soil used to fill the column was sand, so that the effects of sorption of the PAHs by organics in the soil were reduced. The media selected for biofilm growth was rounded

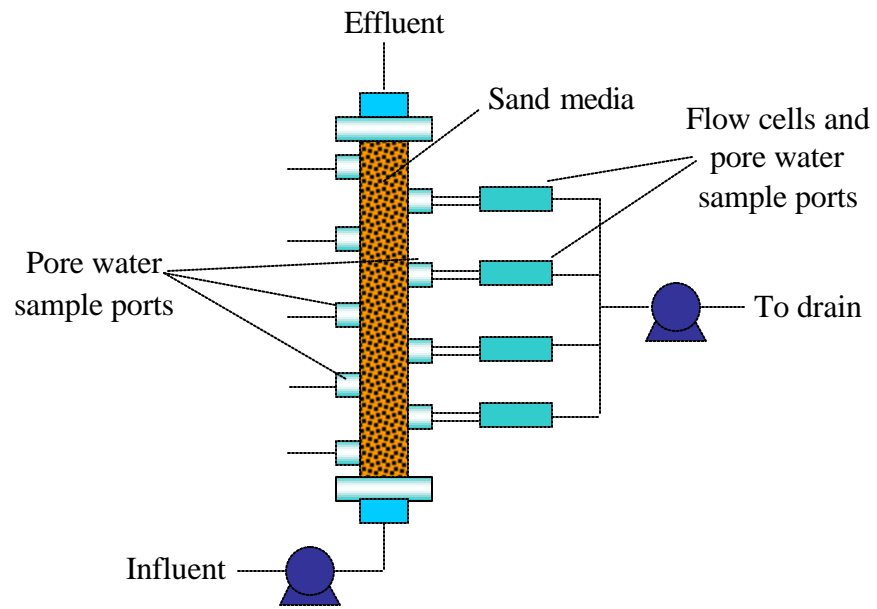


Figure 3.1 Schematic diagram of sand column

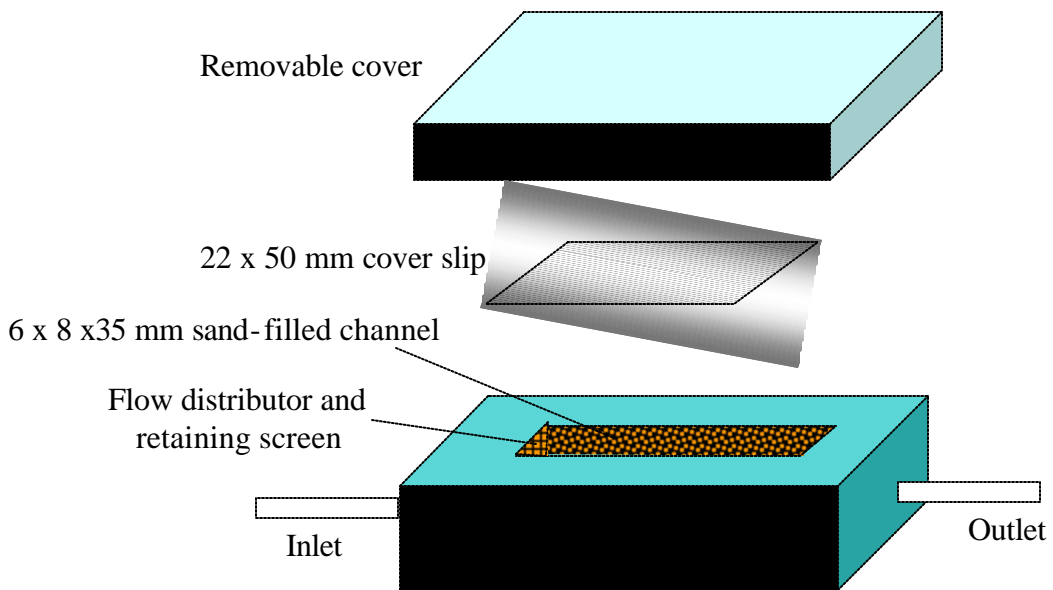


Figure 3.2 Flow cell detail.

fine-to-medium silica sand (ASTM graded sand, C-190) of approximately 0.38 mm median grain size and an effective porosity of 0.44. Sieve analyses were performed to describe in detail the size distribution of the sand, and are available in **Appendix B**.

A nutrient solution was combined with a saturated PAH solution and pumped in an up-flow manner, so that air bubble entrainment was prevented. Due to the diverse range of aqueous solubilities of the compounds used, an alternative method of dissolved PAH generation was adopted through use of feed generation columns; sufficient contact time for feed solution components was allowed in the generating columns to achieve the desired feed PAH concentrations. Details on the PAH generation columns are provided in the correspondent chapter.

Linear pore water velocity through the soil column and the flow cells was maintained at 5 m/d, in order to simulate groundwater flow conditions. A 1-100 rpm MasterFlex pump with LS/14 pump heads (Cole-Parmer Instrument Company, Vernon Hills, IL) operating at a rate of 2.03 mL/min (2.93 L/d) was utilized for the columns, as well as an Ismatec cassette pump (Cole-Parmer Instrument Company, Vernon hills, IL) used to control the liquid flow rate through each flow cell, at approximately 4.4 mL/hr (0.106 L/d).

Sodium acetate solution (10 mg/L) was used in the system for development and enhancement of biofilm; it was continuously injected at the inlet of the column by a syringe pump at a flow rate of 0.25 mL/hr. Aerobic conditions in the reactors were always maintained in the reactors with the aid of a small dose of hydrogen peroxide

solution (3.5%); it was also injected at a rate of 0.25 mL/hr by a syringe pump. Killed control columns were operated simultaneously and at the same conditions as the main columns and were used as a measurement of physical-chemical adsorption mechanisms of contaminants to the sand medium; sodium azide (1 g/L) was added into the system to minimize biomass growth using a syringe pump at 0.25 mL/hr. All columns were operated at room temperature. **Figure 3.3** shows the experimental setup of the system, and a photograph is available in **Appendix A**.

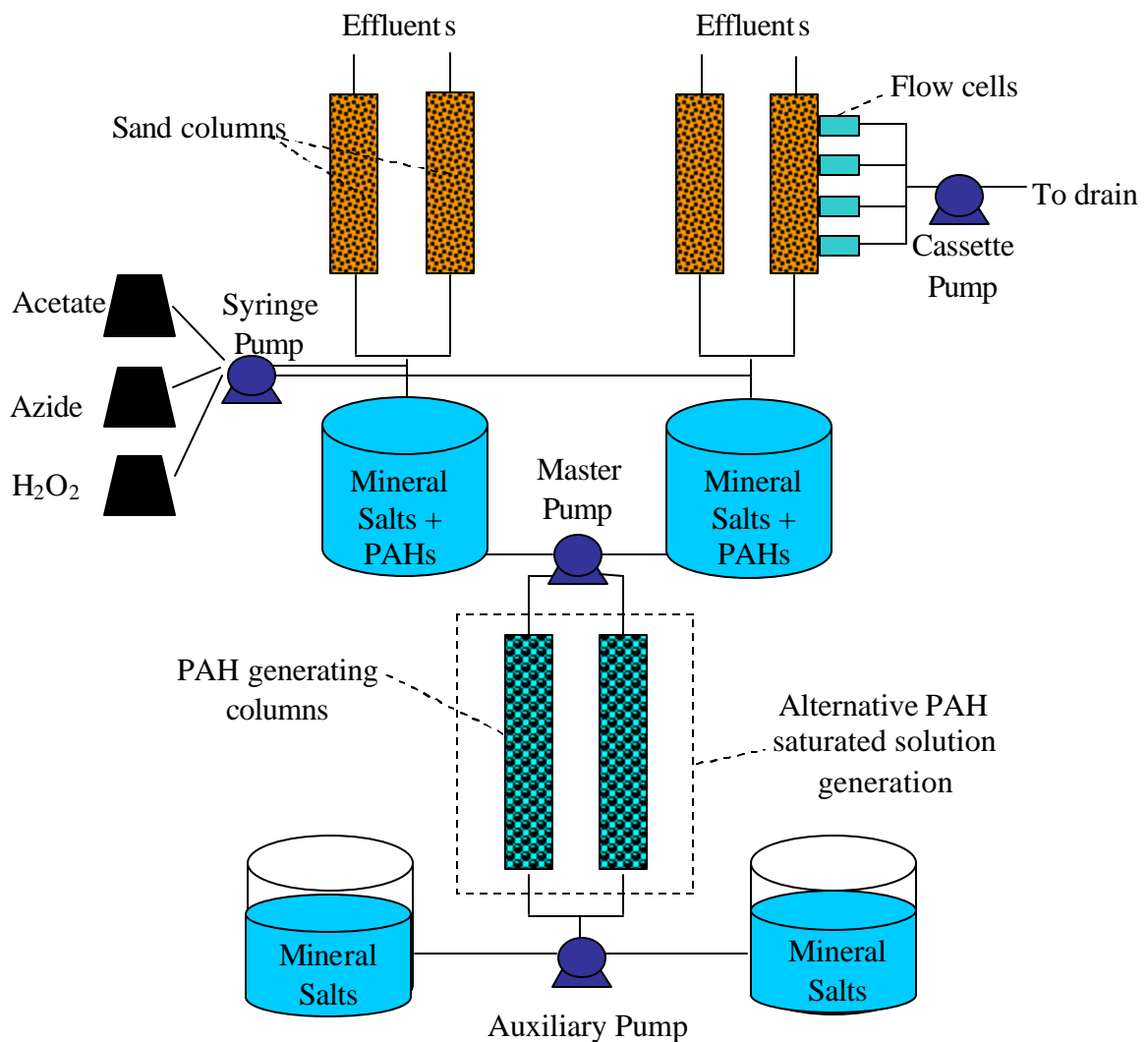


Figure 3.3 Experimental setup of the system.

The enrichment culture for inoculating the soil column was started with a mixed liquor sample from an aeration tank, taken from a domestic wastewater treatment plant (Polk Run WWTP, Cincinnati, OH). The sample was vortexed in centrifuge tubes, and the supernatant containing biomass was collected and mixed as slurry with the soil media. The soil column was slurry-packed to ensure uniform distribution of the inoculum and to minimize subsequent settlement of soil media and entrapment of air bubbles within the media bed. The column was operated for 6 weeks with acetate as a primary substrate, prior to PAH addition, in order to develop a suitable biofilm.

3.3 FEED AND NUTRIENT SOLUTIONS

Feed and nutrient solutions were kept in separate tanks and were fed into the columns by Teflon® lines, to prevent any loss of PAHs due to volatilization or adsorption, during transport. A detailed description of the feed composition is provided in each chapter, as pertaining to that phase of the study. The nutrient solution consisted of essential nutrient salts and excess nitrate so that nutrient and electron acceptor concentrations were not limiting biological growth and activity. The composition of the macronutrients and micronutrients in the nutrient solution is listed in **Table 3.1**.

3.4 CHEMICALS

All chemicals were analytical reagent grade and were purchased from Aldrich (Sigma-Aldrich) (Milwaukee, WI) and Fischer Scientific (Fair Lawn, NJ). All dilutions of these

Table 3.1 Nutrient solution composition.

MACRONUTRIENTS		MICRONUTRIENTS	
Compound	Concentration (mg/L)	Compound	Concentration (mg/L)
NaNO ₃	32	MnSO ₄ .H ₂ O	0.0112
NH ₄ Cl	10	CuSO ₄	0.0007
KH ₂ PO ₄	10	Na ₂ MoO ₄ .2H ₂ O	0.0004
MgSO ₄ .7H ₂ O	3.8	ZnSO ₄ .7H ₂ O	0.012
CaCl ₂ .2H ₂ O	1.4	CoCl ₂ .6H ₂ O	small crystal
FeCl ₃ .6H ₂ O	0.65		
Na ₂ HPO ₄ .7H ₂ O	40		

chemicals were prepared with Milli-Q reagent-grade water (18.2 M Ω -cm), generated by a Milli-Q system (Millipore Inc., Amherst, MA).

3.5 ANALYTICAL METHODS

An overview of the analytical methods used in the different experimental studies is presented in this section. Detailed description of the laboratory procedures are provided in **Appendix C**.

3.5.1 Acetate

Acetate determinations were made using a Dionex DX-120 Ion Chromatography apparatus equipped with two anion columns (AG14-4 and AS14-4) and conductivity detector. Concentrations were based on an acetate standard curve. The detection limit for analysis was approximately 1 mg/L.

3.5.2 Bacterial Viability

The LIVE/DEAD BacLight® bacterial viability kit (Molecular Probes, Eugene, OR) provided a two color fluorescence assay of bacterial viability. Samples were stained with 3 µL/mL fluorescent stain, composed of equal volumes of SYTO 9® and propidium iodide (PI); their excitation/emission maximas were 480/500 nm and 490/635 nm for SYTO and PI, respectively. A Zeiss LSM 510 scanning confocal laser microscope (CLSM) with an upright scope (Carl Zeiss Inc., Thornwood, NY) was used to observe not only the bacterial viability, but also the physical structure, heterogeneity and growth patterns of biofilm in the flow cells.

3.5.3 Carbohydrates

Total carbohydrates were determined by the phenol reaction method of Daniels et al. (1994). Wet sand (0.2 to 0.5 g per sample) was mixed with 1 mL MilliQ water, phenol and sulfuric acid. The absorbances at 488 nm were compared to a glucose calibration standard curve to determine the carbohydrate mass/dry sand mass, using a HACH Portable Datalogging Spectrophotometer DR 2010 (HACH Company, Loveland, CO). The detection limit for this analysis was approximately 1 mg/L.

3.5.4 Dissolved Oxygen (DO)

Dissolved oxygen (DO) was measured by using a MI-730 Micro-Oxygen Electrode with an OM-4 Oxygen Meter (Microelectrodes, Inc. Bedford, NH). Calibration of the microelectrode was performed using pure nitrogen (0% oxygen), 5% oxygen, 10% oxygen and medical air (21% oxygen).

3.5.5 Lipid-Phosphates

Viable biomass was measured by lipid phosphate analysis, using a modified method of Findlay et al. (1989). Sodium chloride (343 mg/L) was added to wet sand (0.2 to 0.5 g per sample), and 2 mL were taken before they were transferred to a new reaction vial, in order to quantify firmly and loosely attached biomass. Samples were extracted with chloroform and methanol, digested with potassium persulfate and dyed with malachite green. The absorbances at 610 nm were compared to a potassium phosphate calibration standard curve to determine the moles/dry sand mass, using a HACH Portable Datalogging Spectrophotometer DR 2010 (HACH Company, Loveland, CO). Total LP varies with microbial strain, but it is an indication of total viable cell mass at approximately 100 μmol LP per g of dry cell weight (White et. al, 1997). The detection limit for this analysis was approximately 0.5 nmol/ampule.

3.5.6 Optical Density (OD)

Optical density measurements were obtained for cell growth analysis. Optical density was measured at 600 nm of absorbance, using a Hewlett-Packard 8345 Diode Array Spectrophotometer.

3.5.7 Polycyclic Aromatic Hydrocarbons

PAH samples (Chapters 4 and 5) were analyzed using a Hewlett-Packard 5890 Gas Chromatograph (GC), equipped with a Flame Ionization Detector (FID) and a Supelco PTA-5 column (30 m length, 0.53 mm ID) (Bellefonte, PA). The column temperature profile during analysis was 50°C for 1 minute, 12 minute ramp to 180°C and then maintained at 180°C for 2 minutes. The injection port and FID temperatures were 250°C and 300°C, respectively. The carrier gas was pre-purified helium, while the FID gases were hydrogen, air and helium (make-up gas). Triplicate samples of 2 mL each were taken from each sample port and extracted with methylene chloride at a ratio of 1:1 (low-molecular-weight PAHs) and of 4:1 (high-molecular-weight PAHs). The samples were compared to a six point standard curve to determine the PAH concentration. The detection limits were approximately 30 µg/L for naphthalene, 10 µg/L for phenanthrene and 10 µg/L for pyrene.

PAH samples (Chapter 6) were analyzed using an Agilent 1100 High Liquid Pressure Chromatograph (HPLC), equipped with a diode array detector. The column used was

Supelcosil LC-18 DB (150 x 4.6 mm) (Bellefonte, PA), with packing material size of 5 μm . An isocratic mobile phase consisting of 40% Milli-Q water and 60% acetonitrile was used to elute the PAH compounds. The flowrate was maintained at 2 mL/min, and the detection limit were approximately 50 $\mu\text{g/L}$ for naphthalene and 50 $\mu\text{g/L}$ for phenanthrene.

3.5.8 pH

Due to the small volume of sample, the pH was measured by using pHydrion Papers 7-11 (Micro Essential Laboratory, Brooklyn, NY).

3.5.9 Proteins

Protein concentrations were determined using the Coomassie® Plus Protein Assay Reagent (#23236) (Pierce Biotechnology, Rockford, IL.). Wet sand (0.2 to 0.5 g per sample) was mixed with MilliQ water and the reagent, and sonicated for 10 minutes. The absorbances at 595 nm were compared to a bovine serum albumin calibration standard curve to determine the protein mass/dry sand mass, using a HACH Portable Datalogging Spectrophotometer DR 2010 (HACH Company, Loveland, CO). The detection limit for this analysis was approximately 1 mg/L.

3.5.10 Triton X-100

Triton X-100 samples were analyzed using an Agilent 1100 High Liquid Pressure Chromatograph (HPLC), equipped with a diode array detector. The column used was Supelcosil LC-18 DB (150 x 4.6 mm) (Bellefonte, PA), with packing material size of 5 μm . An isocratic mobile phase consisting of 40% Milli-Q water and 60% acetonitrile was used to elute the compound. The flowrate was maintained at 2 mL/min and the detection limit were approximately 50 $\mu\text{g/L}$.

3.5.11 Volatile Solids

Volatile solids analyses were performed according to Standard Methods (1998). Wet sand (0.5 to 1.0 g per sample) was dried for 1 hour at 550°C and compared to dry solids for another hour at 105°C. Volatile solids included all biological solids (biomass, protein, carbohydrates and other cellular organic carbon).

3.6 OTHER RESEARCH TOOLS

3.6.1 Flow cells

Flow cells (**Figure 3.2**) were designed and developed in our lab (Ebihara et al., 1997; Ebihara et al., 1999) in order to conduct microscopic soil biofilm examinations, minimizing disturbance to the delicate structures present under laminar flow encountered

in typical *in situ* bioremediation environments. The following criteria were followed during the design of the flow cell: 1) uniform flow distribution across the flow cell cross-section, 2) ability to effectively apply fluorescent stains for examination of three-dimensional microbial cell distributions, 3) preservation of the delicate biofilm growth structures and 4) ability to replicate bulk sand column environmental conditions.

3.6.2 Confocal Scanning Laser Microscopy (CSLM)

Confocal Scanning Laser Microscopy is a technique developed in the 1960s (Minski, 1988), but it was not until the 1980s that researchers started using it in association with several key technologies such as optics, lasers, fluorescence markers, detectors and digital image analysis systems (Inoue, 1995). It can be used to visualize the three-dimensional structure of biofilm growth and microbial cell distributions with a particular fluorophore that is applied to the sample. For this, the sample is illuminated with light at a special wavelength and subsequently emits light at a different wavelength than the illumination source. The emitted light, filtered to obtain only light at the wavelength of the emission maxima, is guided to a photomultiplier tube and recorded as an intensity measurement.

Several biofilm studies have been reported to have used CSLM as a routine tool (Lichtman, 1994; Shotton et al., 1989; Laurent et al., 1994), showing diverse advantages, such as: capability of noninvasive optical sectioning, with virtually no out-of-focus blur; availability of numerous fluorescent and non-fluorescent probes; simultaneous

application of multiple probes and simultaneous multichannel recording of digitally enhanced signals; quantitative static and dynamic analyses of 3D organization of macromolecules, single cells and microcolonies; and 3D multicolor stereoscopic imaging.

Preliminary studies in soil biofilms (Ebihara et al., 1997; Ebihara et al., 1999) showed the formation of surface biofilms and various protrusion and cluster-type structures, with thicknesses between 5 to 15 μm . The monolayers of microbial cells (surface biofilm) were found to be approximately 30-60% of the total viable biomass, while the remainder was loosely attached biofilm to sand grain surfaces.

3.7 QUALITY ASSURANCE AND QUALITY CONTROL (QA/QC)

A quality control plan was developed for the purpose of minimizing the occurrence of data artifacts and experimental error resulting from sampling, instrument calibration or methods used for analysis. Both chemical analysis and liquid and media samples were performed in accordance with this plan, as well as sample blanks, sample duplicates and matrix spikes as needed.

- a) *Sample blanks*: sample blanks allowed the identification of possible laboratory contamination in samples. For aqueous samples, sample blanks consisted of reagent-grade water generated by a MilliQ system (Millipore Inc., Amherst, MA) or dichloromethane (95% purity or higher); for solid samples, clean samples of sand media. A minimum of one sample blank was analyzed for every batch of samples analyzed.

- b) *Sample replicates*: sample replicates established a basis for sample result variation and they were collected and analyzed for all chemical methods used. Duplicates or triplicates were used according to the method of analysis. A minimum of one sample replicate was analyzed for every batch of samples analyzed.
- c) *Matrix spike samples*: matrix spike samples were used to determine the percent recovery for chemical analysis. A minimum of one matrix spike sample was analyzed for every batch of samples analyzed.
- d) *Instrument calibration and maintenance*: all instruments and analytical balances were calibrated and maintained according to standard laboratory operation procedures or manufacturer instructions. Standard curves were generated at regular intervals and for each major sampling event.
- e) *Sample and reagent containers, and sampling equipment*: sample containers, reagent containers and sampling equipment were cleaned to assure negligible external contamination during physical and chemical analysis. All sample containers were cleaned with Liquinox, acid-rinsed and triple rinsed with deionized water.

3.8 REFERENCES

APHA, AWWA, and WEF. (1998). *Standard Methods for the Examination of Water and Wastewater*, 20th ed., Washington, D.C.: American Public Health Association.

Daniels L., R.S. Hanson, J.A. Philips (1994). Chemical Analysis in: *Methods for General and Molecular Bacteriology*, P. Gerhardt, R.G.E. Murray, W.A. Wood and N.R. Krieg Eds, American Society for Microbiology, Washington DC., pp.512-553.

Ebihara, T., Bishop, P.L., (1997), "Examination of biofilms utilized in bioremediation of organic compounds using confocal scanning microscopy techniques", *Superfund Basic Research Program Conference: a decade of improving health through multi-disciplinary research*, Chapel Hill, NC.

Ebihara, T., Bishop, P.L., (1999), "Biofilm structural forms in porous media utilized in organic compounds degradation", *Wat.Sci.&Techn.*, **39**(6),

Findlay R.H., G.M. King, L. Watling (1989). "Efficacy of phospholipids analysis in determining microbial biomass in sediments", *Applied and Environmental Microbiology*, **55**(11), 2888-2893.

Inoue, S., (1995), "Foundations of confocal scanned imaging in light microscopy", in *Handbook of biological confocal microscopy*, Pawley, J.B. Eds., Plenum Press, New York.

Lichtman, J.W., (1994), "Confocal microscopy", *Scientific American*, October, 78-84.

Laurent, M., Johannin, G., Gilbert, N., Lucas, L., Cassio, D., Petit, P.X., Fleury, A., (1994), "Power and limits of laser scanning confocal microscopy", *Biol.Cell.*, **80**, 229-240.

Minski, M., (1988), "Memoir on inventing the confocal scanning microscope", *Scanning*, **10**, 128-138.

Shotton, D., White, N., (1989), "Confocal scanning microscopy: three-dimensional biological imaging", *Trends Biochem.Sci.*, **14**, 435-439.

White, D.C., Pinkart, H.C., Rindberg, D., (1997), "Biomass measurements: biochemical approaches", in C.J.Husrt, Ed., *Manual of Environmental Microbiology*, Washington, D.C., ASM Press, 91-98.

Chapter 4

BIOFILM FUNCTION-STRUCTURE STUDIES DURING BIODEGRADATION OF A LOW-MOLECULAR WEIGHT PAH

4.1 ABSTRACT

A fundamental understanding of the role of biofilms in soil bioremediation systems was developed in this study, in terms of biofilm growth, structure and composition, and the role of the biofilm matrix on mass transport of nutrients and contaminants to the biofilm microorganisms responsible for naphthalene degradation. Sand columns simulated a sandy aquifer contaminated with naphthalene, which was biodegraded to a maximum of 93.5%, using acetate as a co-substrate for enhancement of biofilm growth. Biofilm changes were analyzed over a time period of 18 weeks, showing an increase in total biomass and extracellular polymeric substances; acetate was found to greatly improve the production of live cells and EPS material and, therefore, was considered an important factor for promoting the degradation of naphthalene. A large variety of biological aggregate structures and growth patterns were observed by using confocal microscopy, suggesting that porous media biofilms are heterogeneous and complex matrixes that develop and change with specific environmental conditions. Image analysis was introduced as a tool to three-dimensionally quantify biofilms, in terms of biovolume, biosurface area, biothickness and cell density.

4.2 INTRODUCTION

Polycyclic Aromatic Hydrocarbons (PAHs) are ubiquitous environmental pollutants from incomplete combustion of organic materials. Environmental concern exists about the persistence and toxicity of PAHs, especially high-molecular weight PAHs (Ryan *et al.*, 1991). These compounds exhibit limited solubility in water and adsorb onto soils and particulates, influencing their bioavailability and biodegradation (Ahn *et al.*, 1999). Naphthalene biodegradation has been the best studied of the PAHs because it is the simplest and the most soluble of these hydrocarbons, and naphthalene-degrading bacteria, such as *Pseudomonas*, are easily found in the environment (Stelmack *et al.*, 1999).

The formation of biofilms has long been recognized as an important mechanism of interaction between porous media and biological processes. Biofilm has been defined as an organic material consisting of microorganisms embedded in a polymer matrix of their own making, called extracellular polymeric substances (EPS) (Bishop, 1997). In soil systems there is a large surface available for microorganisms that can either interact or attach to these surfaces, colonizing them and promoting their survival and growth. Viable cells find access to sorbed nutrients and increase their ability to grow and survive in changing environmental conditions.

Biofilm structures vary with the utilized substrate; however there are investigations that support the concept of continuous biofilm formation on the outer surfaces of the soil grain (Taylor *et al.*, 1990), which leads to the growth of layers of maximum thickness;

this was later described as the “open pore” model for permeability reduction. Other studies (Vandevivere et al., 1992a) suggest that bacterial aggregates develop in the pore spaces between coarse soil grains, giving sparse and heterogeneous coverage and limited exopolymer content. Mixed culture biofilm was developed in a simulated sandstone aquifer (Paulsen et al., 1997) showing a biofilm colonization at the beginning, followed by larger cell clusters, and finally development of a “bioweb” network of fibrillar strands, varying in size and shape depending on liquid flow velocity.

The role of biofilms in PAH bioremediation may be crucial to understanding microbial community development, mechanisms of PAH fate and transport in soils, and possible rate-enhancing processes for biodegradation. The structural forms and chemical composition of biofilms in porous media for PAH degradation are currently not well understood because of their complexity and the numerous biotic and abiotic processes. The primary goal of this study was to gain an understanding of the phenomena of biomass growth on soil surfaces in the presence of an easily-degradable PAH, and to investigate qualitatively and quantitatively the role of biofilm, in terms of development, growth, structure and composition, in order to improve bioremediation processes that maximize the useful properties of soil biofilms.

4.3 MATERIALS AND METHODS

Lab-scale reactors were constructed from 30-cm long, 3.8-cm diameter glass columns. The columns were equipped with five sample ports for pore water samples along the

length of the column, as well as four flow cell ports used for examination of biofilm growth. A schematic diagram of the experimental setup can be found in **Chapter 3**. A nutrient solution was combined with a saturated naphthalene solution (10-15 mg/L) and pumped in an up-flow manner at 5 m/d pore water velocity. Sodium Acetate solution (10 mg/L) was used in the system for development and enhancement of biofilm, and a small dose of hydrogen peroxide solution (3.5% v/v) was also injected to provide aerobic conditions in the reactors.

The enrichment culture for inoculating the soil columns was started with a mixed liquor sample from an activated sludge aeration tank, taken from a domestic wastewater treatment plant (Polk Run WWTP, Cincinnati, OH). Yuan *et al.* (2000) and other researchers have shown the broader enzymatic capabilities of mixed cultures, compared to individual bacterial strains; a large diversity of microorganisms enhances degradation rates of PAHs. The columns were operated for a period of 2 weeks with acetate as a primary substrate, prior to naphthalene addition, in order to develop a suitable biofilm.

Pore water samples were taken twice a week and analyzed for the contaminant concentration, dissolved oxygen (DO) and pH. Biofilm composition analysis was performed by taking samples from each flowcell at 1, 11 and 18 weeks of the experimental run. Total and viable biomass (firmly and loosely attached biomass) were measured, as well as carbohydrate and protein concentrations. A scanning confocal laser microscope was used to observe the physical structure, heterogeneity and growth patterns of biofilm in the flow cells. Samples were stained with BacLight® fluorescent stain to

determine viability of cells within the biofilm. Detailed description of analysis procedures and composition of the feed solution can be found in **Chapter 3**.

Quantification of biofilm in terms of cell diameter, cell number (viable/nonviable) per surface area, cell number (viable/nonviable) per volume, biosurface area, biovolume and biothickness, was also conducted by image analysis, using scanning confocal laser microscopy to capture images and MethaMorph® software to process and analyze the images. Samples from flow cells were stained with BacLight® fluorescent stain to distinguish viable/non-viable cells within the biofilm. Biofilm images were collected with a 63x magnification lens, in 32-bit gray-scale TIFF format, consisting of 1024 x 1024 pixels. A total of 30 different samples were available for image analysis; stacks of 39 slices for each sample were taken at random locations within the biofilm, at a 15 µm-depth and at 0.4 µm intervals.

4.4 RESULTS AND DISCUSSION

Duplicate lab-scale reactors were operated in this study for a period of 18 weeks: one main column (Column 2) to test the biodegradation of naphthalene, and one killed control column (Column 1) operated at the same conditions, with the addition of sodium azide (1g/L). **Table 4.1** summarizes the sequence of the experiments. Aerobic conditions were always maintained in the main column with an influent DO of 8-9 mg/L, whereas the effluent ranged between 0.5 and 1.0 mg/L, so that aerobic biological processes were not limited at any moment. The pH was maintained between 7.2 and 7.5 during the run.

Table 4.1 Summary of sequence of experiments.

	Column 1 (Control)	Column 2
Binary mixture (BM)	NAPH, AC + Az	NAPH, AC
Sole-substrate (SS)	NAPH + Az	NAPH

NAPH: naphthalene, AC: acetate, AZ: azide

4.4.1 Biodegradation Studies

The biodegradation of naphthalene was evaluated over time, in the presence and absence of a co-substrate (acetate); the results are shown in **Figure 4.1**. After 2 weeks of initial development of the biofilm with an easily degradable carbon source such as acetate (prior to the main experimental run), the system started to receive naphthalene as an additional substrate (BM). The microbial community seemed to slowly but successfully utilize the 2-ring PAH, with initial removal efficiencies varying from 54 to 75% in the first 6 weeks, indicating a period of acclimation to metabolize the new compound. However, due to problems in the operation of the syringe pump that provided the hydrogen peroxide to the sand column, oxygen levels may have decreased for short periods of time, affecting the degradation of the PAH. This explains the small decreases in naphthalene degradation at the end of weeks 3 and 6.

The system seemed then to recover and achieve excellent naphthalene mineralization, as was demonstrated by the 93.5% maximum removal efficiency at the end of week 11. The acetate-amended sand column showed an efficient metabolizing mechanism occurring within the biofilm.

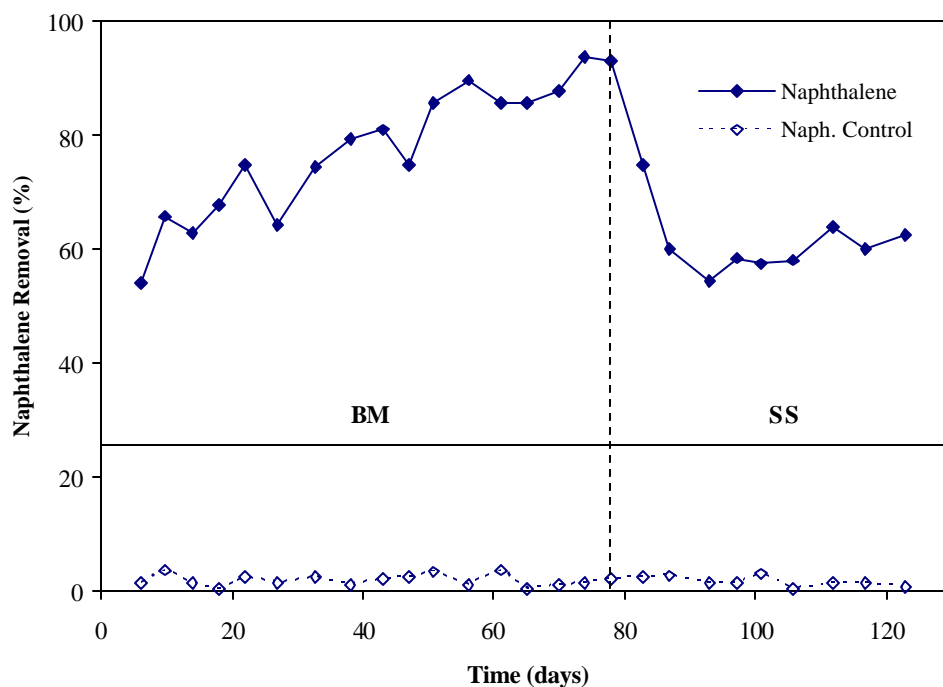


Figure 4.1 Removal efficiency of naphthalene (with and without co-substrate) over a period of 18 weeks.

In order to establish whether the degradation of naphthalene was dependent or not on the presence of acetate, the feed of co-substrate into the system was stopped after 11 weeks of operating with it. The 2-ring PAH acted then as a sole-substrate (SS) in the remaining 7 weeks, where two stages could be observed. On one hand, a 41% decrease in the naphthalene degradation occurred in less than 2 weeks, showing an immediate and strong need for acetate, in order to degrade the PAH. Eventually, though, microorganisms seemed to be able to better utilize naphthalene and its metabolism improved over time, achieving 62.4% removal efficiency.

The dependency on easily-degradable substrates to mineralize higher molecular weight PAHs has been reported in the literature. Yuan *et al.* (2000) investigated the transformation of phenanthrene with addition of acetate, yeast extract, acetate, glucose and pyruvate, and indicated that acetate was the second most preferable carbon source for enhancing phenanthrene degradation. Also, it is known that acetate may produce diverse intermediate products that are important for PAH metabolism, especially by *Pseudomonas* sp. in soil, as it is shown by Juhazs *et al.* (1997). Some researchers (Stringfellow and Atkin, 1995; Bouchez *et al.*, 1999) have reported competitive inhibition during the degradation of PAHs by the presence other compounds. This behavior was not observed in these studies because it is known that naphthalene and acetate are not metabolized by a common enzyme system. Instead, the 2-ring PAH may have used acetate as a growth co-substrate that enhanced its degradation.

Naphthalene biodegradation with sand column distance was also monitored by measuring average bulk naphthalene profiles (**Figure 4.2**). Regardless of the presence of acetate, most of the bulk naphthalene removal occurred within the first 7.5 cm of the sand column inlet, where the active biomass and exopolymeric substances were located. This can be explained because most of the nutrients and contaminants were available at this point, continuously supplying the biofilm with the substrate and oxygen needed for its development and growth. A clear difference was observed between the naphthalene profiles with and without acetate addition. First, a much faster degradation of the 2-ring PAH occurred by the first sample port when the co-substrate was present, which confirmed the enhancement made to naphthalene removal. While 87.4% of the PAH was

removed with acetate's aid in the first 7.5 cm of the sand column, only 68.6% biodegradation was observed when naphthalene was a sole-substrate. Second, a much more solid biofilm matrix seemed to have been established while acetate was being used, helping therefore with the degradation of naphthalene.

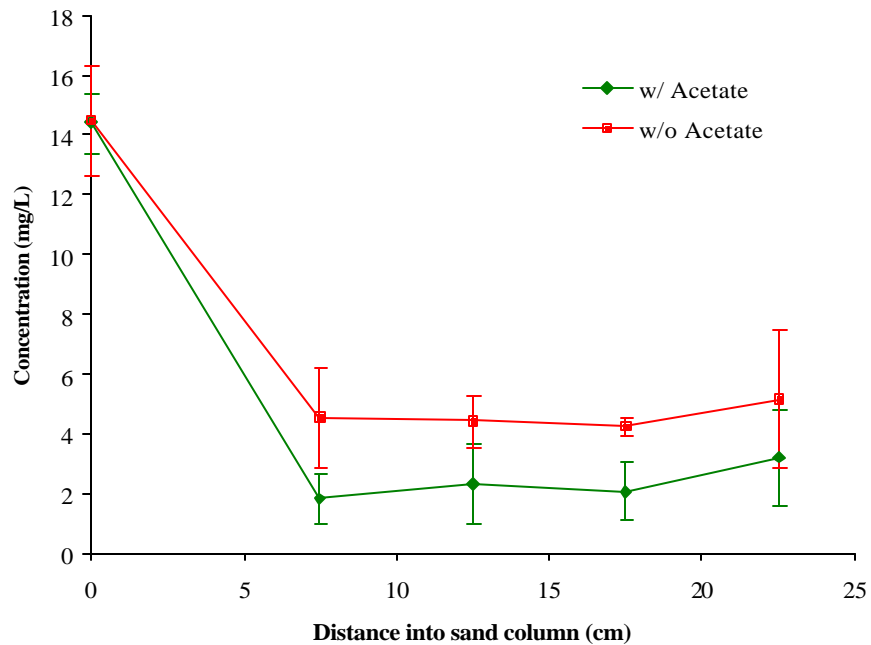


Figure 4.2 Average naphthalene concentration profiles with and without co-substrate.

The residual naphthalene concentration in the remaining distance of the sand column might be due the changes in the dissolved oxygen level, which was not always constant, inducing possible anaerobic periods in the system, inhibiting therefore the degradation of naphthalene. Also, during the acetate-amended period, the 2-ring PAH residual was always lower (around 48% less) than when naphthalene was the only source of organic carbon. A slight increase of bulk naphthalene concentration was observed in the upper 2.5 cm of the sand column for both amended and non-amended cases, probably because

that the contaminant was accumulating due to its hydrophobicity and tendency to strongly adsorb to soils; even so, naphthalene adsorbed onto the media was found to be negligible, as is shown in the sorption-to-sand studies.

4.4.2 Naphthalene Adsorption onto Sand Medium

Final killed biomass naphthalene concentrations in the porous media were obtained at the end of the experimental run, by adding sodium azide to the columns. Results of naphthalene adsorption onto sand media are presented in **Figure 4.3**.

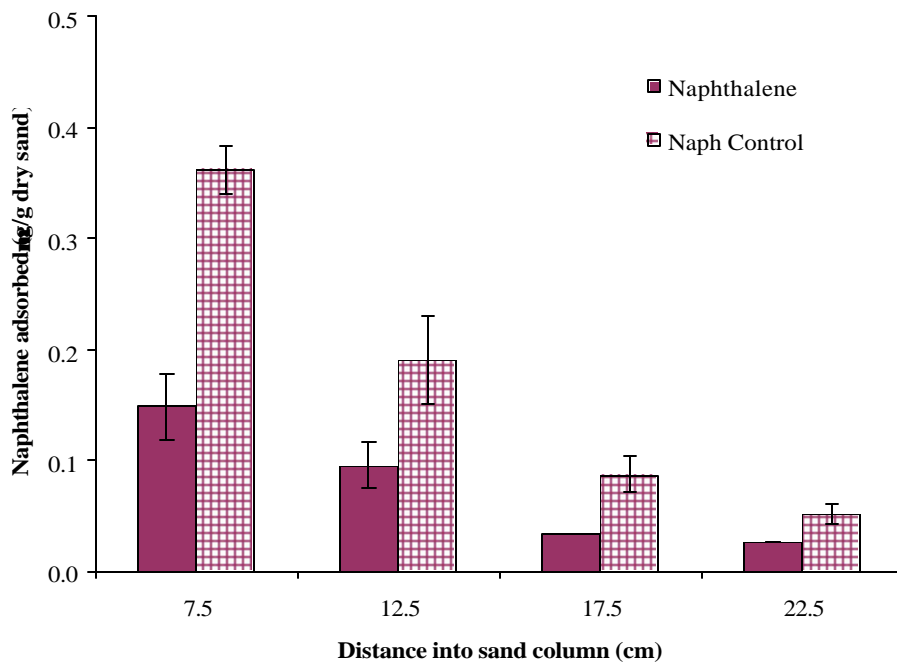


Figure 4.3 Naphthalene adsorbed onto sand after 18 weeks.

The naphthalene concentration at 7.5 cm was $0.149 \pm 0.03 \mu\text{g/g}$ dry sand, indicating the maximum sorption to sand near the inlet of the column. A decreasing profile was

observed with concentrations of 0.09, 0.03 and 0.02 $\mu\text{g/g}$ dry sand at 12.5, 17.5 and 22.5 cm, respectively. This is explained by the low sorption capacity of the porous material, so that removal mechanisms were not attributed to naphthalene adsorption, but instead to biological mechanisms. The control column, which was continuously killed with sodium azide from the beginning of the experiments, showed higher naphthalene concentrations onto the sand with respect to the inoculated column, but these concentrations were still considered insignificant.

Naphthalene concentration profiles in the sand medium seemed to have played a minor role, since final killed biomass concentrations of the three compounds were measured in very low concentrations.

4.4.3 Biofilm Composition

Biofilm components, such as volatile solids, lipid-phosphates, carbohydrates and proteins, were obtained for sampling events at 1, 11 and 18 weeks at various distances along the column, in order to describe the chemical composition of the biomass present in the sand.

Total biomass concentration was quantified by volatile solids, which decreased with depth into the sand column (**Figure 4.4**). Biomass values were observed to be the highest in the first 7.5 cm and increased from 198.4 ± 18 (at 1 week) to 584.4 ± 7 (at 11 weeks) to 787.8 ± 37 $\mu\text{g/g}$ TS (at 18 weeks) of the experimental run. Since most of the

contaminant, co-substrate and nutrients were present and available at the inlet, the majority of the biomass was localized and concentrated at this point. Average total biomasses of 78, 253 and 355 $\mu\text{g/g}$ TS were maintained in the 7.5 to 25 cm depth range of the sand column at 1, 11 and 18 weeks, respectively, indicating a relatively well-distributed biofilm with distance in the column.

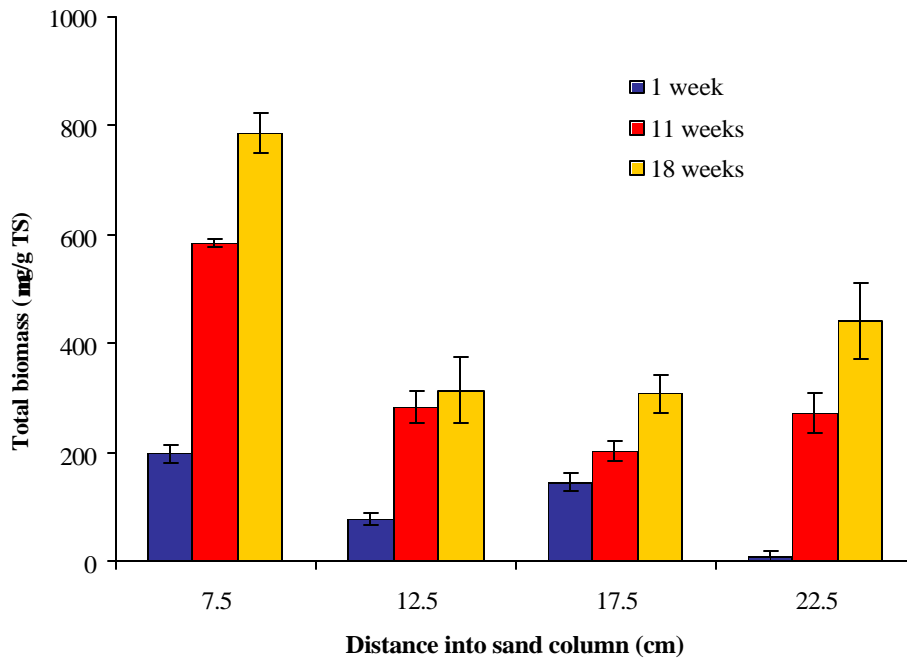


Figure 4.4 Total biomass profile.

An increase of almost three times in the total biomass occurred at the bottom of the column, between the first and the eleventh week, when the binary mixture of naphthalene and acetate was present. A better increase (10-fold on average) in the biomass was observed in the remaining distance of the column (7.5 to 22.5 cm), indicating an even spatial and temporal distribution of biofilm. The co-substrate seemed to have greatly enhanced new cell and exopolymeric substance production, forming a solid biofilm

matrix surrounding the sand grain surfaces. This was confirmed by the increasingly successful PAH biodegradation.

Naphthalene as a sole substrate promoted a small increase in the amount of total biomass compared to the period when binary mixtures were fed; an average of only 200 $\mu\text{g/g}$ TS were produced between weeks 11 and 18, corresponding to a 34.7% increase at the 7.5 cm distance. The other side ports of the sand column showed from 10.7 to 51.8% increase in the biomass caused by naphthalene utilization. It was observed that an average of 21% of the biomass of the main column grew in the killed control column, but this value decrease to 7% in the period of 18 weeks.

Lipid-phosphate analyses were carried out for the purpose of determining the viable cell amount, and the LP was distinguished between firmly attached (biofilm layer directly attached to sand grain surfaces) and weakly attached (protrusion and cell aggregate structures easily separated from the media). **Figure 4.5** presents the viable biomass profile along the sand column with time. An increase of total LP was the main point of observation over the 18-week period, indicating the progressive development of new biomass surrounding the sand grain surfaces. The maximum amount of viable biomass inside the column was located in the first 7.5 cm, where total LP were measured at 161.2 ± 8 (at 1 week), 474.9 ± 12 (at 11 weeks) and 640.9 ± 43 mg/g VS (at 18 weeks). Total LP remained relatively constant across the 7.5 to 25 cm column profile at about 77, 200 and 279 mg/g VS at 1, 11 and 18 weeks, respectively. The major increase in viable biomass was observed in the first 11 weeks, with a 3-fold production of mg of biomass

per mg of VS. This suggests that a large amount of new live cells within the biofilm were being produced, probably due to the presence of acetate which is an easily degradable carbon source. Even so, an additional increase (35%) in the viable biomass occurred in the remaining 7 weeks; this can be directly explained by the absence of the acetate co-substrate, leaving only the heavier molecular weight naphthalene as the sole substrate.

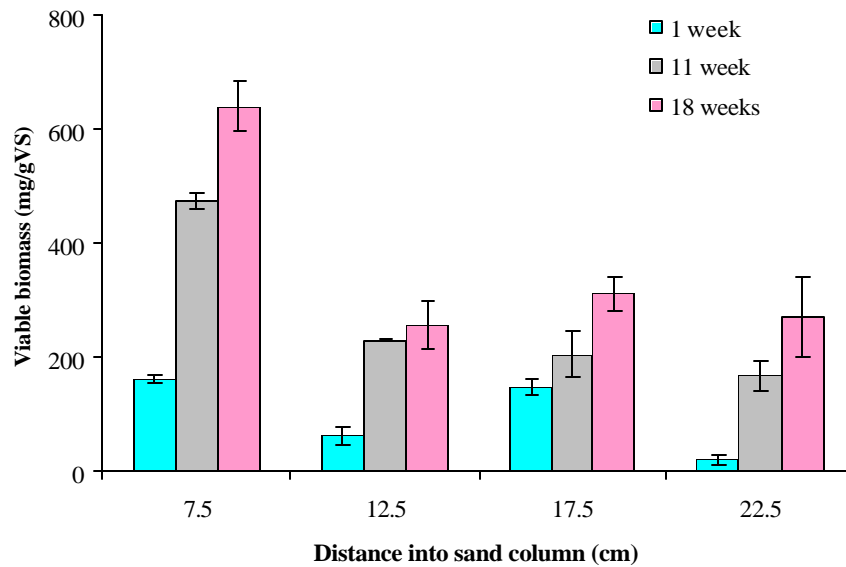
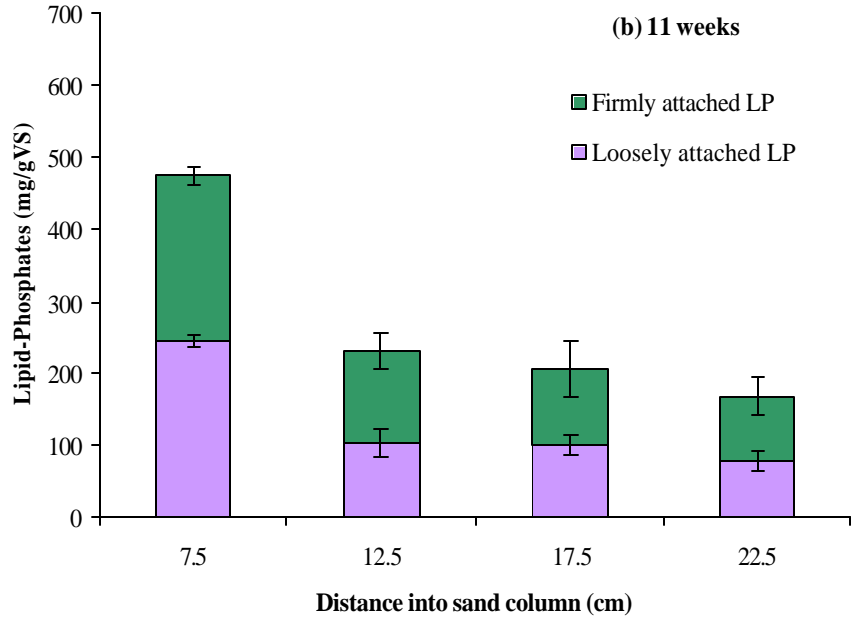
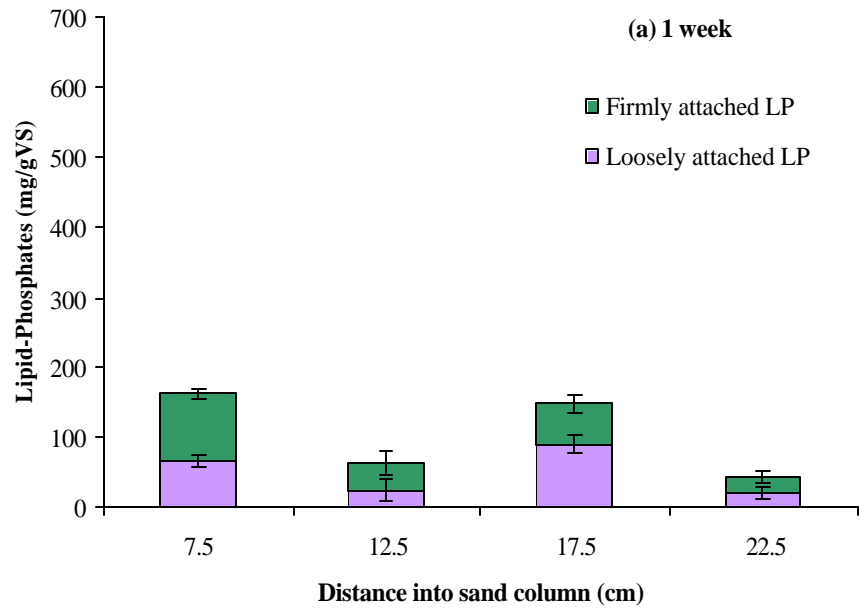


Figure 4.5 Viable biomass profile.

Figure 4.6 (a), (b) and (c) show the firmly and loosely attached biomass, not only with distance into the sand column, but also with time. The most important fraction of the total lipid-phosphates was the firmly attached biomass, which ranged from 59% (at 1 week), to 74% (at 11 weeks) and to 51% (at 18 weeks) of the total LP at the inlet of the sand column. The highest amounts of firmly attached biomass were always measured at the 7.5 cm-depth, with values of 96 ± 3 , 231.2 ± 4 and 237.5 ± 27 mg/g VS at 1, 11 and 18

weeks, respectively. Sampling events during the 11th and 18th weeks, also showed significant LP between the 12.5 and 22.5 cm-range, probably due to residual naphthalene which was biodegraded further into the column, creating a better-established biofilm. As shown by the viable biomass profiles, the binary mixture of acetate and naphthalene caused the highest increase in firmly attached LP, with almost double the concentration of mg of firmly attached biomass per g of VS. Acetate, therefore, contributed to the formation of well-attached biofilm to sand grain surfaces. The degradation of naphthalene alone resulted in only 42% of the amount of firmly attached biomass in the last 7 weeks of the experimental run.

Loosely attached biomass constituted a smaller but still important portion of the lipid-phosphates, with averages of 46.3%, 44.9% and 48.3% of the total lipid-phosphates, along the depth of the column and during the three sampling events. The maximum values of loosely attached biomass were determined to be 65.2 ± 4 , 223.7 ± 8 and 313.4 ± 16 mg/g VS at 1, 11 and 18 weeks, respectively. Particularly at the beginning of the run, loosely attached biomass was evenly distributed with distance into the sand column, at an average of 50 mg/g VS; this can be explained by the newly formed biofilm, which may have not been totally attached to the porous media surfaces. Similarly to the firmly attached biomass, acetate-amended experiments produced more weakly attached biomass between weeks 1 and 11, with an almost 273% increase, while only 28.9% was measured for the naphthalene as sole-substrate period. Firmly and loosely attached biomass in the killed control column were about 9% of the biomass grown in the inoculated column during the 18-week period.



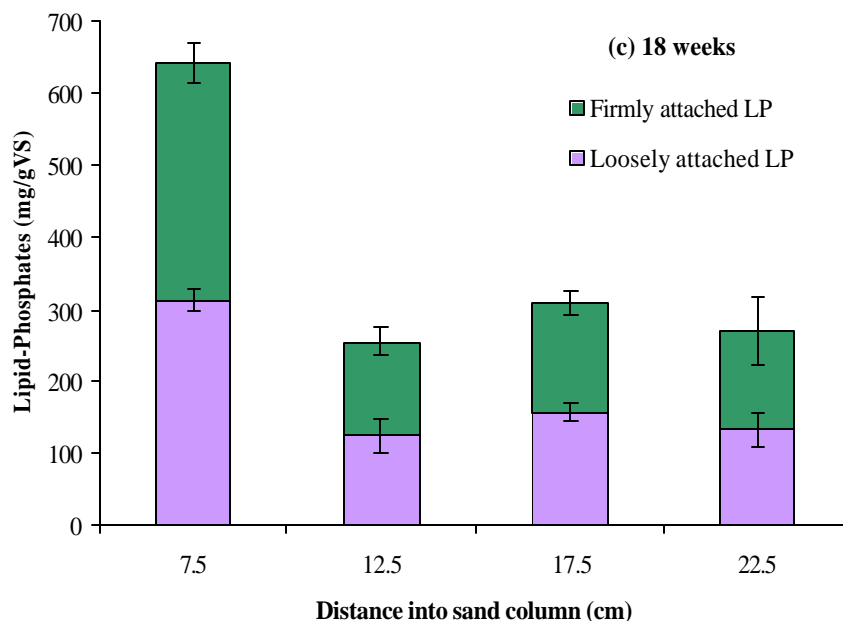


Figure 4.6 Firmly and loosely attached biomass profiles at (a) 1 week, (b) 11 weeks and (c) 18 weeks.

Carbohydrate and protein profiles were used to express the extracellular polymeric substances (EPS) composition of the bio film because they constitute the largest fractions of polymers in the matrix. Carbohydrate profiles are presented in **Figure 4.7**, where the highest amounts of 176.1 ± 10 (at 11 weeks) and 153.4 ± 20 mg/g VS (at 18 weeks) were observed at the bottom of the sand column. The results obtained for the sampling event during the first week showed a relatively constant carbohydrate content along the column distance, with an average amount of approximately 18 mg/g VS. A significant increase of 7 to 9 fold for the carbohydrate mass per volatile solid mass was observed between weeks 1 and 11, because of the acetate amendment in the system. Bacteria seemed to be well-surrounded by a solid exopolymeric matrix, allowing a large colonization of the sand grain surfaces; the binary mixture seemed to function well for the biological processes to

take place, and therefore, higher biodegradation rates of naphthalene were promoted. A slight decrease in the carbohydrate amount occurred in the last 7 weeks of the experimental run, resulting in loss range of about 10 to 57 mg/g VS (or a 13 to 37% decrease with respect to week 11), due to the absence of the co-substrate. Still, the production, when naphthalene was the sole-carbon source, was maintained at 87% of the carbohydrate content obtained in the second sampling event, and a similar tendency was observed along the sand column. An average of 12% of the carbohydrates present in the main column was measured in the killed control column in the first week, and this decreased over time.

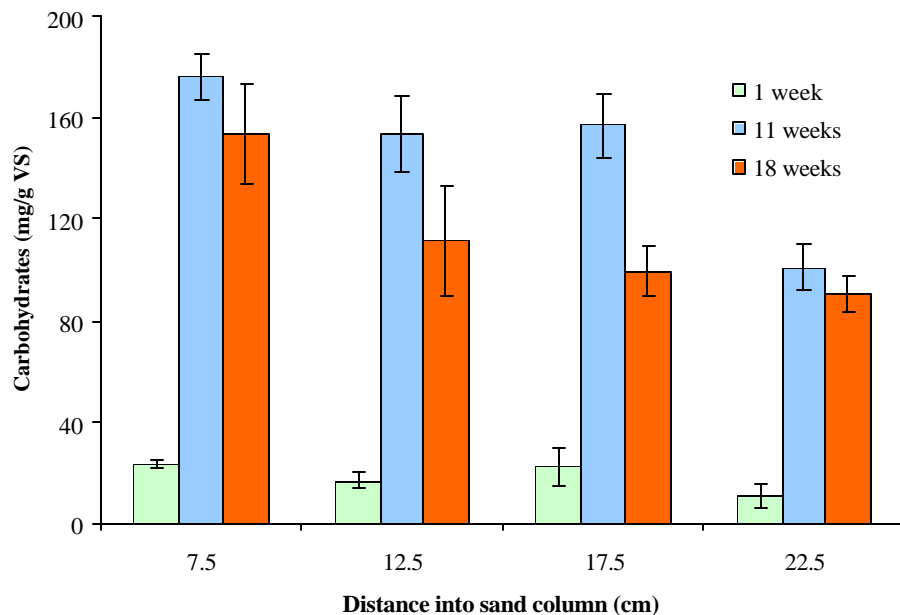


Figure 4.7 Carbohydrate profile.

Profiles of protein concentrations during the 18-week period are shown in **Figure 4.8**. Protein concentrations at the 7.5 cm depth indicated an increase over time from 38.5 ± 2 (at 1 week) to 67.9 ± 7 (at 11 weeks) to 72.9 ± 5 mg/g VS (at 18 weeks). Initial protein

amounts were relatively constant between the 12.5 and 22.5 cm column distance, at an average of 12 mg/g VS after 1 week of experimental run. The protein contents in the middle column were maintained at averages of 51 and 63 mg/g VS, during the second and third sampling events respectively, showing a better spatial distribution of the biomass with depth. The killed control column appeared to show 7% of the protein amounts in the inoculated column.

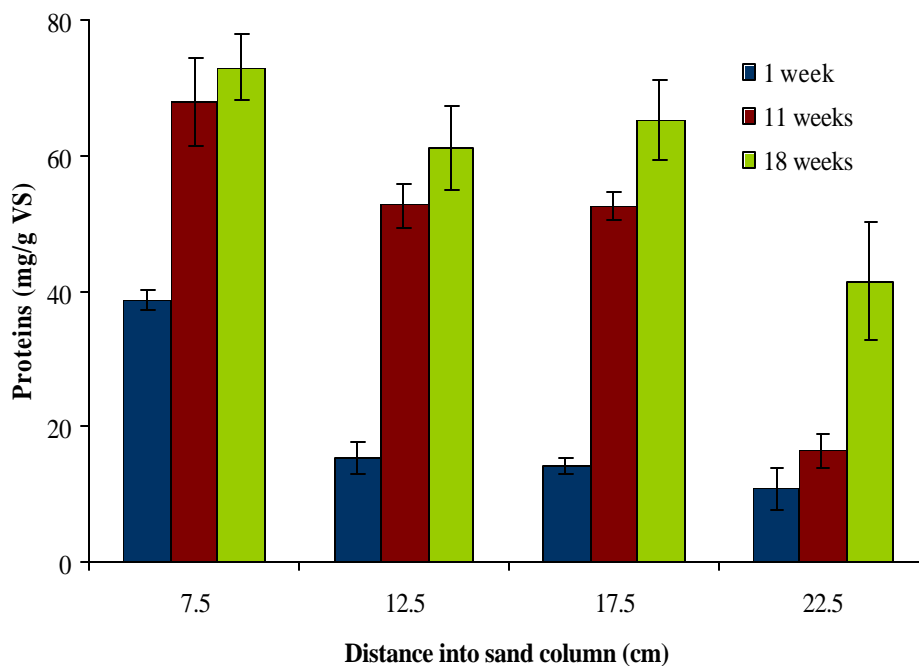


Figure 4.8 Protein profile.

It can be concluded that the production of new proteins was considerably smaller after acetate feed was stopped in the system, showing that the co-substrate plays an important role in biofilm growth and development, because it can not only increase the amount of viable cells present but also the EPS matrix, which are both essential for the contaminant biodegradation.

4.4.4 Biofilm Structure

Physical structures of biofilm from the flow cells in the active zone (0 to 7.5 cm) of the sand columns were examined at 18 weeks, using Confocal Laser Scanning Microscopy. Typical optical sections of biofilms on sand grain surfaces are presented in **Figure 4.9 (a)** and **(b)**. Biofilm coverage of the entire sand grain surfaces was observed, showing a continuous surface biofilm of approximately 15 to 30 μm in thickness. Acetate addition appeared to increase the biomass per unit sand medium, improving the biodegradation function of the microorganisms; the surface biofilm consisted not only of the monolayer of microbial cells, but also of small cluster-type structures in the range of 10 to 15 μm in diameter.

Many structural forms were also observed such as “bridge” formations, protrusion structures and bacterial aggregates. “Bridges” were formed when two or more adjacent surface biofilms became interconnected, creating a web-like system of active biomass called bioweb. Large protrusion structures were very common, varying between 30 to 50 μm in diameter, indicating thick agglomerations of exopolymeric substances, such as carbohydrates and proteins. These were not necessarily attached to the sand grain surfaces, and probably formed during the acetate amendment stage. Bacterial aggregates, or viable cell accumulation, were usually found immediately adjacent to sand grains, with lengths of 20 to 40 μm , occupying available pore spaces.

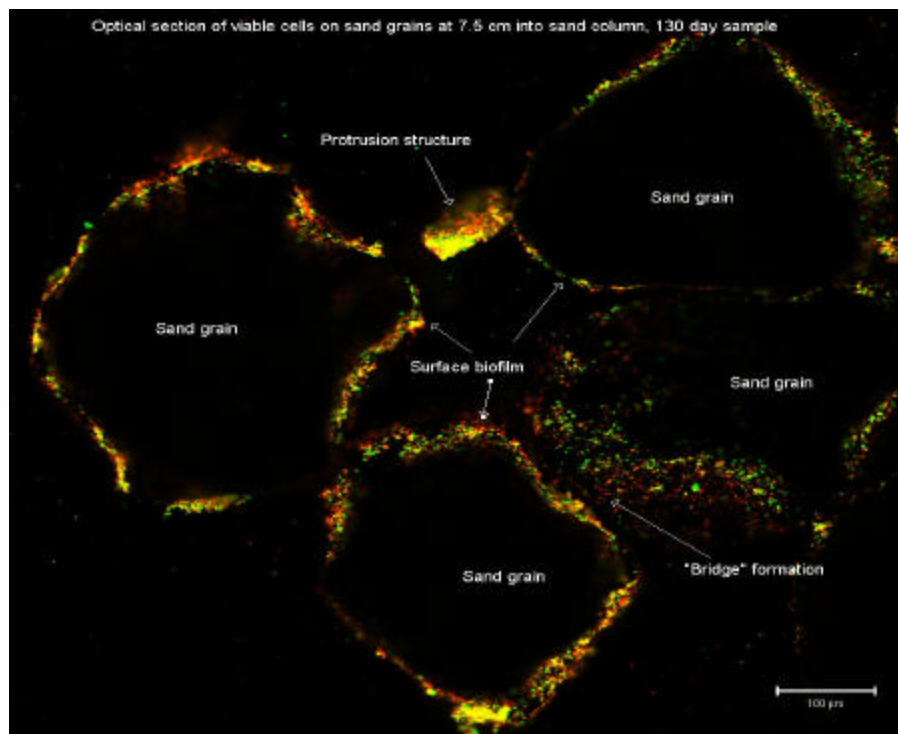
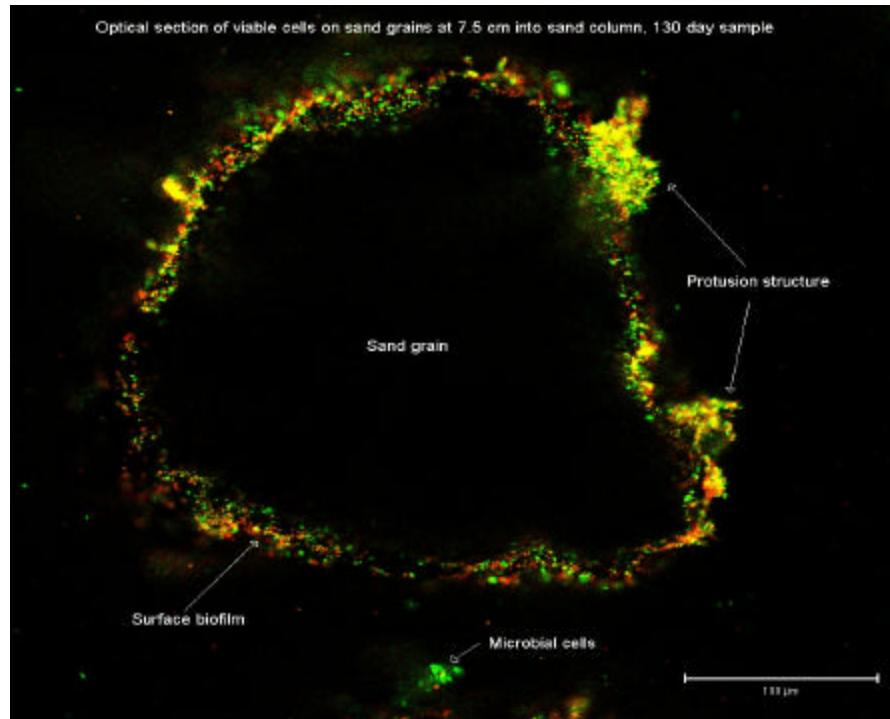


Figure 4.9 Optical sections of biofilms on sand grain surfaces at 7.5 cm (a) at 40x and (b) 20x magnifications, after 18 weeks.

This web-like matrix has been reported previously by Ebihara *et al.* (1997, 1999). Continuous surface films on sand grains were much thinner (5 to 15 μm in thickness) in their studies, and all aggregate structures were much smaller (5 to 30 μm in diameter), compared to this study, probably because of the shorter duration of their experiments (10 weeks, compared to 18 weeks in this study).

Biofilm morphology in porous media has been widely described in the literature (Paulsen *et al.*, 1997; Vandevivere *et al.*, 1992; Dunsmore *et al.*, 2004). Biofilm structured-network has been called “bioweb”, because of the varying strands in size and shape which build a complex matrix with a large surface area. Researchers have reported that, as biofilm depth is minimized, mass transfer resistance between the fluid and the biofilm phase is also decreased, depending on the pore spaces between soil particles and the permeability conditions.

4.4.5 Three-Dimensional Biofilm Quantification

Previous research in biofilm imaging (Yang *et al.*, 2000; Lewandowski *et al.*, 1999; Jackson *et al.*, 2001) has shown that 30 images are statistically adequate to represent and quantify the average biofilm structure. Therefore, in this study 30 different samples of biofilm from flow cells were used to acquire images and conduct quantification analysis.

Initially, a random stack of optically sliced-images (at 100x magnification) was used to estimate the average cell diameter in the biofilm. Cells were identified by defining their

perimeter on each sliced-image, and this process was followed at different depths of the stack; by defining the slice thickness (0.39 μm), MethaMorph® software was used to obtain the superficial area of each cell on each slice and, therefore, its volume. **Figure 4.10** depicts the volume distribution of 38 samples, indicating a great variation in cell volumes; even so, at least 84% of the samples fell in the range between 1.14 and 5.42 μm^3 , which is very close to the average volume. Using Dixon's test (Massart *et al.*, 1997) for the detection of outliers, 6 samples (Cell # 2,4,5,6,9,11) were observed to be measurements outside the typical range and failed the test (with a 5% level of significance) because they were probably big cell clusters; therefore, they were excluded from the following calculations.

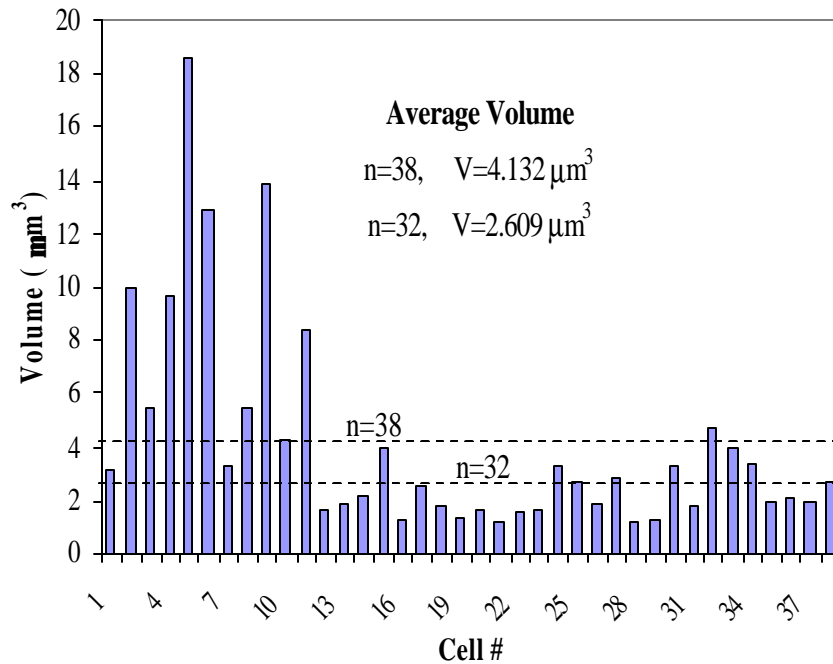


Figure 4.10 Distribution of measured cell volumes.

Assuming cells with spherical shape, the diameter was then calculated. The diameter distribution of the remaining 32 samples is presented in **Figure 4.11**, in which only a small variation between cell diameters is observed.

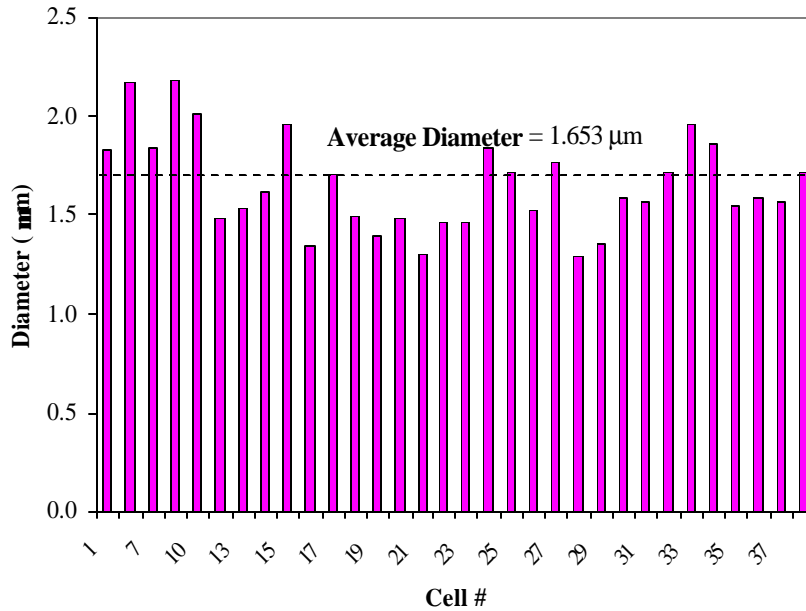


Figure 4.11 Distribution of calculated cell diameters (n=32).

Statistical analyses were then performed with the corrected/uncorrected data; the results are shown in **Table 4.2**. By excluding the 6 outliers and reducing the number of samples to 32, the resulting change in the average volume was almost 200%, indicating the effect the outlying values had on corrupting the data and shifting the tendency of the samples. While the original range of volumes varying from 1.14 to 18.65 μm^3 caused a coefficient of variation of 96.3%, the adjustment to 32 typical samples gave an acceptable standard deviation of 1.21 μm^3 (corresponding to 46.3%). The calculated average diameter was therefore 1.65 μm , with a median 1.59 μm , and a lower coefficient of variation of 14.4%.

Table 4.2 Statistical parameters for cell volume measurements and diameter calculations.

Statistical Parameter	Volume (mm ³)		Diameter (mm)
	n=38	n=32	n=32
Average	4.132	2.609	1.653
Standard Deviation	3.980	1.210	0.239
Minimum	1.140	1.140	1.296
Maximum	18.650	5.420	2.179
Median	2.650	2.150	1.586
Coefficient of Variation (%)	96.314	46.384	14.478

A series of 30 samples were used to acquire images for quantification of biosurface area, biovolume and biothickness. Typical rounded sand grains on each sample were selected and a similar procedure was chosen as in the cell diameter analysis: portions of biofilm visible at 63x magnification were identified by defining their perimeter on each sliced-image, and this process was done at 39 different depths of the stack (for a total of a 15 μm -depth); by defining the slice thickness (0.39 μm), MethaMorph® software was used to obtain the superficial area of each biofilm portion on each slice and therefore, its volume.

A typical stack (Stack #5) of 39 biofilm images in a 15 μm -depth taken by CLSM is shown in **Figure 4.12**. Areas observed in green color represent the live biofilm, while the red-colored areas represent the dead biofilm; dark areas are either bulk fluid or sand grain interior which are not fluorescent. A progressive enlargement of biofilm superficial area is observed as depth increases, indicating the heterogeneous distribution and attachment of biomass on the sand grain surfaces.

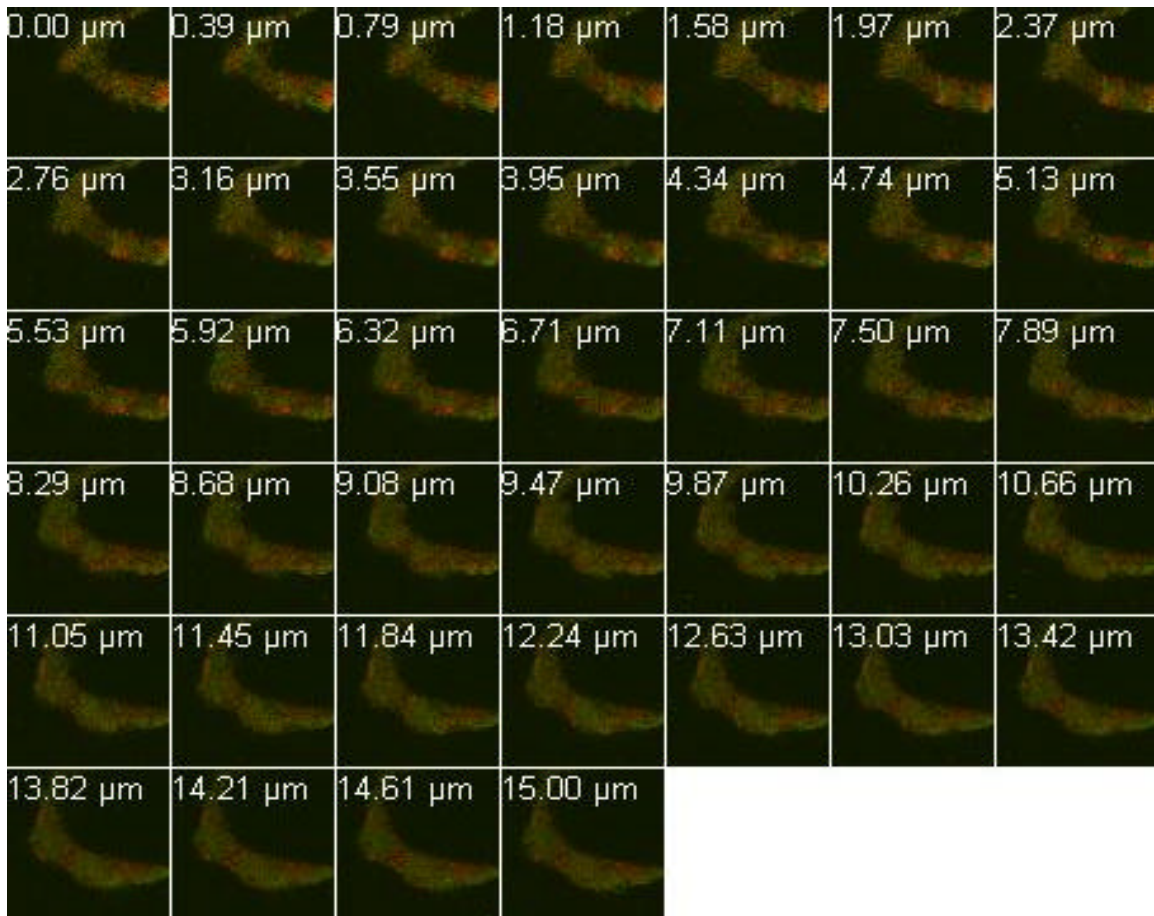


Figure 4.12 Typical stack of 39 biofilm images.

The results of the statistical analyses performed on 30 different biofilm samples are shown in **Table 4.3**. Averages of $41915 \mu\text{m}^3$ and $2310 \mu\text{m}^2$ were found for biovolume and biosurface area, respectively, in biofilm images of $146.2 \times 146.2 \times 15 \mu\text{m}$. Minimums and maximums of biovolumes and biosurface areas indicated a broad range of measured values, probably due to the heterogeneity of the biofilm attached to sand grains. This is confirmed by the qualitative analysis of biofilm structures by CLSM, where it was concluded that the microbial community grows and reproduces in a complex matrix that varies in shape and size; monolayers of biofilm may be present with thicknesses between

10 to 20 μm , but protrusions, cell aggregates and clusters of 30 or even 80 μm in length may also be formed, so that no continuous biofilm structure can be expected to attach to sand grains surfaces. Even so, in this study coefficients of variation were found to be relatively low (33.1% for biovolume and 41.6% for biosurface area) with respect to the variety of biofilm formations on porous media.

Table 4.3 Statistical parameters for biosurface area, biovolume and biothickness.

Statistical Parameter	Biosurface area (mm^2)	Biovolume (mm^3)	Biothickness (mm)
Average	2309.84	41914.52	18.42
Standard Deviation	763.79	17435.39	5.43
Minimum	1062.62	22734.12	12.06
Maximum	3859.45	84271.49	31.30
Median	2298.70	39146.32	16.54
Coefficient of Variation (%)	33.07	41.60	29.49

The average biothickness, or biovolume/biosurface area ratio, was found to be 18.42 μm , very close to the median value of 16.54 μm , so that it can be considered significantly important because it describes with accuracy the tendency of a monolayer biofilm formation. The coefficient of variation was 29.5% with an acceptable standard deviation of 5.43 μm .

Currently, more advanced research is being conducted in order to quantify biofilm heterogeneity and therefore, correlate it numerically with local mass transport rate and local respiration rates measured in biofilms. Several two or three-dimensional software packages based on image analysis by CLSM have been developed to define parameters that adequately represent biofilm morphology for analysis and modeling: COMSTAT

(Heydorn *et al.*, 2000), ISA (Yang *et al.*, 2000) and ISA3D (Beyenal *et al.*, 2004). They not only account for the textural parameters that show the microscale heterogeneity of biofilms (entropy, energy, homogeneity), but also the volumetric parameters that describe size and morphology of biomass (biovolume, surface area, volume/surface area ratio, porosity, mean thickness, run length, diffusion distance, fractal dimension).

Having measured the area of biofilm per slice, live and dead cell areas per slice were also identified, using the BacLight® Live/Dead fluorescent stain that determined viability of cells, by staining the live biofilm green, and the dead biofilm red. Assuming spherical cells with an average diameter of 1.65 μm and an area of 2.15 μm^2 , the total, viable and non-viable number of cells were calculated per slice. Cell numbers were then converted to cell densities (viable and non-viable) per unit area, by normalizing them with the total area of the slice. Cell densities (viable and non-viable) per unit volume were then calculated as the average of cell densities per unit area of two consecutive slices multiplied by the slice thickness (0.39 μm). For each stack of images, the results of 39 slices were averaged and, finally, the results of the 30 samples were averaged. **Table 4.4** presents a summary of the total, viable and non-viable areas and cell densities.

For the small sections of biofilm analyzed, a large portion of coverage on sand grains was observed; more than 60% of the biofilm was viable, indicating an active biomass with potential to rapidly reproduce and colonize surfaces. Only a limited part (around 15%) constituted dead biofilm, which usually is encountered as debris and dead cells within the complex EPS matrix. The variation in area measurements is based on the heterogeneous

growth and attachment of the biofilm to the porous media, so that 41.9%, 12.8% and 38.2% of coefficients of variation for total, viable and non-viable areas, respectively, are considered acceptable.

Table 4.4 Statistical parameters for total, viable and non-viable areas and cell densities.

Statistical Parameter	Area		
	Total (mm ²)	Viable (%)	Non-Viable (%)
Average	85372.27	61.66	15.72
Standard Deviation	35787.58	7.87	6.00
Minimum	39108.63	43.26	7.15
Maximum	178304.48	78.89	26.82
Median	77429.15	60.85	14.88
Coefficient of Variation (%)	41.92	12.77	38.15
	Cell density per unit area (# / mm ²)		
	Total	Viable	Non-Viable
Average	0.2947	0.2350	0.0597
Standard Deviation	0.0346	0.0348	0.0224
Minimum	0.2417	0.1627	0.0269
Maximum	0.3720	0.3155	0.1008
Median	0.2871	0.2289	0.0566
Coefficient of Variation (%)	11.73	14.81	37.50
	Cell density per unit volume (# / mm ³)		
	Total	Viable	Non-Viable
Average	0.1149	0.0916	0.0233
Standard Deviation	0.0136	0.0137	0.0087
Minimum	0.0633	0.0104	0.0940
Maximum	0.1234	0.0395	0.1455
Median	0.0891	0.0221	0.1118
Coefficient of Variation (%)	11.86	14.93	37.52

Cell densities per unit area were found to be around 0.2947 cells/ μm^2 (29.47×10^6 cells/cm²), of which 80% were live cells. Okabe *et al.* (2004) found different areal cell densities in a study with ammonia-oxidizing bacteria grown in slides in rotating discs: while the cell density of *Nitrosomonas* was 1.12 cells/ μm^2 , for *Nitrosospiras* it was half

of that ($0.51 \text{ cells}/\mu\text{m}^2$); the fact that biofilm was produced in a thicker and denser manner, as well as other variables such as cell diameter and primary substrate, may have affected the cell density of specific bacteria. Meanwhile, cell densities per unit volume in this study accounted for $0.1149 \text{ cells}/\mu\text{m}^3$ ($114.9 \times 10^9 \text{ cells}/\text{cm}^3$), which can be closely compared to the value obtained of $98.9 \times 10^9 \text{ cells}/\text{cm}^3$, by Okabe *et al.* (1996). A viable cell density per unit volume of $0.0916 \text{ cells}/\mu\text{m}^3$ was measured in the porous media biofilm, accounting for at least 80% of the total cell density.

Figure 4.13 shows the biosurface area distribution with biofilm depth on a typical stack of images (Stack #5). Firstly, it is observed that the coverage of viable cells is approximately 4 times larger than non-viable cell coverage on each optically-sliced image, indicating an active live biomass that is predominantly present on the surface of sand grains. Although non-viable cell area accounts for only 15% of the total area, debris and dead cells are fundamental in building the biofilm, by giving its structure and mass to the matrix. There is a non-uniform distribution of biofilm coverage within $15 \mu\text{m}$ of depth; the degree and stages of attachment may play an important factor on how the cells start forming the biofilm structure with the exopolymeric materials; it is clear that biofilm is heterogeneous and has great variation on size and shape.

The typical cell density per unit area distribution with biosurface area (taken from Stack #5) is presented in **Figure 4.14**. For total biosurface areas varying between 4300 and $4800 \mu\text{m}^2$, the viable cell densities per unit area ranged between 0.20 and $0.25 \text{ cell}/\mu\text{m}^2$. For non-viable cells, an average cell density per unit area of $0.06 \text{ cell}/\mu\text{m}^2$ was observed.

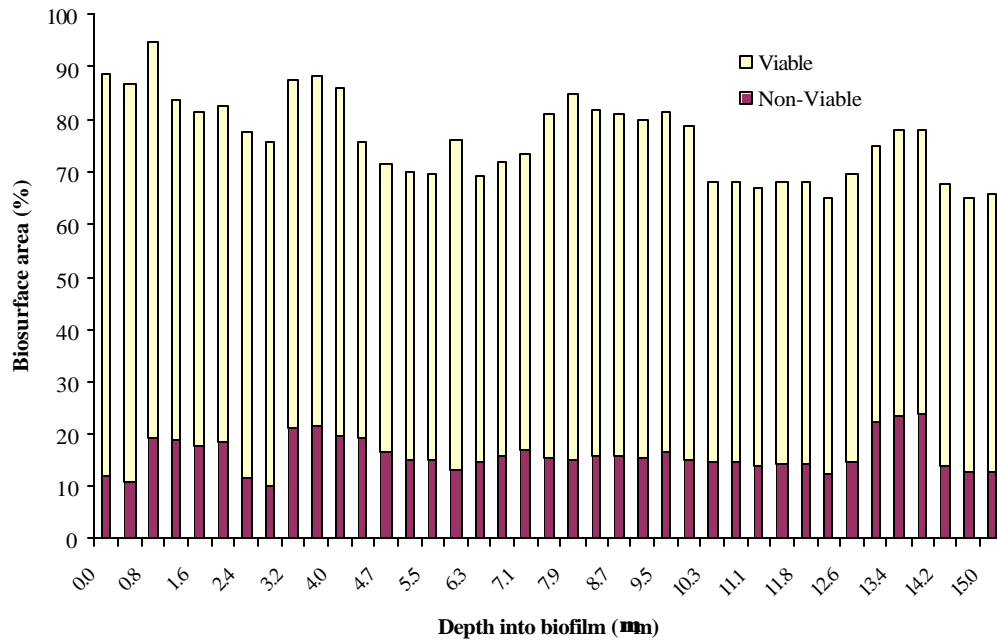


Figure 4.13 Typical biosurface area distribution with biofilm depth.

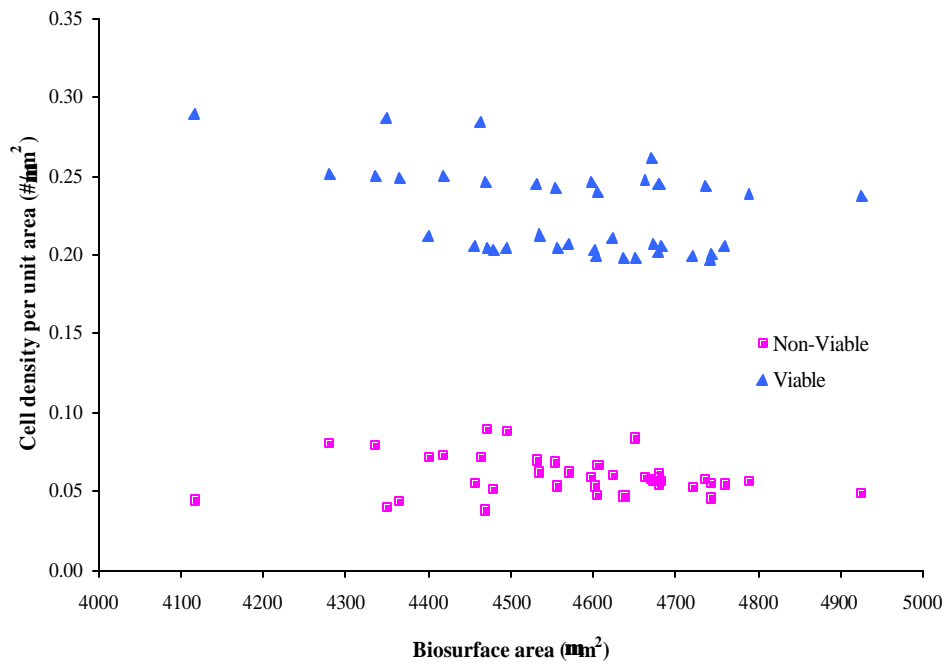


Figure 4.14 Typical cell density per unit area distribution with total biosurface area.

Overall, the distribution of viable and non-viable cells was uniform and did not vary much with the total available biosurface area. Only small clusters or aggregates of cells were observed, where cell densities were the highest, but it can be considered as part of the heterogeneous biofilm structure.

4.5 CONCLUSIONS

Most bulk naphthalene removal occurred within the first 7.5 cm of column depth, with an average of 85.7% removal after 11 weeks (with acetate) and 61.2% after 18 weeks (without acetate), indicating the need for a co-substrate that may enhance a bioremediation system.

Biofilm development and changes in composition were measured at 1, 11 and 18 weeks. Lipid-phosphate profiles indicated that viable biomass increased over time, of which an average of 58% was firmly attached biomass to sand grains surfaces. Extracellular polymeric substances measured as carbohydrates and proteins were found to be an important fraction of the biofilm matrix and, most probably, acetate was the key to enhancing the production of both materials. Microorganisms were, therefore, not only protected by the EPS, but also promoted the successful biodegradation of the PAH. The maximum biomass and exopolymeric material contents were achieved in the first 7.5 cm of depth, where most of the nutrients and contaminant were available.

Biofilm structure examination done by CSLM indicated the presence of continuous surface biofilms on sand grains that were approximately 15 to 30 μm in thickness. A variety of biological aggregate structures ranging from 20 to 50 μm in diameter was also observed: large cluster-and-protusion-type structures, cell aggregate bridging and a thick bioweb-type growth containing viable cells developing in the pore spaces between soil grains.

Image analysis indicated that it is possible to quantify some of the morphological features of biofilms that can be related to processes and conditions occurring in porous media. Characteristics such as biovolume, biosurface area, biothickness, cell diameter and cell density were identified and aided in understanding the relationship between structure and function in biofilms. A more detailed investigation of various biofilm parametric measurements by image analysis should be conducted in the future, by selecting a range of features that better represent the majority of the variation in the biofilm structure.

4.6 REFERENCES

Ahn, Y., Sanseverino, J., Sayler, G., (1999), "Analyses of polycyclic aromatic hydrocarbon-degrading bacteria isolated from contaminated soils", *Biodegradation*, **10**, 149-157.

Beyenal, H., Lewandoski, Z., (2004), "Quantifying biofilm structure: facts and fiction", *Biofouling*, **20**, 1-23.

Beyenal, H., Donovan, C., Lewandoski, Z., Harkin, G., (2004), "Three-dimensional biofilm structure quantification", *J.Microb.Meth.*, **59**, 395-413.

Bishop, P.L. 1997. "Biofilm structure and kinetics", *Wat.Sci. & Techn.*, **36**, 287-294.

Bouchez, M., Blanchet, D., Bardin, V., Haeseler, F., Vandecasteele, J.P., (1999), "Efficiency of defined strains and of soil consortia in the biodegradation of polycyclic aromatic hydrocarbons (PAH) mixtures", *Biodegradation*, **10**, 429-435.

Dunsmore, B., Bass, C., Lappin-Scott, H., (2004), "A novel approach to investigate biofilm and bacterial transport in porous matrices", *Environm.Microbiol.*, **6**(2), 183-187.

Ebihara, T., Bishop, P.L., (1997), "Examination of biofilms utilized in bioremediation of organic compounds using confocal scanning microscopy techniques", *Superfund Basic Research Program Conference: a decade of improving health through multi-disciplinary research*, Chapel Hill, NC.

Ebihara, T., Bishop, P.L., (1999), "Biofilm structural forms in porous media utilized in organic compounds degradation", *Wat.Sci.&Techn.*, **39**(7), 203-210.

Ebihara, T. (1999), "Characterization and enhancement of microbial biofilms in porous media for the biodegradation of polycyclic aromatic hydrocarbons", PhD. Dissertation, University of Cincinnati, Cincinnati, OH.

Heydorn, A., Nielsen, A., Hentzer, M., Stenberg, C., Givskov, M., Ersboll, B.K, Molin, S., (2000), "Quantification of biofilm structures by the novel computer program COMSTAT", *Microbiology UK*, **146**, 2395-2407.

Jackson, G., Beyenal, H., Rees, W., Lewandowski, Z., (2001), "Growing reproducible biofilms with respect to structure and viable cell counts", *J. Microb. Methods*, **47**, 1-10.

Juhasz, A.L., Britz, M.L., Stanley, G.A., (1997), "Degradation of fluoranthene, pyrene, benz[a]anthracene and dibenz[a,h]anthracene by *Burkholderia cepacia*", *J.Appl.Microbiol.*, **83**, 189-198.

Lewandowski, Z., Webb, D., Hamilton, M., Harkin G., (1999), "Quantifying biofilm structure", *Wat.Sci. & Techn.*, **39**, 71-76.

Massart, D., Vandeginste, B., Buydens, L., De Jong, S., Smeyers-Verbeke, J., (1997), *Handbook of Chemometrics and Qualimetrics: Part A, Data Handling in Science and Technology (Vol.20a)*, Elsevier Science, Amsterdam.

Okabe, S., Kindaichi, T., Ito, T., Satoh, H., (2004), "Analysis of size distribution and areal density of ammonia-oxidizing bacterial microcolonies in relation to substrate microprofiles in biofilms", *Biotechn.&Bioengin.*, **85**(1), 86-95.

Okabe, S., Hirata, K., Ozawa, Y., Watanabe, Y., (1996), "Spatial microbial distribution of nitrifiers and heterotrophs in mixed-population biofilms", *Biotechn.&Bioengin.*, **50**, 24-35.

Paulsen, J. 1997. "Biofilm morphology in porous media: a study with microscopic and imaging techniques", *Wat.Sci. & Techn.*, **36**(1), 1-9.

Ryan, J.R., R.C. Loehr, E. Rucker 1991. "Bioremediation of organic contaminated soils", *J.Hazard.Mat.*, **28**,159-169.

Stelmack, P.L., Gray, M.R., Pickard, M.A., (1999), "Bacterial adhesion to soil contaminants in the presence of surfactants", *Appl.Env.Microbiol.*, **65**, 163-168.

Stringfellow, W.T., Aitken, M.D., (1995), "Competitive metabolism of naphthalene, methyl naphthalenes and fluorine by phenanthrene-degrading pseudomonas", *Appl. Environm. Microb.*, **61**, 357-362.

Taylor, S., P. Jaffe 1990. "Biofilm growth and the related changes in physical properties of a porous medium – 1. Experimental Investigation", *Wat.Res.Research.*, **26**(9), 2153-2159.

Vandevivere, P., P. Baveye 1992. "Saturated hydraulic conductivity reduction caused by aerobic bacteria in sand columns", *Soil Science Society of America Journal*, **56**(1), 1-3.

Yang, X., Beyenal, H., Harkin, G., Lewandowski, Z., (2000), "Quantifying biofilm structure using image analysis", *J. Microb. Methods*, **39**, 109-119.

Yuan, S.Y., Wei, S.H., Chang, B.V., (2000), "Biodegradation of polycyclic aromatic hydrocarbons in a mixed culture", *Chemosphere*, **41**, 1463-1468.

Chapter 5

BIOFILM FUNCTION-STRUCTURE STUDIES DURING BIODEGRADATION OF MEDIUM-MOLECULAR WEIGHT PAHS AND MIXTURES

5.1 ABSTRACT

Complex mixtures of polycyclic aromatic hydrocarbons and other organic compounds are usually present in contaminated sites. This may influence biodegradation patterns and changes in biofilm growth and development. Biodegradation studies of naphthalene, phenanthrene and pyrene were conducted in sole-substrate systems and in binary and tertiary mixtures to examine substrate interactions on biofilms in porous media systems. It was shown that phenanthrene and pyrene could not be degraded as sole carbon sources in the system, but binary systems of the 3 and 4-ring PAHs with acetate and naphthalene supplements stimulated their degradation, with up to 87.9% and 70.1% removal efficiencies, respectively. However, in the tertiary systems the presence of phenanthrene inhibited pyrene degradation. Adsorption of PAHs to sand media was determined to be negligible. Biofilm growth, development and changes in composition were analyzed over time; these showed increases in both firmly and loosely attached viable biomass, as well as extracellular polymeric substance production that formed a complex matrix. Heterogeneous surface films and a variety of biological aggregate structures and growth patterns were observed by confocal microscopy.

5.2 INTRODUCTION

The contamination of soil and groundwater at Superfund sites by Polycyclic Aromatic Hydrocarbons (PAHs) is very common. PAHs are a group of aromatic compounds, usually produced by the incomplete combustion of coal, oil and gas, garbage and other organic substances. The main concern with PAHs is based on their unique characteristics: high levels of toxicity, microbial recalcitrance, high potential for bioaccumulation and high occurrence in the environment (Ryan *et al.*, 1991).

Substrate interactions complicate the biodegradation kinetics in PAH-contaminated environments. When in mixtures, PAHs can influence positively or negatively the rate and extent of biodegradation of other PAH components. Sometimes, cometabolic interactions enhance degradation of higher molecular weight PAHs, when soil consortia utilize inter-metabolites. In other cases, competitive inhibition was observed when PAHs were metabolized by a common enzyme system, with the degradation of 2 or 3-ring compounds preferred, and delay or decrease of the degradation of more persistent PAHs. Tiehm and Fritzsche (1995) showed that compounds such as anthracene, fluorene and pyrene do not support the growth of an aerobic mixed culture as a sole carbon source, but necessarily depended on the presence of more soluble PAHs. On the other hand, inhibition was reported by Stringfellow and Aitken (1995), who found that phenanthrene degradation was decreased in the presence of naphthalene, methylnaphthalene or fluorene. Both cometabolic and inhibitory effects have frequently been observed and

widely reported in the literature (McNally *et al.*, 1999; Bouchez *et al.*, 1999; Yuan *et al.*, 2001; Dean-Ross *et al.*, 2002).

The objective of this study was to examine the cometabolism/cross feeding and competitive inhibition effects of multisubstrate utilization of PAHs by biofilms in porous media. Naphthalene, phenanthrene and pyrene were studied in varying mixture combinations under aerobic conditions in simulated sandy aquifers. This study contributes to expanding the information on PAH biodegradation from single to multisubstrates in contaminated sites, and the role of the biofilm matrix in transporting nutrients and PAH-contaminants to biofilm microorganisms.

5.3 MATERIALS AND METHODS

Lab-scale reactors were constructed from 30-cm long, 3.8-cm diameter glass columns. The columns were equipped with five sample ports for pore water samples along the length of the column, as well as four flow cell ports used for examination of biofilm growth. A schematic diagram of the experimental setup can be found in **Chapter 3**. A nutrient solution was pumped through PAH feed generation columns filled with glass beads coated with solid PAHs, to produce dissolved PAH concentrations; sufficient contact time (around 45 minutes) for feed solution components was allowed in the generating columns to achieve the desired feed PAH concentrations of approximately 10 mg/L naphthalene, 1.0 mg/L phenanthrene and 0.1 mg/L pyrene. Generation columns were regenerated with solid PAHs every two weeks, in order to keep the influent PAH

concentrations constant. **Table 5.1** shows the parameters for the PAH feed generation columns used in these series of experiments. Details on the preparation of these columns are described in **Appendix D**.

Table 5.1 PAH feed generation column parameters.

Length/diameter	90 cm/4.75 cm
Glass bead diameter	4 mm
Flowrate	4 mL/min
Detention time	45 min
Mass of PAH(s) dissolved in solvent per mass of glass beads	15 g NAPH, 10 g PHE, 10 g PYR in 100 mL DCM per 1 Kg of glass beads

NAPH: naphthalene, PHE: phenanthrene, PYR: pyrene, DCM: dichloro-methane

Linear pore water velocity through the silica sand column was maintained at 5 m/d, and a sodium acetate solution (10 mg/L) was used in the system for development and enhancement of biofilm. Aerobic conditions were always maintained in the reactors with the aid of a small dose of hydrogen peroxide (3.5%).

The enrichment culture for inoculating the soil columns was started with a mixed liquor sample from an activated sludge aeration tank, taken from a domestic wastewater treatment plant (Polk Run WWTP, Cincinnati, OH). Mixed cultures have been shown to degrade several PAHs at significantly higher rates than individual bacterial strains because of their broader enzymatic capabilities (Yuan *et al.*, 2000). The columns were

operated for a period of 6 weeks with acetate as a primary substrate, prior to PAH addition, in order to develop a suitable biofilm.

Pore water samples were taken twice a week and analyzed for the contaminant concentration, dissolved oxygen (DO) and pH. Biofilm composition analysis was performed by taking samples from each flowcell at 1, 14 and 22 weeks of the experimental run. Total and viable biomass (firmly and loosely attached biomass) were measured, as well as carbohydrate and protein concentrations. A scanning confocal laser microscope was used to observe the physical structure, heterogeneity and growth patterns of biofilm in the flow cells. Samples were stained with BacLight® fluorescent stain to determine viability of cells within the biofilm. Detailed description of analysis procedures and composition of the feed solution can be found in **Chapter 3**.

5.4 RESULTS AND DISCUSSION

Two main columns were used in this study (Columns 2 and 4) to test the biodegradation of sole-substrate, binary and tertiary mixtures of PAHs. Killed control columns (Columns 1 and 3) were operated simultaneously and at the same conditions as the main columns, but with the addition of sodium azide (1g/L), to minimize biomass growth. **Table 5.2** summarizes the sequence of the experiments over a period of 22 weeks. Influent DO was maintained at 8-9 mg/L, whereas the effluent ranged between 0.5 and 1.0 mg/L, so it can be inferred that aerobic conditions were not limiting biological processes. The pH was maintained between 7.2 and 7.5 during the run.

Table 5.2 Summary of sequence of experiments.

	Pyrene Studies	
	Column 1 (Control)	Column 2
Binary mixture 1 (BM1)	PYR, AC + Az	PYR, AC
Sole-substrate (SS)	PYR + Az	PYR
Binary mixture 2 (BM2)	PYR, NAPH + Az	PYR, NAPH
Tertiary mixture (TM)	PYR, NAPH, PHE + Az	PYR, NAPH, PHE
	Phenanthrene Studies	
	Column 3 (Control)	Column 4
Binary mixture 1 (BM1)	PHE, AC + Az	PHE, AC
Sole-substrate (SS)	PHE + Az	PHE
Binary mixture 2 (BM2)	PHE, NAPH + Az	PHE, NAPH
Tertiary mixture (TM)	PHE, NAPH, PYR + Az	PHE, NAPH, PYR

PHE: phenanthrene, PYR: pyrene, NAPH: naphthalene, AC: acetate, AZ: azide

5.4.1 Phenanthrene Biodegradation Studies

Biodegradation of phenanthrene was initially enhanced by the addition of acetate (BM1) for the first 9 weeks, during which 87.9% removal of phenanthrene was achieved (**Figure 5.1**). Phenanthrene as a sole-substrate (SS) was then tested for the following 3 weeks and a sudden decrease in its biodegradation (to only 8.5% removal) was observed; the metabolism of the contaminant appeared to be strongly dependent on the more easily-degradable carbon source. Similar behaviors on the transformation of phenanthrene with addition of acetate, yeast extract, acetate, glucose and pyruvate were reported by Yuan *et al.* (2000), with acetate being the second most preferable carbon source for enhancing phenanthrene degradation. In addition, phenanthrene metabolism by *Pseudomonas* sp. in soil is known to produce pyruvate and/or acetate as intermediate products (Juhazs *et al.*, 1997), which may act as co-substrates. Reapplication of acetate for a period of 1 week

then allowed the system to recover back to the initial phenanthrene removal efficiency (around 92.3%).

A binary mixture of phenanthrene and naphthalene (BM2) was then added into the columns between weeks 13 and 20. Two main points were observed for the two PAHs during this phase: first, a transition stage of 2 weeks occurred where the biofilm was getting acclimated to utilizing the 2-ring PAH and, therefore, a decrease in the 3-ring PAH degradation efficiency was observed, down to 31.7%. Second, naphthalene was later readily biodegraded, and its removals were measured to be as high as 99.9%, while phenanthrene degradation slowly increased up to 75.6%. This indicates the strong need of

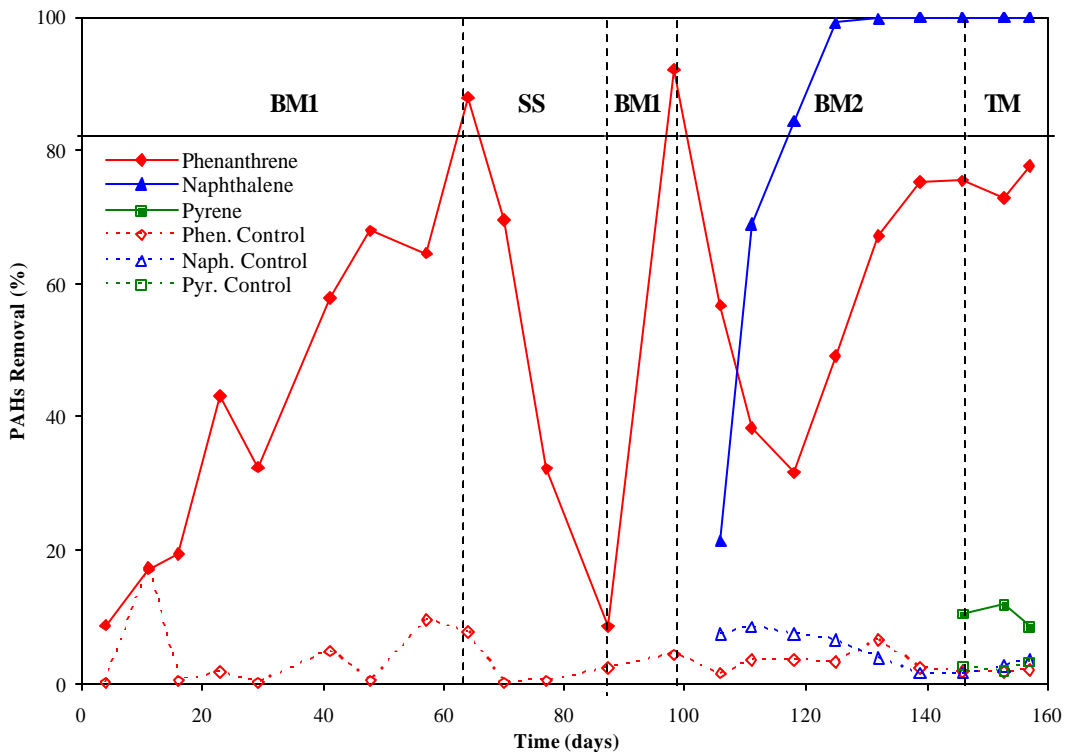


Figure 5.1 Removal efficiencies for sole-substrate and binary and tertiary mixtures of PAHs during phenanthrene studies.

a co-substrate, as in the first binary mixture. Previous reports have documented that PAH-degrading bacteria utilize common enzymes for the degradation of two or more PAHs, while cometabolism is occurring. It has been shown that enzymes for naphthalene degradation in certain strains were found to be involved in the degradation of phenanthrene and anthracene, especially in *Pseudomonas* (Menn *et al.*, 1993). Several researchers (Stringfellow and Atkin, 1995; Bouchez *et al.*, 1999) observed a competitive inhibition during the degradation of phenanthrene in the presence of a second PAH, whether the second PAH was used as a growth substrate or cooxidized, and such competition can be expected when PAHs are metabolized by a common enzyme system. On the contrary, in other studies (Mueller *et al.*, 1989; Tiehm and Fritzsche, 1995; McNally *et al.*, 1999), it was shown that naphthalene enhanced the degradation of phenanthrene through cometabolic mechanisms.

Tri-component experiments (TM) were then carried out in the final two weeks of the run. Naphthalene degradation did not appear to be affected by the presence of phenanthrene or pyrene, and phenanthrene degradation was maintained at 77.8%. This has been confirmed by McNally *et al.* (1999) and Guha *et al.* (1999), but naphthalene biodegradation was shown to occur slower in ternary mixtures than in the sole-substrate system. In the experiments, pyrene failed to biodegrade, probably due to competition for the common enzymes in the system; the final biodegradation percentage of pyrene was around 11.2% in the tertiary mixture, indicating a preference for more soluble PAHs. Similar inhibition behaviors have been reported by Stringfellow and Aitken (1995), Dean-Ross *et al.* (2002) and McNally *et al.* (1999) in suspended culture: mixtures of three or more PAHs usually

compromised the degradation of the higher molecular weight PAHs, because of products and/or toxicity produced during metabolism of other PAHs (Bouchez *et al.*, 1999) and consumption of common enzymes.

5.4.2 Pyrene Biodegradation Studies

Column experiments with pyrene and acetate (BM1) were conducted for 10 weeks, as shown in **Figure 5.2**. Two important stages were observed: a lag phase of 7 weeks, when pyrene degradation was delayed, probably due to an acclimation period of the mixed culture to utilize the enzymes needed for the metabolism of the 4-ring PAH, and the subsequent 3 weeks, when it was successfully biodegraded (up to 54.8%). Acetate clearly enhanced pyrene degradation, acting as a co-substrate, which may have increased the biomass of degraders, and therefore, the enzymatic capabilities for the removal of a more recalcitrant compound, such as the 4-ring PAH.

Degradation of pyrene was then measured when it was used as a sole-substrate (SS) for the mixed culture, but removal significantly decreased to 14.8% in less than 3 days; in this case, cells showed total inability to utilize pyrene in the absence of the primary substrate. Several authors (Clinge *et al.*, 2001, Guieysse *et al.*, 2001) have reported the poor biodegradation of pyrene individually, usually less than 20%, while others (Ramirez *et al.*, 2001, Eriksson *et al.*, 2002) have found pyrene in soil-water slurries can achieve up to 50-60% removal efficiencies. The reason of these different trends can be attributed to distinct pure cultures acclimated for the 4-ring PAH and microbial interactions in the

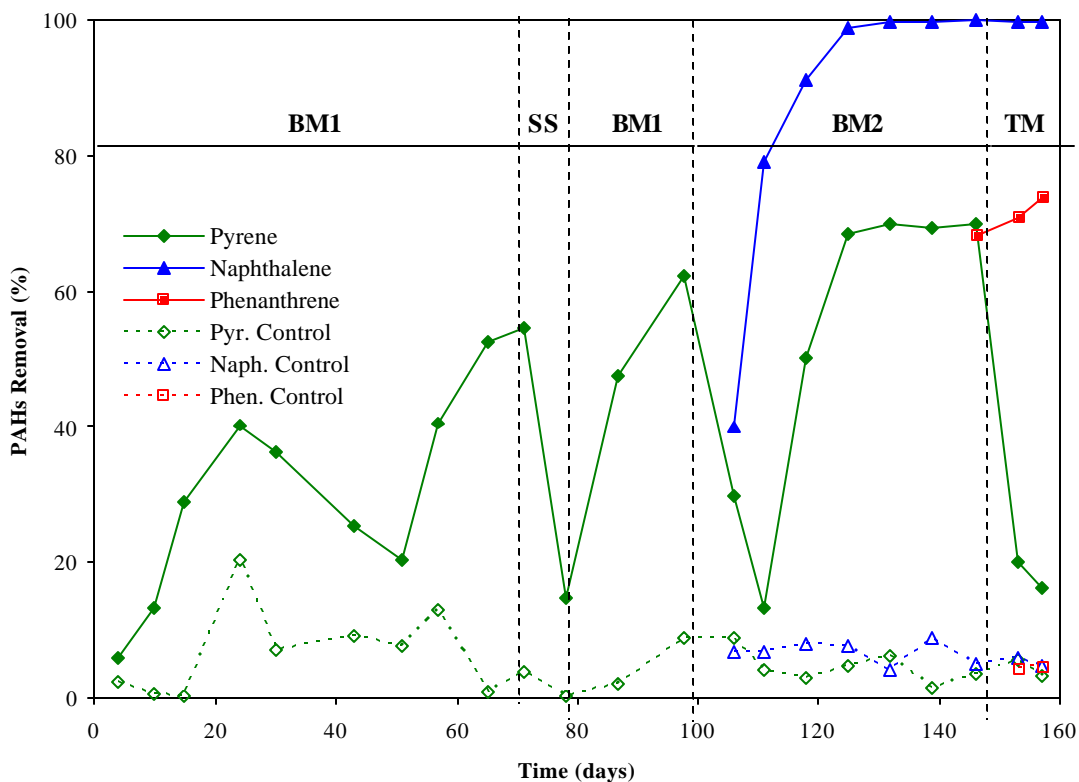


Figure 5.2 Removal efficiencies for sole-substrate and binary and tertiary mixtures of PAHs during pyrene studies.

consortia. Song (1999) reported the mineralization of sole-carbon source pyrene by white rot fungi in soils, but only 15% was achieved compared to biodegradation experiments with bacteria, and an average of 30% was incorporated into fungal biomass, either as precipitated or adsorbed pyrene. In these experiments, pyrene degradation increased to 62.2% after once again amending with acetate for another 2.5 weeks and recovering the initial successful removal efficiency.

A binary mixture of pyrene and naphthalene (BM2) was later evaluated between weeks 13 and 20; it showed similar behavior as in the acetate addition experiment. Naphthalene

was easily degraded within 2 weeks, up to 99.7%, while pyrene experienced a lag phase, with a decrease of its degradation down to 13.1% followed by an increase to 70.1%, due to cometabolism. This could be explained by the results of Bouchez *et al.* (1999), who have suggested that compounds with structural similarities and the broad specificity of some enzymes may enhance substrate interactions, especially for higher molecular weight PAHs.

Tertiary mixtures (TM) run over the remaining 2 weeks showed the 3-ring PAH significantly inhibiting pyrene from degrading. Phenanthrene reached 73.4% removal, while pyrene achieved only 16.1% removal in the 3-component system. McNally *et al.* (1999) described exactly the same behavior for a 2-, 3- and 4-ringed PAH mixture in the presence of pure batch cultures. The inhibitory behavior of phenanthrene on pyrene has been shown in several studies (Stringfellow and Aitken, 1995, Molina *et al.*, 1999), where competition for the initial enzymes in the biodegradation pathway could result in competitive inhibition of substrates with higher molecular weight; slow induction of enzymes could also cause the lag in biodegradation of 4 and more ring PAHs (Lotfabad *et al.*, 2002). Even when acclimated bacterial strains were used for individual PAH degradation, their performance was not really as satisfactory for the degradation of the mixtures as when mixed cultures were utilized, because of the inability of some microorganisms to use byproducts and enzymes of other microorganisms. In these experiments, pyrene degradation was not totally inhibited by phenanthrene, as it is reported in the majority of studies in the literature, meaning that mixed consortia may provide a wider variety of bacteria that demonstrates an advantage in soil bioremediation.

5.4.3 PAH adsorption onto sand medium

PAH concentration profiles in the sand media were obtained at the end of the experimental run, after 22 weeks, for both the phenanthrene and pyrene studies. They represent final killed biomass PAH concentrations, after sodium azide addition. Results of PAH adsorption to sand media are presented in **Figure 5.3** (for phenanthrene biodegradation studies) and **Figure 5.4** (for pyrene biodegradation studies).

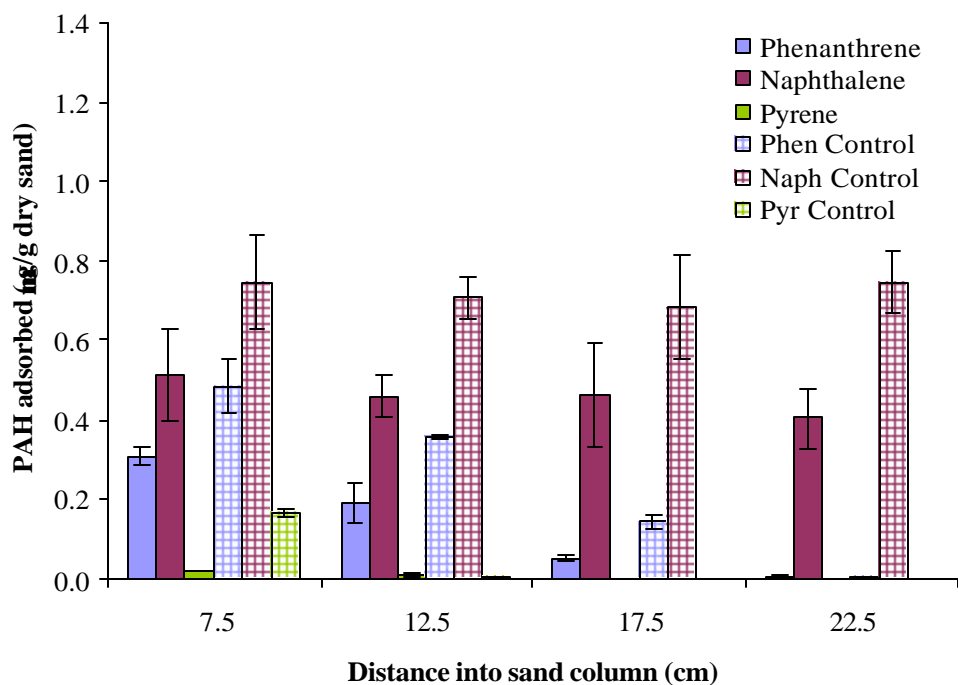


Figure 5.3 PAH adsorbed onto sand during phenanthrene studies after 22 weeks.

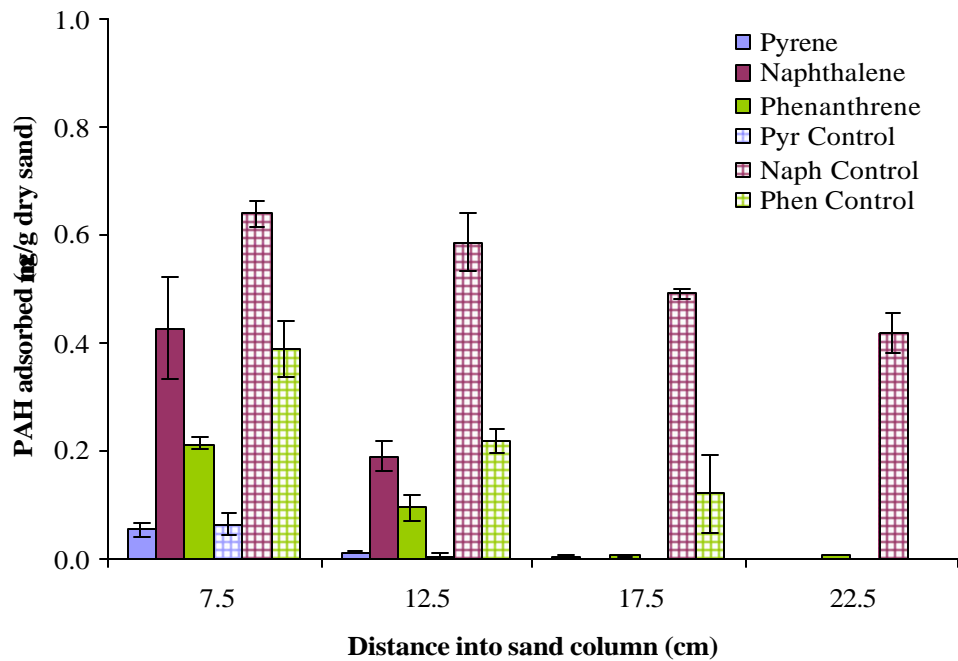


Figure 5.4 PAH adsorbed onto sand during pyrene studies after 22 weeks.

In the phenanthrene studies, the phenanthrene concentration at 7.5 cm was 0.31 ± 0.02 $\mu\text{g/g}$ dry sand, and decreased to 0.18, 0.05 and 0.01 $\mu\text{g/g}$ dry sand at 12.5, 17.5 and 22.5 cm, respectively. Additionally, an average of 0.46 ± 0.07 $\mu\text{g/g}$ dry sand of naphthalene was found adsorbed on the media throughout the sand column. Pyrene concentrations were almost negligible (less than 0.02 $\mu\text{g/g}$ dry sand), even at the inlet of the column. The control column, continuously killed with sodium azide from the beginning of the experiments, showed increases in PAH concentrations onto the sand with respect to the inoculated column of 31% for phenanthrene, 35% for naphthalene and 87% for pyrene, at the inlet of the column, although all the PAH concentrations are still considered insignificant.

In the case of the pyrene studies, a similar trend was observed for PAH sorption onto sand. Pyrene concentrations varied from 0.05 $\mu\text{g/g}$ dry sand (at 7.5 cm) to non-detectable (at 17.5 and 22.5 cm). Naphthalene showed maximum sorption at the inlet of the column with $0.43 \pm 0.09 \mu\text{g/g}$ dry sand; this was decreased by half in the following 5 cm and became non-detectable later in the sand column. Phenanthrene concentration at 7.5 cm was $0.21 \pm 0.01 \mu\text{g/g}$ dry sand, and decreased to 0.09 and 0.01 $\mu\text{g/g}$ dry sand at 12.5, 17.5 and 22.5 cm respectively. Again, the control column showed higher increase in PAH sorption onto sand with respect to the inoculated column, with increases of 13% for pyrene, 44% for naphthalene and 33% for phenanthrene.

Sand medium PAH concentration profiles therefore played little or no role in the removal mechanisms, since final killed biomass concentrations of the three compounds were measured in very low concentrations. Biological degradation was therefore the main component in the mineralization of the three PAHs and their mixtures.

5.4.4 Biofilm composition

Biofilm development and changes in composition were obtained at 1, 14 and 22 weeks. During the phenanthrene experiments, the highest total biomass values were observed in the first 7.5 cm of the column at 145 (at 1 week), 801 (at 14 weeks) and 2375 $\mu\text{g/g}$ TS (at 22 weeks) during the experimental run (**Figure 5.5**). These values decreased with depth into the column, localizing most of the biomass at the inlet where most of the contaminant and nutrients were present and available.

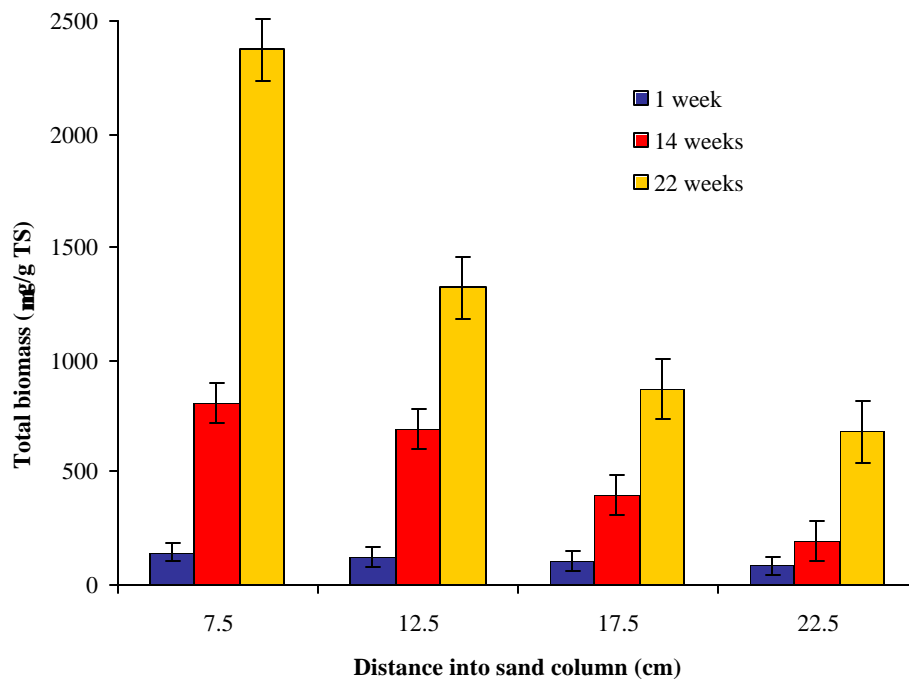


Figure 5.5 Total biomass profile during phenanthrene studies.

Total biomass seemed to increase almost 4 times between the first and the fourteenth week, which was the period when binary mixtures (phenanthrene-acetate and phenanthrene-naphthalene) were fed, indicating the ability of cells to increase their numbers and amount of polymeric substances produced in the presence of low-molecular weight PAHs and easily biodegradable substrates. This may have helped in the establishment of a solid biofilm matrix surrounding the sand grain surfaces and, therefore, promoting successful PAH biodegradation. The presence of tertiary mixtures tripled the amount of total biomass in the sand column (at 7.5 cm) between weeks 14 and 22, indicating a good production of both living cells and exopolymeric substances; the other side ports of the sand column showed at least 100% increase in the biomass, producing an even spatial and temporal distribution of biofilm along the depth of the

column. The killed control column showed 26% of the biomass grown in the main columns, which remained constant over the period of 20 weeks.

During the pyrene studies, an average total biomass of 87 $\mu\text{g/g}$ TS was observed in the first week, showing an even distribution of cells and exopolymeric substances with distance in the column, as described in **Figure 5.6**. An increase of 92% along the column was then found at the second sampling event during the presence of both acetate and naphthalene with the pyrene, as occurred in the phenanthrene experiment; in the last 8 weeks of the run, total biomass increased an average of 28% or 382 $\mu\text{g/g}$ TS. The maximum values of total biomass occurred at the inlet of the column and were 1462 ± 113 (at 14 weeks) and 2034 ± 198 $\mu\text{g/g}$ TS (at 22 weeks). An average of one tenth of total biomass in the inoculated column was found in the killed control column.

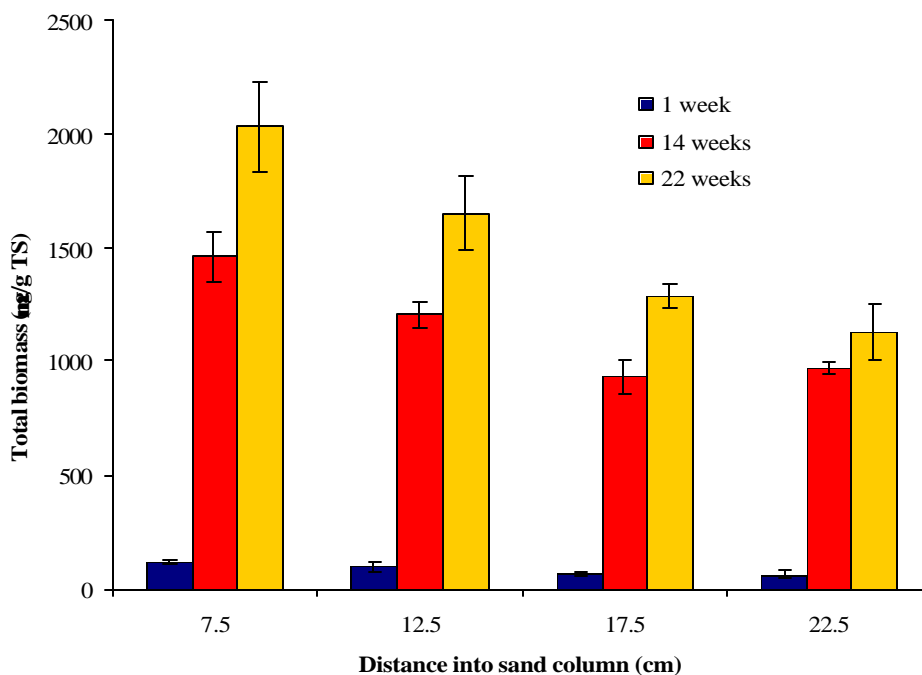


Figure 5.6 Total biomass during pyrene studies.

Results from lipid-phosphate profiles during the phenanthrene run are shown in **Figure 5.7**, indicating that viable biomass increased significantly over time, from 131 ± 20 (at 1 week) to 486 ± 16 (at 14 weeks) and to 682 ± 22 mg/g VS (at 22 weeks) at 7.5 cm. Most of the production of new cells (73% increase at 7.5 cm) was achieved while binary mixtures were present, because acetate and naphthalene were easily usable substrates, and at the same time improved phenanthrene biodegradation. Similar trends of progressive production of new viable biomass were observed across the column, with 50-80% increase in mg LP/mg VS in the first 14 weeks. In the last 8 weeks, the viable biomass amount increased only 32% on average across the depth of the column, which can be explained by an already well-established biofilm whose purpose was to degrade the tertiary mixtures for sustenance and not to create new living cells. The total LP remained relatively constant at the end of the run, with an average of 559 mg/g VS.

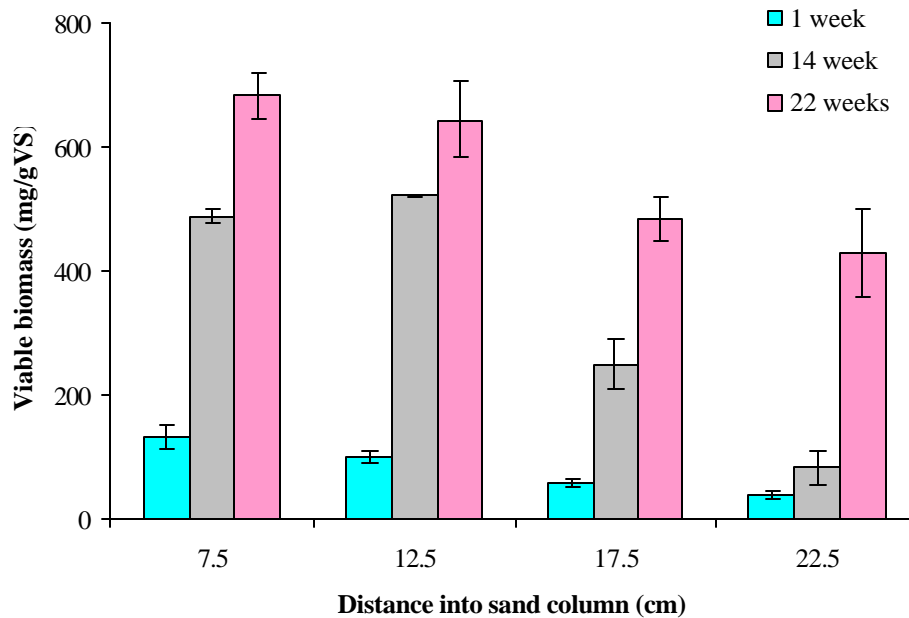
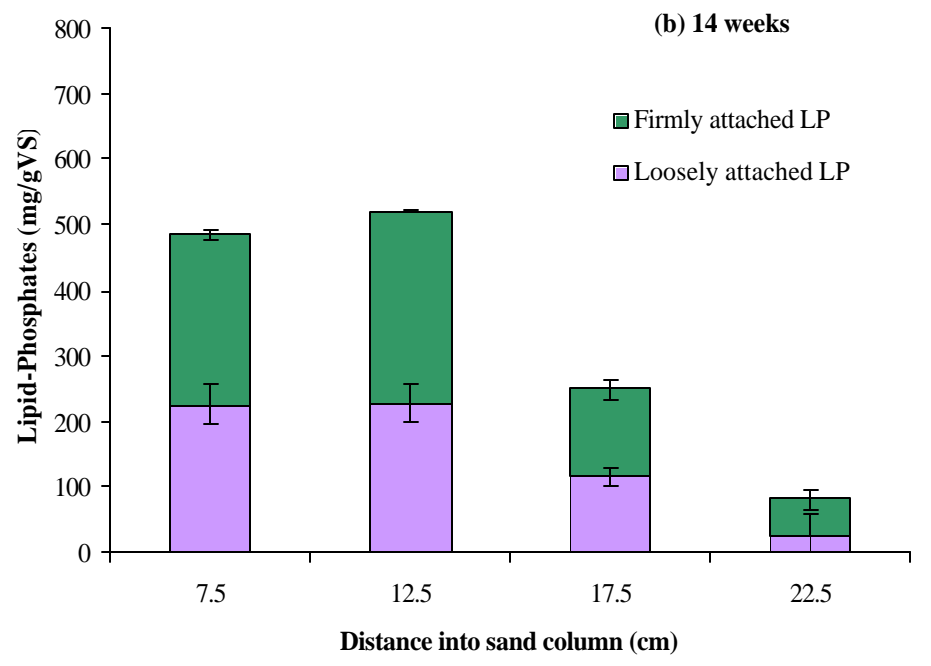
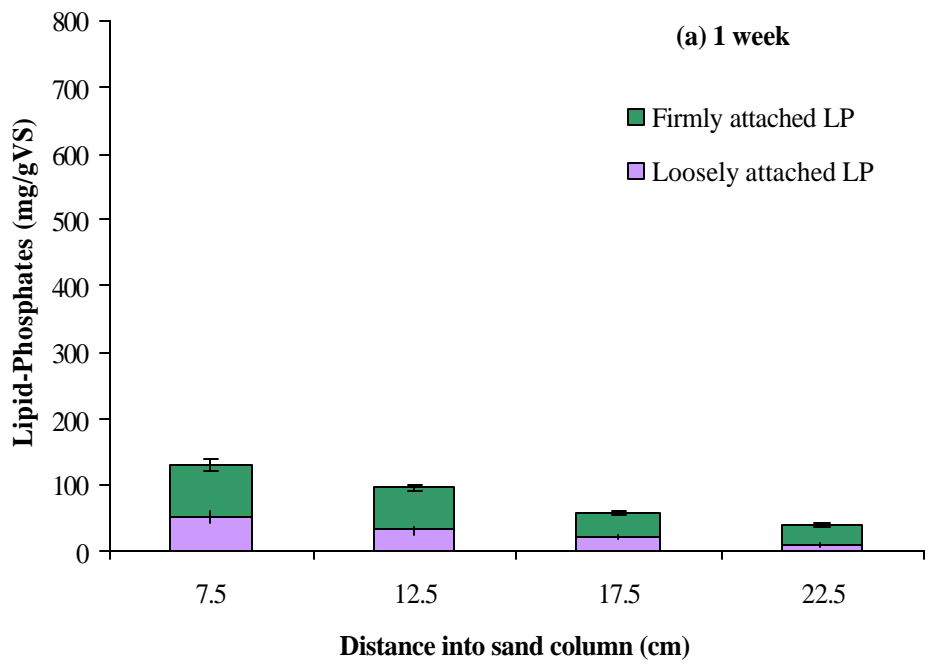


Figure 5.7 Viable biomass profile during phenanthrene studies.

In the killed control column it was observed that the viable biomass was only one tenth of that in the inoculated column; sodium azide concentrations may not have been strong enough to kill all of the biomass during the phenanthrene experiments.

Firmly attached biomass (monolayer of surface biofilms directly attached to sand grain surfaces) and loosely attached biomass (cell aggregates and protrusion bodies easily separated from the media) compose the viable biomass. During the phenanthrene run, firmly attached biomass was observed to be the most important fraction of the total lipid-phosphates, not only with distance into the sand column, but also with time (**Figure 5.8 (a), (b) and (c)**). It averaged at 65.6% (at 1 week), 57.8% (at 14 weeks) and 56.1% (at 22 weeks) of the total LP, along the depth of the column. Maximums at 7.5 cm from the inlet were measured at 79 ± 10 (at 1 week), 261 ± 4 (at 14 weeks) and 366 ± 30 mg/g VS (at 22 weeks), but during the 14th and 22nd weeks, firmly attached biomass was also significantly important at 12.5 cm. This may be the result of the biodegradation of the medium molecular weight PAH further into the column, once the more easily-degradable substrates were mineralized at the inlet, because of a better-established biofilm. The highest increase in firmly attached biomass occurred while the binary mixtures were present, which contributed to the formation of well-attached biofilm to sand grains; an almost 355 mg/g VS increase was observed at the inlet of the column in the first 14 weeks, while 196 mg/g VS were produced in the last 8 weeks.

Loosely attached biomass remained relatively constant along the depth of the column during the three sampling events. The averages measured were 29, 149 and 249 mg/g



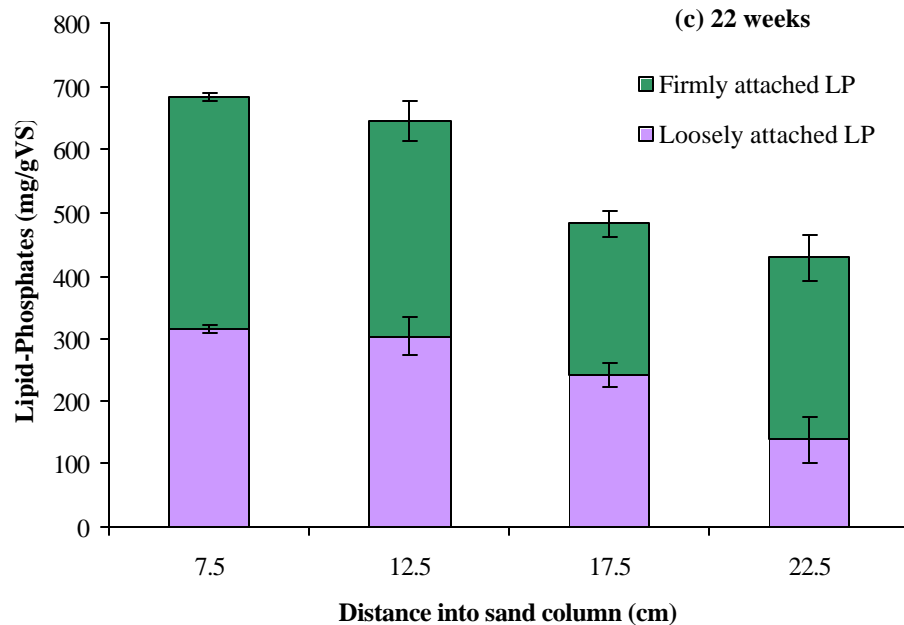


Figure 5.8 Firmly and loosely attached biomass profiles at (a) 1 week, (b) 14 weeks and (c) 22 weeks, during phenanthrene studies.

VS at 1, 14 and 22 weeks, which constituted 34.4%, 42.2% and 43.9%, respectively, of the total lipid-phosphates. Similar to the firmly attached biomass, acetate- or naphthalene-phenanthrene mixtures produced more weakly attached biomass between weeks 1 and 14, with a 77% increase, while only 29% was measured for the periods when tertiary mixtures were present.

The changes in viable biomass distribution, especially between 12.5 and 22.5 cm depths, do not appear to be explained by simple movement of weakly attached biomass further into the sand column, becoming entrapped and creating new firmly attached biomass. Both fractions equally increased over time, indicating growth of both types of biofilm structural forms proportionally to the PAH contaminants. The killed control column

showed a range of 5% to 13% of the firmly and loosely attached biomass grown in the inoculated column during the phenanthrene experiments.

During the pyrene studies, lipid-phosphate analyses provided the profiles indicated in **Figure 5.9**, where viable biomass followed the trend of decreasing concentrations with distance into the column, but increasing amounts over the 22-week period. At the first port, viable biomass was measured to be the highest, with values of 83 ± 17 (at 1 week), 412 ± 38 (at 14 weeks) and 549 ± 60 mg/g VS (at 22 weeks), which were very similar to the concentrations found during the phenanthrene run. At 22 weeks the total LP remained relatively constant along the depth of the column, with an average of 491 mg/g VS. Binary mixtures greatly improved the production of new biomass compared to tertiary mixtures; acetate and naphthalene were the main contributors as substrates to form new

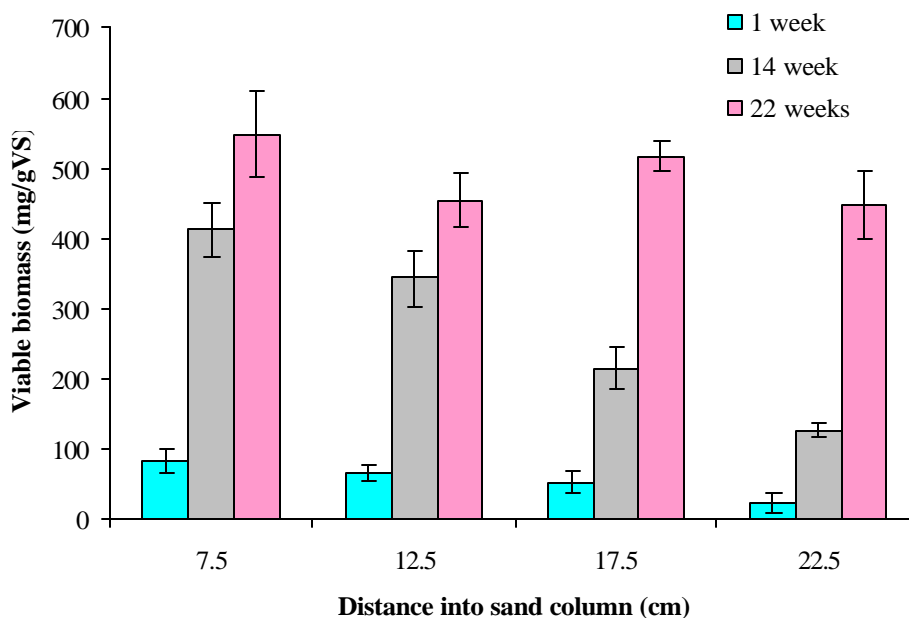
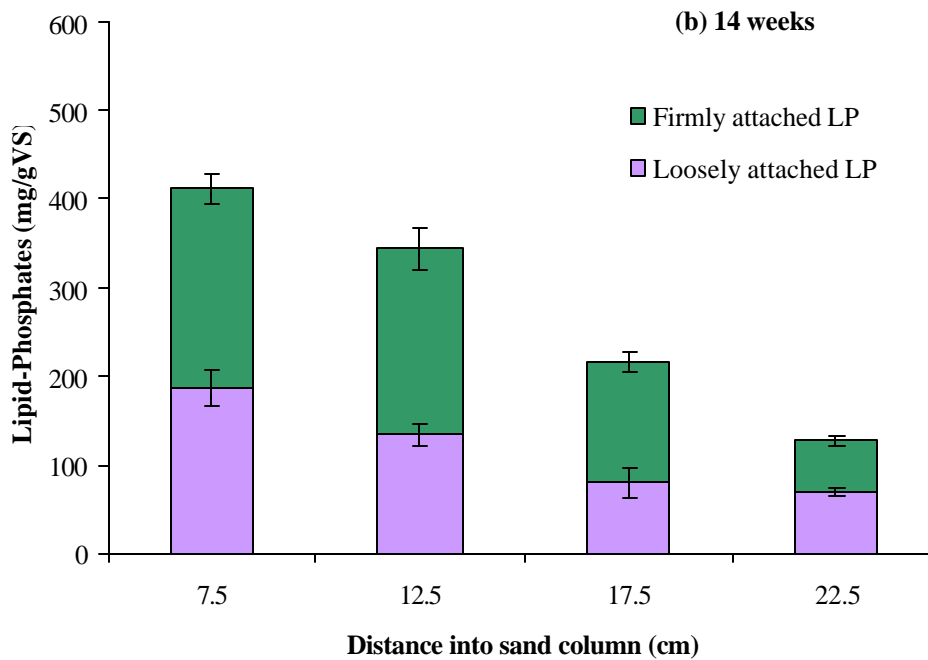
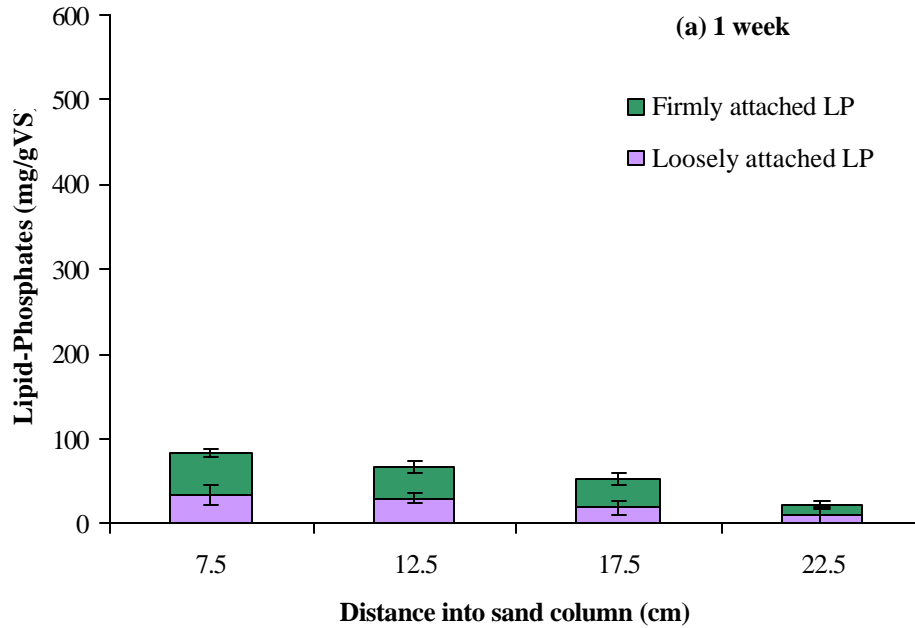


Figure 5.9 Viable biomass profile during pyrene studies.

living cells. This explains the average increase between weeks 1 and 14 that was around 83%, while over the remaining 8 weeks only a 25% increase was observed. The viable biomass in the killed control column during the pyrene experiments ranged from 5 to 15%, with respect to the inoculated column.

Figure 5.10 (a), (b) and (c) describes the firmly and loosely attached biomass in the pyrene studies during the three sampling events. Firmly attached biomass concentrations were always greater than loosely attached biomass, with percent averages of 57.8% (at 1 week), 56.1% (at 14 weeks) and 61.8% (at 22 weeks) of the total lipid-phosphates. The inlet of the column had the maximum concentrations of both fractions of LP, even though the values at 7.5 cm and 12.5 cm seemed to indicate little or no difference for firmly and loosely attached biomass, probably due to the degradation of the medium molecular weight PAHS further into the column. Particularly at the end of the run, loosely attached biomass was evenly distributed with distance into the sand column, at an average of 189 mg/g VS. An increase of 177.6 mg/g VS (at 7.5 cm) in the firmly attached biomass was observed between weeks 1 and 14, which was actually two times the increase over the remaining 8 weeks, thanks to the presence of binary mixtures 1 and 2. The same was the case for the weakly attached biomass, in which the increase in the first 14 weeks corresponded to 151.4 mg/g VS (at 7.5 cm), being three times the increase between the 14th and the 22nd week.

A range from 3 to 12% of the firmly and loosely attached biomass grown in the inoculated column was measured in the killed control column during the pyrene experiments.



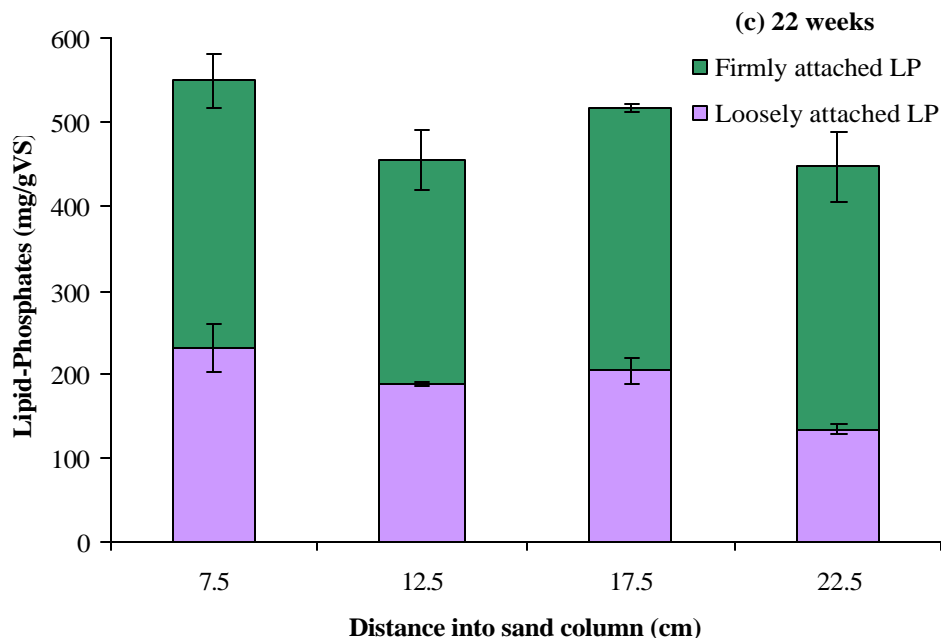


Figure 5.10 Firmly and loosely attached biomass profiles at (a) 1 week, (b) 14 weeks and (c) 22 weeks, during pyrene studies.

Extracellular polymeric substances (EPS) were characterized by measuring carbohydrate and protein contents, which constitute the largest fractions of polymers in the biofilm matrix. Carbohydrate profiles for the phenanthrene studies are shown in **Figure 5.11**, where maximum values of 54 ± 5 (at week 1), 133 ± 7 (at week 14) and 149 ± 37 mg/g VS (at week 22) were observed at 7.5 cm. The first week of the experimental run showed the most even distribution of carbohydrates compared to weeks 14 and 22, with an average of 40 mg/g VS along the depth of the column. A significant increase of 56 to 70% in the carbohydrate amount was observed in the first 14 weeks along the column, explained by the contribution of both binary mixtures 1 and 2. The formation of a solid exopolymeric matrix, which surrounded the bacteria, allowed for colonization of the sand grain surfaces, and promoted higher biodegradation rates of the PAHs. A smaller amount of

new carbohydrate production of 6.8 to 15.7 mg/g VS (or 5 to 11% increase) occurred in the last 8 weeks, due to the presence of the tertiary mixture. A range, varying from 18 to 27% of the carbohydrates present in the main phenanthrene column, was measured in the killed control column in the first week and decreased over time.

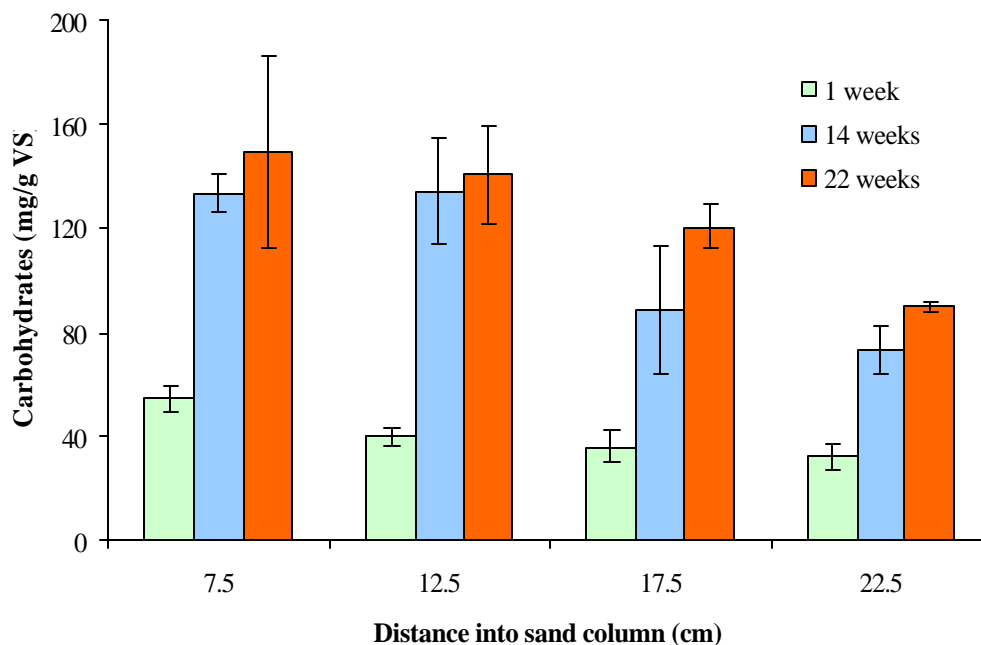


Figure 5.11 Carbohydrate profile during phenanthrene studies.

Figure 5.12 describes the carbohydrate profile during the pyrene studies. As shown, during the three sampling events, the amounts of carbohydrates measured were relatively well distributed along the column, with averages of 25 (at week 1), 85 (at week 14) and 110 mg/g VS (at week 22); particularly at 14 weeks, and between the inlet and 17.5 cm into the sand column, carbohydrates leveled at 96 mg/g VS with a very small standard deviation. The reason was probably the presence of the acetate- or naphthalene-phenanthrene mixtures. The increases between weeks 1 and 14, and 14 and 22 were 64

and 27%, respectively, showing a similar trend compared to the phenanthrene column. An average of 25 mg/g VS were measured along the killed control column, but biomass did not increase with time, thanks to the inhibitor sodium azide.

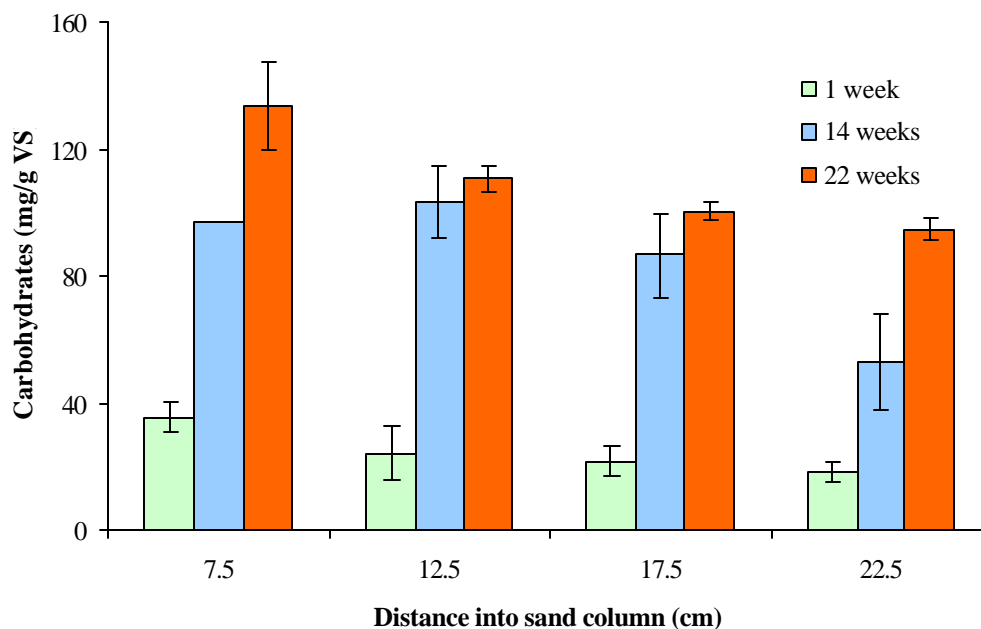


Figure 5.12 Carbohydrate profile during pyrene studies.

During the phenanthrene experiments, the proteins mass per volatile solid mass progressively decreased with increasing distance into the sand bed for the three sampling events, even though week 1 had an average of 8 mg/g VS with a very small standard deviation (**Figure 5.13**). At 7.5 cm, the amounts of proteins were 10.6 ± 5 (at 1 week), 47.2 ± 5 (at 14 weeks) and 63.2 ± 14 mg/g VS (at 22 weeks), which corresponded to the well-formed and established biofilm matrix. Again, like with the carbohydrate results, the protein production was higher at higher substrate loadings and with more easily degradable contaminants (78% increase acetate- or naphthalene-phenanthrene mixtures),

and was also not found to be enhanced in a significant way by the tri-component PAHs (25% increase). Protein results in the killed control column indicated low concentrations during the 22-week experiments.

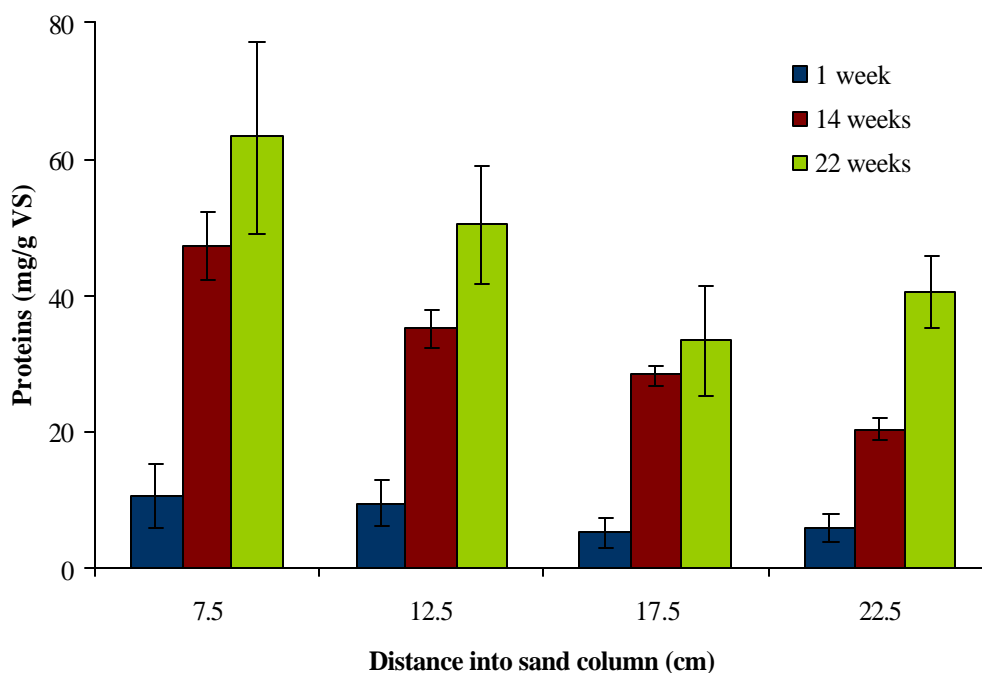


Figure 5.13 Protein profile during phenanthrene studies.

Profiles of protein concentrations during the pyrene studies are shown in **Figure 5.14**. Initial protein amounts were relatively constant with sand column distance, at an average of 7 mg/g VS after 1 week of experimental run, which is a similar result to that found in the phenanthrene column. At weeks 14 and 22, the maximum protein values were observed near the inlet of the column, at 30.9 ± 1 and 42.5 ± 8 mg/g VS respectively. Protein amounts then decreased with depth and leveled out to averages of 16 and 24 mg/g VS, respectively, indicating a better distribution of protein at different locations in the column. It was observed that a higher increase in the protein production (at a percentage

of 74%) occurred in the first 14 weeks, due to the binary mixtures, confirmed also by the carbohydrate results. In the remaining 8 weeks, the increase was not as significant and led to a 27% new production of proteins. The killed control column appeared to show 10% of the protein amounts in the inoculated column.

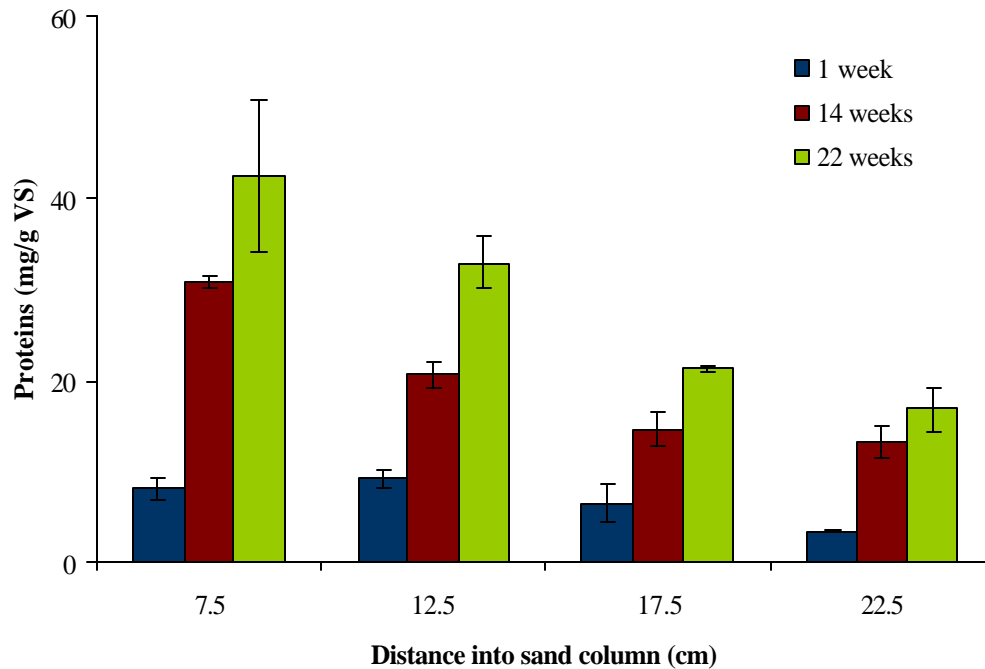


Figure 5.14 Protein profile during pyrene studies.

5.4.5 Biofilm structure

Biofilm structure examination by Confocal Scanning Laser Microscopy was conducted at the second (14 weeks) and the third (22 weeks) sampling events using the flowcells located in the active zone of the sand columns (7.5 cm). **Figure 5.15 (a)** and **(b)** show optical sections of biofilms grown after 14 weeks of the phenanthrene experimental run. Dense biofilm coverage was observed on sand grain surfaces, indicating the presence of

heterogeneous surface biofilms of approximately 20 to 40 μm thickness. Surface biofilms consisted not only of monolayer biofilms, but also of occasional small cluster and cell aggregate structures in the range of 15 to 20 μm in diameter, directly attached to the continuous biofilms. Large cluster-and-protrusion-type structures, ranging from 40 to 80 μm in thickness, were also observed and appeared to actively develop in the pore spaces between soil grains, creating a thick bioweb-type growth. Binary mixtures seemed to increase the biomass per unit sand medium, thanks to easily degradable substrates, such as acetate and naphthalene. The living cells and exopolymeric substances grown under these conditions created a stable biofilm matrix, which not only supported the colonization and survival of a diverse microbial community, but also improved the biodegradation rates of medium molecular weight PAHs and their mixtures over time.

Biofilms grown during the addition of the tertiary mixtures of PAHs are indicated in **Figure 5.16 (a) and (b)**, after 22 weeks of the phenanthrene studies. In this case, thinner surface biofilms were observed, with thicknesses varying from 10 to 20 μm , producing a more continuous distribution of biomass on the sand grains. The appearance of small cluster and cell aggregates weakly attached to the surface biomass was less frequent and smaller in size (between 10 to 15 μm). Large protrusions of 80 to even 100 μm were noted to be growing in selected zones, but these structures may have been formed in early stages of the run and slowly enlarged during the tri-component mixtures, which confirms the small new production of lipid-phosphates, proteins and carbohydrates in the last 8 weeks.

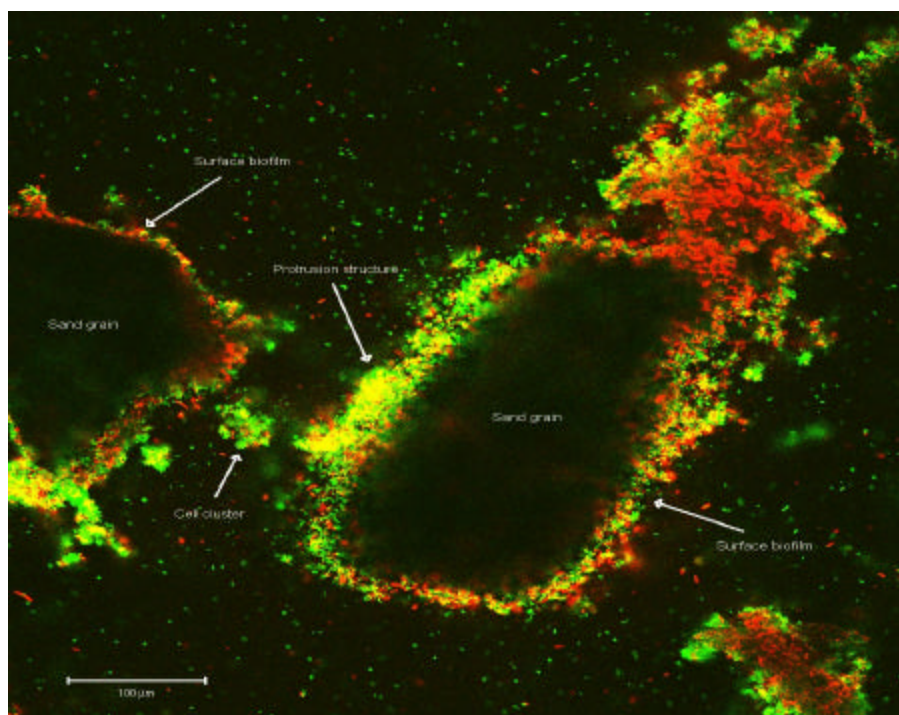
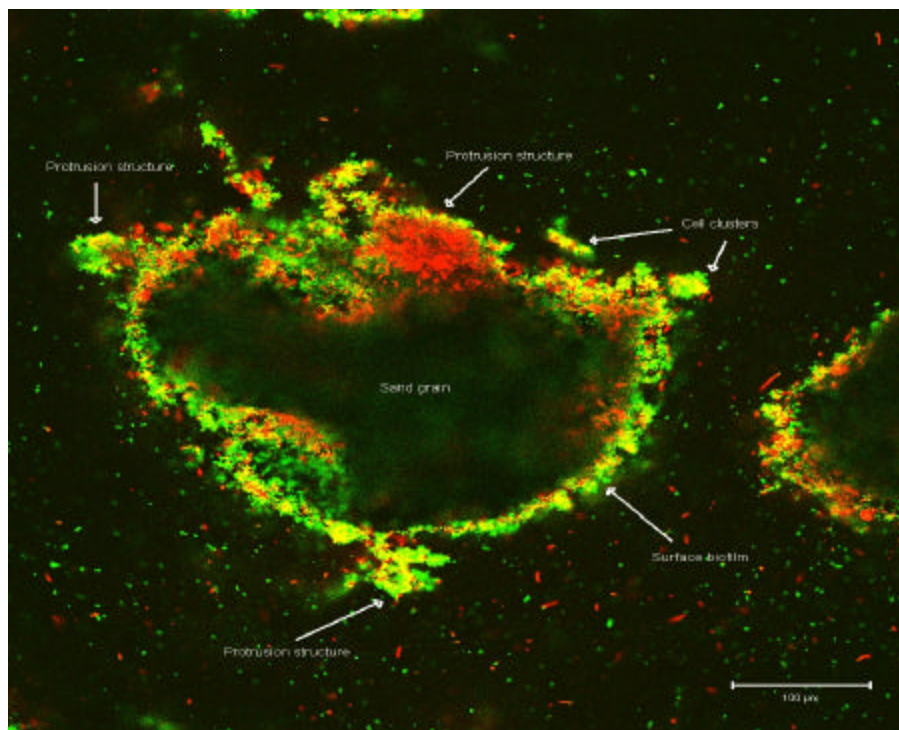


Figure 5.15 Optical sections of biofilms on sand grain surfaces at 7.5 cm (a) at 40x and (b) 20x magnifications, during phenanthrene studies after 14 weeks.

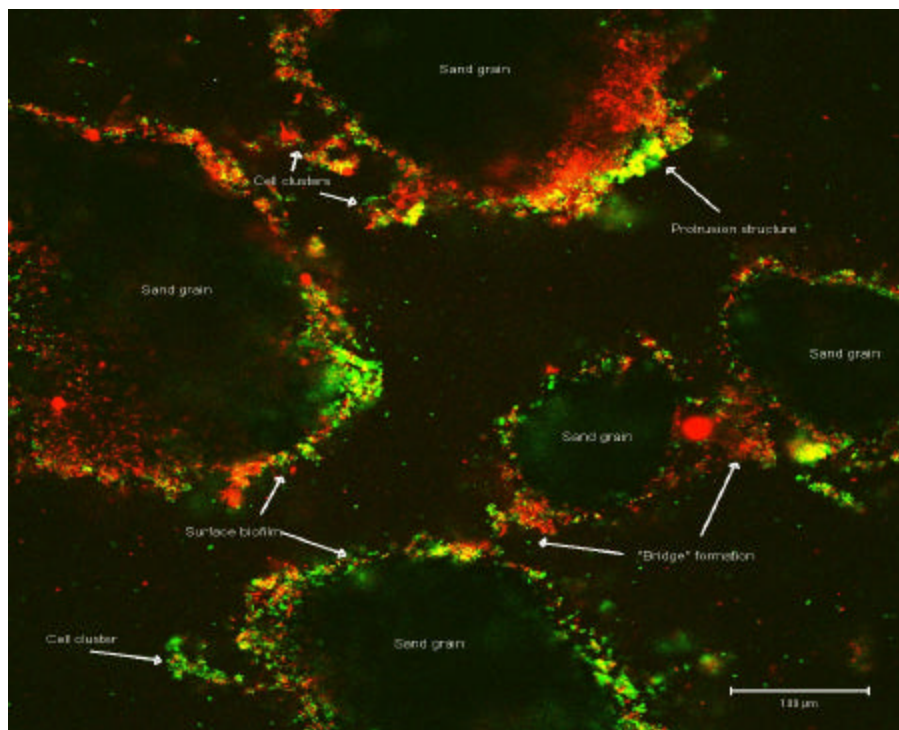
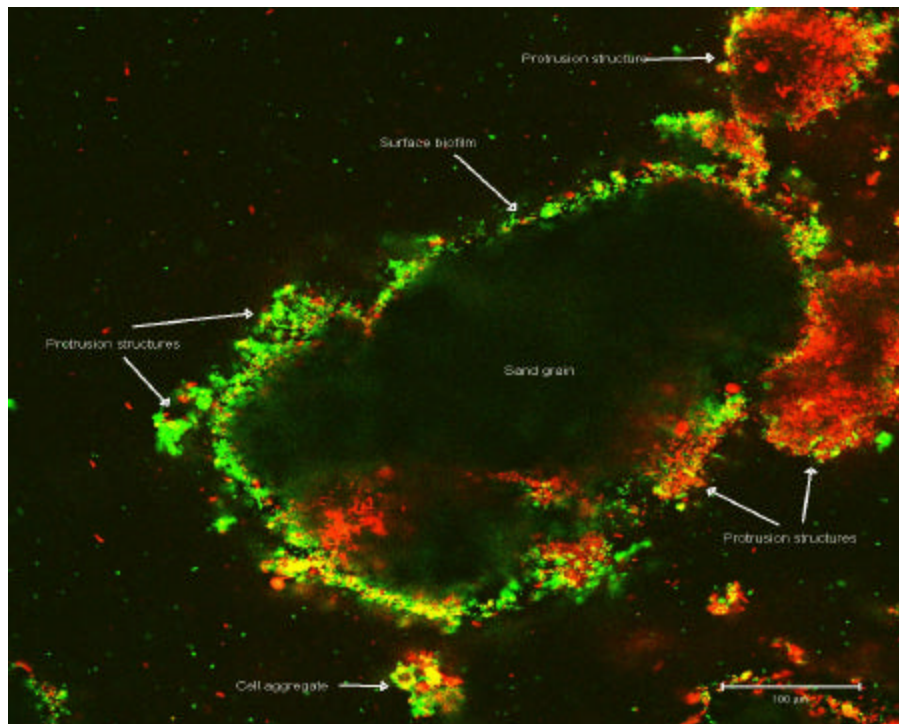


Figure 5.16 Optical sections of biofilms on sand grain surfaces at 7.5 cm (a) at 40x and (b) 20x magnifications, during phenanthrene studies after 22 weeks.

The optical sections of biofilms grown at the inlet of the pyrene column after 14 weeks are shown in **Figure 5.17 (a)** and **(b)**. Monolayer-type growth was common, with a base biofilm of approximately 15 to 20 μm in thickness; even so, frequent small cell clusters (10-15 μm in diameter) were also present, creating a heterogeneous surface biofilm. Other structures such as protrusions and aggregates were formed in areas of low pore water velocity; living cells and EPS material may have been accumulated in such a dense manner that they created large clusters, ranging between 50 and 90 μm in diameter. The pore spaces between sand grains were frequently filled with “biofilm bridges”, which were the interconnections of surface biofilms between two or more soil particles. This explained the “bioweb” network of fibrillar strands, with sparse and heterogeneous coverage of bacterial aggregates, varying in size and shape.

After 22 weeks of operating the pyrene column, a surface biofilm covered the sand grains with layers of 10 to 15 μm in thickness, as shown in **Figure 5.18 (a)** and **(b)**. Some localized small diameter strands and aggregates of cells (of approximately 10 to 20 μm in size) were also present, but the major protrusions observed were the large clusters formed between immediately adjacent sand grains. The size of these protrusions was between 50 to 100 μm in length, creating a web-like system of active biomass. These thick aggregates and cluster-type structures were not necessarily attached to soil particles and were probably formed during the binary mixture stage.

Ebihara *et al.* (1997, 1999) conducted similar work on structural characterization of biofilm grown on porous media, while degrading PAHs. His results indicated the

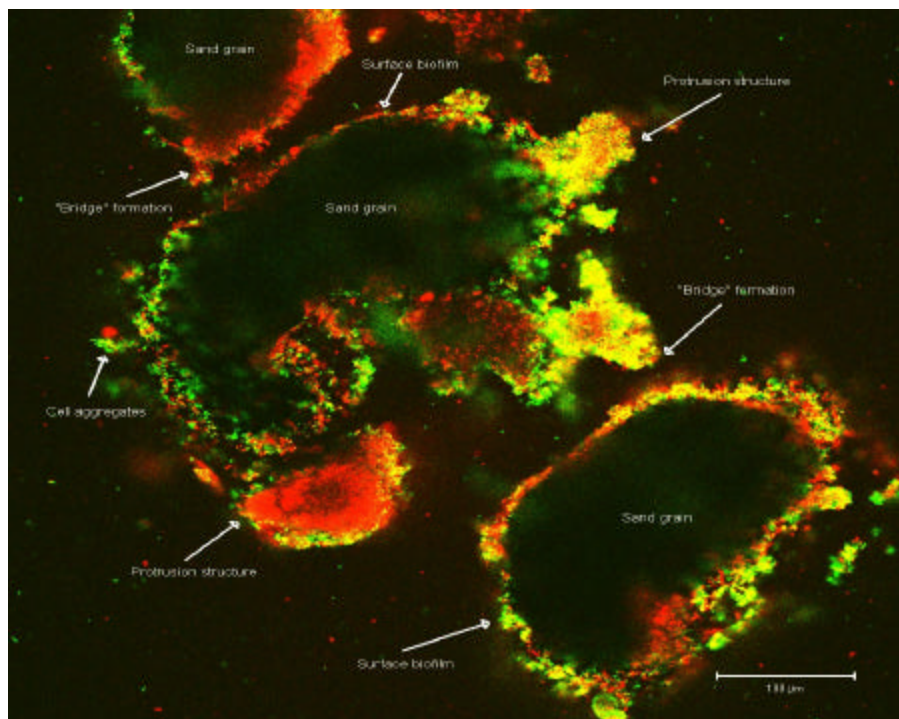
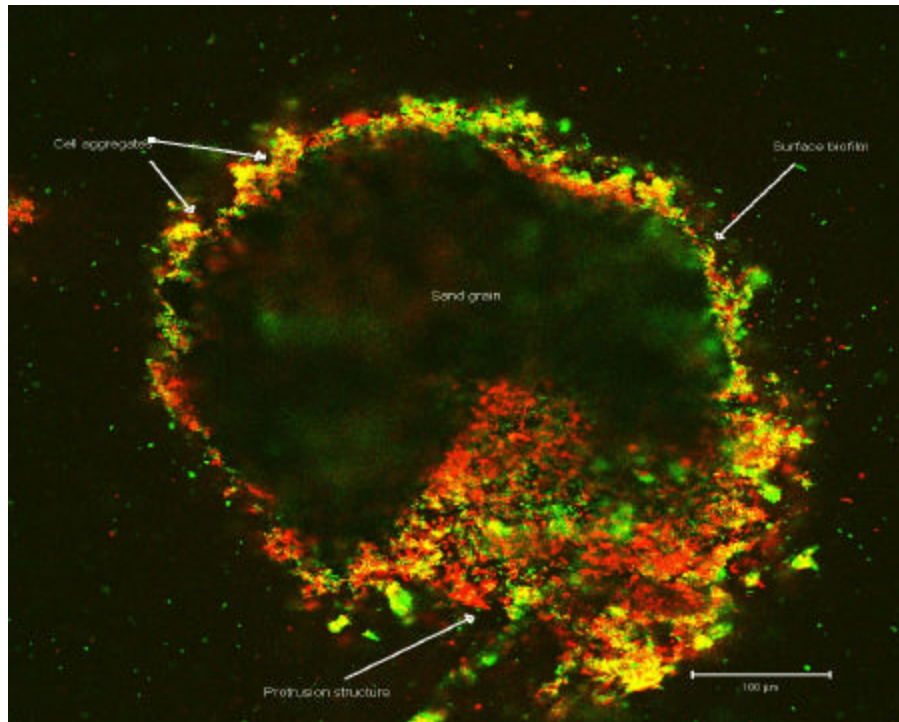


Figure 5.17 Optical sections of biofilms on sand grain surfaces at 7.5 cm (a) at 40x and (b) 20x magnifications, during pyrene studies after 14 weeks.

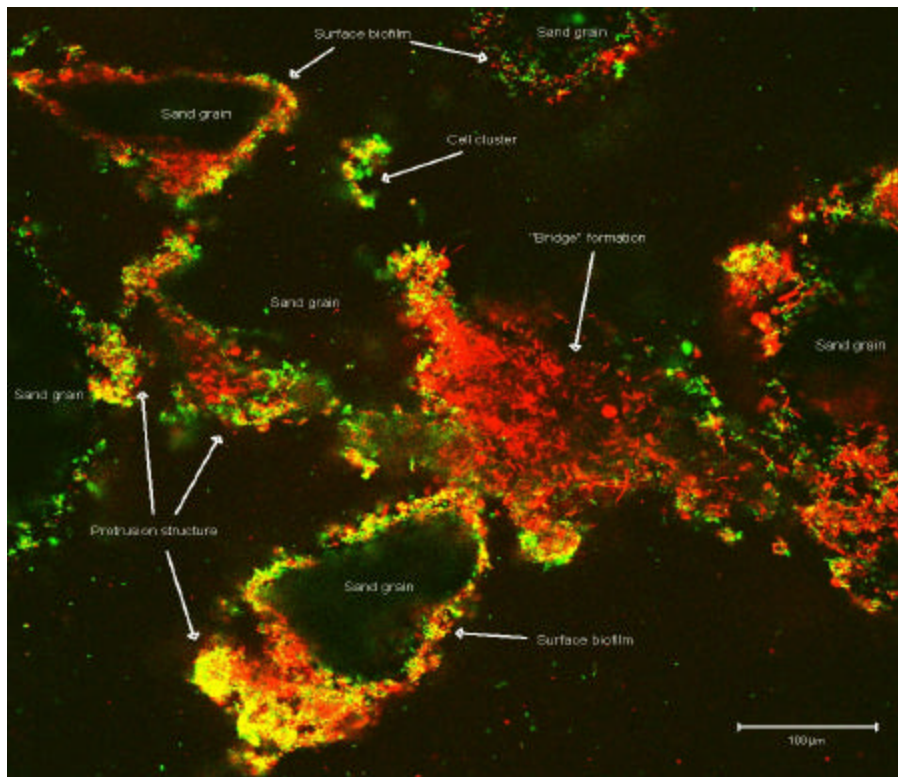
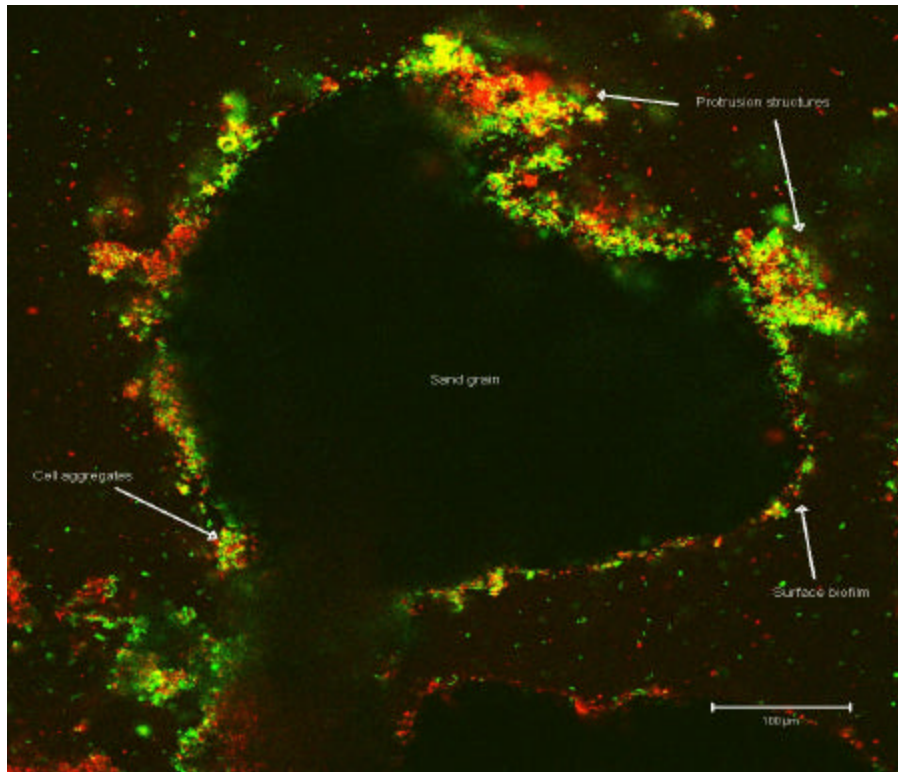


Figure 5.18 Optical sections of biofilms on sand grain surfaces at 7.5 cm (a) at 40x and (b) 20x magnifications, during pyrene studies after 22 weeks.

presence of thinner, continuous surface films on sand grains (5 to 15 μm in thickness) and smaller biological aggregate structures (5 to 30 μm in diameter). This could be explained by a shorter acclimation period (2 weeks, compared to 6 weeks in this study) and duration of the experiment (10 weeks, compared to 22 weeks in this study). Ebihara *et al.* (1997, 1999) also used an alternate growth substrate for the purpose of improving PAH biodegradation rates; it was shown that biomass content in sand medium increased, increasing the thickness of surface biofilms and the occurrence of cluster-and-protusion-type structures.

Paulsen *et al.* (1997) also described the biofilm morphology in porous media, calling it “bioweb”, or a spider web where each strand varies in size and shape. The biofilm maintained a large surface area and a minimum depth, minimizing mass transfer resistance between the fluid and the biofilm phase, under the conditions tested. Dunsmore *et al.* (2004) also found complex structural forms in biofilms, with thicknesses of about 30 μm , but with strands varying in length up to 40 μm , depending on the pore spaces between soil particles and the permeability conditions.

5.5 CONCLUSIONS

Multiple substrate utilization is a very important process, especially in bioremediation of contaminated soils, where various mixtures of pollutants are often present. The substrate interactions of the degradation of a mixture of compounds in the field are most likely complex, resulting in a number of degradation patterns. This is supported by many

studies that have shown PAH-degraders are capable of degrading a range of PAHs, while others have reported a narrow range of substrate utilization for PAH-degraders. Consequently, these degradation phenomena are system specific, where environmental conditions may affect the degrading capabilities of microbial communities.

The potential interactions of three PAH-based substrates were shown in this study: positive effects, resulting in an increase in biodegradation of at least one of the components, and negative effects, such as inhibition of the medium molecular weight PAHs were observed. Sole-substrate experiments indicated that phenanthrene and pyrene were not able to be biodegraded alone, but instead they were cross-fed and required a co-substrate or degradation intermediates from a more soluble and easily degradable compound such as acetate or naphthalene.

Biofilm composition indicated a great dependence on the substrate present; as easily degradable compounds are mineralized, living cells reproduce rapidly and release more exopolymeric material, which helps in building the biofilm attached to the porous media. Biofilm structure analysis suggested a heterogeneous web-like matrix with different aggregate formations of bacteria and exopolymeric substances, varying in size and shape. The presence of binary and tertiary mixtures favored the formation of clusters and protrusions, increasing the biomass per unit sand area.

More complex mixtures of PAHs in soils need to be investigated in the future, in order to give a better understanding of the potential interactions during PAH biodegradation by mixed cultures.

5.6 REFERENCES

Bouchez, M., Blanchet, D., Bardin, V., Haeseler, F., Vandecasteele, J.P., (1999), "Efficiency of defined strains and of soil consortia in the biodegradation of polycyclic aromatic hydrocarbons (PAH) mixtures", *Biodegradation*, **10**, 429-435.

Cingle, C., Gejlsbjerg, B., Ekelund, F., Madsen, T., (2001), "Effects of sludge-amendment on mineralization of pyrene and microorganisms in sludge and soil", *Chemosphere*, **45**, 625-634.

Dean-Ross, D., Moody, J., Cerniglia, C.E., (2002), "Utilization of mixtures of polycyclic aromatic hydrocarbons by bacteria isolated from contaminated sediment", *Microb. Ecol.*, **41**, 1-7.

Dunsmore, B., Bass, C., Lappin-Scott, H., (2004), "A novel approach to investigate biofilm and bacterial transport in porous matrices", *Environm. Microbiol.*, **6**(2), 183-187.

Ebihara, T., Bishop, P.L., (1997), "Examination of biofilms utilized in bioremediation of organic compounds using confocal scanning microscopy techniques", *Superfund Basic Research Program Conference: a decade of improving health through multi-disciplinary research*, Chapel Hill, NC.

Ebihara, T., Bishop, P.L., (1999), "Biofilm structural forms in porous media utilized in organic compounds degradation", *Wat.Sci.&Techn.*, **39**(7), 203-210.

Ebihara, T. (1999), "Characterization and enhancement of microbial biofilms in porous media for the biodegradation of polycyclic aromatic hydrocarbons", PhD. Dissertation, University of Cincinnati, Cincinnati, OH.

Eriksson, M., Dalhammar, G., Mohn, W., (2002), "Bacterial growth and biofilm production on pyrene", *Microbiol.Ecol.*, **40**, 21-27.

Guha, S., Peters, C., Jaffe, P., (1999), "Multisubstrate biodegradation kinetics of naphthalene, phenanthrene and pyrene mixtures", *Biotechn.&Bioengineer.*, **65**(5), 491-499.

Guieysse, B., Cirne, M., Mattiasson, B., (2001), "Microbial degradation of phenanthrene and pyrene in a two-liquid phase-partitioning bioreactor", *Appl.Microb.Biotechnol.*, **56**, 796-802.

Hwang., S., Cutright, T., (2002), "Biodegradability of aged pyrene and phenanthrene in a natural soil", *Chemosphere*, **47**, 891-899.

Juhasz, A.L., Britz, M.L., Stanley, G.A., (1997), "Degradation of fluoranthene, pyrene, benz[a]anthracene and dibenz[a,h]anthracene by *Burkholderia cepacia*", *J.Appl.Microbiol.*, **83**, 189-198.

Lotfabad, S., Gray, M., (2002), "Kinetics of biodegradation of mixtures of polycyclic aromatic hydrocarbons", *Appl.Microb.Biotechnol.*, **60**, 361-365.

McNally, D., Mihelcic, J.R., Luenking, D., (1999), "Biodegradation of mixtures of polycyclic aromatic hydrocarbons under aerobic and nitrate-reducing conditions", *Chemosphere*, **38**(6), 1313-1321.

Menn, F.M., Applegate, B.M., Sayler, G.S., (1993), "NAH-plasmid mediated catabolism of anthracene and phenanthrene to naphthoic acid", *App. Environm. Microbiol.*, **59**, 1938-1942.

Molina, M., Araujo, R., Hodson R.E., (1999), "Cross-induction of pyrene and phenanthrene in a *Mycobacterium* sp. isolated from polycyclic aromatic hydrocarbons contaminated river sediments", *Can.J.Microbiol.*, **45**, 520-529.

Mueller, J.G., Chapman, P., Pritchard, P., (1989), "Action of a fluoranthene-utilizing bacterial community on polycyclic aromatic hydrocarbon components of creosote", *Appl.Environm.Microbiol.*, **55**, 3085-3090.

Paulsen, J., Oppen, E, Bakken. R., (1997), "Biofilm morphology in porous media: a study with microscopic and imaging techniques", *Wat.Sci.& Techn.*, **36**(1), 1-9.

Ramirez, N., Cutright, T., Ju, L., (2001), "Pyrene biodegradation in aqueous solutions and soil slurries by *Mycobacterium* PYR-1 and enriched consortium", *Chemosphere*, **44**, 1079-1086.

Rodriguez, S., Bishop, P.L., (2004). "Biofilm growth, structure and composition during *in-situ* bioremediation of naphthalene", *Proceed. 4th Int'l Conf. on Remediation of Chlorinated and Recalcitrant Compounds*, Monterey, CA, May 24-27th.

Ryan, J.R., Loehr, R.C., Rucker, E., (1991), "Bioremediation of organic contaminated soils", *J.Hazard.Mat.*, **28**,159-169.

Song, H.G., (1999), "Comparison of pyrene biodegradation by white rot fungi", *W.J.Microbiol.&Biotechn.*, **15**, 669-672.

Stringfellow, W.T., Aitken, M.D., (1995), "Competitive metabolism of naphthalene, methyl naphthalenes and fluorine by phenanthrene-degrading pseudomonas", *Appl. Environm. Microb.*, **61**, 357-362.

Tiehm, A., Fritzsche, C., (1995), "Utilization of solubilized and crystalline mixtures of polycyclic aromatic hydrocarbons by *Mycobacterium* sp.", *Appl. Microb. Biotechnol.*, **42**, 964-968.

Yuan, S.Y., Wei, S.H., Chang, B.V., (2000), "Biodegradation of polycyclic aromatic hydrocarbons in a mixed culture", *Chemosphere*, **41**, 1463-1468.

Yuan, S.Y., Chang, J.S., Yen, J.H., Chang, B.V., (2001), "Biodegradation of phenanthrene in river sediment", *Chemosphere*, **43**, 273-278.

Chapter 6

SOLUBILIZATION AND SORPTION STUDIES OF PAHS WITH A NONIONIC SURFACTANT

6.1 ABSTRACT

This study sought to examine the solubilization of polycyclic aromatic hydrocarbons in a solution of a nonionic surfactant, as well as the sorption of surfactant and/or PAHs to the sand medium and biofilm. Water solubility enhancements of naphthalene, phenanthrene and pyrene were achieved by using micellar solutions of Triton X-100, above the critical micelle concentration (CMC): the solubilities of the 2-, 3- and 4-ringed PAHs were successfully increased 2, 16 and 100 times, respectively. The molar solubilization ratio (MSR) and the micelle/water partition coefficient (K_m) were calculated in order to evaluate the effectiveness of the surfactant in solubilizing the three PAHs.

Batch experiments were also conducted to investigate the sorption effects of PAHs and/or Triton X-100 to the porous media, as well as the partitioning to live/killed biofilms. An average amount of 17 $\mu\text{g/g}$ of Triton X-100 was sorbed onto sand, and it decreased with higher sand doses; however the removal of surfactant from the solution was always less than 2%, indicating extremely low affinity of Triton X-100 for the porous media. The presence of Triton X-100 increased PAH sorption onto sand; however, sorbed concentrations of the 2-, 3- and 4-ringed PAHs were still considered negligible.

Surfactant appeared to adsorb at approximately 7.2 and 6.4 $\mu\text{g}/\text{mg}$ VS, for live and killed biofilm, respectively; the highest amounts of naphthalene, phenanthrene and pyrene that were found within the biofilm, were 0.39, 0.17 and 0.10 $\mu\text{g}/\text{mg}$ VS, representing a minimal percentage of PAH sorption.

6.2 INTRODUCTION

The contamination of soil and water by organic pollutants is a widespread environmental problem, and different physical, chemical, biological and combined technologies have been attempted to remediate polluted soils. Surfactants have been suggested as a promising tool for the removal of polycyclic aromatic hydrocarbons, by improving the aqueous-phase concentration via micelle-microemulsion formation or by mobilization of the PAH phase, and hence, improving their bioavailability (Zhu and Feng, 2003; Park *et al.*, 2000; Jeong *et al.*, 2000).

In general, surfactant molecules have a hydrophilic head and one or two hydrophobic tails; the polar head, often ionizable, acts to increase solubility in water while the tail, usually a long hydrocarbon chain, has the opposite effect. Surfactants can accumulate along the air-liquid and liquid-liquid interfaces and thus reduce both surface tension and interfacial tension at the same time. In addition, if the surfactant concentration exceeds a certain threshold, known as the critical micelle concentration (CMC), surfactant monomers in aqueous solution will tend to aggregate to form micelles in colloidal-size to achieve segregation of their lipophilic parts from water. The major types of micelles

appear to be small spherical, elongated cylindrical (rod-like), lamellar (disk-like) and vesicles. Under those conditions, the hydrophobic solubilizates are incorporated in the hydrophobic cores of the micelles, which is often termed as solubilization (Guha and Jaffe, 1996; Li and Chen, 2002). This mechanism, however, is dependent of the surfactant nature, solute, temperature, ionic strength, concentration, surfactant-soil interactions and time of contact between the contaminant and soil (Rosen, 1989).

The effective critical micelle concentration in soil has been found to be reduced in pore water relative to clean water, especially for anionic and cationic surfactants, due to the ionic strength of the water (Haigh, 1996). It has also been reported that the degree of adsorption of surfactants to soils increases with its organic content, clays and colloidal materials; however, the sorption characteristics of nonionics will always be lower than other surfactants, which give them the potential to interact with the hydrophobic compounds (Liu *et al.*, 1992). Biodegradation of surfactants can occur, as shown by several authors (Kim *et al.*, 2001; Doong and Lei, 2003); in their studies, microorganisms showed rapid utilization of nonionic Brij 30, Brij 35 and Tween 80, as easy sources of carbon, due to their low molecular weight.

Several effects of surfactants have been observed on the fate of PAHs in soil. Surfactants enhance solubilization of these pollutants, increasing linearly the desorptive mechanism from soil (Kim *et al.*, 2001; Doong and Lei, 2003). But they can also improve their adsorption by forming hydrophobic adsorbate layers (called hemimicelles), into which the organics can partition (Haigh, 1996; Klumpp *et al.*, 1991; Edwards *et al.*, 1994). The

reason for this negative effect can be attributed to the soil composition; a low surface area and large number of positively adsorption charged sites facilitates the formation of hemimicelles at low surfactant concentrations.

There are conflicting views as to whether the presence of surfactants in soil enhances or inhibits the degradation of PAHs. Overall, the evidence favors the suggestion that solubilization of sorbed PAHs by surfactants can also enhance their degradation, because of their better bioavailability for the microorganisms (Kim *et al.*, 2001; Doong and Lei, 2003; Fortin *et al.*, 1997; Tiehm, 1994). However, it has also been reported that surfactant toxicity and preferential degradation of surfactant may interfere with the mineralization of PAHs (Bramwell and Laha, 2000; Laha and Luthy, 1991, 1992).

The objectives of this study were to investigate the ability of a nonionic surfactant (Triton X-100) to enhance the water solubility of PAHs, the surfactant toxicity to biofilm, and sorption of the surfactant to sand and biofilm in the presence of PAHs. Microbial growth, sorption and solubility batch tests of sole-substrate/binary mixtures of naphthalene, phenanthrene and pyrene were conducted to ascertain if a Triton X-100 solution with concentrations near the CMC may be used in the surfactant-enhanced remediation of polycyclic aromatic hydrocarbons.

6.3 MATERIALS AND METHODS

The nonionic surfactant Triton X-100 was chosen in this study because of its commercial use in the bioremediation of organics in soils (Zhu and Feng, 2003; Li and Chen, 2002, Yuan *et al.*, 2000; Churchill *et al.*, 1995; Backhus *et al.*, 1997). Its properties are listed in **Table 6.1**.

Table 6.1 Selected properties of surfactant Triton X-100.

Name	Polyoxyethylene(10)octynolphenol
Molecular Formula	$C_8H_{17}C_6H_4(OC_2H_4)_{10}OH$
Molecular Weight (g/mol)	625

Microbial Growth

The microbial consortia utilized to perform the cell growth experiments was started with a mixed liquor sample taken from an aeration tank at a domestic wastewater treatment plant (Polk Run WWTP, Cincinnati, OH). The sample was vortexed in centrifuge tubes, and the concentrated biomass was collected. Cell growth was evaluated using several concentrations of non ionic surfactant Triton X-100 (25 mg/L, 50 mg/L, 100 mg/L, 125 and 200 mg/L) in the presence of an excess quantity of ground naphthalene crystals (1 g/L), in triplicate cultures. Each vial contained 17.5 mL of the respective surfactant solution prepared in sterile mineral salt solution (see **Chapter 3** for nutrient composition) and was inoculated with 1 mL of the liquid culture described above; also, 0.07 mL of 1% H₂O₂ was added to each vial in order to provide aerobic conditions. Due to the high volatility of naphthalene, vials were not allowed to have head-space and silicone-teflon

septa were used to seal them. Controls for each surfactant concentration were also prepared in the same conditions, with no initial inoculum.

Five separate samples were taken at 0, 24, 48, 72 and 144 hours. Ten minutes were allowed for the naphthalene crystals to settle to avoid removing naphthalene with the cells. The optical densities of the microbial solutions were measured as absorbances using a Diode Array Spectrophotometer, at a wavelength of 600 nm (OD_{600}).

Plate counts on the initial mixed culture (used as inoculum for the experiments) were also carried out, in order to establish the ratio of initial to final cfu/mL per unit of OD_{600} .

Solubility of PAHs

Aqueous solubility experiments were performed using three different concentrations of surfactant Triton X-100 (50 mg/L - below the CMC, and 100 mg/L and 125 mg/L, - above the CMC) in the presence of excess quantities of ground naphthalene, phenanthrene and pyrene crystals. Due to the high volatilization of naphthalene, 17.5-mL vials with silicone-teflon septa were used and no head-space was allowed. Vials were continuously mixed on a rotary shaker (20 rpm) and samples were sacrificed once opened. For the 3- and 4-ring PAHs, 500-mL flasks were utilized, and solutions were mixed with magnetic stirrers at 200 rpm.

Samples were taken with glass syringes on five separate sampling events at 2, 5, 24, 48 and 96 hours. Samples were then filtered with a 0.1 µm membrane filter to separate the undissolved portion of PAHs. All the glassware and filter holders were cleaned with Milli-Q water and methanol, in order to minimize residuals of any of the target compounds, and new filters were used every time for each independent sample. HPLC was used to measure the PAH and Triton X-100 concentrations in the samples.

Sorption Tests

The rate and extent of sorption of the three PAHs to the sand medium and to the biofilm (live/killed), in the presence of two concentrations of Triton X-100 (100 and 125 mg/L), were measured in batch experiments.

The medium used in these studies was the same rounded fine-to-medium silica sand (ASTM graded sand, C-190) of approximately 0.38 mm median grain size and an effective porosity of 0.44, used in the column biodegradation studies. Details on the size distribution of the sand are available in **Appendix B**. To evaluate the effect of mass amount of sand on sorption of PAH and/or surfactant, three masses of 1, 2 and 5 grams of sand per vial were chosen.

Surfactant-to-sand sorption was tested using 17.5-mL vials with silicone-teflon septa and no head-space. Solutions of Triton X-100 were prepared ahead of time, in order to allow for equilibrium conditions of the surfactant in water. Vials were then prepared and

continuously mixed inside a rotary shaker (20 rpm); samples were sacrificed once opened, so sufficient vials were prepared. Samples were taken on seven separate sampling times at 1, 3, 5, 24, 48, 72 and 168 hours. Controls for each surfactant concentration were also prepared in the same conditions, with no sand dose, in order to record any loss of surfactant.

Vials of 17.5 mL with silicone-teflon septa were used for the PAH/surfactant-sand sorption case, and no head-space was allowed, due to the high volatility of naphthalene. Solutions of PAHs and/or Triton X-100 were prepared ahead of time, in order to allow for equilibrium conditions (24 hours for naphthalene, and 48 hours for phenanthrene and pyrene). A rotary shaker (20 rpm) continuously mixed the vials, and samples were sacrificed once opened, so sufficient vials were prepared. Controls for each surfactant concentration and PAH were also prepared in the same conditions.

For the PAH/surfactant-biofilm sorption case, a 2-L wide mouth glass jar without headspace was used, where biofilm was grown attached to glass slides for about two weeks before the sorption experiments. Live and killed biofilm (by adding 1g/L sodium azide) were combined with the solutions of PAHs and/or Triton X-100, which were prepared ahead of time and allowed to reach equilibrium conditions, in addition to a sterile mineral salt solution (see **Chapter 3** for nutrient composition) and 0.07 mL of 1% H₂O₂ to provide aerobic conditions; solutions were mixed with magnetic stirrers at 50 rpm. Liquid samples were taken at 2, 10, 18, 24 and 48 hours and triplicates of biofilm samples were analyzed for volatile solids content at each sampling event. Controls were

also prepared containing only surfactant or only biofilm and were maintained at the same conditions, in order to establish losses of surfactant or biomass changes.

Samples were always taken with glass syringes and then filtered with a 0.1 μm membrane filter to separate the undissolved portion of PAHs or retain any particulate matter. All the glassware and filter holders were cleaned with Milli-Q water and methanol, in order to minimize residuals of any of the target compounds, and new filters were used every time for each independent sample. HPLC was used to measure the PAH and Triton X-100 concentrations of the samples.

6.4 RESULTS AND DISCUSSION

The Critical Micelle Concentration (CMC) is the value at which the surface-active molecules do not exist as monomers, but as aggregates with hydrophobic groups located at the center of the cluster and hydrophilic groups towards the solvent. It has been measured as the point of inflection where surface tension becomes constant with increasing surfactant concentration, and in the case of Triton X-100, it has been reported as 13.6 mg/L (Kim *et al.*, 2001), 43 mg/L (Shiau *et al.*, 1995), 101 mg/L (Doong and Lei, 2003), 130 mg/L (Prak and Pritcard, 2002), 140 mg/L (Guha and Jaffe, 1996), 145 mg/L (Boonchan *et al.*, 1998), 160 mg/L (Chen *et al.*, 2000). The wide variation in CMC values of Triton X-100 is due to different interpretations of the plot of surface tension versus concentration. An average of 100 mg/L was chosen as the Triton X-100's CMC value in these studies.

6.4.1 Microbial Growth

Data shown in **Figure 6.1** represent the growth of a mixed culture on naphthalene with concentrations of Triton X-100 from 25 to 200 mg/L. In all cases cells grew as free suspensions and the average initial OD₆₀₀ was observed to be around 0.062±0.012. The OD₆₀₀ values increased rapidly over the first 24 hours, where linear growth was observed, due to the rapid consumption of water-soluble substrate. Previous studies have reported on growth on solid PAHs, where slow dissolution does not permit exponential growth (Volkering *et al.*, 1995; Chen *et al.*, 2000). Samples with 25, 50 and 200 mg/L of Triton X-100 showed a stable trend for cell growth after the first day of the experiments, with average final OD₆₀₀ values of 0.11, 0.12 and 0.09, respectively. Meanwhile, the 100 and 125 mg/L Triton X-100 concentrations were described as having a continuing increase up to 48 hours, after which optical densities decreased and stabilized over time.

The least effect of toxicity/inhibition to the mixed culture, if any, was observed for the 50, 100 and 125 mg/L concentrations of the surfactant, where maximum OD₆₀₀ values reached 0.12. Even so, in order to produce micelles that contribute to the solubilization of the PAHs, just the last two concentrations were chosen for the column biodegradation studies, which are both above the CMC of Triton X-100.

The plate count of inoculum used in these experiments indicated that it contained 10⁹ cell/mL, which gave a consistent ratio of 10⁸ cfu/mL for each 0.1 unit of OD₆₀₀. Any adhesion of cells to the surface of the naphthalene crystals would not give a significant

error in OD_{600} measurement, due to cell attachment on the low surface area of the naphthalene particles.

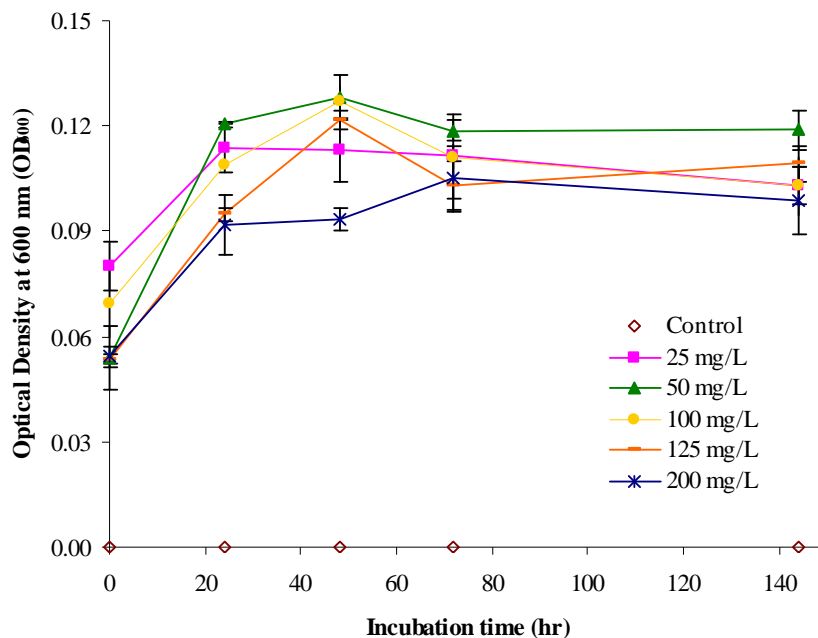


Figure 6.1 Microbial growth of naphthalene in the presence of Triton X-100.

In parallel to the optical density observations, naphthalene and surfactant concentrations were also monitored from the same samples used for microbial growth; the objective was to investigate the possible competitive effects between the two substrates for cell growth. **Figures 6.2 (a)** and **(b)** show the consumption of naphthalene and surfactant over a period of 144 hours. In the first plot, naphthalene was almost completely degraded in the presence of 25 mg/L of Triton X-100 after 24 hours, with 78% consumption; slower rates were observed with increasing surfactant concentration for the remaining cases, but eventually, after 72 hours, all the samples reached the same value of 1 mg/L of naphthalene. Overall, the total percentage of naphthalene consumed by the mixed culture

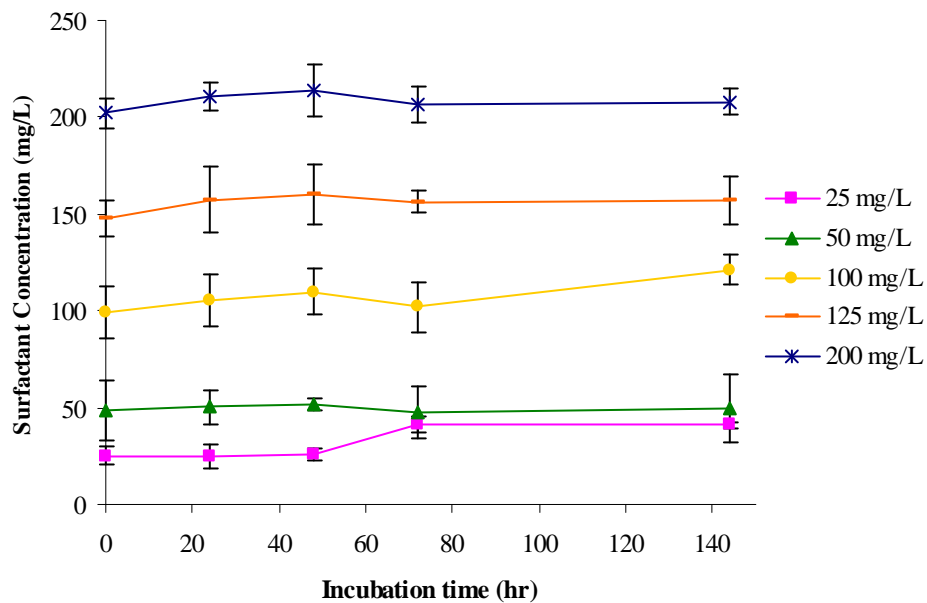
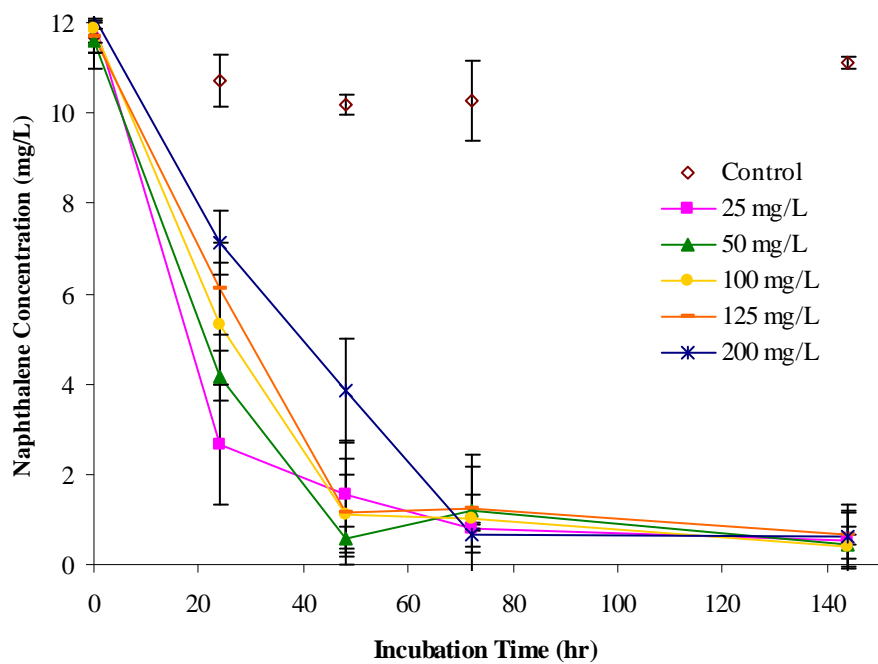


Figure 6.2 Consumption of (a) naphthalene and (b) Triton X-100 by a mixed culture during microbial growth experiments.

in the presence of different surfactant concentrations over a period of 5 days ranged from 93 to 95%.

Triton X-100 concentrations remained constant with time, indicating that the surfactant was not being used as a substrate for cell growth. This could be explained by the fact that Triton X-100 is a high molecular weight compound, whose structure is composed of stable benzene rings; the same behavior has been reported in the literature (Kim *et al.*, 2001; Doong and Lei, 2003). There were no concentration changes observed in the control samples for either naphthalene or surfactant.

6.4.2 Solubility of PAHs

Nonionic surfactant Triton X-100 was used to optimize conditions for the biodegradation of high molecular weight PAHs and their mixtures. The apparent solubilities of naphthalene, phenanthrene and pyrene were measured in the presence of the surfactant below, above and at the CMC. In **Figures 6.3, 6.4 and 6.5**, the solubilities of naphthalene, phenanthrene and pyrene were plotted as a function of time for different surfactant solution concentrations.

Above the CMC, the added surfactant formed the micelles and enhanced the PAH's solubility. Naphthalene concentration was increased by 58% and 80% after 24 hours for the 100 and 125 mg/L Triton X-100 solutions, respectively. After one day of mixing, an equilibrium stage was reached giving constant naphthalene concentrations (31 ± 0.4 for

100 mg/L and 35 ± 0.7 for 125 mg/L of Triton X-100), even when 5 days passed. The solubility of phenanthrene increased from 0.5 mg/L (with no surfactant) up to 6.5 ± 0.2 (with 100 mg/L Triton X-100) and 8.1 ± 0.2 mg/L (with 125 mg/L Triton X-100), after 48 hours of mixing, when the concentration was equilibrated. Finally, pyrene experienced the major enhancement in its solubility, because it increased more than 100 times for both surfactant concentrations above the CMC during the 5-day experiments. Below the surfactant concentrations above the CMC during the 5-day experiments. Below the CMC, the surfactant mainly existed as monomers and did not contribute to the solubility of the PAHs; this was confirmed by the unchanged soluble concentrations of naphthalene, phenanthrene and pyrene at 50 mg/L of Triton X-100.

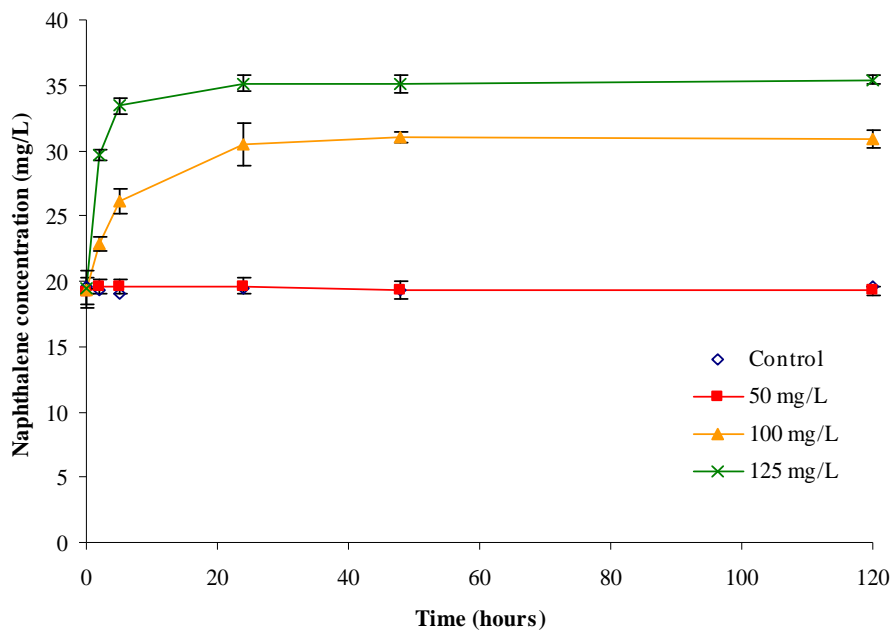


Figure 6.3 Naphthalene solubility at different Triton X-100 concentrations.

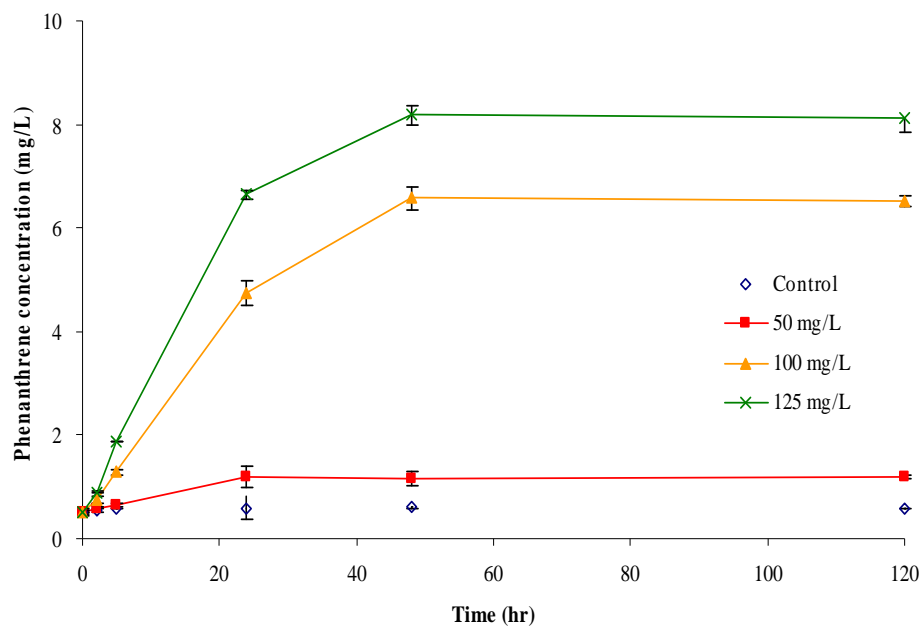


Figure 6.4 Phenanthrene solubility at different Triton X-100 concentrations.

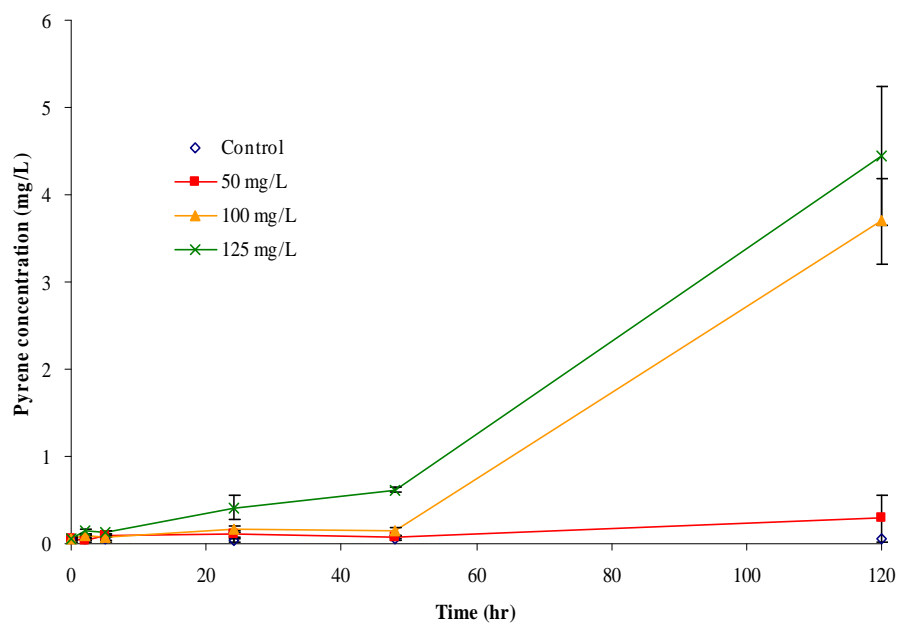


Figure 6.5 Pyrene solubility at different Triton X-100 concentrations.

Higher concentrations of Triton X-100 have been used in other studies for solubilizing PAHs, usually between 0.5 and 20 g/L (Kim *et al.*, 2001, Boonchan *et al.*, 1998; Li and Chen, 2002; Prak and Pritchard, 2002; Guha *et al.*, 1998). Increases from 500-fold to 10⁴-fold have been obtained in similar experiments for most PAHs (even high molecular weight ones), and linear proportionality between PAHs and surfactant concentrations has always been observed above the CMC, because the concentration of the surfactant monomers remains relatively constant.

The effectiveness of a surfactant in solubilizing a given PAH can be assessed by determining the molar solubilization ratio (MSR) and the micelle/water partition coefficient (K_m). MSR is described as the moles of PAH solubilized by per mole of surfactant above its CMC, which is shown as follows (Edwards *et al.* 1991):

$$MSR = \frac{C - C_{cmc}}{C_{surf} - CMC} \quad (1)$$

where C is the total apparent solubility of PAH in micellar solution at the particular surfactant concentration equal to C_{surf} ; and C_{cmc} is the saturation concentration of PAH at the CMC. The micelle-water partition coefficient K_m is a parameter that indicates the distribution of molecules between the micellar phase and the aqueous phase:

$$K_m = \frac{\left(\frac{MSR}{1 + MSR} \right)}{X_a} \quad (2)$$

where the numerator is the mole fraction of PAH in the micellar pseudophase, expressed in terms of MSR, and X_a is the mole fraction of PAH in the micellar-free aqueous phase

(Edwards *et al.* 1991). X_a can be expressed as $V_w C_{cmc}$, where V_w is the molar volume of water at 30°C (0.018015 L mol⁻¹) and C_{cmc} is the apparent solubility of the PAH at CMC.

In this study, the concentrations of added PAHs were well in excess of aqueous saturation concentrations; therefore, the molar solubilization ratio (MSR) for each compound was calculated as the slope of the curve generated from a plot of PAH concentration versus surfactant concentration, according to Edwards *et al.*, (1991); the micelle/water partition coefficients K_m were then obtained from Equation (2). The correspondent values of MSR and K_m found in this study for naphthalene, phenanthrene and pyrene are shown in **Table 6.2.**, as well as reported values.

Table 6.2 Solubilization parameters of PAHs by surfactant Triton X-100.

PAH	MSR (mol/mol)	Log K_m	Reference
Naphthalene	0.223	4.58	This study
	0.186	5.24	Kim <i>et al.</i> (2001)
Phenanthrene	0.18	5.34	This study
	0.118	5.72	Li and Chen (2002)
	0.13 +/- 0.01	6.10	Prak and Pritchard (2002)
Pyrene	0.054	5.16	This study
	0.0352	5.84	Boonchan <i>et al.</i> (1998)
	0.062	5.97	Guha <i>et al.</i> (1998)
	0.056 +/- 0.004	6.6 +/- 0.3	Prak and Pritchard (2002)

According to the MSR values, naphthalene was the compound with the most moles solubilized by per mole of Triton X-100, compared to the 3- and 4-ring PAHs. Log K_m values showed that phenanthrene had the best micelle-water distribution of molecules between the micellar phase and the aqueous phase, followed by pyrene and naphthalene.

The results of MSR as well as of Log K_m for the three PAHs were found to be higher and lower, respectively, than the reported literature values. This can be explained by the fact that this study was conducted for very low surfactant concentrations, near the average CMC value of Triton X-100; other researchers have used at least 500 mg/L of the surfactant to enhance PAH solubilities (Kim *et al.*, 2001, Boonchan *et al.*, 1998; Li and Chen, 2002; Prak and Pritchard, 2002; Guha *et al.*, 1998), four times the concentration used in the present study. Also, the shape of the micelles may vary with surfactant concentration (above the CMC) changing the solubilization rates: with concentrations such as those used previously in the literature, not only the equilibrium solubilities are increased but also the solubilization rates of hydrophobic compounds.

Hydrophilic lipophilic balance (HLB) is another good indicator to judge to solubilization capacity of surfactants. Triton X-100 has a low HLB value (13.5) compared to other surfactants commercially used, such as Tergitol 15-S-12 (HLB=14.7), Tween 20 (HLB=16.7) and Tween 80 (HLB=15.0) (Li and Chen, 2002); this increases its solubilization capacity, increasing also its hydrophobicity. In aqueous solutions, a surfactant like Triton X-100 will tend to form micelles that contain a more hydrophobic environment in the cores of the micelles, which is favorable for hydrocarbons to reside in. Micelles also possess a larger volume, holding more hydrocarbon molecules. These two reasons translate into a higher solubilization capacity for Triton X-100 with PAHs, as confirmed in several studies (Kim *et al.*, 2001, Li and Chen, 2002).

6.4.3 Surfactant Sorption-to-Sand Tests

The results for the batch sorption study of the surfactant onto sand are present in **Figure 6.6**. Sand dose was used to assess the influence on the adsorption capacity (amount of surfactant sorption per unit dry weight of sand) and was varied from 59 to 325 g/L, using 100 and 125 mg/L of Triton X-100.

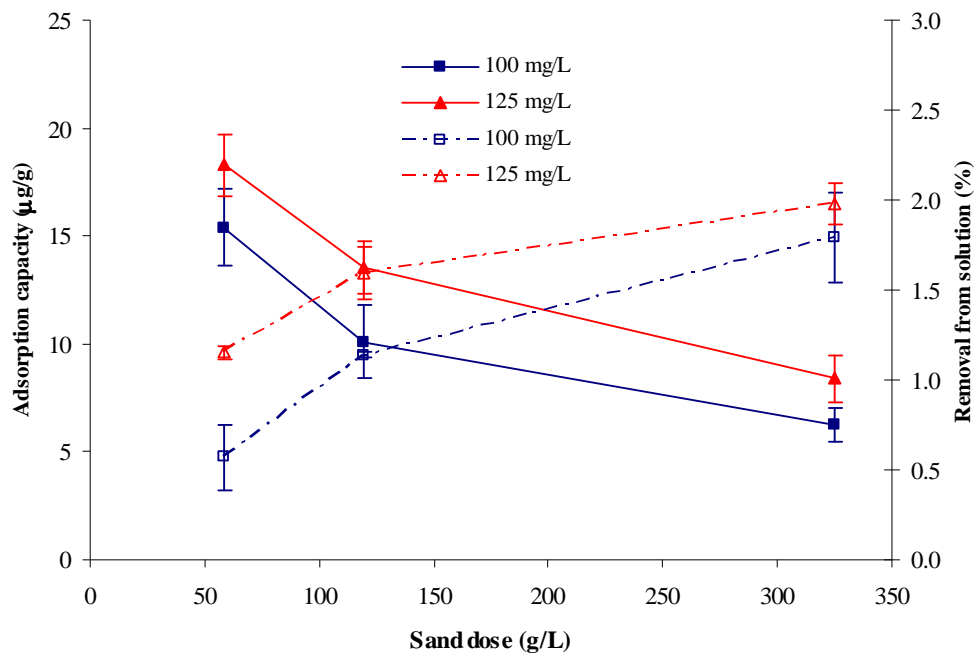


Figure 6.6 Adsorption capacity onto sand of Triton X-100 (filled symbols, Y axis at left) and removal from solution (open symbols, Y axis at right) with sand dose (after 24 hours).

After 24 hours of initial stirring, Triton X-100 appeared to have reached equilibrium conditions, and sorption was not dependent on the experimental time. The adsorption capacities of sand decreased as the sand dose increased; the maximum amounts of

surfactant adsorbed on sand were found to be 15.4 ± 1 and 18.3 ± 1 $\mu\text{g/g}$ for 100 and 125 mg/L of Triton X-100, respectively, at the 58.48 g/L sand dose. When the sand dose was higher than 325 g/L, the adsorption capacities for both surfactant concentrations were observed to start becoming constant, at an average adsorption capacity of approximately 7.3 $\mu\text{g/g}$. However, the removal of surfactant increased since the equilibrium concentration of Triton X-100 in solution was lower in the presence of high sand doses. Only 1.79% (for 100 mg/L) and 1.98 % (for 125 mg/L) of the surfactant could be removed from solution when sand dose was 324.68 g/L, after which the removal seemed to achieve stable values.

The adsorptive capacity of Triton X-100 onto sand was therefore considered negligible, as was expected because that this porous material has no organic content and very low surface area. Such small removal percentages indicate that adsorption does not play a major role in Triton X-100 removal from solution, so it may not be important when compared to biological removal mechanisms.

Usually two different isotherm shapes are commonly observed for sorption of nonionic surfactants on porous material. On one hand, Langmuir sorption isotherm has been reported, with a plateau above the CMC value for the surfactant (Liu *et al.*, 1992; Pennell *et al.*, 1993). On the other hand, S-shaped sorption isotherms are also common, with the first part behaving as a Langmuir isotherm, followed by a plateau and a subsequent increase of sorption at higher surfactant concentrations (Rosen, 1989; Abdul and Gibson, 1991). This first part of the S-shape isotherms is attributed to sorption of a monolayer of

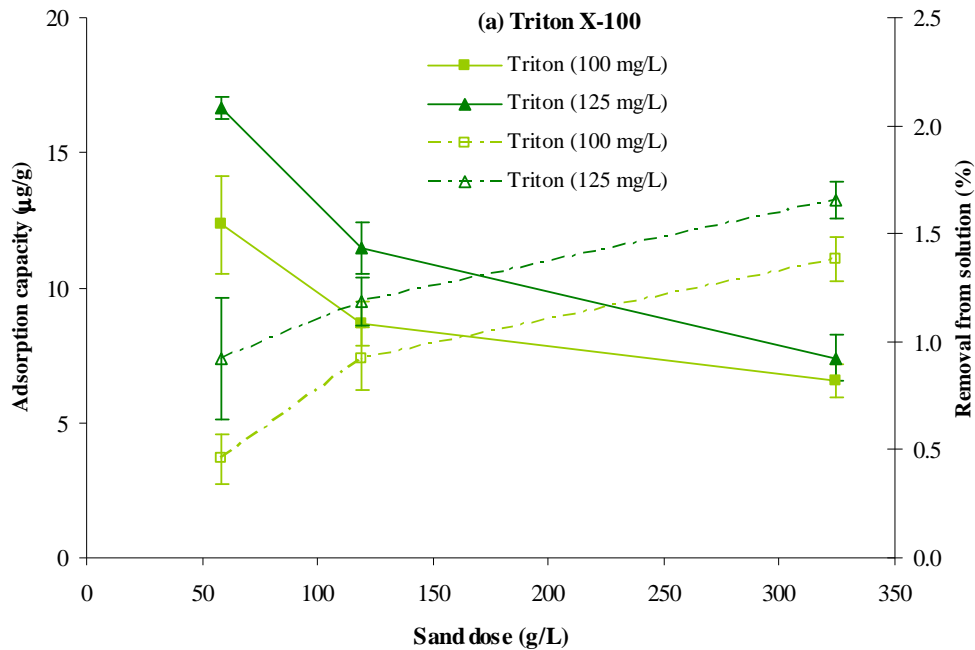
surfactant, and the increase in adsorption beyond the monolayer is due to the adsorption of micelles (surfactant-surfactant interaction) (Abdul and Gibson, 1991; Pennell *et al.*, 1993).

The surfactant sorption isotherm obtained in this study does not seem to follow any of the shapes commonly reported, because Triton X-100 concentrations were near the CMC and experiments were conducted on sand with no organic carbon content, leading to very small amounts of sorption. This behavior was also reported by Fortin *et al.* (1997) and Backhus *et al.* (1997).

According to Somesundaran and Hanna (1977), adsorption isotherms near or above the CMC exhibit shapes that are not often encountered. Adsorption at and above the critical micelle concentration can involve factors such as micellar exclusion from the interfacial region, competition between various monomeric and micellar species, and even phase separation and precipitation. According to several authors (Fortin *et al.*, 1997; Somesundaran and Hanna, 1977), the properties of the solid surface are a major factor governing adsorption above the critical micelle concentration. This results in different shapes of sorption isotherms on different solid substrates.

6.4.4 PAH/Surfactant Sorption-to-Sand Tests

In the case of naphthalene/Triton X-100 (100 mg/L) sorption experiments (**Figure 6.7**), the maximum surfactant concentration ($12.32 \pm 1.8 \mu\text{g/g}$) on the sand was measured at the lowest sand dose, and then decreased to 8.66 ± 0.8 and $6.54 \pm 0.6 \mu\text{g/g}$, respectively, for the other two sand doses. Surfactant sorption followed the same trend at 125 mg/L of Triton X-100, with an average of 32% increase in the mass sorbed onto sand. Most of the surfactant remained in solution, with average removal efficiencies of 0.92 and 1.25% for 100 and 125 mg/L Triton X-100, respectively. On the other hand, naphthalene was found to be sorbed at $1.2 \mu\text{g/g}$ onto sand for both Triton X-100 concentrations, when 58.48 g/L sand dose were used in the batch experiments; a decrease in naphthalene sorption of approximately 35% was observed for the subsequent two sand doses.



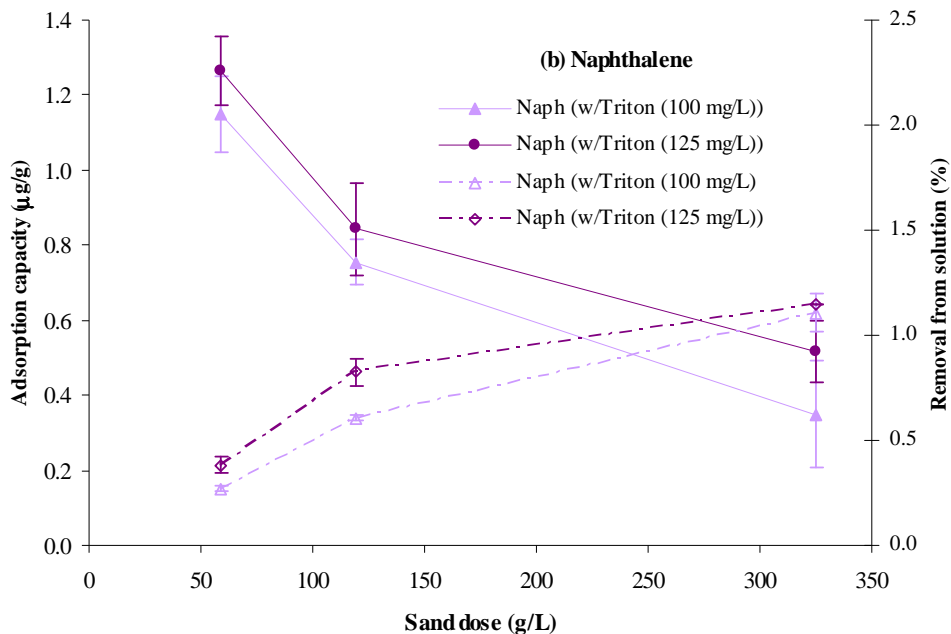


Figure 6.7 Adsorption capacity onto sand of (a) Triton X-100 and (b) naphthalene (filled symbols, Y axis at left) and their removal from solution (open symbols, Y axis at right) with sand dose.

A minimal loss by sorption to sand (less than 1.1%) of the 2-ring PAH was observed, indicating the high solubility of naphthalene and its stability in the micellar solution.

Batch sorption-to-sand studies of phenanthrene and surfactant are shown in **Figure 6.8**. A similar trend was observed for both Triton X-100 concentrations and the 3-ring PAH, as observed for the 2-ring PAH. Surfactant showed an average sorption of 8.22 and 9.51 µg/g dry with sand dose; its maximum values were 37% (for 100 mg/L Triton X-100) and 44% (for 125 mg/L Triton X-100) higher than the average and were observed at 58.48 g/L sand dose. Surfactant removals from the solution of 1.12 and 1.34 % for 100 and 125 mg/L of Triton X-100, respectively, were observed in these experiments, indicating

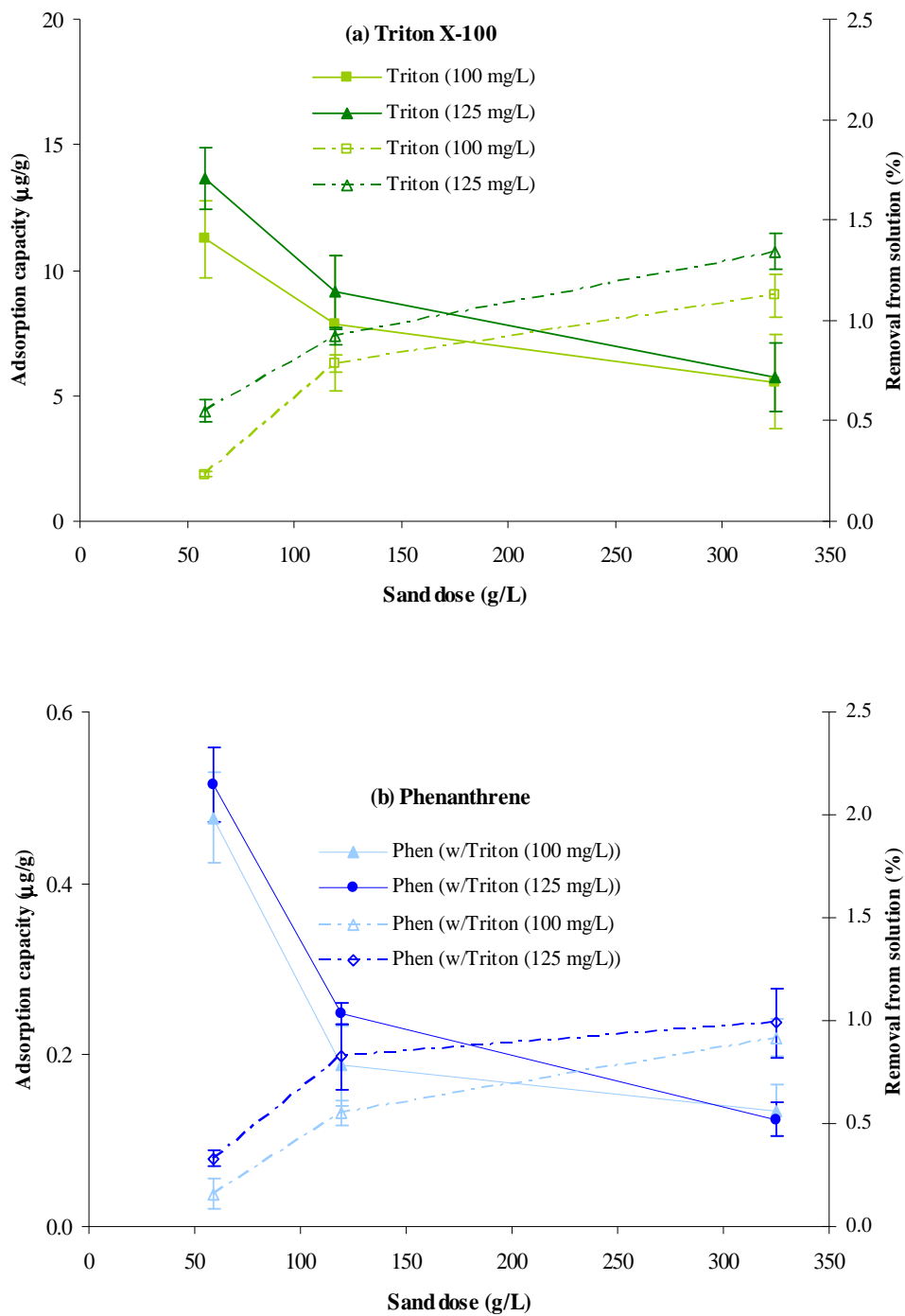


Figure 6.8 Adsorption capacity onto sand of (a) Triton X-100 and (b) phenanthrene (filled symbols, Y axis at left) and their removal from solution (open symbols, Y axis at right) with sand dose.

insignificant loss of surfactant by sorption onto sand. Phenanthrene was found to be adsorbed at 0.48 ± 0.05 (for 100 mg/L Triton X-100) and 0.52 ± 0.04 $\mu\text{g/g}$ (for 125 mg/L Triton X-100) at the sand dose of 58.48 g/L; its concentrations decreased approximately 75% at the highest sand dose for both surfactant concentrations. Averages of phenanthrene removal due to sorption mechanisms were observed to be at 0.54 and 0.71% for 100 and 125 mg/L of Triton X-100.

Finally, pyrene/surfactant sorption-to-sand batch studies were also conducted and the results are provided in **Figure 6.9**. For 100 mg/L of Triton X-100, the surfactant adsorbed onto sand at 9.11 ± 0.32 , 4.68 ± 0.27 and 2.60 ± 0.15 $\mu\text{g/g}$ for 58.48, 119.05 and 324.68 g/L of sand doses, respectively; increases of 8, 48 and 37% on Triton X-100 sorption (125 mg/L) were observed at the three different sand doses. Removal of surfactant due to sorption increased with high sand doses, as was indicated with naphthalene-surfactant and phenanthrene-surfactant experiments, but values were always found to be less than 0.75%. Pyrene concentrations sorbed onto sand followed the trend of decreasing sorption with increasing sand doses; the mass of pyrene adsorbed onto the porous medium varied from 0.22 ± 0.02 to 0.09 $\mu\text{g/g}$ (for 100 mg/L Triton X-100) and from 0.25 ± 0.02 to 0.11 ± 0.01 $\mu\text{g/g}$ (for 125 mg/L Triton X-100). Although pyrene's solubility was highly improved by the addition of surfactant and its sorption to sand was therefore increased, the sorbed amounts were still considered to be relatively low.

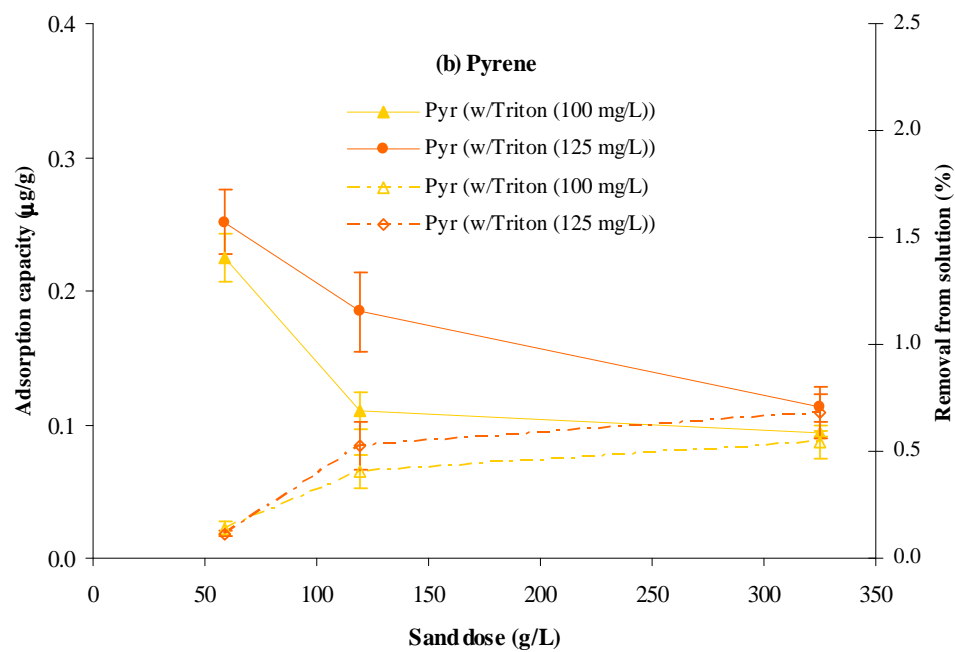
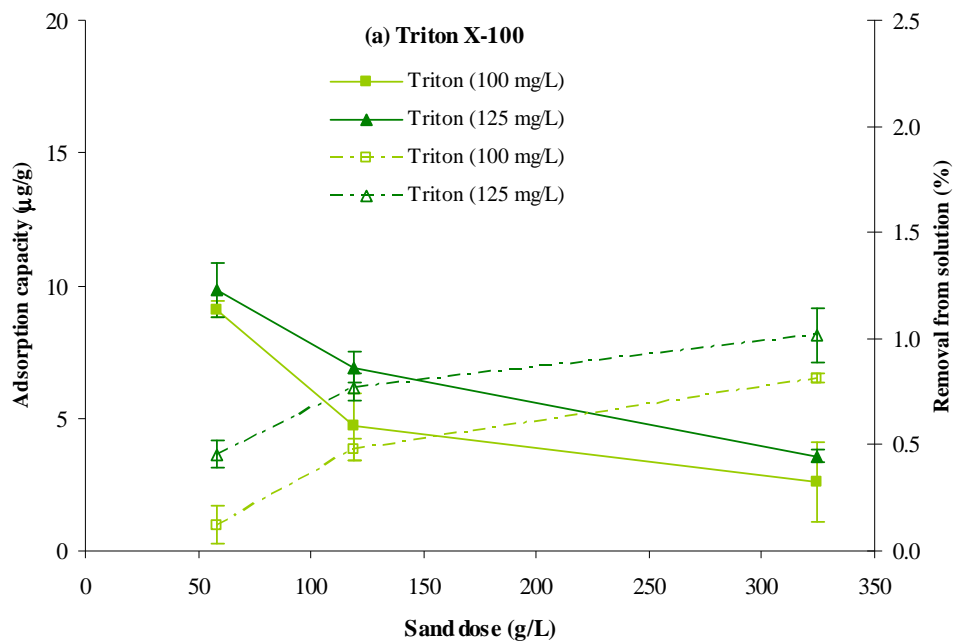


Figure 6.9 Adsorption capacity onto sand of (a) Triton X-100 and (b) pyrene (filled symbols, Y axis at left) and their removal from solution (open symbols, Y axis at right) with sand dose.

6.4.5 Surfactant Sorption-to-Biofilm Tests

Sorption batch tests of Triton X-100 (at 100 mg/L) onto live and killed biofilm are shown in **Figure 6.10**. An initial rapid sorption of surfactant to live and killed biofilm up to an average of 3.4 $\mu\text{g}/\text{mg}$ VS was observed in the first 10 hours of the experiments, probably due to the initial availability of sites within the biofilm, especially in the EPS material, which has been reported to contain diverse cationic and anionic groups. A slower rate of increasing adsorption was then observed in the subsequent 14 hours, showing 40% and 33% increase for live and killed biofilm, respectively. After 24 hours, surfactant sorption stabilized in both biofilms, probably due to the saturation of the sites on microorganisms and their exopolymeric material; averages of 6.04 (in live biofilm) and 5.14 $\mu\text{g}/\text{mg}$ VS (in killed biofilm) were measured during the remaining sorption experimental time.

In the case of using Triton X-100 at 125 mg/L, a similar trend was observed for the adsorption capacity in the biofilm. An initial rapid increase in the surfactant sorption was found, with 3.32 ± 0.36 and 3.55 ± 0.14 $\mu\text{g}/\text{mg}$ VS for live and killed biofilm, respectively; values of 6.83 ± 0.18 (for live biofilm) and 6.15 ± 0.25 $\mu\text{g}/\text{mg}$ VS (for killed biofilm) were then measured at 24 hours and increased little in the following 24 hours. The difference in adsorption capacity of Triton X-100 between live and killed biofilm does not appear to be due to biodegradation of the surfactant, and is mainly explained by the available sorptive sites in a live functioning structure. Besides, Triton X-100 is known to be

difficult to mineralize by microorganisms due to its high molecular weight and its stable benzene structure.

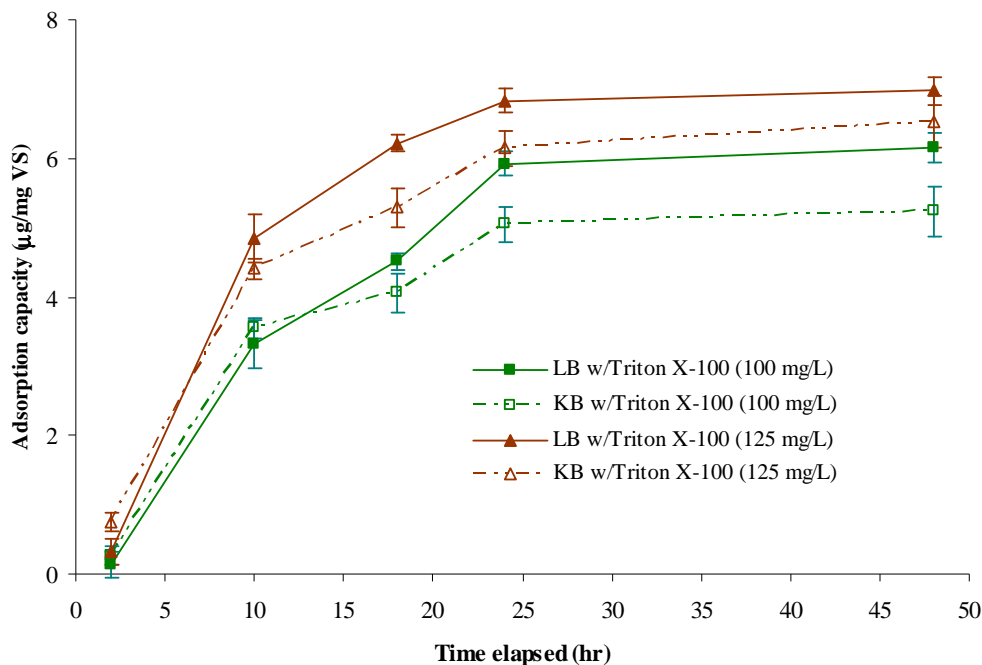


Figure 6.10 Adsorption capacity onto live biofilm (LB) and killed biofilm (KB) of Triton X-100 with time.

It can be concluded that there was a tendency of increasing adsorption capacity over time for both surfactant concentrations, which can be attributed not only to the surfactant characteristics of having both polar and nonpolar regions on the same micelle molecule, but also to the diversity of cationic and anionic groups present in the EPS matrix of the biofilm. However, the adsorption capacity of the biofilm is still limited for a heavy compound such as Triton X-100, and the values that are reported in this study can be neglected, compared to other main removal mechanisms like biodegradation.

It has been reported in the literature that surfactants could change microbial adhesion by adsorbing to the surfaces of microorganisms, or to the surfaces of hydrocarbons, or both (Neu, 1996). Chen *et al.* (2000) reported that Triton X-100 could bind to the *Mycobacterium* sp., covering approximately 20% of the surface of the cells (considering a hydrophobic tail of Triton X-100 of 0.6 nm x 0.3 nm, and a 0.5 x 2 µm rod-shaped cell). These levels of coverage would be sufficient to significantly alter the hydrophobicity or hydrophilicity of the surfaces, depending on the orientation of the surfactant. The authors found that the inhibition that was observed for *Mycobacterium* sp. suggested that the interaction with surfactant was saturable, consistent with a surface coverage mechanism. Dispersion of bacteria from hydrophobic surfaces by surfactants can also significantly reduce the growth rate, even when the bacteria are not growing as a biofilm (Stelmack *et al.*, 1999; Chen *et al.*, 2000).

6.4.6 PAHs/Surfactant Sorption-to-Biofilm Tests

Batch experiments with Triton X-100 (in concentrations of 100 and 125 mg/L) in the presence of naphthalene, phenanthrene and pyrene were also conducted to evaluate the portion of PAHs adsorbed onto live and killed biofilm due to the presence of the surfactant. **Figure 6.11** presents the sorption of Triton X-100 onto live and killed biofilm, while the three PAHs were also in solution. The adsorption capacity curve is very similar to the one without the hydrocarbons, although the results indicated lower affinity to both types of biofilms at maximum surfactant sorption concentrations of 4.15 ± 0.21 and 4.46 ± 0.37 µg/mg VS, for 100 and 125 mg/L of Triton X-100, respectively. This can be

explained by the fact that there was probably competition between the surfactant and the PAHs for the available sites within the biofilms, reducing the overall adsorbed amount of Triton X-100 by an average of 34%. Killed biofilms seemed to adsorb the same amount of surfactant at an average of 3.58 $\mu\text{g}/\text{mg}$ VS for both surfactant concentrations.

The adsorption of PAHs onto live biofilm, when 100 mg/L of Triton X-100 were added into solution, is shown in **Figure 6.12**. The mass of naphthalene per unit biomass appeared to progressively increase over the 48-hour run, although the major adsorption took place during the first 18 hours at 0.28 ± 0.07 $\mu\text{g}/\text{mg}$ VS; the amount of naphthalene increased only 25% in the last 30 hours. The 3- and 4-ringed PAHs showed a slower increase of sorption to biomass with 0.13 ± 0.01 and 0.08 $\mu\text{g}/\text{mg}$ VS, respectively, after 10

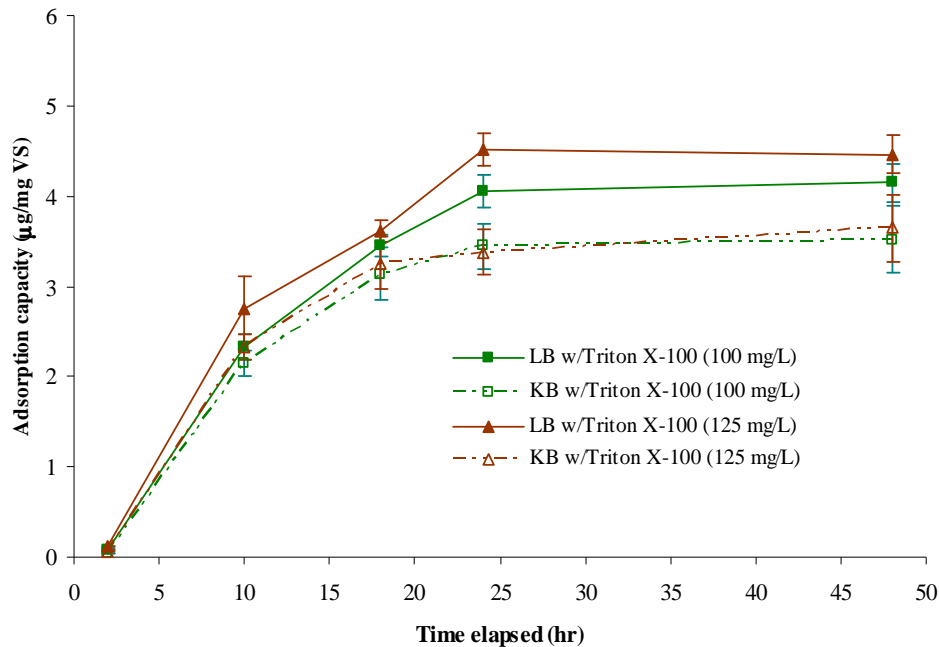


Figure 6.11 Adsorption capacity onto live biofilm (LB) and killed biofilm (KB) of Triton X-100 with time, in the presence of PAHs.

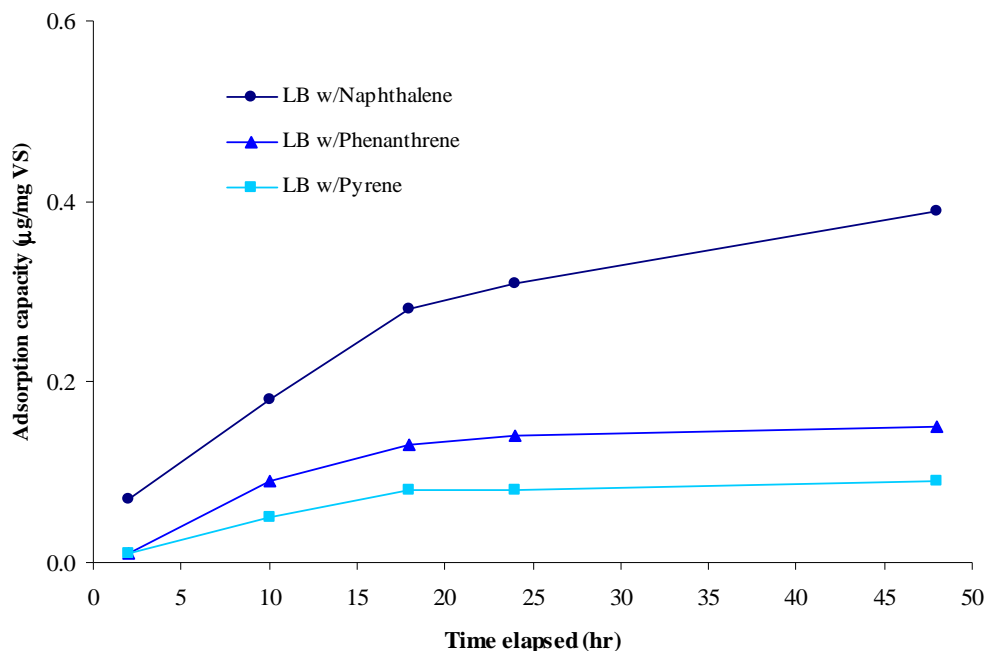


Figure 6.12 Adsorption capacity onto live biofilm (LB) of PAHs with time, in the presence of Triton X-100 (100 mg/L).

hours, but these amounts constituted an average of 88% of the total adsorbed capacity reached at 48 hours of these PAHs.

A similar tendency was observed for the batch experiments with 125 mg/L of Triton X-100 (**Figure 6.13**). The average increase in sorption capacity of naphthalene, phenanthrene and pyrene onto live biofilm was reported to be 10%, due to the increase in surfactant concentration; however, this increase is not considered significant and sorption. Sorption effects may be more evident if much higher concentrations of Triton X-100 are used. Killed biofilm results showed almost the same levels for the 2-, 3- and 4-ring PAHs as in the live biofilm experiments.

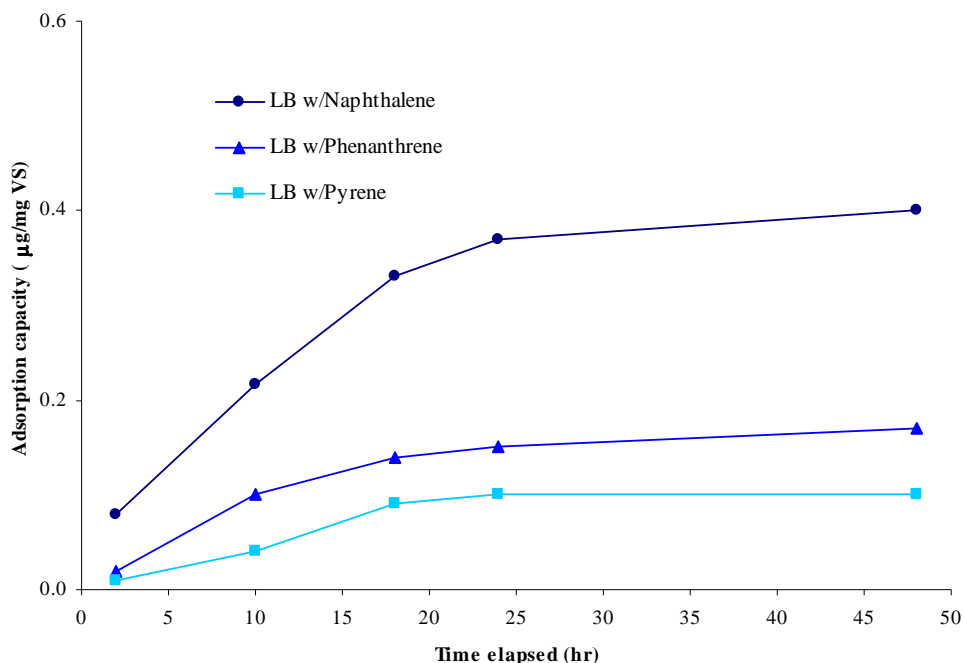


Figure 6.13 Adsorption capacity onto live biofilm (LB) of PAHs with time, in the presence of Triton X-100 (125 mg/L).

It can be concluded that both Triton X-100 concentrations may have increased the amount of PAHs sorbed into the biofilm, because of the increased solubilities of the compounds, but at the same time, sorption may not play an important role within the biofilm, other than making PAHs more available for the microorganisms.

6.5 CONCLUSIONS

The use of surfactants for enhancing the solubilities of hydrophobic compounds such as PAHs has been widely reported in the literature. The extent of solubilization, toxicity

effects and other diverse interactions between surfactant and PAHs, and even with the supporting medium where PAHs persist needs to be deeply investigated.

Triton X-100 did not appear to show any toxic effects to microorganisms, although the surfactant concentrations were very close to the critical micelle concentration. Also, no competitive effects between Triton X-100 and an easily degradable substrate like naphthalene were observed while conducting cell growth experiments; this can be explained by the stable structure of the surfactant.

It was shown that Triton X-100 could considerably enhance the solubilities of naphthalene, phenanthrene and pyrene by 2, 16 and 100 times, respectively. Even though several studies in the literature have indicated that solubilities of PAHs can be better increased, from 500-fold to even 10^4 -fold, by using high concentrations of surfactants, the solubility results from this study are considered more than satisfactory, taking into account the low concentration of Triton X-100 used, which was around its CMC. The effectiveness of the surfactant in solubilizing the three PAHs was assessed by determining the molar solubilization ratio (MSR) and the micelle/water partition coefficient (K_m), which were generally around the range reported for PAHs and Triton X-100 in other studies.

Adsorption capacities of Triton X-100 to sand and live/killed biofilm were found to be almost negligible, considering the porous medium has no organic content, the surfactant is a non-easily degradable compound (thanks to its high molecular weight and stable

ringed-structure) and that the concentrations used were around the CMC. Due to increased solubilities of PAHs, these compounds were found to adsorb slightly onto sand and biofilm, but these values were not still considered to be significant, compared to their concentrations that remained in solution.

Future research should look into testing a wide variety of surfactants for the solubilization of single and multiple PAHs, as well as the use of mixed surfactants to evaluating synergistic solubilizing effects on hydrocarbons. The surfactant's structure and PAH-PAH and/or surfactant-PAHs interactions should also be investigated, because PAH concentrations in the micelles may change in different systems.

The physical properties of hydrocarbons in soils can be expected to range from liquid to high-viscosity semi-solid due to weathering and prior biodegradation. Consequently, dispersion of bacteria from hydrocarbon surfaces by sub- and upper-CMC concentrations of surfactant may inhibit growth and concomitant bioremediation, for a range of hydrocarbon properties.

Surfactants, and especially Triton X-100, are promising materials for the development of novel environmental remediation applications, but needs further investigation of its properties and its effects on PAHs.

6.6 REFERENCES

- Abdul, A., Gibson, T., (1991), "Laboratory studies of surfactant-enhanced washing of polychlorinated biphenyl from sandy material", *Env.Sci.&Techn.*, **25**, 665-671.
- Backhus, D., Picardal, F., Johnson, S., Knowles, T., Collins, R., Radue, A., Kim, S., (1997), "Soil- and surfactant reductive dechlorination of carbon tetrachloride in the presence of *Shewanella putrefaciens* 20 ", *Contam.Hydrol.*, **28**, 337-361.
- Boonchan, S., Britz, M.L., Stanley, G.A., (1998), "Surfactant-enhanced biodegradation of high-molecular weight polycyclic aromatic hydrocarbons by *Stenotrophomonas maltophilia*", *Biotechnol&Bioengin.*, **59**(4),482-494.
- Bramwell, D., Laha S., (2000), "Effects of surfactant addition on the biomineralization and microbial toxicity of phenanthrene", *Biodegradation*, **11**, 263-277.
- Chen, P., Pickard, M., Gray, M., (2000), "Surfactant inhibition of bacterial growth on solid anthracene", *Biodegradation*, **11**, 341-347.
- Churchill, P., Dudley, R., Churchill, S., (1995), "Surfactant-enhanced bioremediation", *Wast.Managem.*, **15**(5/6), 371-377.
- Doong, R., Lei, W., (2003), "Solubilization and mineralization of polycyclic aromatic hydrocarbons by *Pseudomonas putida* in the presence of surfactant", *J.Hazard.Mater.*, **B96**, 15-27.
- Edwards, D., Luthy, R., Liu, Z., (1991), "Solubilization of polycyclic aromatic hydrocarbons in micellar nonionic surfactant solutions", *Env.Sci.&Techn.*, **25**, 127-133.
- Edwards, D., Adeel, Z., Luthy, R., (1994), "Distribution of nonionic surfactant and phenanthrene in a sediment/aqueous system", *Env.Sci.&Techn.*, **28**, 1550-1560.
- Fortin, J., Jury, W., Anderson, M., (1997), "Enhanced removal of trapped non-aqueous phase liquid from saturated soil using surfactant solutions", *J.Contam.Hydrol.*, **24**, 247-267.
- Guha S., Jaffe, P., Peters, C., (1998), "Solubilization of PAH mixtures by a nonionic surfactant", *Env.Sci.&Techn.*, **32**, 930-935.
- Guha, S., Jaffe, P., (1996), "Biodegradation kinetics of phenanthrene partitioned into the micellar phase of ionic surfactant", *Env.Sci.&Techn.*, **25**(30), 605-611.
- Jeong, S., Corapcioglu, M., Roosevelt, S., (2000), "Micromodel study of surfactant foam remediation of residual trichloroethylene", *Env.Sci.Tecn.*, **34**, 3456-3451.

Kim, I.S., Park, J., Kim, K., (2001), "Enhanced biodegradation of polycyclic aromatic hydrocarbons using nonionic surfactants in soil slurry", *App. Geochemist.*, **16**, 1419-1428.

Klumpp, E., Heitman, H., Schwuger, M., (1991), "Interactions in surfactant/pollutant/soil mineral systems", *Tens.Surfact.Deterg.*, **28**, 441-446.

Haigh, S., (1996), "A review of the interaction of surfactants with organic contaminants in soil", *The Science of the Total Environment*, **185**, 161-170.

Laha, S., Luthy, R.G., (1991), "Inhibition of phenanthrene mineralization by nonionic surfactants in soil-water systems", *Env.Sci.Tecn.*, **25**, 1920-1930.

Laha, S., Luthy, R.G., (1992), "Effects of nonionic surfactants on the solubilization and mineralization of phenanthrene in soil-water systems", *Biotechn.Bioengineer.*, **40**, 1367-1380.

Li, J.L., Chen, B.H., (2002), "Solubilization of model polycyclic aromatic hydrocarbons by nonionic surfactants", *Chem.Eng.Sci.*, **57**, 2825-2935.

Liu, Z., Edwards, A., Luthy, R.G., (1992), "Non-ionic surfactant sorption onto soil", *Wat.Sci.& Techn.*, **26**, 2337-2340.

Neu, R., (1996), "Significance of bacterial surface-active compounds in interaction with bacteria with interfaces", *Microb.Rev.*, **60**, 151-166.

Park, D., Abriola, L., Weber Jr., W, Bocskay, K., Pennels, K., (2000), "Solubilization rates of *n*-alkanes in micellar solutions of nonionic surfactants", *Env.Sci.&Techn.*, **34**, 476-482.

Pennell, K., Abriola, M., Weber, W., (1993), "Surfactant-enhanced solubilization of residual dodecane in soil columns, 1. Experimental investigation", *Env.Sci.&Techn.*, **27**, 2332-2340.

Prak, D., Pritcard, P., (2002), "Solubilization of polycyclic aromatic hydrocarbon mixtures in micellar nonionic surfactant solutions", *Water Research*, **36**, 3463-3472.

Rosen, M.J., (1989), "Surfactant and interfacial phenomena", (2nd Ed.), New York, Wiley.

Somesundaran, P., Hanna, H., (1977), "Physico-chemical aspects of adsorption at solid/liquid interfaces". In D. Shah and R. Schechter Editors, Improved oil recovery by surfactant and polymer flooding. Academic Press, London, pp.205-252.

Shiau, B.J., Sabatini, D, Harwell, J., (1995), “Properties of food grade surfactants affecting subsurface remediation of chlorinated solvent”, *Env.Sci.&Techn.*, **29**, 2929-2935.

Stelmack, P., Gray, M., Pickard, M., (1999), “Bacterial adhesion to soil contaminants in the presence of surfactants”, *Appl.Environm.Microb.*, **65**, 163-168.

Tiehm, A., (1994), “Degradation of polycyclic aromatic hydrocarbons in the presence of synthetic surfactants”, *Appl.Environm.Microbiol.*, **60**, 258-263.

Volkering, F., Breure, A.M., Sterkenburg, A., Van Andel J., Rulkens, W., (1995), “Influence of nonionic surfactants on bioavailability and biodegradation of polycyclic aromatic hydrocarbons”, *Appl.Env.Microbiol.*, **61**, 1699-1705.

Yuan, S.Y., Wei, S.H., Chang, B.V., (2000), “Biodegradation of polycyclic aromatic hydrocarbons in a mixed culture”, *Chemosphere*, **41**, 1463-1468.

Zhu, L., Feng, S., (2003), “Synergistic solubilization of polycyclic aromatic hydrocarbons by mixed anionic-nonionic surfactants”, *Chemosphere*, **53**, 459-467.

Chapter 7

EFFECTS OF NONIONIC SURFACTANT ADDITION ON THE BIODEGRADATION OF PAHS

7.1 ABSTRACT

The application of surfactants for the bioremediation of contaminated sites with polycyclic aromatic hydrocarbons has been widely reported, because they are known to increase PAH solubility and desorption, enhancing thereby their bioavailability to biofilm microorganisms. The effects of a nonionic surfactant on the biodegradation of PAHs in porous media, as well as the fate of the surfactant, were investigated in this study. Column experiments in the presence of the surfactant showed that, while the degradation of the 2-ring PAH alone was not affected, there was a small enhancement of 3- and 4-ring PAH degradation when they were present as sole-substrates and when using Triton X-100, thanks to the higher solubility of the PAHs. Biofilm seemed to respond well to binary mixtures of phenanthrene-naphthalene and pyrene-naphthalene with removals of 45.5% and 24.1%, respectively, in the presence of the surfactant; however, higher biodegradations were always achieved by having just PAH mixtures without the surfactant, indicating the importance of cometabolic / cross feeding mechanisms over improved solubilization of PAHs. Biofilm composition was measured at the end of the experimental run and showed a good production of viable biomass, as well as EPS material. Optical sections taken using a confocal laser scanning microscope allowed

observation of a heterogeneous web-like matrix of biofilm, with diverse biological aggregate structures.

7.2 INTRODUCTION

Polycyclic aromatic hydrocarbons (PAHs) are major recalcitrant hydrophobic compounds, usually produced by industrial activities, disposal of processing wastes and incomplete combustion of organic materials. The decontamination of PAH-polluted sites is of substantial importance because many of these are either known or suspected carcinogens and mutagens to humans. Due to the low aqueous solubility and strong sorption properties of PAHs, the extent and rate of their biodegradation are restricted by limited bioavailability, so that contaminated soils are not easily treated by biological means.

Surfactants have been suggested for the bioremediation of PAH-contaminated sites, because they are mobilizing agents that enhance the desorption and solubility of hydrophobic compounds, increasing their availability for biodegradation (Backhus et al., 1997). At high concentrations, particularly above the surfactant's critical micelle concentration (CMC), these substances can alter the distribution of the contaminant between aqueous and solid phases, in which spherical micelle clusters may be formed. Their interior is a non polar phase and may dissolve appreciable quantities of non polar solutes which are virtually insoluble in normal aqueous solutions, increasing the apparent solubility of compounds such as PAHs.

There is little information concerning the effects of surfactants on the biodegradation of PAHs and furthermore, the available studies have reported inconclusive results at sub- or super-CMC concentrations (Margessin and Schinner, 1999). Some studies showed enhanced effects (Kim *et al.*, 2001; Lee *et al.*, 1995; Zheng and Obbard, 2001; Churchill *et al.*, 1995), in which not only low molecular weight PAHs were degraded successfully, but even compounds containing four, five, six and seven rings. Boonchan *et al.* (1998) reported the improvement by 30% of the degradation of PAH mixtures (three to seven benzene rings) by using the nonionic surfactant Tergitol NP-10 (10 g/L), and it was explained by a dynamic exchange of PAH molecules between the micelles and the liquid, that served to replenish the supply of PAHs more quickly into the aqueous pseudophase as they were degraded.

However, several studies showed inhibitory effects when using surfactant on PAH biodegradation (Laha and Luthy, 1991, 1992). Bramwell and Laha (2000) reported a decrease of the mineralization of 3-ring PAHs even at low doses of surfactants; toxicity tests suggested that solubilized phenanthrene increased the toxic effect by a 100-fold. Yuan *et al.* (2000) also found repeated inhibition of phenanthrene and other PAHs by common surfactants such as Brij 30 and 35, and longer lag phases caused by Triton X-100 and Triton N101, due to a decrease in the microbial activity and the presence of hydrophilic molecules as inhibitors. Guha and Jaffe (1996) and Liu *et al.* (1995) have explained the negative impacts by the inaccessibility of the microorganisms to micelle-bound PAHs; this might be related to cell surface hydrophobicity that influences the transfer of PAH from micelles to cells, because of complex microbial membrane

processes. Tiehm (1994), Deschenes *et al.* (1995) and Hutchins *et al.* (1991) reported in some cases the preferential utilization of surfactants over PAHs, as primary substrates, especially when they have simple molecular structures, which may exclude the degradation of heavier compounds such as PAHs.

The objective of this study was to evaluate the capacity of a nonionic surfactant (Triton X-100) to affect the biodegradation of PAHs and to define the effects of the surfactant on biofilm composition and structure in porous media environments. Sand column experiments with sole-substrate/binary mixtures of naphthalene, phenanthrene and pyrene were conducted to establish the effectiveness of Triton X-100 on their mineralization. This study provides an important guideline for the development of more effective remediation strategies in future field applications of the surfactant flushing remediation technology.

7.3 MATERIALS AND METHODS

The commercial nonionic surfactant Triton X-100 used in this study has been extensively evaluated for enhanced-bioremediation technologies (Zhu and Feng, 2003; Li and Chen, 2002, Yuan *et al.*, 2000; Churchill *et al.*, 1995; Backhus *et al.*, 1997). Details on its properties can be found in **Chapter 6**.

Study of the biodegradation of PAHs in the presence of a nonionic surfactant was conducted with lab-scale reactors of 30-cm length. Five sample ports for pore water

samples along the length of the column, as well as four flow cell ports for examination of biofilm growth, were used for this purpose. Details on the experimental system can be found in **Chapter 3**. A nutrient solution was combined with a PAH-surfactant solution and then pumped into the column at a linear pore water velocity of 5 m/d; when PAHs alone were needed in the system, a similar PAH generation mode was operated as is explained in **Chapter 5**. Sodium acetate solution (10 mg/L) was used in the system for development and enhancement of biofilm, and a small dose of hydrogen peroxide solution (3.5%) was also injected to maintain aerobic conditions in the reactors.

The inoculum for the soil columns was a mixed liquor sample from an activated sludge aeration tank, taken from a domestic wastewater treatment plant (Polk Run WWTP, Cincinnati, OH). A period of 6 weeks with acetate and naphthalene as substrates, prior to PAH-surfactant addition, was allowed in order to develop a suitable biofilm.

Columns were operated for a total of 22 weeks. Pore water samples were taken twice a week and analyzed for the contaminant concentration, dissolved oxygen (DO) and pH. Biofilm composition analysis was performed by taking samples from each flow cell at the end of the experimental run, when total and viable biomass (firmly and loosely attached biomass), carbohydrate and protein concentrations were measured. Biofilm structure examination was also conducted at the 22nd week using scanning confocal laser microscopy, in order to observe the physical structure, heterogeneity and growth patterns of biofilm in the flow cells. Detailed descriptions of analysis procedures and composition of the feed solution can be found in **Chapter 3**.

7.4 RESULTS AND DISCUSSION

Two main columns were used in this study (Columns 1 and 3) to test the biodegradation of PAHs (as sole-substrates and binary mixtures) in the presence of nonionic surfactant Triton X-100, added in two different concentrations (100 and 125 mg/L). Killed control columns (Columns 2 and 4) were operated simultaneously and at the same conditions as the main columns, but with the addition of sodium azide (1g/L) to minimize biomass growth. **Table 7.1** summarizes the sequence of the experiments over a period of 22 weeks. Aerobic conditions were always maintained in the reactors and did not limit biological processes; influent DO was kept at 8-9 mg/L and effluent DO ranged between 0.5 and 1.0 mg/L. The pH was measured to be from 7.3 to 7.5 during the run.

Table 7.1 Summary of sequence of experiments.

	Triton X-100 at 100 mg/L	
	Column 1	Column 2 (Control)
Sole-substrate 1 (SS1)	NAPH	NAPH + Az
Sole-substrate 2 (SS2)	PHE	PHE + Az
Binary mixture 1 (BM1)	PHE, NAPH	PHE, NAPH + Az
Sole-substrate 3 (SS3)	PYR	PYR + Az
Binary mixture 2 (BM2)	PYR, NAPH	PYR, NAPH + Az
	Triton X-100 at 125 mg/L	
	Column 3	Column 4 (Control)
Sole-substrate 1 (SS1)	NAPH	NAPH + Az
Sole-substrate 2 (SS2)	PHE	PHE + Az
Binary mixture 1 (BM1)	PHE, NAPH	PHE, NAPH + Az
Sole-substrate 3 (SS3)	PYR	PYR + Az
Binary mixture 2 (BM2)	PYR, NAPH	PYR, NAPH + Az

PHE: phenanthrene, PYR: pyrene, NAPH: naphthalene, AZ: azide

7.4.1 Biodegradation studies at 100 mg/L of Triton X-100

The biodegradation of PAHs in the presence of 100 mg/L of Triton X-100 was conducted in Columns 1 and 2 (**Figure 7.1**). In the first week and a half, naphthalene was supplied as the sole-substrate (SS1) while the surfactant was added into the system; naphthalene did not appear to be affected since its removal efficiency was maintained at 99.7%.

Phenanthrene was then introduced in a binary mixture (BM1) with naphthalene. It was seen that bacteria began to degrade (in less than a week) the higher molecular weight PAH in the presence of the more easily degradable co-substrate, reaching a removal efficiency of 75.5%. At this point and for the following 3.5 weeks, phenanthrene was then fed to the columns as the sole carbon source along with the surfactant (SS2). Two stages were observed for the 3-ring compound: first, the degradation of phenanthrene decreased suddenly to about 30.9%; it seemed the PAH was being rapidly solubilized by the 100 mg/L of Triton X-100, but was still not sufficiently available for the biofilm because of micellar phenanthrene not being directly usable, so that it moved through the column and was released with only a small portion being degraded. Second, and after approximately 2 weeks, the removal slightly increased to 39.9%, probably due to some solubilized phenanthrene which had been accumulated on the biofilm and then mineralized. The increase in the biodegradation of the 3-ring PAH was not caused by cometabolic mechanisms with Triton X-100, because the surfactant biodegradation was always minimal (less than 2%), as shown in the microbial growth studies; the surfactant has a stable benzene structure with a high molecular weight that makes it not easily used

as a primary substrate. Later, surfactant addition was stopped for a week, during which time phenanthrene nearly totally failed to degrade; the removal efficiency was measured to be only 9.6%, indicating the inability of being mineralized individually.

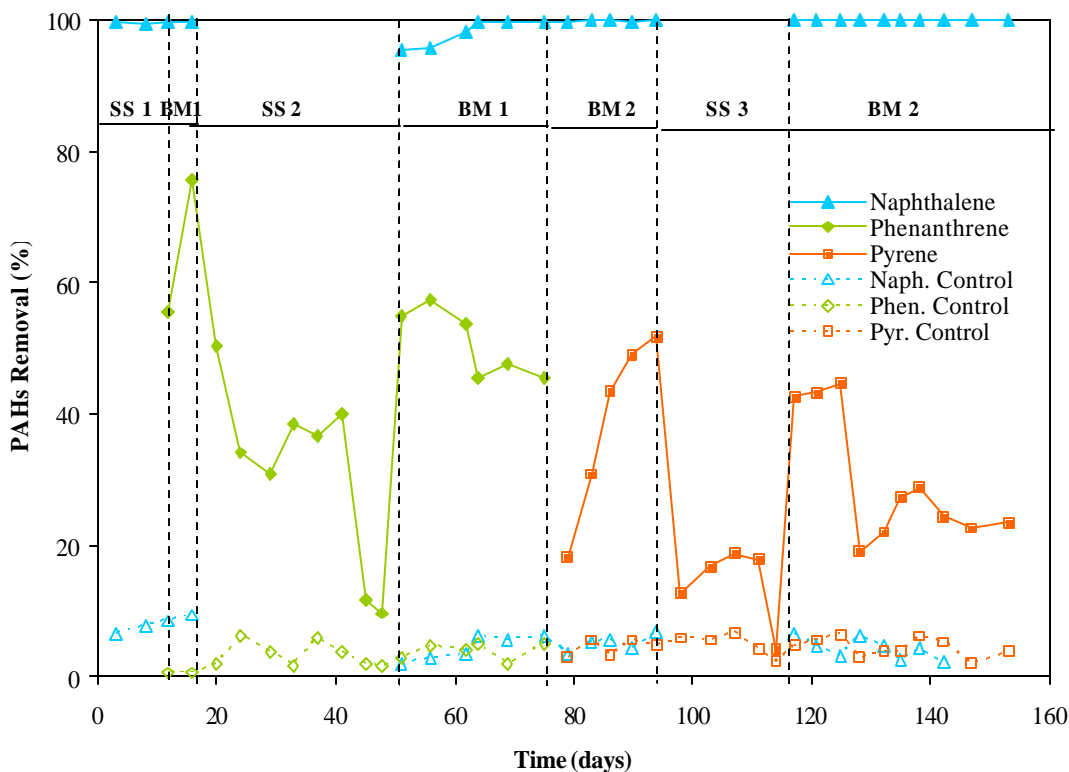


Figure 7.1 Removal efficiencies of PAHs in the presence of 100 mg/L Triton X-100 (Shaded areas indicate addition of surfactant).

Overall, the presence of the surfactant did not appear to improve the degradation of the 3-ring PAH to a significant level; with or without Triton X-100, phenanthrene biodegradation could not occur by itself. The solubility of the compound was improved, but the availability to the biofilm was limited. Similar results with phenanthrene as the sole-substrate were already explained in **Chapter 5** and confirm these results.

Reapplication of naphthalene for a period of 2 weeks allowed the system to recover back to good phenanthrene (53.7%) and naphthalene (98.3%) removal efficiencies. The binary mixture (BM1) was then maintained and evaluated for another 2 weeks, during which 100 mg/L of Triton X-100 were added. The 2-ring PAH maintained its satisfactory biodegradation (around 99.8%), while the 3-ring PAH biodegradation decreased to 45.5%, indicating the preference of the bacteria to use phenanthrene only in the presence of an easily degradable co-substrate and independently of the presence of the surfactant, since the degradation was not enhanced from both naphthalene and Triton X-100. Higher degradation efficiency for the binary mixture was observed for the two PAHs alone, as seen in **Chapter 5**, indicating that cometabolism was occurring in the system.

From days 75 to 94, the system was acclimatized to a second binary mixture (BM2) of naphthalene and pyrene; they reached removals of 99.8 and 51.7%, respectively, thanks to a well-developed biomass which most probably utilized enzymes for the 2-ring degradation that were also involved in the 4-ring degradation. Pyrene as a sole-substrate (SS3) was then tested in the presence of the surfactant, but its removal decreased to 12.6% in only 4 days, probably due to a sudden solubilization and mobilization of the PAH. However, in the following 11 days a slow but small increase in the biodegradation was observed up to 17.9%, because the biofilm was able to use the more soluble PAH, but neither removal rates were comparable to results achieved during the application of binary mixtures. Without the surfactant, bacteria were totally unable to break down pyrene; in less than three days, the removal efficiency dropped to 4.1%.

Pyrene was allowed around ten days to recover its degradation with a mixture with naphthalene (BM2), thanks to the amending capacity of the co-substrate. Once the 2- and 4-ring PAHs reached removal efficiencies of 99.9% and 44.7% respectively, the system was evaluated for its performance while adding Triton X-100. During a period of 4 weeks, complete naphthalene removal was obtained, which was coherent with the sole-substrate and binary mixtures 1 and 2 for naphthalene experiments. However, pyrene removal showed a sudden decrease to 19.1% removal in just a few days, where the PAH was probably being mobilized along the reactor but minimally biodegraded; however, it slowly recovered to an average of 24% removal efficiency during the application period of the binary mixture.

7.4.2 Biodegradation Studies at 125 mg/L of Triton X-100

Experiments in the presence of 125 mg/L of Triton X-100 were conducted in Columns 3 and 4 and are shown in **Figure 7.2**. Naphthalene as sole-substrate (SS1) was initially tested in the presence of the nonionic surfactant, and it was found that the 2-ring PAH biodegradation was maintained at 99.3% over a 1.5 week period.

The biofilm in the reactors was then acclimated to utilize a binary mixture of naphthalene and phenanthrene (BM1) for a short period of time; both PAHs achieved high removal efficiencies of about 99.4 and 77.1%, respectively; phenanthrene seemed to follow a cometabolic mechanism of biodegradation.

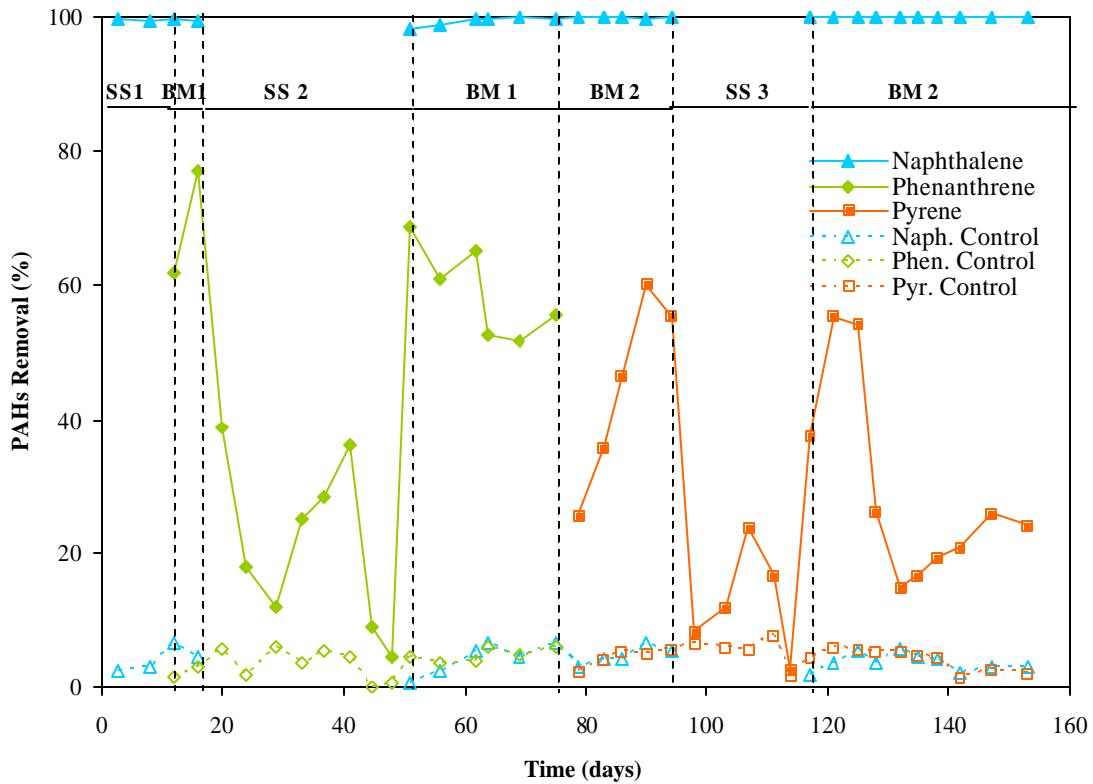


Figure 7.2 Removal efficiencies of PAHs in the presence of 125 mg/L Triton X-100. (Shaded areas indicate addition of surfactant).

Phenanthrene as sole-substrate (SS2) was evaluated from weeks 3 to 5 while Triton X-100 was being added into the system. It was determined in the first 13 days that biodegradation of the 3-ring PAH dramatically decreased to 11.9%, a similar trend as observed in the sand column with 100 mg/L Triton X-100, indicating not only rapid solubilization of phenanthrene but also its inability to be transferred to the biofilm to be utilized. However, more than a week later, the removal efficiency was improved to 36.0%, which can be explained by the time that was allowed for the bacteria to degrade the soluble phenanthrene. Phenanthrene as sole substrate was also evaluated as to its

performance without surfactant addition in the system; a very low biodegradation (down to 4.5%) was the response, because, once again, the metabolism of the contaminant appeared to be dependent on a more easily degradable carbon source.

The addition of a binary mixture of naphthalene and phenanthrene allowed the system to recover for a week and removal efficiencies of 98.8 and 68.7%, respectively, were measured. The binary mixture (BM1) was then evaluated in the presence of Triton X-100 for another 3.5 weeks. While naphthalene removal did not appear to be affected by either phenanthrene or the surfactant, maintaining an average of 99.7% biodegradation, the 3-ring PAH removal decreased to 55.6%. Even though the removal efficiency of phenanthrene was improved considerably from that as a sole-substrate to that of the binary mixture (both with Triton X-100), the 3-ring PAHs always showed a better performance thanks to co-substrates in the system. Solubilization of the high molecular weight PAH played a minor role in enhancing the removal efficiency, but only when phenanthrene was present as a sole-substrate and after a period of 2 or 3 weeks of running under those conditions.

A second binary mixture (BM2) of naphthalene and pyrene was introduced into the sand column for 3 weeks, in order to acclimate the bacteria to cometabolic/cross feeding mechanisms for the combined biodegradation of the two compounds; removals of 99.9 and 59.9% were achieved in this period for naphthalene and pyrene, respectively. Sole-substrate (SS3) experiments with pyrene were then carried out in the presence of the surfactant. These showed high solubilization of the contaminant, inducing its

mobilization through the column instead of its biodegradation; in just a few days the removal efficiency of pyrene went down to 8.4%, but then it slowly increased to 16.6%. At day 111, when the surfactant was not present anymore, pyrene removal failed when pyrene was the sole substrate, and the observed removal was down to 1.9% in only 4 days, because of the absence of an appropriate co-substrate to produce intermetabolites for the biofilm to use.

Naphthalene and pyrene were later reintroduced into the system as the second binary mixture (BM2), to reestablish favorable metabolic conditions for the microbial population; degradation of the two compounds were measured to be of 99.9% and 55.3%, respectively, which was very similar to that shown in PAH mixture biodegradation in **Chapter 5**. From days 125 to 153, the surfactant solution was added to the columns, and during this period naphthalene maintained its highest removal efficiency. However, pyrene showed two main phases that followed the same biodegradation trend as when 100 mg/L Triton X-100 was used: first, a rapid decrease to 15.1% removal was observed in less than a week, where pyrene was solubilized but not efficiently biodegraded; second, a recovery up to 24.2% removal after accumulation and mineralization of pyrene within the biofilm.

The results from the two series of column experiments are summarized in **Table 7.2**. It is shown that naphthalene biodegradation was always successfully completed (higher than 99.5%), independent of the presence of Triton X-100. This was expected since the 2-ring PAH is a low molecular weight compound, with the highest solubility of all PAHs and is

most easily degradable because of its structure. The addition of surfactant definitely improved phenanthrene and pyrene biodegradations as sole-substrates, due to the contaminants' higher solubilities, which made them more available to the bacteria within the biofilm. The improvements due to the surfactant addition were on average from 7 to 37% (for the 3-ring PAH) and from 3 to 20% (for the 4-ring PAH), even though the metabolic mechanisms from carbon source utilization were not totally successful because of the absence of a co-substrate and the production of the appropriate enzymes that stimulated further the mineralization process; this was confirmed by the use of binary mixtures in the presence of Triton X-100, and as previously described in **Chapter 5**.

Table 7.2 Summary of effects of addition of Triton X-100 during PAH biodegradation.

	w/Triton X-100	w/o Triton X-100
Naphthalene	0	0
Phenanthrene	+	-
Pyrene	+	-
Naphthalene + Phenanthrene	+	++
Naphthalene + Pyrene	+	++

Binary mixtures of naphthalene-phenanthrene and naphthalene-pyrene behaved in a similar way; while a little improvement on the degradation was observed with the presence of the surfactant, it was not as high as the excellent enhancements with just the mixtures and without Triton X-100. The predominant mechanism in both cases was cometabolism, which allowed the production of essential enzymes by the bacteria during the 2-ring PAH mineralization for the utilization of the 3- and 4-ring PAHs, as was previously observed and explained in **Chapter 5**. The use of Triton X-100 appeared to

improve the solubilities of all the compounds; however, in the short term the high-molecular weight PAHs were transported rapidly throughout the column, and biofilm was unable to use them. Over a longer period of time, a small increase in the biodegradation efficiencies was observed in both systems, even though removal percentages were always lower for the binary mixture alone than when surfactant was added. Surfactant concentration did not seem to affect the overall removal efficiencies of single PAHs or their mixtures because both 100 and 125 mg/L surfactant were concentrations near the CMC value of Triton X-100, and because the results obtained showed similar trends in columns 1 and 3 for sole-substrates and binary mixtures.

According to several studies, naphthalene has always been known to be more easily biodegradable than other PAHs, and the effects of surfactant addition are typically negligible to non-existent (Kim *et al.*, 2001; Ghosh *et al.*, 1995). In a few cases, researchers have observed lower rates of biodegradation, as evidenced by an increased lag period, but the overall removal efficiency of the compound was not changed (Chen *et al.*, 2001). However, Auger *et al.* (1995) reported a case of “overflow metabolism”, in which reduced biodegradation of naphthalene in the presence of a nonionic surfactant was observed; the carbon source was in such abundance that it created incomplete metabolized by-products which became inhibitory as they accumulated.

Contradictory results have been found in the literature on the use of surfactants in bioremediation applications of high-molecular weight PAHs; some researchers have shown biodegradation enhancements in the presence of surfactants for phenanthrene,

pyrene, fluorene, anthracene, benzo[a]anthracene, chrysene and benzo[a] pyrene, which have very stable structures and are very recalcitrant compounds. Márquez-Rocha *et al.* (2000) reported an increase removal from 23 to 75% (for the 3-ring PAH) and from 12 to 75% (for the 4-ring PAH), when Tween 40 (1.5 g/L) surfactant was added to a contaminated soil. Complete biodegradation of phenanthrene was achieved by Kim *et al.* (2001) by using Brij 30 (1.5 g/L), but this was combined with the surfactant biodegradation which actually acted as a co-substrate for the 3-ring PAH. Also the rates of biodegradation of PAHs can be increased in surfactant-enhanced environments: Churchill *et al.* (1995) showed that by using Inipol EAP 22 (1 g/L) the rates for phenanthrene mineralization increased by two-fold, as a result of increased biomass in the samples and excellent solubilization of the compound. In another study (Boonchan *et al.*, 1998), the addition of Tergitol NP-10 and Brij 35 (10 g/L) increased the maximum specific PAH degradation rate by 30% and decreased the lag period normally seen for PAH degradation for single PAHs and mixtures, for 4 to 7 ring compounds.

On the other hand, some inhibitory effects have also been reported, explained by the toxicity of the surfactant. Branwell and Laha (2000) found reduced removal efficiencies for phenanthrene by one half, due to reduced biomass growth and microbial inability to adapt to the presence of surfactants. Also, Guha and Jaffe (1996) explained the decrease in biodegradation rates of PAHs by concluding that parts of solubilized PAHs in the micellar phase of the surfactant may not be directly available for the degraders; in fact, they demonstrated that this portion decreased as micelle concentration increased with a

fixed amount of phenanthrene in the system. This has been confirmed by several authors such as Deschenes *et al.* (1995) and Laha and Luthy (1991).

7.4.3 PAH/Surfactant Adsorption onto Sand Medium

Final killed biomass PAH-surfactant concentrations in the sand media, after sodium azide addition and at 22 weeks, are provided in **Figure 7.3** (for biodegradation studies at 100 mg/L of Triton X-100) and **Figure 7.4** (for biodegradation studies at 125 mg/L).

In the case of the addition of 100 mg/L of surfactant, the maximum naphthalene concentration on the sand was measured at 7.5 cm (0.75 ± 0.16 $\mu\text{g/g}$ dry sand), and then decreased to an average value of 0.54 $\mu\text{g/g}$ dry sand along the remaining distance into sand column. Phenanthrene was found to be adsorbed at 0.35 ± 0.09 $\mu\text{g/g}$ dry sand at the inlet; its concentrations decreased to 0.22 , 0.08 and 0.04 $\mu\text{g/g}$ dry sand at 12.5, 17.5 and 22.5 cm depth, respectively. The presence of Triton X-100 seemed to result in a doubling of the naphthalene and phenanthrene concentrations in the sand medium, due to their higher resulting solubilities; on the other hand, the pyrene concentration at the inlet of the column was increased by ten times by the addition of the surfactant, and this can be explained by the 100-fold increase in the pyrene soluble fraction when surfactants were added. Even so, adsorption of pyrene to the porous media was still considered negligible, being less than 0.2 $\mu\text{g/g}$ dry sand. The killed control column showed higher increases in PAH sorption onto sand with respect to the inoculated column, with increases of 45% for

naphthalene and 56% for phenanthrene, while a decrease of 15% was measured for pyrene samples.

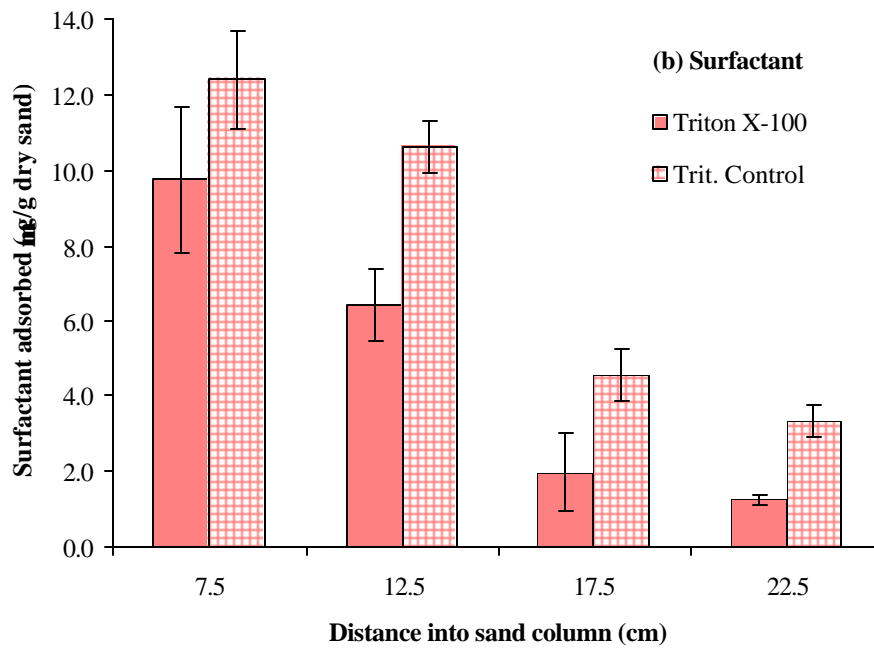
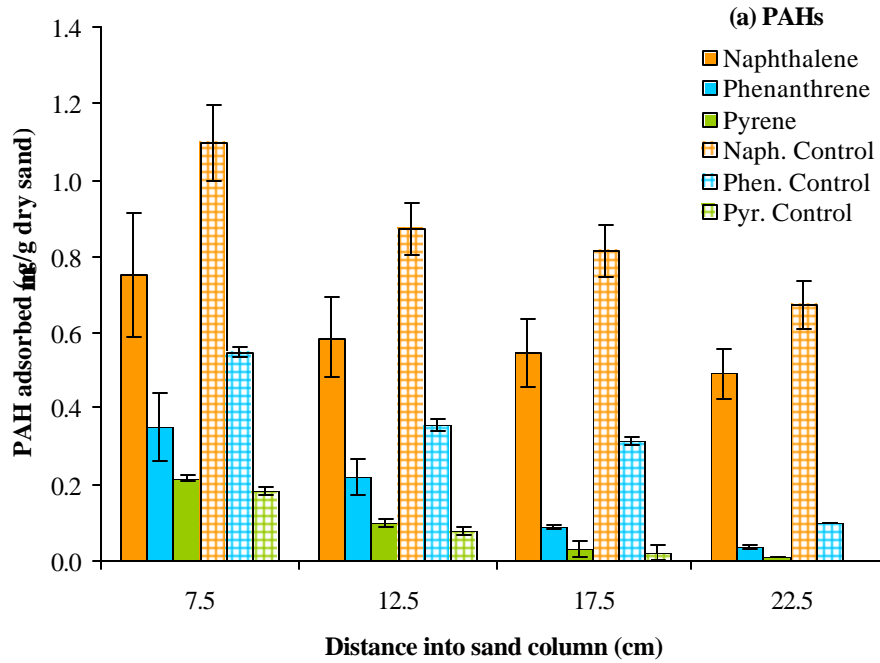


Figure 7.3 Sorption of (a) PAHs and (b) surfactant (100 mg/L) onto sand.

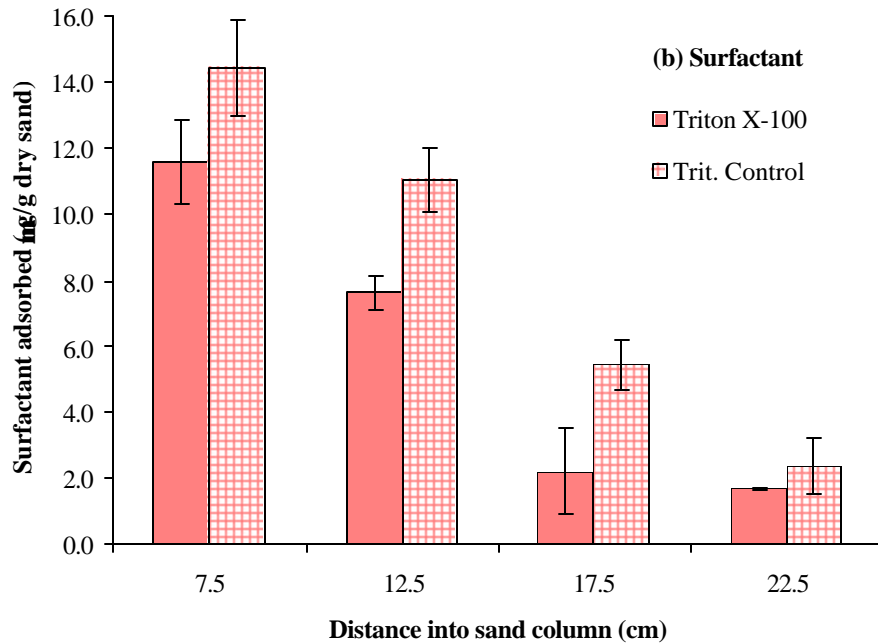
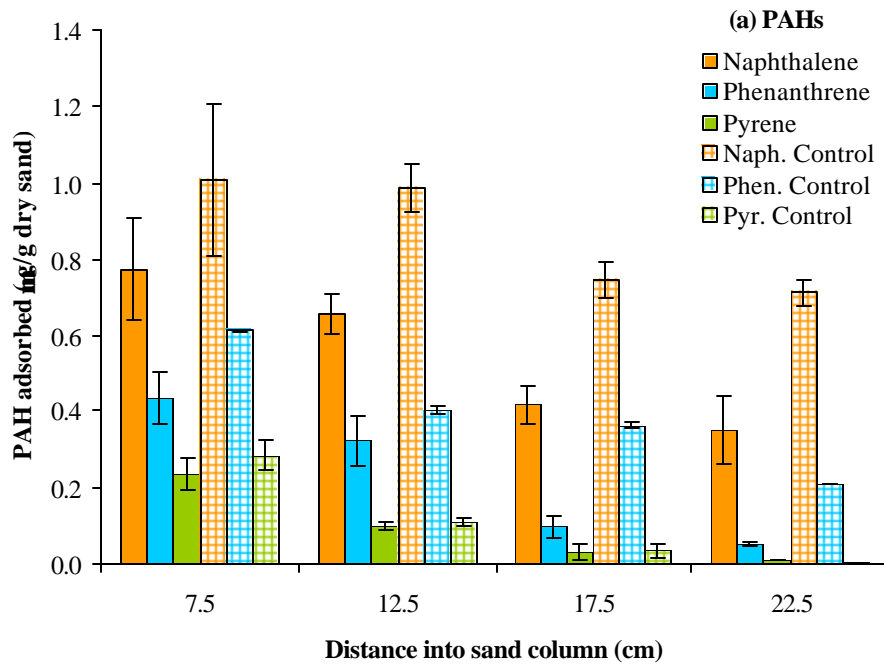


Figure 7.4 Sorption of (a) PAHs and (b) surfactant (125 mg/L) onto sand.

Evaluation of the amount of Triton X-100 (at 100 mg/L) sorption to sand during the biodegradation studies was also carried out. The highest surfactant concentrations adsorbed to the porous media were observed at 7.5 and 12.5 cm from the inlet of the column and they were 9.77 ± 1.93 and 6.43 ± 0.95 $\mu\text{g/g}$ dry sand, respectively. In the remaining distance, an average of 3.5 $\mu\text{g/g}$ dry sand was adsorbed. Although, the Triton X-100 concentrations appeared to be 13, 29 and 45 times higher than PAH concentrations on the sand media, the removal of the surfactant was still determined to be below 1.5%, which corresponds to a removal of less than 1 mg/L of surfactant from solution.

A similar trend was observed for PAH sorption onto sand in the columns that received 125 mg/L of Triton X-100. Naphthalene showed an average sorption of 0.55 $\mu\text{g/g}$ dry sand along the depth of the column; its maximum value was 41% higher than the average and was observed at the 7.5 cm depth. The phenanthrene concentration at 7.5 cm was 0.435 ± 0.07 $\mu\text{g/g}$ dry sand, and decreased to 0.32, 0.09 and 0.05 $\mu\text{g/g}$ dry sand at 12.5, 17.5 and 22.5 cm respectively. Pyrene concentrations varied from 0.23 $\mu\text{g/g}$ dry sand (at 7.5 cm) to almost non-detectable at 0.01 $\mu\text{g/g}$ dry sand (at 22.5 cm). Although all the PAH concentrations are still considered insignificant, increases of 30% for naphthalene, 41% for phenanthrene and 21% for pyrene were observed with respect to the inoculated column. Again, the maximum amount of Triton X-100 adsorbed onto sand was observed at the inlet of the column at 11.57 ± 1.26 $\mu\text{g/g}$ dry sand, but it decreased by 34% in the following 5 cm and by 80% across the distance of the column. Removal-wise, the surfactant concentration did not decrease more than 2% from its initial concentration in solution.

It can be concluded that profiles for both PAH and surfactant did not show significant concentration changes across the columns, indicating the low adsorptive capacity of the sand medium for these compounds, as expected. Therefore, biodegradation can be considered to be the main removal mechanism for the PAHs, when present both as sole-substrates and in mixtures.

7.4.4 Biofilm Composition

The composition of biofilm across the depth of the columns was analyzed at the end of the experimental run (week 22). **Figure 7.5** shows the profiles for total biomass in the presence of Triton X-100. No significant difference was observed between the two surfactant concentrations, due to their proximity to the CMC value. Highest biomass values were measured at the inlet of the columns at 2626 ± 145 and 2596 ± 326 $\mu\text{g/g}$ TS for 100 and 125 mg/L of Triton X-100, respectively, due to the major availability of contaminants and nutrients at this location. Total biomass values decreased with depth into the columns until 12.5 cm, after which cells and EPS material were maintained at an average of 1155 $\mu\text{g/g}$ TS for both surfactant cases. The increased solubilization of the PAHs, especially phenanthrene and pyrene, may have contributed to a relative well-distributed biomass with distance into the column, because of their mobilization and transport within the surfactant micelles. Eventually, PAHs were biodegraded with time and good production of both living cells and exopolymeric substances were observed towards the outlets of the sand columns. The killed control columns showed only 20-26%

of the biomass grown in the main columns, which remained constant over the period of 22 weeks.

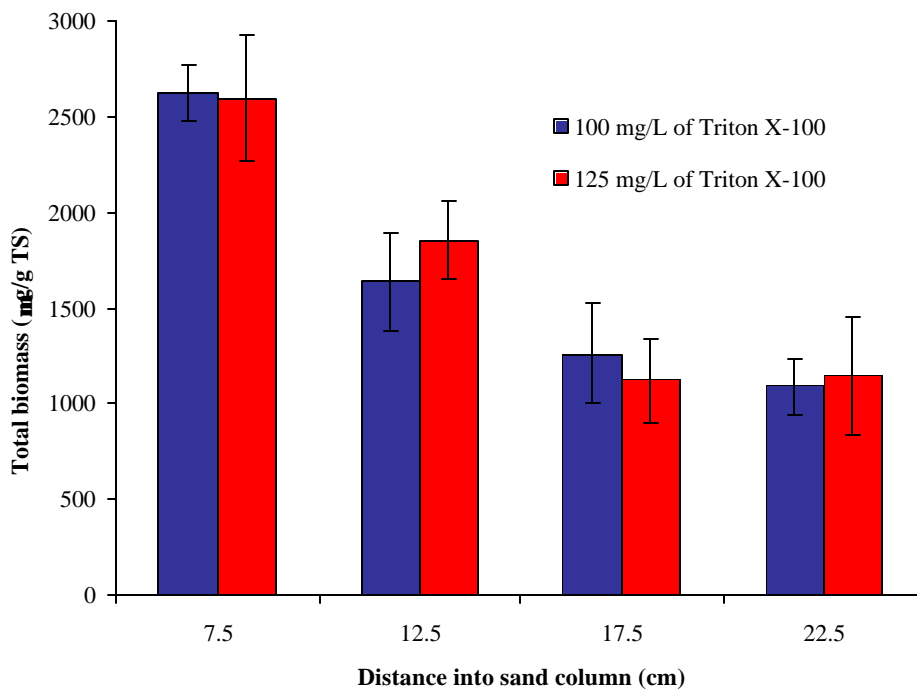


Figure 7.5 Total biomass profile in the presence of Triton X-100.

Results from lipid-phosphate profiles for both surfactant concentrations are shown in **Figure 7.6** and indicate that the maximum production of viable biomass occurred at 7.5 cm depth, with 463 ± 39 mg/g VS (for 100 mg/L Triton X-100) and 524 ± 88 mg/g VS (for 125 mg/L Triton X-100). The presence of naphthalene in the first weeks of the experimental run greatly improved the growth of new living cells, because of the ability to mineralize completely the 2-ring compound. This also helped with the establishment of an active biofilm matrix at the bottom of the sand columns; however, the biodegradation of binary mixtures could have supplied additional viable biomass because of the higher solubilities of phenanthrene and pyrene, which made them more available for biofilm

utilization. Averages of 253 and 261 mg/g VS for 100 mg/L and 125 mg/L of Triton X-100, respectively, were measured across the sand columns at the 12.5 cm depth; only small standard deviations were calculated, so only a slight decrease in mg LP/g VS was reported with distance. Both main columns seemed to show a similar behavior concerning the production of viable biomass during the 22-week period under the two surfactant concentrations; an average of only 10% of the viable biomass grown in the inoculated columns was found in the killed controls.

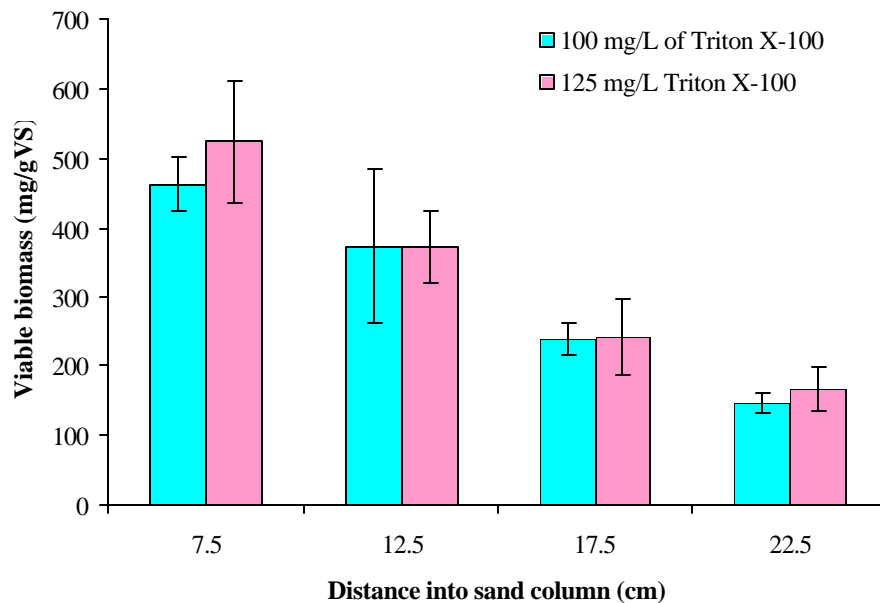


Figure 7.6 Viable biomass in the presence of Triton X-100.

The viable biomass could be distinguished in this study in both the firmly attached biomass (base biofilm attached to the surface of the porous media) and loosely attached biomass (all aggregates easily separated from the sand). **Figure 7.7 (a)** and **(b)** describes the firmly and loosely attached biomass at the end of the experimental run for both Triton

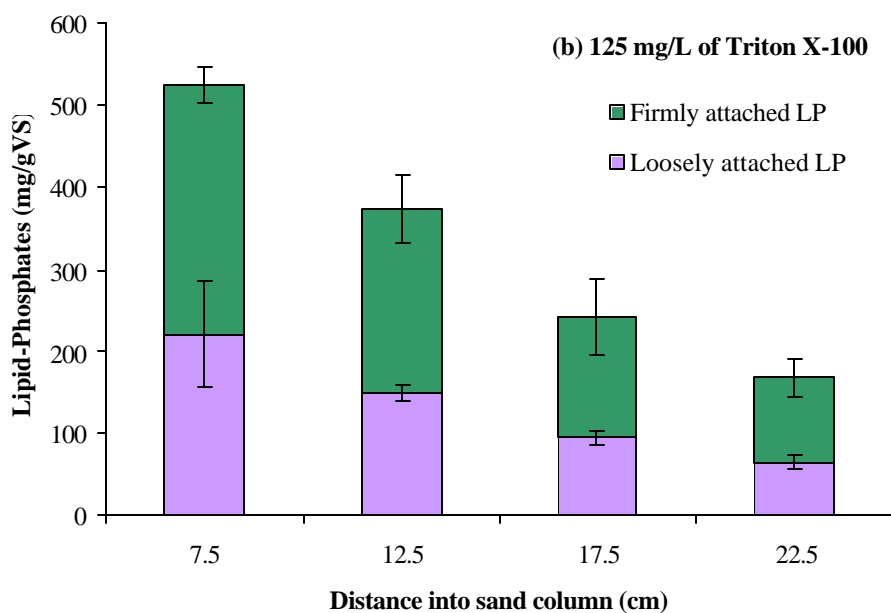
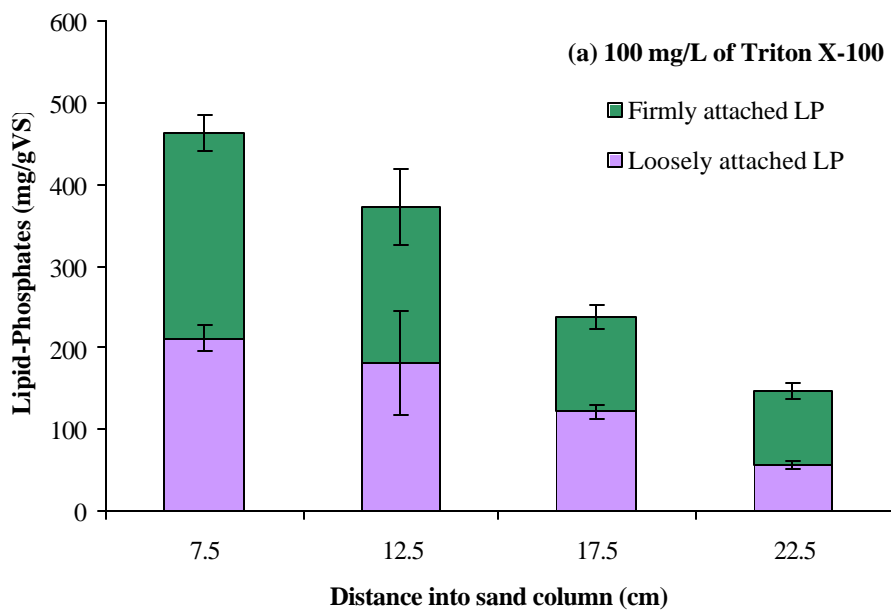


Figure 7.7 Firmly and loosely attached biomass profiles in the presence of (a) 100 mg/L and (b) 125 mg/L of Triton X-100.

X-100 concentrations. It can be seen that firmly attached biomass accounted for 54 to 61% of the total lipid-phosphates, indicating that there was a major fraction of viable biomass directly attached to sand grain surfaces; this was evident for both 100 and 125 mg/L of surfactant and also along the depth of the columns. Maximum concentrations of firmly attached biomass were found at the inlet of the columns, with values of 250 ± 22 (for 100 mg/L Triton X-100) and 303 ± 22 mg/g VS (for 125 mg/L Triton X-100). This may be the result of the degradation of naphthalene as a sole-substrate at the early stages of the experimental run, as well as use of naphthalene as a co-substrate during the binary mixture applications. It was evident mostly at the 7.5 cm distance.

Loosely attached biomass seemed to be more evenly distributed with distance across the sand columns, because of the mobilization of the more soluble and higher molecular weight PAHs (phenanthrene and pyrene) further into the columns over the 22-week period. The existent firmly biofilm produced more living cells, which may have been entrapped and transported from 12.5 to 22.5 cm of distance, creating new biomass, first weakly attached and later on, firmly attached. Averages of 143 and 132 mg/g VS were measured for 100 and 125 mg/L of Triton X-100, respectively, with this distance. A range from 6 to 11% of the firmly and loosely attached biomass grown in the inoculated columns was measured in the killed control columns after 22 weeks.

Characterization of the extracellular polymeric substances (EPS) was also conducted at the end of the experimental run, by analyzing carbohydrate and protein contents in the biofilm. **Figure 7.8** describes the carbohydrate profile for both Triton X-100

concentrations. As shown, the maximum value of carbohydrates at 100 mg/L of surfactant was measured to be 162 ± 21 mg/g VS at 7.5 cm into sand column, due to the biodegradation of the easily degradable naphthalene in the first weeks; between the 12.5 and 22.5 cm ports, the amounts leveled out to an average of 116 mg/g VS. This was probably due to the utilization of phenanthrene and pyrene during their binary mixture addition with the 2-ring PAH, because they were more soluble and, therefore, were transported and mineralized further into the column. The column that received 125 mg/L of Triton X-100 followed a similar trend, even though higher concentrations were found at 7.5-cm and at 12.5-cm depths, with carbohydrate amounts of 174 ± 10 and 139 ± 13 mg/g VS, respectively; more soluble compounds could have stimulated the production of new carbohydrates. An average of 32 mg/g VS was measured along the killed control columns, which remained constant during the 22 weeks.

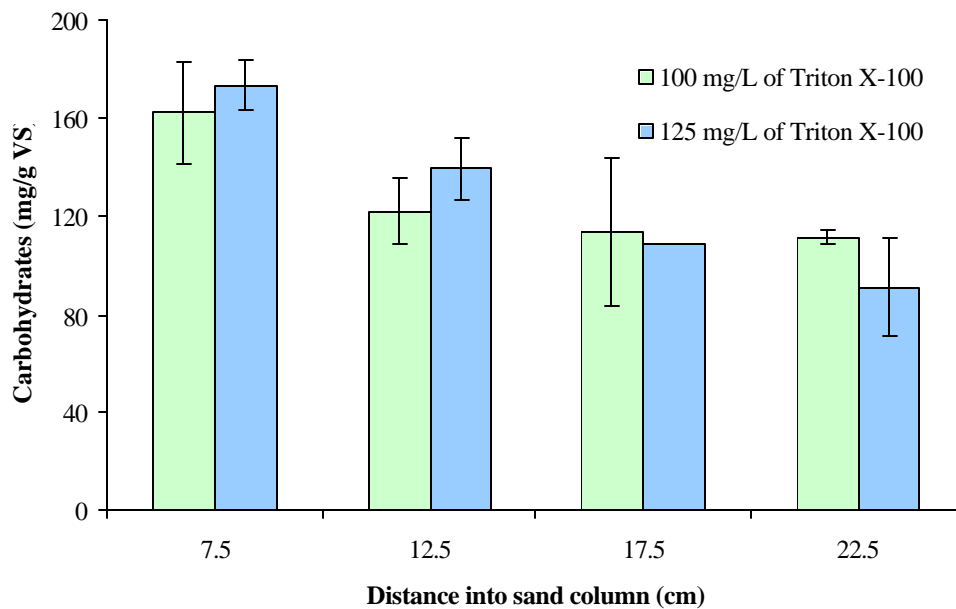


Figure 7.8 Carbohydrate profile in the presence of Triton X-100.

The profile of protein concentrations during a 22-week run are shown in **Figure 7.9**. Progressive decrease of protein mass per volatile solid mass with increasing distance into the sand column was observed for both Triton X-100 concentrations. At the inlet of the columns, the amounts of proteins were 72 ± 9 and 61 ± 4 mg/g VS for 100 and 125 mg/L of surfactant, respectively, and these, as in the carbohydrate case, indicate a good production of EPS material in a well-established biofilm in the presence of the 2-ring PAH. The degradation of binary mixtures seemed to have contributed to significant amounts of proteins along the columns, due to the higher solubilities of phenanthrene and pyrene in the presence of surfactant, with averages of 42 and 37 mg/g VS that were measured between the 12.5 and 22.5 cm depths. Very low concentrations of proteins were found in the killed control columns.

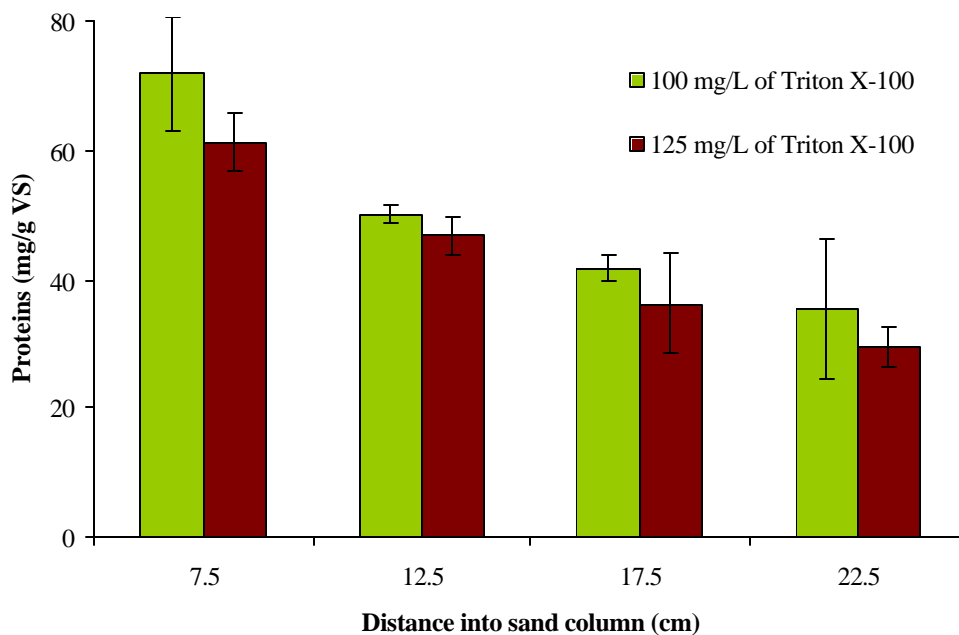


Figure 7.9 Protein profile in the presence of Triton X-100.

7.4.5 Biofilm Structure

The active zone of the columns at 7.5 cm of depth was used for biofilm structure examination at the end of the experimental run (week 22), using Confocal Scanning Laser Microscopy. The optical sections of biofilms grown in the presence of 100 mg/L of Triton X-100 are shown in **Figure 7.10 (a)** and **(b)**. Sand grains seemed to be covered by a base biofilm with layers of variable thickness between 15 to 25 μm ; however, a heterogeneous surface of biomass was observed, consisting not only of continuous biofilms, but also small cell clusters of approximately 20-25 μm in diameter, that were still weakly attached to the main monolayer. The formation of large structures, such as protrusions and aggregates of 40-60 μm , was commonly seen as a result of the biodegradation of naphthalene, which contributed to the establishment of a solid biofilm matrix. Consequently, the amount of biomass per unit sand medium was increased in the early stages of the experimental run. A thick bioweb-type growth was also observed because of the presence of biofilm material in the pore spaces between sand grains; “biofilm bridges” were formed as the interconnections of two or more surface biofilms of soil particles. The areas filled with new living cells and EPS substances were probably due to the mobilization of soluble 3- and 4-ring PAHs, whose degradation contributed on the creation of weakly attached biomass that was transported in the pore spaces.

Figure 7.11 (a) and **(b)** shows optical sections of biofilms grown after 22 weeks of the study with PAHs and 125 mg/L of Triton X-100. In this case, surface biofilms of 10-15 μm thickness were observed, in combination with numerous small cell clusters,

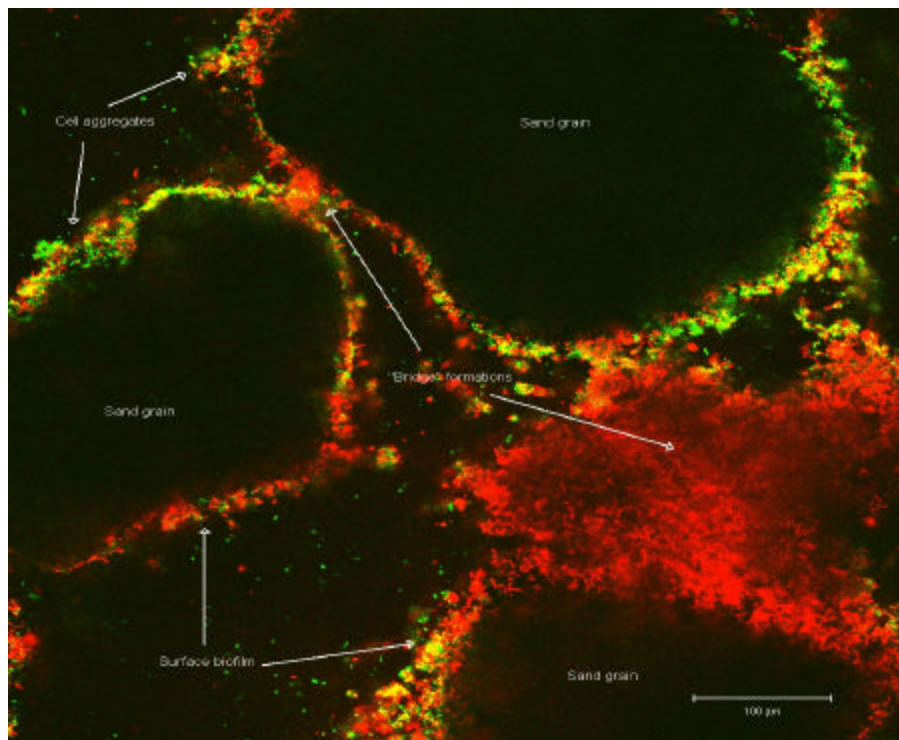
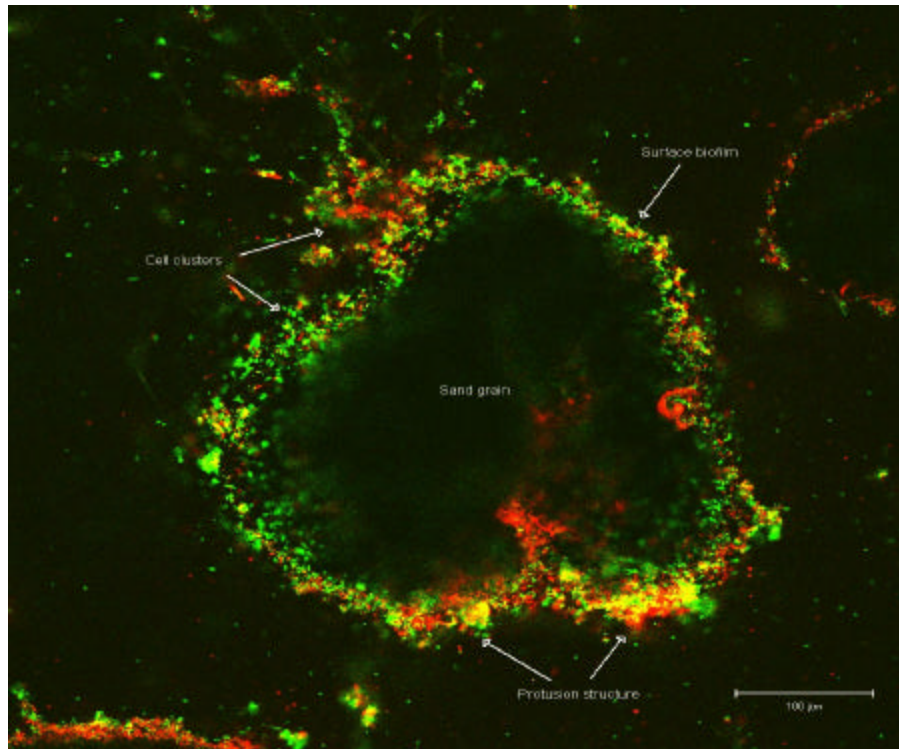


Figure 7.10 Optical sections of biofilms on sand grain surfaces at 7.5 cm (a) at 40x and (b) 20x magnifications, in the presence of 100 mg/L of Triton, after 22 weeks.

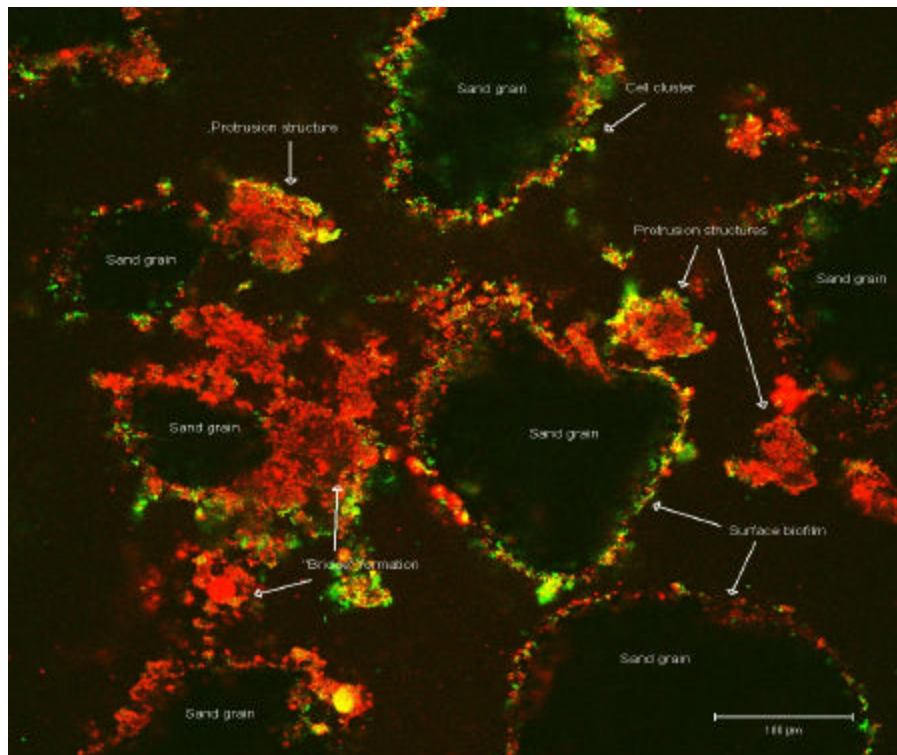
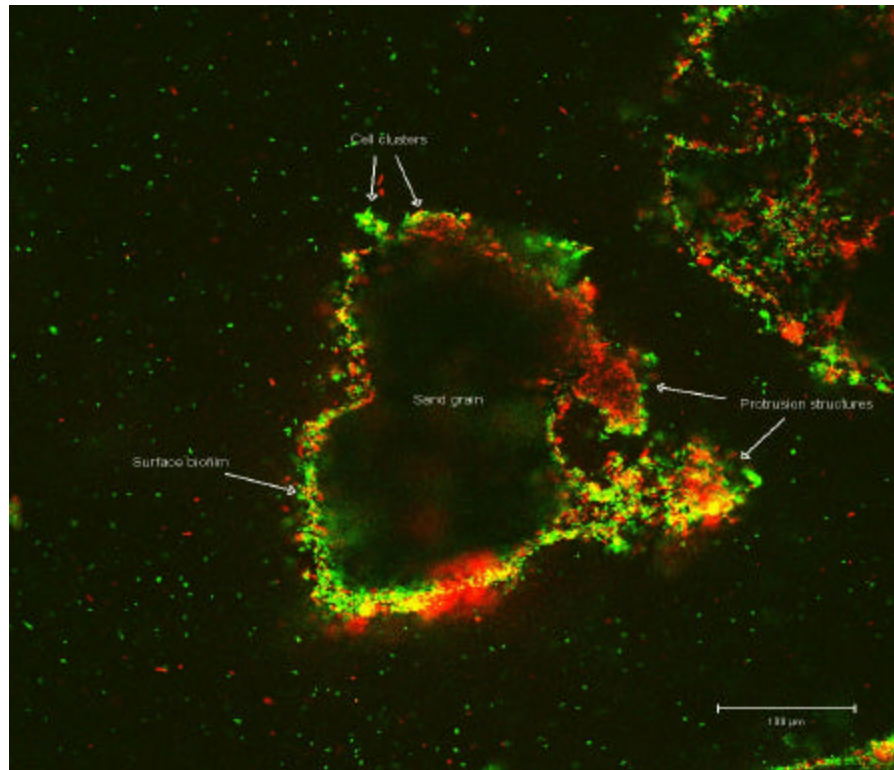


Figure 7.11 Optical sections of biofilms on sand grain surfaces at 7.5 cm (a) at 40x and (b) 20x magnifications, in the presence of 125 mg/L of Triton, after 22 weeks.

ranging from 15 to 20 μm in diameter; this biofilm seemed to provide a sparse matrix, where a diverse microbial community allowed for the successful biodegradations of PAHs and their mixtures. The appearance of large cluster-and-protrusion-type structures was more frequent and larger in size (40-60 μm), compared to the sand columns with 100 mg/L of Triton X-100. These biofilm bodies may have been formed by the degradation of the 2-ring PAH as a sole-substrate and in the binary mixtures. Therefore, a dense and heterogeneous coverage of aggregates, not necessarily attached to sand grains, created a “bioweb” network of strands of different shapes and sizes.

Similar biofilm structures were shown in **Chapter 5**, when PAHs and their mixtures were used without the addition of any surfactant. This may explain the sparse and heterogeneous coverage of bacteria on porous media. The individual processes that control the formation and persistence of biofilm (such as adsorption, growth, attachment, desorption and detachment) are common to porous media. Once microorganisms find the way to interact or attach to the media surfaces, colonizing them and promoting their survival and growth, viable cells will find access to sorbed nutrients and increase their ability to grow and survive in changing environmental conditions.

Other studies (Paulsen *et al.*, 1997; Dunsmore *et al.*, 2004; Ebihara *et al.*, 1997, 1999) have described the diverse morphology of biofilms growing on soil particles. In general, the presence of continuous monolayers maximizing the coverage of a large surface area of the porous media is very common, but at the same time, structures such as clusters,

protrusions, strands and bridges may form in the interstitial spaces, creating a complex and heterogeneous “bioweb” with biofilm bodies of varying shape and size.

7.5 CONCLUSIONS

Highly hydrophobic compounds, such as PAHs, have limited biodegradability, due to their low aqueous solubilities. The use of surfactants may increase the PAH partitioning fractions between the solid and liquid phases, but at the same time, they may affect positively and negatively the mineralization of the more soluble substrates. This has been confirmed by a number of studies in the literature, which have reported both enhanced-biodegradation and inhibition-toxic effects on PAHs.

The use of Triton X-100 on an easily-degradable substrate, such as naphthalene, did not appear to change the biological mechanisms of degradation; successful removals were always achieved for the 2-ring PAH. For more complex compounds like phenanthrene and pyrene, it was observed that their biodegradation may be improved as sole-substrates by the addition of surfactants, due to their resulting higher solubilities which made them more available to the bacteria within the biofilm. Even so, the need for an additional carbon source was evident because of the absence of the inter-metabolites produced by the bacteria to carry out the complete mineralization process, as was shown to occur during the binary-mixture study in **Chapter 5**.

In the case of the biodegradation of a two-PAH mixture, the results indicated that cometabolism was the main mechanism driving the biodegradation of the 3- and 4-ring PAHs, rather than the use of the surfactant. Triton X-100 may have enhanced the soluble fractions of the compounds, but at the same time they were not made more readily available for the biofilm, and instead, they were transported rapidly throughout the sand columns.

Although it was not the case in this study, soil and ground water may be significantly contaminated by the addition of surfactants. Studies on synergistic solubilization of PAHs by mixed surfactants should be conducted to decrease the costs and the impacts of using high concentrations of single surfactants, while maintaining the efficiency of surfactant solutions.

Biofilm composition analyses showed the presence of a large amount of living cells and exopolymeric material, as a result of the degradation of simple substrates such as naphthalene. The addition of a nonionic surfactant did not seem to play a major role in the composition of the bio-matrix. A heterogeneous biofilm structure was observed by confocal microscopy, indicating the complex formation of monolayers, clusters, aggregates, protrusions and “bridges” that varied in size and shape. The presence of naphthalene in the feed at early stages of the experiments contributed to the formation of a solid biofilm matrix, which remained active and well-established during the 22-week run.

In general, the application of surfactants in *in-situ* bioremediation needs the development of a predictive framework for surfactant-amended biodegradation of PAHs. Tests should be conducted extensively on different types of surfactants, their physical and chemical characteristics, their solubilizing ability for PAHs, their sorptive properties, their toxicity concentrations to microorganisms and their biodegradability, before their widespread application in the field, in order to establish the specific conditions for feasible and improved usage.

7.6 REFERENCES

- Auger, R., Jacobson, A., Domach, M., (1995), "Effect of nonionic surfactant addition on bacterial metabolism of naphthalene: assessment of toxicity and overflow metabolism potential", *J.Hazard.Mater.*, **43**, 263-272.
- Backhus, D., Picardal, F., Johnson, S., Knowles, T., Collins, R., Radue, A., Kim, S., (1997), "Soil- and surfactant reductive dechlorination of carbon tetrachloride in the presence of *Shewanella putrefaciens* 20 ", *Contam.Hydrol.*, **28**, 337-361.
- Boonchan, S., Britz, M.L., Stanley, G.A., (1998), "Surfactant-enhanced biodegradation of high-molecular weight polycyclic aromatic hydrocarbons by *Stenotrophomonas maltophilia*", *Biotechnol&Bioengin.*, **59**(4),482-494.
- Bramwell, D., Laha S., (2000), "Effects of surfactant addition on the biomineralization and microbial toxicity of phenanthrene", *Biodegradation*, **11**, 263-277.
- Chen G., Strevett, K., Vanegas, A., (2001), "Naphthalene, phenanthrene and surfactant biodegradation", *Biodegradation*, **12**, 453-442.
- Churchill, P., Dudley, R., Churchill, S., (1995), "Surfactant-enhanced bioremediation", *Wast.Managem.*, **15**(5/6), 371-377.
- Deschenes *et al.* (1995), Surfactant influence in PAH biodegradation in creosote-contaminated soil", pp.51-58, In: R.Hinchee, F. Brockman, and C. Vogel Eds., Microbial processes for bioremediation. Battelle Press, Columbus, OH.
- Dunsmore, B., Bass, C., Lappin-Scott, H., (2004), "A novel approach to investigate biofilm and bacterial transport in porous matrices", *Environm.Microbiol.*, **6**(2), 183-187.

Ebihara, T., Bishop, P.L., (1997), "Examination of biofilms utilized in bioremediation of organic compounds using confocal scanning microscopy techniques", *Superfund Basic Research Program Conference: a decade of improving health through multi-disciplinary research*, Chapel Hill, NC.

Ebihara, T., Bishop, P.L., (1999), "Biofilm structural forms in porous media utilized in organic compounds degradation", *Wat.Sci.&Techn.*, **39**(7), 203-210.

Ebihara, T. (1999), "Characterization and enhancement of microbial biofilms in porous media for the biodegradation of polycyclic aromatic hydrocarbons", PhD. Dissertation, University of Cincinnati, Cincinnati, OH.

Ghosh, M., Yeom, I., Shi, Z., Cox, C., Robinson, K., (1995), Surfactant-enhanced bioremediation of PAH- and PCB-contaminated soils", pp.15-23, In: R.Hinchee, F. Brockman, and C. Vogel Eds., *Microbial processes for bioremediation*. Battelle Press, Columbus, OH.

Guha, S., Jaffe, P., (1996), "Biodegradation kinetics of phenanthrene partitioned into the micellar phase of ionic surfactant", *Env.Sci.&Techn.*, **25**(30), 605-611.

Kim, I.S., Park, J., Kim, K., (2001), "Enhanced biodegradation of polycyclic aromatic hydrocarbons using nonionic surfactants in soil slurry", *App. Geochemist.*, **16**, 1419-1428.

Hutchins, R., Sewell, G., Kovacs, D., Smiths, G., (1991), "Biodegradation of aromatic hydrocarbons by aquifer microorganisms under denitrifying conditions", *Env.Sci.&Techn.*, **25**(1), 68-76.

Laha, S., Luthy, R.G., (1991), "Inhibition of phenanthrene mineralization by nonionic surfactants in soil-water systems", *Env.Sci.Tecn.*, **25**, 1920-1930.

Laha, S., Luthy, R.G., (1992), "Effects of nonionic surfactants on the solubilization and mineralization of phenanthrene in soil-water systems", *Biotechn.Bioengineer.*, **40**, 1367-1380.

Lee, M., Gregory, G., White, D., Fountain, J., Shoemaker, S., (1995), "Surfactant-enhanced anaerobic bioremediation of a carbon tetrachloride DNAPL". In: R.Hinchee, A. Leeson, L. Semprini (Eds), *Bioremediation of chlorinated solvents*. Battelle Press, Columbus, OH, pp147-151.

Li, J.L., Chen, B.H., (2002), "Solubilization of model polycyclic aromatic hydrocarbons by nonionic surfactants", *Chem.Eng.Sci.*, **57**, 2825-2935.

Liu, Z., Jacobson, A., Luthy, R., (1995), "Biodegradation of naphthalene in aqueous nonionic surfactant systems", *Appl.Environmental Microbiol.*, **61**, 145-151.

Márquez-Rocha, F., Hernández-Rodríguez, V., Vázquez-Duhalt, R., (2000), "Biodegradation of soil-adsorbed polycyclic aromatic hydrocarbons by the white rot fungus *Pleurotus ostreatus*", *Biotechn.Lett.*, **22**, 469-472.

Margessin, R., Schinner, F., (1999), "Biodegradation of diesel oil by cold-adapted microorganisms in the presence of sodium dedecyl sulfate", *Chemosphere*, **38**(15), 3463-3472.

Paulsen, J., Oppen, E, Bakken. R., (1997), "Biofilm morphology in porous media: a study with microscopic and imaging techniques", *Wat.Sci.& Techn.*, **36**(1), 1-9.

Tiehm, A., (1994), "Degradation of polycyclic aromatic hydrocarbons in the presence of synthetic surfactants", *Appl.Environment.Microbiol.*, **60**, 258-263.

Yuan, S.Y., Wei, S.H., Chang, B.V., (2000), "Biodegradation of polycyclic aromatic hydrocarbons in a mixed culture", *Chemosphere*, **41**, 1463-1468.

Zheng, Z., and Obbard, J., (2001), "Effects of nonionic surfactants on elimination of polycyclic aromatic hydrocarbons (PAHs) in soil-slurry by *Phanerochaete chrysosporium*", *J.Chem.Techn.Biotechn.*, **76**, 423-429.

Zhu, L., Feng, S., (2003), "Synergistic solubilization of polycyclic aromatic hydrocarbons by mixed anionic-nonionic surfactants", *Chemosphere*, **53**, 459-467.

Chapter 8

CONCLUSIONS AND RECOMMENDATIONS

8.1 CONCLUSIONS

This research provides an improved understanding of the transport and degradation mechanisms involved in soil bioremediation systems for low and medium molecular weight PAHs, as well as the important role of the biofilm matrix, in terms of growth and development, structure, composition and chemistry during *in situ* PAH biodegradation.

The following conclusions can be drawn from this study:

1. A low molecular PAH (naphthalene) was demonstrated to be easily degradable in the presence of a co-substrate, which enhanced its metabolism by 30%. Acetate also promoted the production of viable biomass and extracellular polymeric substances, creating a thick 'bioweb' network of combined surface biofilms and a variety of biological aggregate structures.
2. Image analysis was demonstrated to be a powerful tool to three-dimensionally quantify some of the morphological features of biofilms that relate to processes and conditions occurring in porous media. Characteristics such as biovolume, biosurface area, biothickness, cell diameter and cell density were identified and aided in understanding the relationship between structure and function in biofilms.

3. Multiple substrate utilization for a system with sole-substrate and binary/tertiary PAH mixtures was investigated. Two potential interactions of three PAH-based substrates were observed: positive effects (resulting in an increase in biodegradation of at least one of the components) and negative effects (inhibition of the medium molecular weight PAHs).
4. Biofilm composition was substrate dependent: the mineralization of easily degradable compounds contributed to the rapid reproduction of living cells, which released more exopolymeric material and helped in building the biofilm attached to the porous media. Binary and tertiary mixtures favored the formation of clusters and protrusions, increasing the biomass per unit sand area.
5. A nonionic surfactant was used to enhance the solubilities of PAHs, by 2, 16 and 100 times for naphthalene, phenanthrene and pyrene, respectively. Adsorption capacities of Triton X-100 to sand and live/killed biofilm were found to be almost negligible, considering the porous medium has no organic content, the surfactant is a non-easily degradable compound (thanks to its high molecular weight and stable ringed-structure) and that the concentrations used were around the CMC.
6. The use of Triton X-100 on naphthalene did not appear to change the biological mechanisms of degradation, but for more complex compounds like phenanthrene and pyrene, it was observed that their biodegradation may be improved as sole-substrates by the addition of surfactants, due to their resulting higher solubilities which made them more available to the bacteria within the biofilm. Even so, the need for an additional carbon source was evident because of the absence of the

inter-metabolites produced by the bacteria to carry out the complete mineralization process.

8.2 RECOMMENDATIONS

Degradation phenomena, where environmental conditions may affect the degrading capabilities of microbial communities, are system specific. Therefore, a more detailed study should be conducted on a wider range of PAH-degraders, under different scenarios of substrate utilization, especially high molecular weight PAHs and their mixtures. A better understanding of the potential interactions during PAH biodegradation by mixed cultures should be obtained in order to simulate more realistic field applications.

Image analysis (with available software) should be used to deeply investigate biofilm morphology and structure. A wide range of the textural and volumetric features should be selected to better represent the majority of the variation within the biofilm, so that the relationship between biofilm heterogeneity and the underlying processes (such as mass transport dynamics, substrate concentrations and species variations) can be properly quantified.

The application of surfactants into PAH bioremediation should be carefully evaluated because of PAH-PAH and/or surfactant-PAH interactions that may alter biological mechanisms. A wide variety of surfactants for the solubilization of single and multiple

PAHs, as well as the use of mixed surfactants to evaluating synergistic solubilizing effects on hydrocarbons should be thoroughly tested.

In general, *in situ* bioremediation needs the development of a predictive framework for biodegradation of Polycyclic Aromatic Hydrocarbons, before its application in the field, in order to establish the specific conditions for feasible and improved usage.

Appendix A

SAND COLUMN DESIGN AND OPERATION

Sand column design and operating details are summarized in this Appendix. Pictures of experimental setup are also available.

Sand column design summary:

Column diameter (ID):	3.8 cm
Column length:	30 cm
Pore water sample ports:	5, 10, 15, 20 and 25 cm
Flow cell port locations:	7.5, 12.5, 17.5 and 22.5 cm

Sand column operation summary:

Feed flowrate:	2.03 mL/min
Linear pore water velocity:	5 m/d
Flow cell flowrate:	4.4 mL/hr
H ₂ O ₂ solution concentration:	3.5 % (v/v)
H ₂ O ₂ feed rate:	0.25 mL/hr
NaAc solution concentration:	484 mg/L
NaAc feed rate:	0.06 mL/min
NaAz solution concentration:	13450 mg/L
NaAz feed rate:	0.06 mL/min

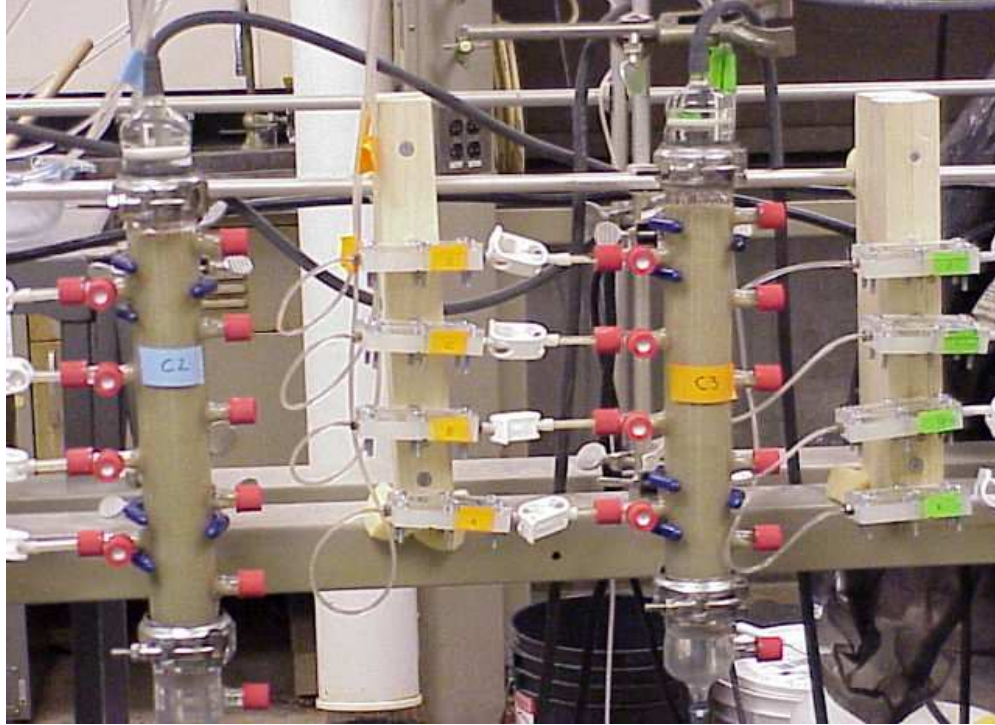


Figure A.1 Experimental setup of single sand column and flowcells.

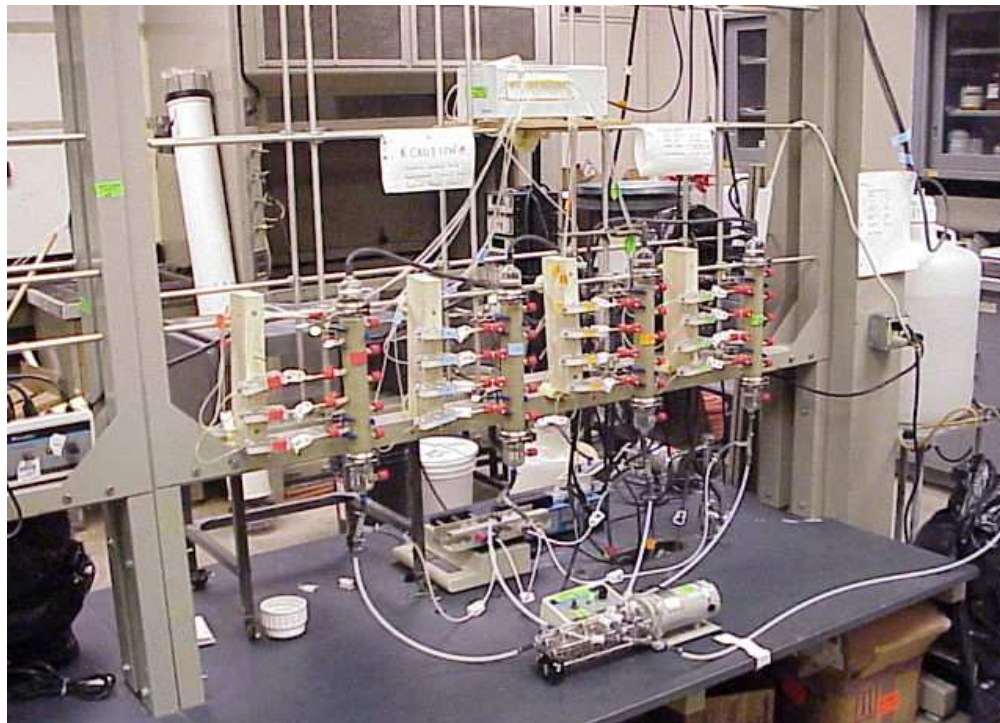


Figure A.2 Complete experimental setup.

Appendix B

PHYSICAL PROPERTIES OF SAND MEDIA

The bulk properties of the sand media used in column and batch experiments are presented in this Appendix. Physical properties include particle density, bulk density, porosity and particle size distribution.

Sand medium: ASTM silica sand (C-190)

Particle density: 2.65 g/cm^3

Bulk density: 1.70 g/cm^3

Effective porosity: 0.36

Median grain size: 0.38 mm

Size distribution: **Figure B.1**

08/06/2002

Type of sand: silica sand ASTM C-190

Mass of dry sample + dish: 786.91 g

Mass of dish: 192.31 g

Mass of dry sample: 594.6 g

Sieve N°	Diam. (mm)	Mass retained (g)	% retained	% passing
10	2	0.00	0.0000	100.0000
20	0.85	0.30	0.0504	99.9496
40	0.425	200.27	33.6707	66.2789
60	0.25	334.54	56.2451	10.0338
100	0.15	54.39	9.1444	0.8894
140	0.106	4.74	0.7969	0.0925
200	0.075	0.44	0.0740	0.0185
pan		0.11	0.0185	0.0000
	Total	594.79	100.0000	

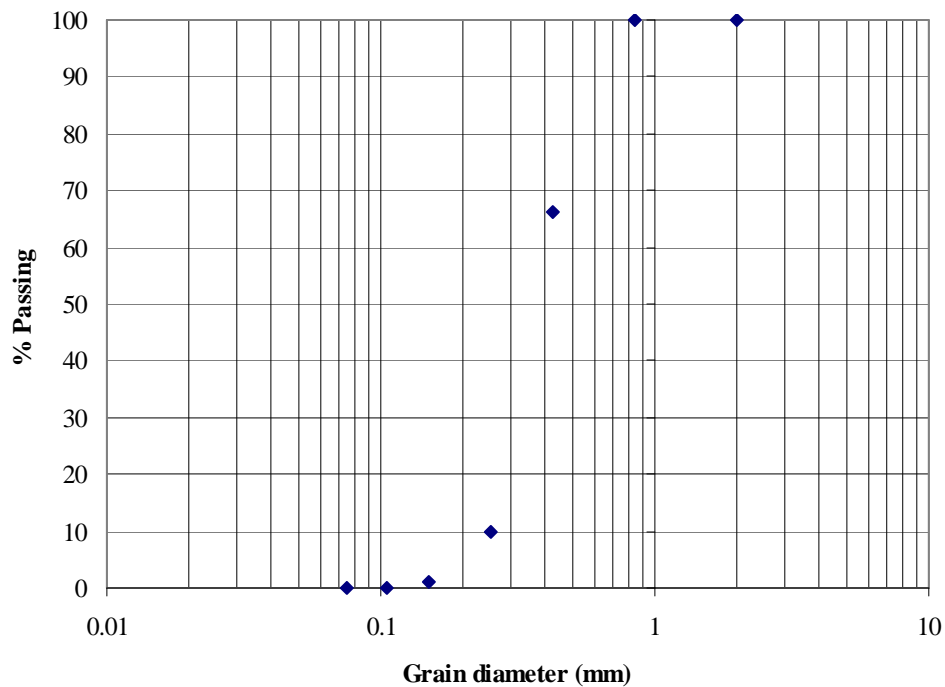


Figure B.1 Grain size distribution for ASTM silica sand (C-190).

Appendix C

CHEMICAL AND PHYSICAL ANALYSIS PROCEDURES

Procedures for the following chemical and physical analyses are presented in this

Appendix:

Appendix C.1	Naphthalene analysis by GC/FID
Appendix C.2	Phenanthrene analysis by GC/FID
Appendix C.3	Pyrene analysis by GC/FID
Appendix C.4	PAHs/Triton X-100 analysis by HPLC
Appendix C.5	Protein analysis
Appendix C.6	Carbohydrates analysis
Appendix C.7	Lipid-Phosphate analysis
Appendix C.8	Bacterial viability staining

Appendix C.1 Naphthalene analysis by GC/FID

Naphthalene was analyzed by Gas Chromatography/Flame Ionization Detection.

Column: Supelco PTA-5, 0.53 mm capillary, 30 m length
Carrier gas: Pre-purified helium at 6.11 cc/min
FID gases: Pre-purified hydrogen at 32.2 cc/min
Air at 359 cc/min
Helium at 26.2 cc/min (makeup)
Inlet temperature: 310 °C
Detector temperature: 300 °C
Temperature program: 100 °C for 1 min
12 °C/min up to 180 °C
Hold at 180 °C for 2 min
Run time: 11.83 min
Peak: 9.1 min

Calibration Curve preparation:

1. Prepare 1000 mg/L naphthalene solution by dissolving 0.1 g naphthalene in 100 mL DCM
2. Prepare standards in 1 mL DCM as following:

<u>Concentration (mg/L)</u>	<u>µL Stock Solution</u>
1	1
2	2
5	5
10	10
20	20
30	30

or use conveniently prepared dilutions.

4. Add 10 µL DCB internal standard stock solution (of 1.2828 g/L) into each standard (12.828 mg/L concentration in 1 mL standard)

Appendix C.2 Phenanthrene analysis by GC/FID

Phenanthrene was analyzed by Gas Chromatography/Flame Ionization Detection.

Column: Supelco PTA-5, 0.53 mm capillary, 30 m length
Carrier gas: Pre-purified helium at 6.11 cc/min
FID gases: Pre-purified hydrogen at 32.2 cc/min
Air at 359 cc/min
Helium at 26.2 cc/min (makeup)
Inlet temperature: 310 °C
Detector temperature: 300 °C
Temperature program: 100 °C for 2 min
30 °C/min up to 230 °C
Hold at 230 °C for 2 min
Run time: 8.33 min
Peak: 7.3 min

Calibration Curve preparation:

3. Prepare 1000 mg/L phenanthrene solution by dissolving 0.1 g phenanthrene in 100 mL DCM
4. Prepare 100 mg/L phenanthrene stock solution by diluting 1:10, by adding 10 mL from previous solution into 90 mL DCM
5. Prepare standards in 1 mL DCM as following:

<u>Concentration (mg/L)</u>	<u>μL Stock Solution</u>
0.10	1.0
0.20	2.0
0.25	2.5
0.50	5.0
1.0	10.0
2.0	20.0

or use conveniently prepared dilutions.

4. Add 5 μL DCB internal standard stock solution (of 1.2828 g/L) into each standard (6.414 mg/L concentration in 1 mL standard)

Appendix C.3 Pyrene analysis by GC/FID

Pyrene was analyzed by Gas Chromatography/Flame Ionization Detection.

Column: Supelco PTA-5, 0.53 mm capillary, 30 m length
Carrier gas: Pre-purified helium at 6.11 cc/min
FID gases: Pre-purified hydrogen at 32.2 cc/min
Air at 359 cc/min
Helium at 26.2 cc/min (makeup)
Inlet temperature: 310 °C
Detector temperature: 300 °C
Temperature program: 100 °C for 2 min
30 °C/min up to 260 °C
Hold at 260 °C for 2 min
Run time: 9.33 min
Peak: 8.5 min

Calibration Curve preparation:

6. Prepare 1000 mg/L pyrene solution by dissolving 0.1 g pyrene in 100 mL DCM
7. Prepare 50 mg/L pyrene stock solution by diluting 1:20, by adding 5 mL from previous solution into 95 mL DCM
8. Prepare standards in 1 mL DCM as following:

<u>Concentration (mg/L)</u>	<u>μL Stock Solution</u>
0.05	1.0
0.125	2.5
0.25	5.0
0.50	10.0
1.0	20.0
2.0	40.0

or use conveniently prepared dilutions.

4. Add 5 μL DCB internal standard stock solution (of 1.2828 g/L) into each standard (6.414 mg/L concentration in 1 mL standard)

Appendix C.4 PAHs/Triton X-100 analysis by HPLC

PAHs and Triton X-100 were analyzed by High Performance Liquid Chromatography.

Column:	Supelcosil LC-18 DB (150 x 4.6 mm)
Packing material size:	5 μm
Mobile phase:	40% Milli-Q water - 60% acetonitrile
Flowrate:	2 mL/min
Detection limits:	50 $\mu\text{g/L}$ for naphthalene and phenanthrene 100 $\mu\text{g/L}$ for pyrene

Appendix C.5 Protein analysis

Reagents:

Comassie Plus Reagent (bring to room temperature prior to use)

Albumin standard stock solution: 2 g/L bovine serum albumin in 0.9% saline and 0.05% sodium azide (ampules)

Procedure:

1. Dilute albumin stock solution 1:10 with MilliQ water just before use: 200 μ L BSA stock solution in 1800 μ L (1.8 mL) MilliQ water (200 mg/L BSA solution).
2. Prepare standard curve in 10 mL COD vials as following (do triplicates):

Standard	Concentration (mg/L)	μL of albumin stock solution	mL of MilliQ water
Blank	0	0	2.00
St 2.5	2.5	25	1.975
St 7.5	7.5	75	1.925
St 15	15	150	1.85
St 20	20	200	1.80
St 25	25	250	1.75
St 50	50	500	1.50

Add stock solution first, then MilliQ water, from low to high concentration.

3. Add 2 mL Comassie plus reagent to standards.

For wet sand samples:

4. Place 0.25 to 1 g wet sand medium into 10 mL COD vial, record wet sample mass for each sample.
5. Add 2 mL MilliQ water.
6. Add 2 mL Comassie plus reagent to sample/duplicate.
7. Sonicate standard/sample for 10 min.
8. Read absorbance at 595 nm immediately.

Reference: Protein Assay Technical Handbook (Pierce).

Appendix C.6 Carbohydrates analysis

Reagents:

- Phenol solution: 5 g phenol in 100 mL MilliQ water (5% phenol)
Benzoic acid: 0.15 g benzoic acid in 100 mL MilliQ water
(0.15% benzoic acid)
Glucose stock solution: 100 mg glucose in 100 mL 0.15% benzoic acid
(1g/L glucose solution)
Concentrated sulfuric acid

Procedure:

1. Dilute glucose stock solution 1:5 with MilliQ water just before use: 20 mL glucose stock solution in 80 mL MilliQ water (200 mg/L glucose solution).
2. Prepare standard curve in 10 mL COD vials as following:

Standard	Concentration (mg/L)	mL of glucose stock solution	mL of MilliQ water
Blank	0	0.00	1.00
St 10	10	0.05	0.95
St 20	20	0.10	0.90
St 40	40	0.20	0.80
St 60	60	0.30	0.70
St 80	80	0.40	0.60
St 100	100	0.50	0.50

3. Place 0.25 to 1 g wet sand medium into 10 mL COD vial, record wet sample mass.
4. Add 1 mL MilliQ water to wet sand sample.
5. Add 1 mL phenol solution to standard/sample and mix rapidly.
6. Add 5 mL concentrated sulfuric acid and mix rapidly. Let stand for 10 min.
7. Place COD vials in water bath at 25°C for 15 min.
8. Read absorbance at 488 nm.

Reference: Daniels, L., Hanson, R., Phillips, J., (1994), "Chemical Analysis". In Methods for General and Molecular Bacteriology. Eds P. Gerhardt, R. Murray, W. Wood and N. Krieg. American Society for Microbiology. Washington, D.C.

Appendix C.7 Lipid-Phosphate analysis

Reagents:

0.0306 M H ₂ SO ₄ :	1.7 mL H ₂ SO ₄ in 1 L MilliQ water
0.36 N H ₂ SO ₄ :	1 mL H ₂ SO ₄ in 100 mL MilliQ water
5.72 N H ₂ SO ₄ :	15.8 mL H ₂ SO ₄ in 100 mL MilliQ water
5% Potassium persulfate solution:	5 g persulfate in 150 mL beaker (tared), add 100 mL 0.36 N H ₂ SO ₄
2.5% Ammonium molybdate solution:	2.5 g molybdate in 150 mL beaker (tared), add 100 mL 5.72 N H ₂ SO ₄
0.111% Polyvinil solution:	0.111 g PVA in in 100 mL MilliQ water at 80°C
0.011% Malachite green solution:	0.011 g malachite in 100 mL MilliQ water, add 100 mL PVA solution at 25°C
0.05M K ₂ HPO ₄ stock solution:	1.742 g K ₂ HPO ₄ in 200 mL MilliQ water (store at 4°C). Dilute same day to 0.25 mM (1 mL stock solution in 199 mL MilliQ water)
343 mg/L sterile saline (NaCl) solution	
ACS grade chloroform	
ACS grade methanol	

Extraction Procedure:

1. Place 0.5 to 1 g wet sand medium in 20 mL vial, record wet sample mass.
2. Add 2 mL saline solution water and swirl gently for 15 seconds.
3. Remove 1.8 mL of supernatant and place in a clean 20 mL vial. Analyze by total lipid phosphate using following procedure (this is loosely-attached biomass fraction).
4. Add 1.8 mL saline solution to the vial from which supernatant was removed. Analyze by total lipid phosphate using following procedure (this is firmly-attached biomass fraction).

LP Procedure:

5. Add 5 mL methanol and 2.5 mL chloroform to the sample; shake for 2 minutes. Extract for 2 hours.
6. Add 2.5 mL 0.0306 M H₂SO₄ and 2.5 mL chloroform and allow phases to separate overnight.
7. Remove methanol layer (upper layer) with a disposable pipette and discard. Transfer 1 mL of chloroform layer (lower layer) to 5 mL glass ampule and evaporate with nitrogen gas in a warm waterbath at 30°C for 8-10 min.
8. Add 0.9 mL persulfate solution and seal ampules.
9. Digest samples in a 100°C oven for 18 hours. Remove from oven and allow to cool down to room temperature.
10. Break ampules and add 0.2 mL molybdate solution. Let stand for at least 10 minutes.
11. Add 0.9 mL malachite solution and let stand for 30 minutes.

12. Prepare standard curve as following:

Standard	Concentration (nmoles/ampoule)	μL of K_2HPO_4 stock solution	mL of MilliQ water
Blank	0	0.00	2.00
St 2.5	2.5	10	1.99
St 7.5	7.5	30	1.97
St 15	15	60	1.94
St 20	20	80	1.92
St 25	25	100	1.90
St 50	50	200	1.80

Follow LP procedure for the standards after digestion.

13. Add 2 mL MilliQ water to standards/samples.

14. Read absorbance at 610 nm.

Reference: Findlay, R., King, G., Watling, L., (1989), "Efficacy of phospholipids analysis in determining microbial biomass in sediments", *Appl. & Envir. Microb.*, **55**(11), 2888-2893.

Appendix C.8 Bacterial viability staining

Reagents:

Component A: propidium iodide (PI)

Component B: SYTO 9®

Phosphate Buffer Saline, adjusted to pH 7.2

Stain preparation:

1. Add 1.5 μ L of Component A and 1.5 μ L of Component B to 1.0 mL PBS solution and mix thoroughly.
2. Store at 4°C in amber microtubes.

Sample staining:

1. Stain samples with 0.5 mL of fluorescent stain
2. Incubate flow cells for 20 minutes in darkness at lab temperature
3. Adjust excitation/emission maximas of 480/500 nm and 490/635 nm for SYTO and PI, respectively.
4. Analyze under a scanning confocal laser microscope (CLSM) with an upright scope.

Reference: LIVE/DEAD BacLight® Bacterial Viability Kit (Molecular Probes, Eugene, OR).

Appendix D

PAH FEED GENERATION COLUMNS

The PAH feed generation apparatus consists of two stainless steel columns, 4.75 cm diameter and 90 cm length, each filled with 2.4 kg of 3 mm soda lime glass beads coated with solid PAH. This generator column apparatus was a modification of an approach used by De Maagd *et al* (1998). Each kg of glass beads for PAH Generation Column was coated with 15 g of naphthalene, 10 g of phenanthrene, and 10 g of pyrene. PAHs were dissolved in approximately 100 mL of methylene chloride (DCM) and mixed with glass beads under a laboratory fume hood, allowing methylene chloride to evaporate completely and deposit a solid residue covering glass bead surfaces (Total: 36 g naphthalene, 24 g phenanthrene, 24 g pyrene).

Note: This is sort of a messy procedure, and MUST be done in the lab hood with the face of the hood as closed as far as possible. Use a steel tray lined with aluminum foil as a container to coat the beads. When most of the solvent is gone, the beads can be spread out in a “monolayer” on some aluminum foil to speed up the process and get a more uniform coating on the beads. Some PAH “dust” residue will be left over things. To keep the particulate PAHs out of the feed stream going to the column bioreactor the fine inlet and outlet stainless steel screens are essential. Used a steel spatula to mix the beads as the DCM was evaporating to get an even coating of the beads. DCM diffuses through

the latex or nitrile gloves so try not to touch the beads with your gloved hands too much, but just in case, use double gloves.

REFERENCES

De Maagd, P.G., Ten Hulscher, D.T.E.M., Van Den Heuvel, H., Opperhuizen, A. Sims, D.T.H.M., (1998), "Physicochemical properties of polycyclic aromatic hydrocarbons: aqueous solubilities, n-octanol/water partition coefficients and henry's law constants", *Environm.Toxicol.Chem.* **17**, 251-257.

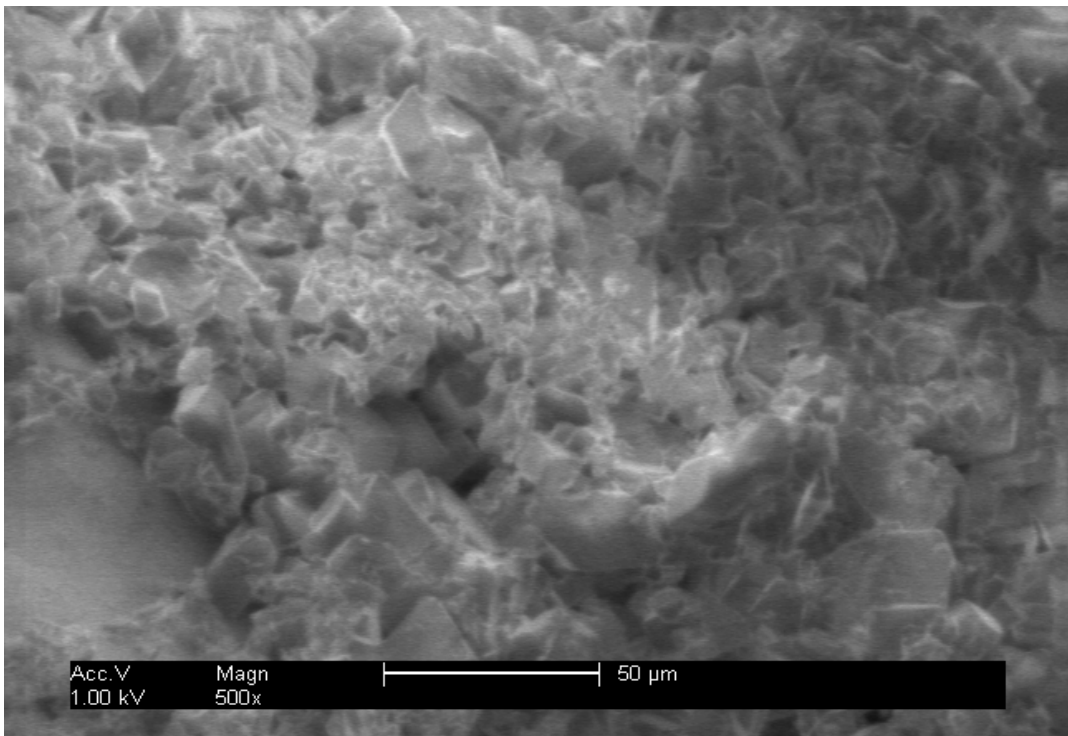
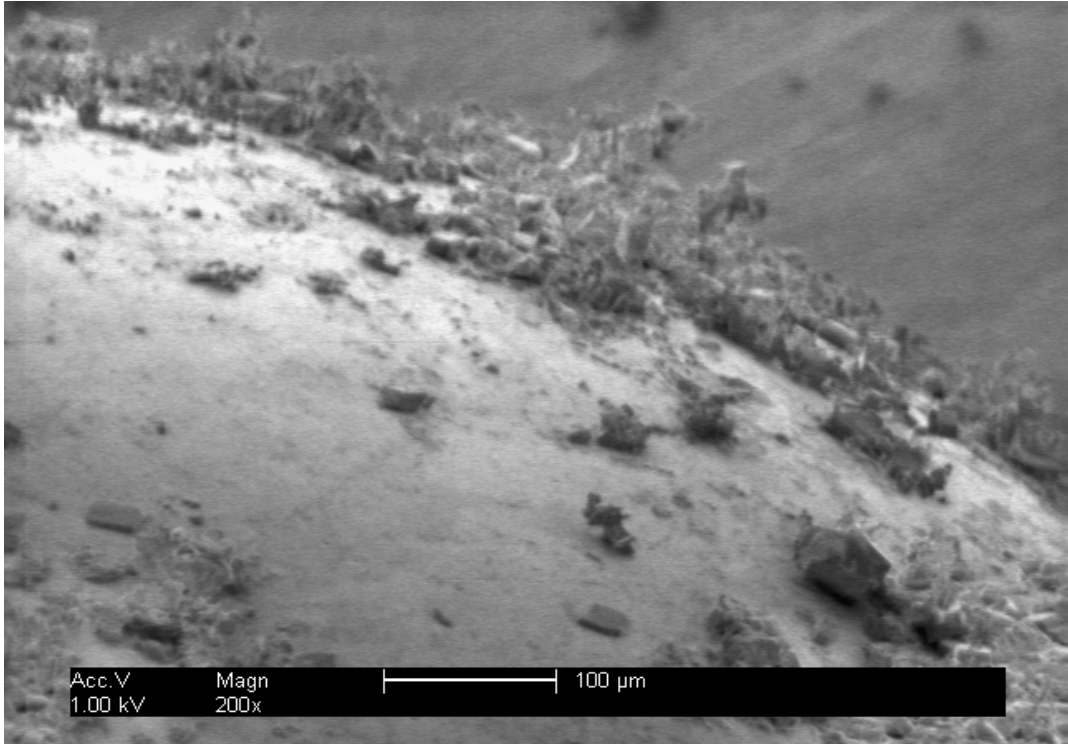


Figure D.1 ESEM picture of typical PAH coating on glass beads at 200x and 500x magnifications.